

# INSIGHT INTO THE MULTICOPPER OXIDASES STABILITY

**André João Tavares Fernandes**

*Dissertation presented to obtain the PhD degree in Biochemistry at the Instituto  
de Tecnologia Química e Biológica, Universidade Nova de Lisboa*

Supervisor: Prof. Lúcia O. Martins

Co-supervisor: Prof. Eduardo P. Melo



**Oeiras, February of 2011**

Apoio financeiro da FCT e do FSE no âmbito do Quadro Comunitário de  
Apoio, BD nº SFRH/BD/31444/2006

**FCT** Fundação para a Ciência e a Tecnologia  
MINISTÉRIO DA CIÊNCIA, TECNOLOGIA E ENSINO SUPERIOR Portugal





*Supervisor:* Prof. Lúcia O. Martins

*Co-supervisor:* Prof. Eduardo P. Melo

*President of Jury:* Prof. Carlos Romão

*Examiners:* Prof. Giovanni Sannia, Prof. Rui Brito and Prof. Margarida Bastos



## ACKNOWLEDGMENTS

Getting to the end of this, almost, life project would not be possible without the precious help and contributions of some people to whom I would like to acknowledge all of their support.

My first words are directed to my Supervisor, Prof. Lgia O. Martins. She was my professor during my college degree and even without being a regular presence in her class room (well, in some disciplines...), she told me that is better not going to a class room without the correct will, and always supported me when the will was the correct one. A few semesters later, with all my will and motivation, and almost at the end of my fourth year in college, I met her and ask if I could participate in her lab as a volunteer (the beginning of the Quest...). When I first came to ITQB to meet her in the lab I got a huge surprise...never saw a lab completely empty. I was the first student in the lab. Those months afterwards were of so much fun and learning, because, together with science I and Prof. Lgia were looking to material and equipment to acquire and off course negotiating with the providers. In 2006 she gave me the honour to work with her in close collaboration in the organization of a European meeting at ITQB. I have no words to thank her enough for all the science that she provide me to develop at ITQB, for all the knowledge that I obtained under her supervision, and for all the fun that I had in other lab works that were not science (at least directly...). Her strong personality made me a bigger scientist/person. Her strong support made me want to continue, even in those really bad days. Her permanent presence is a safe shelter for all of the students that may need some support. Her constant fight to provide us better science conditions is strongly acknowledged by me, and honestly it is with deep pride that my supervision was carried out by Prof. Lgia O. Martins. For all this I want to express my deep gratitude to her for being my “Boss” during these last years.

I would also like to acknowledge Prof. Eduardo P. Melo in participating in all my work. During this period, Prof. Eduardo taught me different techniques that we further developed to specific purposes according to our work. His deep knowledge on those different techniques provided me the opportunity to further develop my scientific work and background. His collaboration was in fact fundamental to all my work since it provided, until now, insight in the obscureness of some particularities of these enzymes. His patience, without giving up gave me some windows that we further developed even if swimming against the current. For all his friendship, patience, and persistency I want to deeply thank to Prof. Eduardo, that without him certainly that this thesis would be completely different.

I only present in this thesis the work developed directly by me, but obviously, this would not be possible or at least it would be much more difficult (than what it was...) if I didn't have lab mates. Therefore I would like to acknowledge firstly three past members for their friendship and support, Paulo Durão, Luciana Pereira, and Carlos Covinha. I also want to express all my gratitude to the current lab members, Vânia Brissos, Zhenjia Chen, Sónia Mendes, Tânia Rosado and Rita Catarino, even if some of them did not participate directly in the work. I want to acknowledge them, because I know it is not really easy to live with me 9/10 hours a day 5 days a week... Even so it were some wonderful years or months (for some of them) to work closely with them. Their support on the bad days, the sharing of joys in the good days and more importantly their friendship was essential during all this time period.

Importantly, I also would like to thank the great contributions of Manuela Pereira, Smilja Todorovic, Isabel Bento, Catarina Silva, João M. Damas and Cláudio Soares and to Peter F. Lindley. Thank you for all the input you have given into the presented work in this dissertation.

I am thankful to Instituto de Tecnologia Química e Biológica (ITQB), the institution that made this work possible by providing me the facilities and

equipment. I would also like to thank Instituto de Biologia Experimental e Biotecnológica (IBET), the European projects, Sophied and Biorenew, and off course to all FCT projects as well and again to FCT for my grant.

In last, I would like to thank to parents and brother for their constant presence, their constant support and their constant friendship. To Vanessa I would like to thank her for listening to all my complaints (only in those bad days...) without complaining herself, to all her love and friendship.





## DISSERTATION ABSTRACT

This dissertation portrays recent development on the knowledge of the stability determinants and of functional characteristics of multicopper oxidases (MCO). Multicopper oxidases are a family of enzymes that includes laccases (benzenediol oxygen oxidoreductase; EC 1.10.3.2), ascorbate oxidase (L-ascorbate oxygen oxidoreductase, EC 1.10.3.3) and ceruloplasmin ( $\text{Fe}^{2+}$  oxygen oxidoreductase, EC 1.16.3.1). MCO are characterized by having four copper ions that are classified into three distinct types of copper sites, namely type 1 (T1), type 2 (T2) and type 3 (T3). The classical T1 copper site comprises two histidine residues and a cysteine residue arranged in a distorted trigonal geometry around the copper ion with bonding distances approx.  $2.0 \text{ \AA}$  ( $1 \text{ \AA} = 0.1 \text{ nm}$ ); a weaker fourth methionine ligand completes the tetrahedral geometry. The copper–cysteine linkage is characterized by an intense  $\text{S}(\pi) \rightarrow \text{Cu}(\text{d}_x^2 - \text{d}_y^2)$  CT (charge transfer) absorption band at approximately 600 nm, and a narrow parallel hyperfine splitting  $A_{\parallel} = (43\text{--}90) \times 10^{-4} \text{ cm}^{-1}$  in the electron paramagnetic resonance (EPR) spectrum. The function of the T1 copper site is to shuttle electrons from substrates to the trinuclear copper centre where molecular oxygen is reduced to two molecules of water during the complete four-electron catalytic cycle. The trinuclear center contains a T2 copper coordinated by two histidine residues and one water molecule, lacks strong absorption bands and exhibits a large parallel hyperfine splitting in the EPR spectrum ( $A_{\parallel} = (150\text{--}201) \times 10^{-4} \text{ cm}^{-1}$ ). The T2 copper site is in close proximity to two T3 copper ions, which are each coordinated by three histidine residues and typically coupled, for example, through a dioxygen molecule. The T3 or coupled binuclear copper site is characterized by an intense absorption band at 330 nm originating from the bridging ligand and by the absence of an EPR signal due to the antiferromagnetically coupling of the copper ions.

These are enzymes that catalyze the oxidation of various substituted phenolic compounds, aromatic amines and even certain inorganic compounds by using molecular oxygen as the electron acceptor. Their substrate versatility makes

laccase highly interesting for various applications, including textile dye bleaching, pulp bleaching and bioremediation, where enzymatic catalysis could serve as a more environmentally friendly alternative than the current used chemical processes. However, using an enzyme in industrial environment requires a high stability, since most of the industrial activities are carried out at high temperatures, extreme pH values, high pressures among other physico-chemical adverse conditions. Natural enzymes are usually, far from optimally functioning under these harsh conditions. The work developed in this thesis focus precisely in the study of molecular determinants of stability in MCO. Having these in mind two different strategies were followed. We searched for hyperthermophilic MCO and simultaneously we have used site directed mutagenesis in a well characterized bacterial laccase, CotA-laccase from *Bacillus subtilis* whose structure is known. Two MCO from hyperthermophilic microorganism were isolated and characterized, one from the *Bacterium Aquifex aeolicus*, and the other from the *Archaeon Pyrobaculum aerophilum*. Unlike most of the hyperthermophiles both *A. aeolicus* and *P. aerophilum* can withstand the presence of oxygen, growing efficiently in microaerophilic conditions, and using it as electron acceptor in a chemiolitoautotrophic metabolism. *Aquifex aeolicus* isolated from a shallow submarine hydrothermal system at Volcano, Italy is one of the most hyperthermophilic bacteria known so far ( $T_{op}$  89°C) and belongs to an ancient lineage within the bacterial domain. *Pyrobaculum aerophilum* was isolated from a boiling marine water hole at Maronti Beach in Italy as an optimal growth temperature of 100°C. *P. aerophilum* is able to grow autotrophically by oxidation of molecular hydrogen, thiosulfate or sulphur, using oxygen, as electron acceptors and is a strictly aerobic organism, a rare feature among hyperthermophiles.

The first gene to be cloned in this work was the one corresponding to the MCO from the hyperthermophilic bacterium *Aquifex aeolicus* and the recombinant protein expressed in *E. coli*. The *mcoA* gene is localized in the genome as part of a putative copper-resistance determinant. The purified recombinant enzyme

shows spectroscopic and biochemical characteristics typical of the well-characterized MCO. McoA presents higher specificity ( $k_{\text{cat}}/K_{\text{m}}$ ) for cuprous and ferrous ions than for aromatic substrates and is therefore designated as a metallo-oxidase. Addition of copper is required for maximal catalytic efficiency. A comparative model structure of McoA has been constructed and a striking structural feature is the presence of a Met-rich region (residues 321–363), reminiscent of those found in copper homeostasis proteins. The kinetic properties of a mutant enzyme, McoA $\Delta$ P321-V363, deleted in the Met-rich region, provide evidence for the key role of this region in the modulation of the catalytic mechanism. McoA probably contributes to copper and iron homeostasis in *A. aeolicus*.

In order to understand the stability determinants in this family of enzymes we analyzed in more detail the thermodynamic stability of McoA. The deconvolution of the DSC traces shows that thermal unfolding is characterized by an average melting temperature of 110°C, showing that this enzyme is highly thermotolerant. Furthermore, McoA has an optimal catalytic temperature of 75 °C and presents remarkable heat stability at 80 and 90 °C, with activity lasting for up to 9 and 5 h, respectively. However, chemical denaturation studies revealed that McoA displays, at room temperature, a very low stability (2.8 kcal/mol). Stopped-flow kinetics was performed to obtain additional information regarding the mechanism of unfolding and the role of copper in the stabilization of the protein. In McoA which is highly prone to aggregation, the kinetic partitioning between unfolding and aggregation should constitute the main factor behind the unusual low chemical stability of the enzyme. Moreover, McoA exhibits a small difference in stability between the folded and unfolded states in a broad range of temperatures. Actually, the flattening of the  $\Delta G_{\text{stab}}$  curvature as a function of temperature due to a low heat capacity change is one mechanism used by other thermophilic proteins, for balancing a high melting temperature with the thermodynamic stability needed for optimal activity, and

this mechanism should explain, at least partially, the hyperthermophilic nature of McoA.

The second MCO (McoP) to be cloned and studied was from the hyperthermophilic archaeon *Pyrobaculum aerophilum*. The enzyme consists of a single subunit with 49.6 kDa and the combined results of UV-visible, circular dichroism (CD), electron paramagnetic resonance (EPR) and resonance Raman (RR) showed the typical spectroscopic characteristics of the MCO family. McoP is an efficient metallo-oxidase that catalyzes the oxidation of  $\text{Cu}^+$  and  $\text{Fe}^{2+}$  metal ions with turnover rate constants of 356 and 128  $\text{min}^{-1}$ , respectively, at 40°C. Noteworthy, McoP that follows a ping-pong mechanism presents a 3-fold higher catalytic efficiency when using nitrous oxide ( $\text{N}_2\text{O}$ ) as electron acceptor as compared with dioxygen, the typical oxidizing substrate of multicopper oxidases. This finding led us to propose that McoP represents a novel archaeal nitrous oxide reductase most probably involved in the final step of the denitrification pathway of *P. aerophilum*. The analysis of McoP sequence, showing similarities with bacterial MCO, allowed deriving its structure by comparative modelling methods. Mutants were designed to elucidate the substrate specificity as well as the low redox potential of the T1 center. We show that the low redox potential of this enzyme is at least in part related to a negatively charged residue (Glu296), near T1 (7.8 Å) that should stabilize the oxidized state of the copper ion, reducing the center redox potential. McoP has an optimum reaction temperature of 85°C and is a hyperthermostable enzyme, with a half-life of inactivation of around 6 h at 80°C, being one of the most hyperthermostable MCO studied so far. To gain further insight into the thermal stability of McoP we have analyzed its melting temperatures by DSC. Similar to other MCO, the endothermic peak revealed a complex and irreversible thermal transition, characterized by three independent non two-state transitions with melting temperatures ranging from 97 to 112°C.

We also evaluated the stability determinants of MCO by using site directed mutagenesis in a well characterized MCO, CotA-laccase from *Bacillus subtilis*.

The first work performed was to evaluate the effect of the axial Met in the T1 copper center reduction potential. We have replaced the Met by a Leu or Phe residue in order to increase the redox potential of the enzyme. In fact, these mutations led to an increase of the T1 redox potential by approximately 100 mV relative to the wild-type enzyme but severely compromised the catalytic rate of the enzyme. This decrease in the catalytic efficiency was unexpected as the X-ray analysis of mutants has shown that replacement of Met ligand did not lead to major structural changes in the geometry of the T1 center or in the overall fold of the enzyme. However, these point mutations have a profound impact on the thermodynamic stability of the enzyme. The fold of the enzyme has become unstable especially with the introduction of the larger Phe residue and this instability should be related to the decrease in the catalytic efficiency. This instability of the folded state resulted in the accumulation of an intermediate state, partly unfolded, in between native and unfolded states. Quenching of tryptophan fluorescence by acrylamide has further revealed that the intermediate state is partly unfolded.

With the aim at evaluating the copper content effect on the thermal stability of CotA-laccase we have studied different forms of CotA-laccase with respect to copper content. The data shows that copper content of CotA-laccase has a profound impact in the kinetic and thermal stability as assessed by long term stability (at 80°C) and DSC. Indeed, HoloCotA, produced in recombinant *Escherichia coli* under microaerobic conditions, is a very stable enzyme, followed by ApoCotA reconstituted *in vitro* with  $\text{Cu}^+$ , and by ApoCotA reconstituted with  $\text{Cu}^{2+}$ . These results showed additionally, that copper incorporation into the protein seems to occur more effectively during the *in vivo* folding of the enzyme and is dependent on its oxidation state, a higher Cu:protein ratio is achieved with  $\text{Cu}^+$  than with  $\text{Cu}^{2+}$  form. CotA-laccase has an intradomain disulfide bridge between Cys229 and Cys322. Disulfide bridges are known stabilizers of protein structures; we have used site directed mutagenesis, in a well known laccase, in order to mutate Cys322 to remove the disulfide

bond of CotA-laccase. Surprisingly the results show that this disulfide bridge is not involved in the protein stability. Furthermore, the mutagenesis of Cys322 did not alter the kinetic and spectroscopic properties of the enzyme. However, the removal of the S-S bond resulted in an enzyme with a higher dynamics for copper incorporation/bleaching as assessed by stopped-flow spectroscopy unfolding studies. Removal of the S-S bond causes a destabilizing effect on the copper coordination.

## SUMÁRIO DA DISSERTAÇÃO

Esta dissertação retrata os desenvolvimentos recentes no conhecimento dos determinantes de estabilidade e também das características funcionais de oxidases de múltiplos cobres. As oxidases de múltiplos cobres (OMCs) são uma família de enzimas que inclui lacases (oxidoreductases de benzenodiol e oxigénio, EC: 1.10.3.2.), ascorbato oxidase (oxidoreducase de L-ascorbato e oxigénio, EC: 1.10.3.3) e ceruloplasmina (oxidoreductase de  $\text{Fe}^{2+}$  e oxigénio, EC: 1.16.3.1). As OMCs são caracterizadas por terem 4 centros de cobre distintos, nomeadamente, tipo 1 (T1), tipo 2 (T2) e tipo 3 (T3). O centro de cobre T1 clássico é composto por dois resíduos de histidinas e um de cisteína que estão organizados numa geometria trigonal distorcida, em torno do átomo de cobre com distâncias de ligação de aproximadamente 2,0 Å (1 Å=0.1 nm); a geometria tetraédrica é completada com a presença de um quarto ligando fraco, um resíduo de metionina. A ligação entre o cobre e a cisteína é caracterizada por ter uma transferência de carga (TC) intensa entre  $\text{S}(\pi) \rightarrow \text{Cu}(\text{d}_x^2 - \text{d}_y^2)$  que resulta numa banda de absorção a aproximadamente 600 nm, e uma separação do paralelo hiper-fino estreito,  $A_{\parallel} = (43-90) \times 10^{-4} \text{ cm}^{-1}$ , no espectro de ressonância paramagnética (ERP). A função do centro de cobre T1 é transferir os electrões subtraídos aos substratos para o centro trinuclear, onde durante um ciclo completo de quatro electrões, a molécula de oxigénio é reduzida a duas moléculas de água. O centro trinuclear é composto por um centro de cobre tipo 2 (T2) coordenado por duas histidinas e uma molécula de água, não tem bandas de absorção fortes e exhibe um paralelo hiper-fino largo no espectro de ressonância paramagnética (ERP) ( $A_{\parallel} = (150-201) \times 10^{-4} \text{ cm}^{-1}$ ). O centro de cobre T2 está muito próximo dos dois cobres do tipo T3, em que cada um é coordenado por três resíduos de histidinas e são tipicamente acoplados, por exemplo, por uma molécula de oxigénio. O centro de cobre do tipo T3 ou centro binuclear é caracterizado por uma banda de absorção intensa a 330 nm, que é originada pelo ligando acoplado e também pela ausência de um sinal de ERP devido ao acoplamento antiferromagnético dos dois átomos de cobre.

As laccases são enzimas que catalisam a oxidação de uma variedade de compostos fenólicos substituídos, aromáticos, aminas e, também, de alguns compostos inorgânicos, usando o oxigénio como aceitador final de electrões. A sua versatilidade de substratos faz com que as lacases sejam muito interessantes para várias aplicações biotecnológicas, incluindo descoloração de corantes têxteis, branqueamento da pasta do papel e bioremediação, onde a catálise enzimática poderá servir como uma alternativa, mais amiga do ambiente, aos processos químicos actuais. No entanto, o uso de enzimas em ambiente industrial requer que estas tenham uma elevada estabilidade, uma vez que a maioria dos processos industriais realizam-se a temperaturas elevadas, valores de pH extremos, pressões altas entre outras condições físico-químicas adversas. As enzimas naturais estão normalmente longe de funcionar optimamente sob estas condições adversas. O trabalho desenvolvido nesta tese foca precisamente o estudo dos determinantes moleculares de estabilidade das OMCs. Tendo isto em mente, foram seguidas duas estratégias. Procurámos OMCs hipertermófilas e simultaneamente usámos mutagénesis dirigida numa lacase bacteriana bem caracterizada cuja estrutura tridimensional é conhecida, a CotA-lacase de *Bacillus subtilis*. Duas OMCs de microrganismos hipertermófilos foram isoladas e caracterizadas, uma da *Bacteria Aquifex aeolicus* e outra do *Archeaum Pyrobaculum aerophilum*. Ao contrário da maioria dos hipertermófilos, ambos *A. aeolicus* e *P. aerophilum* toleram a presença de oxigénio, crescendo de forma eficiente em condições de microaerofilia, usando, O<sub>2</sub> como aceitador de electrões num metabolismo quimiolitotrófico. *Aquifex aeolicus* foi isolado de um sistema hidrotermal pouco profundo em Volcano, em Itália sendo a bactéria mais hipertermófila conhecida ( $T_{opt}=89^{\circ}C$ ) e pertence a uma linhagem antiga dentro do domínio *Bacteria*. O *Pyrobaculum aerophilum* foi isolado num buraco de água marinha fervente na praia de Maronti, em Itália, tendo uma temperatura óptima de crescimento de 100°C. O *P. aerophilum* é capaz de crescer autotroficamente através da oxidação de hidrogénio molecular, tiosulfato ou sulfato, usando o oxigénio como aceitador de electrões, característica rara entre os hipertermófilos.



Neste trabalho a primeira OMC a ser clonada e a proteína recombinante expressa em *E. coli* foi a da bactéria hipertermófila *Aquifex aeolicus*. O gene *mcoA* está inserido no genoma como parte de um possível determinante genético de resistência ao cobre. A enzima pura tem as características espectroscópicas e bioquímicas típicas de outras OCMs conhecidas. A McoA é designada como oxidase de metais uma vez que tem uma especificidade ( $k_{\text{cat}}/K_m$ ) elevada para o ião  $\text{Cu}^+$  e para  $\text{Fe}^{2+}$  quando comparado com substratos aromáticos. Para atingir a máxima eficiência catalítica é necessária a adição de cobre ( $\text{Cu}^{2+}$ ) às misturas reacionais. Um modelo comparativo da McoA foi construído e, uma característica interessante que foi detectada, foi a presença de um segmento rico em metioninas (resíduos 321-363) reminescente de outras enzimas envolvidas na homeostase de cobre. As propriedades cinéticas da enzima mutante McoA $\Delta$ P321-V363, em que se removeu a região rica em metioninas, apontam para o papel crucial desta região na modulação do mecanismo catalítico. A McoA provavelmente contribui para a homeostase de  $\text{Cu}^+$  e  $\text{Fe}^{2+}$  em *A. aeolicus*.

Para estudar os determinantes de estabilidade nesta família de enzimas, analisámos com mais pormenor a estabilidade termodinâmica da McoA. A desconvolução dos termogramas de DSC mostra que o ‘unfolding’ térmico é caracterizado por uma temperatura de ‘melting’ média de 110°C, mostrando assim a termotolerância desta enzima. Além do mais, a McoA tem uma temperatura óptima de catálise de 75°C, a também uma elevada estabilidade cinética a 80 e 90°C, temperaturas às quais a enzima permanece activa durante 9 e 5 horas, respectivamente. No entanto, estudos de estabilidade química demonstraram que a McoA, à temperatura ambiente, tem uma estabilidade muito baixa (2.8 kcal mol<sup>-1</sup>). Para perceber melhor o mecanismo de ‘unfolding’ e também o papel dos iões de cobre na estabilidade da enzima, obtivemos informação adicional por meio de técnicas de mistura rápida, concretamente cinéticas de fluxo interrompido. Na McoA que tem tendência a agregar, a partição cinética entre ‘unfolding’ e agregação deverá constituir o factor

principal que determina a baixa estabilidade à temperatura ambiente. No entanto, a McoA apresenta uma baixa diferença de energia livre ( $\Delta G_{\text{stab}}$ ) entre os estados nativo e desnaturado num intervalo largo de temperaturas. Na verdade, o alargamento e diminuição da curva de  $\Delta G_{\text{stab}}$  em função da temperatura, devido a um baixo valor de variação da capacidade calorífica ( $\Delta C_p$ ), é um mecanismo usado por outras proteínas termófilas para balancear uma temperatura de ‘unfolding’ elevada com a necessária estabilidade termodinâmica para uma actividade catalítica óptima, sendo que este mecanismo poderá explicar, pelo menos em parte, a natureza hipertermófila da McoA.

A segunda OCM (McoP) a ser clonada e estudada foi do archaeum hipertermófilo *Pyrobaculum aerophilum*. A enzima é um monómero com 49.6 kDa, em que os resultados combinados de UV-Visível, dicroísmo circular, ressonância electrónica paramagnética e ressonância de Raman, mostraram que a enzima contém as características espectroscópicas típicas da família das OCM. A McoP é uma oxidase de metais eficiente com um ‘turnover’ a 40°C de 356 e 128 min<sup>-1</sup> para o Cu<sup>+</sup> e Fe<sup>2+</sup>, respectivamente. De realçar, que a McoP segue um mecanismo tipo ‘ping-pong’ e apresenta uma eficiência 3 vezes superior usando o óxido nítrico (N<sub>2</sub>O) como aceitador final de electrões quando comparado com o substrato típico das OCMs, o oxigénio. Esta descoberta levou-nos a propor que a McoP representa um novo tipo de reductase de óxido nítrico envolvida no último passo da via de desnitrificação do *P. aerophilum*. A análise da sequência mostra similaridades com outras OCM’s bacterianas o que permitiu a construção de um modelo estrutural comparativo da McoP. Alguns mutantes foram construídos para elucidar a especificidade dos substratos, bem como o baixo potencial redox do centro de cobre T1. Mostrámos que o baixo potencial redox desta enzima é, pelo menos em parte, relacionado com a presença, perto do T1 (7.8 Å), de um resíduo de carga negativa (Glu296) que deverá estabilizar o estado oxidado do centro levando a valores relativamente baixos do potencial de redução. A McoP tem uma temperatura óptima de

catálise de 85°C e, é uma enzima hipertermoestável com um tempo de meia vida de 6 horas a 80°C, sendo uma das OCM's conhecidas mais estáveis. Com o objectivo de analisar em maior pormenor a estabilidade térmica da McoP, analisámos as temperaturas de 'melting' por DSC. À semelhança do que aconteceu para outras OCM's, o pico endotérmico mostrou tratar-se de uma transição complexa e irreversível, caracterizada por três transições independentes, com temperaturas de 'melting' de 97 a 112°C.

Estudámos também os determinantes de estabilidade das OCM's usando mutagénesis dirigida numa enzima bem caracterizada, a CotA-lacase de *Bacillus subtilis*. No primeiro estudo que desenvolvemos, avaliámos o efeito do ligando axial metionina do centro de cobre T1. Substituímos a metionina por resíduos de leucina e fenilalanina, com o objectivo de aumentar o potencial de redução da enzima. De facto, estas mutações permitiram aumentar o potencial de redução do centro de cobre T1, em relação à enzima nativa, em 100 mV aproximadamente, no entanto, a velocidade catalítica das enzimas ficou severamente comprometida. Esta diminuição da eficiência catalítica não era expectável, uma vez que a análise das estruturas de raio-X das proteínas mutantes, mostrou que a substituição do ligando metionina, não causou alterações na geometria do centro de cobre T1 nem no enrolamento geral da proteína. No entanto, estas mutações pontuais tiveram um impacto profundo na estabilidade termodinâmica da enzima. O enrolamento das enzimas mutantes tornou-se instável, especialmente com a introdução do resíduo de fenilalanina de maiores dimensões, o que deverá estar relacionado com a diminuição da eficiência catalítica. Esta instabilidade no enrolamento das enzimas causa a acumulação de um estado intermediário, parcialmente desenrolado, entre os estados nativo e desenrolado. Estudos de extinção da fluorescência de triptofanos usando acrilamida, revelaram que este estado intermediário é uma estrutura parcialmente desenrolada. Com o objectivo de avaliar o efeito do teor em cobre na estabilidade térmica da CotA-lacase, estudámos diferentes variantes da enzima com diferentes teores em cobre. Os dados mostram que o

teor em cobre na CotA-lacase, tem um efeito profundo na estabilidade cinética e térmica, tal como determinado por estudos de estabilidade cinética a 80°C e também por varrimento diferencial de calorimetria. De facto, a holoCotA recombinante, produzida em *Escherichia coli* sob condições micoraeróbicas, é uma enzima muito estável, seguido da apoCotA reconstituída *in vitro* com  $\text{Cu}^+$  e pela apoCoA reconstituída com  $\text{Cu}^{2+}$ . Estes resultados mostram, adicionalmente, que a incorporação de cobre na proteína ocorre de forma mais eficiente durante o enrolamento da enzima *in vivo* e que é dependente do estado de oxidação do metal, uma vez que um rácio maior de Cu:proteína, é conseguido com cobre no estado I do que com cobre no estado II. A enzima CotA-lacase tem uma ponte disulfureto intradomínio entre a cisteína 229 e a cisteína 322. Com recurso a mutagénese dirigida substituímos a cisteína 322 por uma alanina, de forma remover a ponte disulfureto da CotA-lacase. As pontes disulfureto são conhecidas por aumentarem a estabilidade estrutural nas proteínas. Surpreendentemente, os resultados mostraram que a ponte de disulfureto não está envolvida na estabilidade da proteína. Além do mais, a remoção da ponte disulfureto não afectou as propriedades cinéticas da enzima. No entanto, a substituição deste resíduo, causou um aumento da dinâmica na proteína em relação à incorporação/remoção de cobre dos centros catalíticos causando um efeito destabilizar na manutenção dos centros activos, tal como verificado por recurso a cinéticas de fluxo interrompido.

## LIST OF PUBLICATIONS

Paulo Durão, Isabel Bento, **André T. Fernandes**, Eduardo P. Melo, Peter F. Lindley, and Lígia O. Martins. 2006. Perturbations of the T1 copper site in the CotA-laccase from *Bacillus subtilis*: Structural, Biochemical, Enzymatic and Stability Studies. J. Biol. Inorg. Chem. 11:514-526.

**André T. Fernandes**, Cláudio M. Soares, Manuela M. Pereira, Robert Huber, Gregor Grass, Lígia O. Martins. 2007. A robust metallo-oxidase from the hyperthermophilic bacterium *Aquifex aeolicus*. The FEBS Journal. 274:11 2683-2694

Paulo Durão, Zhenjia Chen, **André T. Fernandes**, Peter Hildebrandt, Daniel H. Murgida, Smilja Todorovic, Manuela M. Pereira, Eduardo P. Melo, Lígia O. Martins. 2008. Copper incorporation into recombinant CotA-laccase from *Bacillus subtilis*: characterization of fully copper loaded enzymes. J. Biol. Inorg. Chem. 13:183-93

**André T. Fernandes**, Lígia O. Martins, Eduardo P. Melo. 2009. The hyperthermophilic nature of the metallo-oxidase from *Aquifex aeolicus*. Biochimica et Biophysica Acta. 1794: 75-83

**André T Fernandes**, João M. Damas, Smilja Todorovic, Robert Huber, M. Camilla Baratto, Rebecca Pogni, Cláudio M. Soares and Lígia O. Martins. 2010. The multicopper oxidase from the archaeon *Pyrobaculum aerophilum* shows nitrous oxide reductase activity. FEBS J. 277: 3176-3189

**André T Fernandes**, Manuela M. Pereira, Catarina I. Silva, Isabel Bento, Peter F. Lindley, Eduardo P. Melo and Lígia O. Martins. The removal of a disulfide bridge of CotA-laccase changes the slower motion dynamics involved in copper binding but has no effect on the thermodynamic stability. J. Biol. Inorg. Chem. DOI: 10.1007/s00775-011-0768-9.



## TABLE OF CONTENTS

DISSERTATION ABSTRACT .....	IX
SUMÁRIO DA DISSERTAÇÃO.....	XV

---

<b>1 General Introduction .....</b>	<b>27</b>
-------------------------------------	-----------

---

<b>1.1. WHITE BIOTECHNOLOGY .....</b>	<b>2</b>
1.1.1. Enzymes in White Biotechnology .....	5
<b>1.2. MULTICOPPER OXIDASES .....</b>	<b>6</b>
1.2.1. Overall fold of multicopper oxidases.....	7
1.2.2. Copper centers in multicopper oxidases .....	9
1.2.3. reaction mechanism of Multicopper oxidases.....	13
1.2.4. Metallo-oxidases substrate specificity .....	17
1.2.5. Distribution and role of Multicopper oxidases .....	20
1.2.6. Biotechnological applications .....	25
<b>1.3. PROTEIN STABILITY .....</b>	<b>29</b>
1.3.1. Techniques to measure protein stability .....	30
1.3.2. Thermal stability .....	32
1.3.3. Protein folding .....	35
1.3.4. Molecular determinants of stability .....	41
1.3.5. Stability in metallo-proteins.....	44

---

<b>2 A Robust Metallo-Oxidase from the Hyperthermophilic Bacterium <i>Aquifex aeolicus</i> .....</b>	<b>49</b>
--	-----------

---

<b>2.1. INTRODUCTION .....</b>	<b>51</b>
<b>2.2. EXPERIMENTAL PROCEDURES .....</b>	<b>53</b>
<b>2.3. RESULTS AND DISCUSSION .....</b>	<b>59</b>

**3 The hyperthermophilic nature of the metallo-oxidase from *Aquifex aeolicus* .....73**

---

<b>3.1. INTRODUCTION.....</b>	<b>75</b>
<b>3.2. EXPERIMENTAL PROCEDURES.....</b>	<b>77</b>
<b>3.3. RESULTS .....</b>	<b>80</b>
<b>3.4. DISCUSSION.....</b>	<b>94</b>

**4 The Multicopper Oxidase from the Archaeon *Pyrobaculum aerophilum* shows Nitrous Oxide Reductase Activity .....101**

---

<b>4.1. INTRODUCTION.....</b>	<b>103</b>
<b>4.2. EXPERIMENTAL PROCEDURES.....</b>	<b>105</b>
<b>4.3. RESULTS .....</b>	<b>110</b>
<b>4.4. DISCUSSION.....</b>	<b>124</b>
<b>4.5. SUPPLEMENTARY MATERIAL .....</b>	<b>127</b>

**5 Stability studies in CotA-Laccase from *Bacillus subtilis* .....129**

---

<b>5.1. EFFECT OF THE REPLACEMENT OF THE AXIAL LIGAND IN THE REDOX PROPERTIES OF COTA.....</b>	<b>132</b>
5.1.1. Experimental Procedures .....	134
5.1.2. Thermodynamic stability of M502 mutants.....	136
5.1.3. Concluding remarks .....	142
<b>5.2. EFFECT OF COPPER CONTENT IN THE STABILITY OF COTA-LACCASE .....</b>	<b>143</b>
5.2.1. Experimental Procedures .....	144
5.2.2. Copper incorporation into CotA-laccase .....	145
5.2.3. Thermal stability of CotA variants .....	149
5.2.4. Concluding Remarks.....	153



<b>5.3. THE REMOVAL OF A DISULFIDE BRIDGE OF COTA CHANGES THE SLOWER MOTION DYNAMICS INVOLVED IN COPPER BINDING BUT HAS NO EFFECT ON THE THERMODYNAMIC STABILITY .....</b>	<b>155</b>
5.3.1. Abstract .....	155
5.3.2. Introduction.....	155
5.3.3. Experimental procedures .....	158
5.3.4. Results and Discussion .....	161
 <b>6 General Discussion.....</b>	 <b>175</b>
 <b>7 References .....</b>	 <b>193</b>
 <b>8 Annexes .....</b>	 <b>223</b>
 <b>8.1. MCOA SUBSTRATE SPECIFICITY: CHARACTERIZATION OF MUTANT ENZYMES .....</b>	 <b>225</b>
8.1.1. Experimental Procedures .....	225
8.1.2. Results .....	227
8.1.3. Discussion .....	235



# 1 GENERAL INTRODUCTION

---

<b>1.1.</b>	<b>WHITE BIOTECHNOLOGY .....</b>	<b>2</b>
1.1.1.	Enzymes in White Biotechnology .....	5
<b>1.2.</b>	<b>MULTICOPPER OXIDASES .....</b>	<b>6</b>
1.2.1.	Overall fold of multicopper oxidases.....	7
1.2.2.	Copper centers in multicopper oxidases .....	9
1.2.3.	reaction mechanism of Multicopper oxidases.....	13
1.2.4.	Metallo-oxidases substrate specificity .....	17
1.2.5.	Distribution and role of Multicopper oxidases.....	20
1.2.6.	Biotechnological applications .....	25
<b>1.3.</b>	<b>PROTEIN STABILITY .....</b>	<b>29</b>
1.3.1.	Techniques to measure protein stability .....	30
1.3.2.	Thermal stability .....	32
1.3.3.	Protein folding .....	35
1.3.4.	Molecular determinants of stability .....	41
1.3.5.	Stability in metallo-proteins .....	44

## **1.1. WHITE BIOTECHNOLOGY**

Biotechnology can be defined as the field of applied biology involving the use of living organisms in engineering, medicine, agriculture and in products of the day to day life. The use of the term includes genetic engineering as well as cell and tissue culture technologies. This concept encompasses a wide range of procedures for modifying nature according to human purposes, going back to domestication of the living organism. Biotechnology draws on the pure biological sciences (genetics, microbiology, animal cell culture, molecular biology, biochemistry, and cell biology) and in many instances is also dependent on the knowledge and methods, outside the sphere of biology, from chemical engineering, bioprocess engineering. Biotechnology is divided in different branches and in order to better identify the terms of the biotechnology application, a code of colours was created;

The Green biotechnology is applied to agricultural processes. An example is the designing of transgenic plants to grow under specific environments in the presence or absence of chemicals, or the engineering of a plant to express a pesticide, thereby ending the need of external application of pesticides.

Red biotechnology is applied to medical processes. The designing of organisms to produce antibiotics is an example, or the engineering of genetic cures through genetic manipulation, by developing DNA or RNA vaccines.

Blue biotechnology is a term that has been used to describe the marine and aquatic applications of biotechnology, but its use is relatively rare. It involves the use of marine organisms, and their derivatives, for purposes such as increasing seafood supply and safety or controlling the proliferation of noxious water-borne organisms.

Industrial biotechnology, also known as White biotechnology, is the application of biotechnology for the sustainable production of biochemicals, biomaterials and biofuels from renewable resources, using living cells and/or their enzymes.

The aim is to develop cleaner processes with minimum waste generation and energy use. White biotechnology is not an end of the pipe cleaning technology; it is a clean production process that minimizes waste before it is even produced. It has substantial potential to reduce environmental impact. For example, air and water pollution can be reduced, energy use lowered, fewer raw materials needed, and waste could be diminished or substituted by biodegradable materials. White biotechnology has become more broadly applicable due to recently developed genetic techniques. Multiple enzymes variants, for example, can now be created at high speed, which are then screened to better fit the desired applications. A wide range of useful products can be produced by industrial biotechnology. These fall within the categories of fine chemicals, pharmaceuticals, food additives and supplements, colorants, vitamins, pesticides, bio-plastics, solvents, bulk chemicals and biofuels (Figure 1.1.) (EuropaBio, 2003).

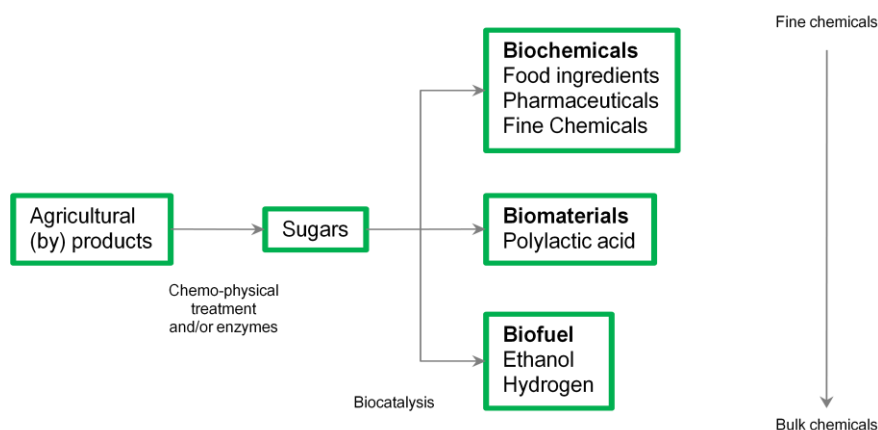


Figure 1.1: The Industrial Biotechnology Value Chain.

White biotechnology can maximize the economic value of current waste and by-products streams through new and potentially energy saving bio-processes, at the same time reducing carbon emissions. The wide production and use of bioproducts can therefore make a considerable impact on reduction of industry green house gases emissions. In parallel, the economy will benefit as

biotechnology enables the introduction of more efficient, less energy-intensive processes. Developments are also making their first inroads into larger volume segments such as polymers, bulk chemicals and biofuels, and many other industrial sectors. Although numbers may differ, all studies agree that industrial biotechnology will play an increasingly significant role in the chemical and other manufacturing industries in the future.

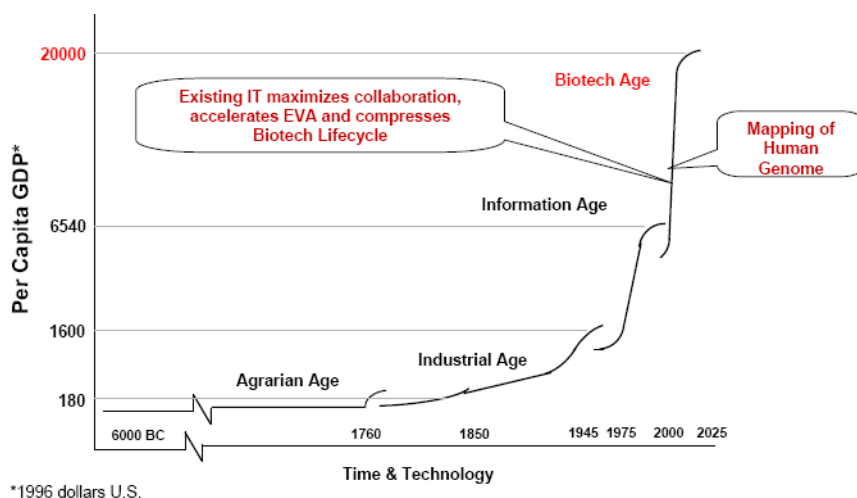


Figure 1.2: Evolution of gross domestic product according to the Humanity important marks.

The introduction of new key technologies has changed societies. The enormous impact of inventions like steam power, the internal combustion engine and mains electricity is well known. Information technology (IT) and biotechnology are the two most recent waves of innovation which are reshaping the way we live. Biotechnology is indeed in the vanguard of industrial development. It has an unique capacity to enable the economy to contribute to the key policy objectives of increasing competitiveness, employment and sustainable development. The bio-based economy is a term encompassing a future society no longer wholly dependent on fossil fuels for energy and industrial raw materials. Currently, most of our power comes from burning coal, oil or gas: once extracted and used, we have to find and exploit new resources. We don't know when they will begin to run out, but as demand increases, the prices

increase, therefore now is the time to focus attention on alternatives. It is crucial for industries to secure abundant, competitively priced and stable resources. And natural renewable resources constitute an interesting and reliable set of feedstocks.

### **1.1.1. ENZYMES IN WHITE BIOTECHNOLOGY**

Enzymes are molecules present in all living organisms. The function of these biocatalysts is to catalyze chemical reactions *in vivo* by lowering the activation energy of the chemical reactions. Enzymes can be considered the catalytic machinery of living systems. Industrial biotechnology aims to utilize this enzymatic capability in industrial processes. Nowadays, the industrial enzyme producers use them over a wide variety of applications. The estimated value of world market is presently about US\$ 2 billion. Detergents (37%), textiles (12%), starch (11%), baking (8%) and animal feed (6%) are the main industries, which use about 75% of industrially produced enzymes. A very important field in which enzymes have proved to be of great value over the last 15-20 years is the starch industry. In 1950s, fungal amylase was used in the manufacture of specific types of syrup, which could not be produced by the conventional acid hydrolysis. The real turning point was reached early in the 1960s when the enzyme glucoamylase that completely hydrolyze starch into glucose was used for the first time. Within a few years, almost all glucose production was reorganized and enzyme hydrolysis was used instead of acid hydrolysis due to the better benefits such as greater yield, higher degree of purity and easier crystallization (James and Lee, 1997).

Other representative large scale application of enzymes in industry is in detergents. Enzymes such as proteases and lipases are used in detergents. Some of these have been genetically engineered to be more stable in the hostile environment of washing machines with several different chemicals present, including anionic detergents, oxidizing agents and high pH. In the early 90's the

detergents composition was upgraded with cellulases. Cellulase is actually an enzyme complex capable of degrading crystalline cellulose to glucose. In textile, washing cellulases remove cellulose microfibrils, which are formed during washing of cotton based cloths. This can be seen as colour brightening and softening of the material. An important area of research is the investigation of enzymes that can tolerate, or even have higher activities, in hot and cold temperatures. The search for thermotolerant and cryotolerant enzymes has spanned the globe. These enzymes are especially desirable for improving laundry processes in hot water cycles and/or at low temperatures for washing colours and darks.

In contrast with hydrolases, such as lipases and proteases, some industrial processes would benefit with oxidation/reduction based enzymatic reactions. For these processes, the suitable enzymes are oxidoreductases. Most of these, usually need the addition of exogenous co-factors, electron donor/acceptors (NAD(P)H and FMNH<sub>2</sub>) which would make the process extremely expensive and not suitable for industrial application. Among the biological group of oxidoreductases, there is a ubiquitous and interesting group of enzymes that show great potential for biotechnological and environmental applications, laccases, which are a functional class among the multicopper oxidases. Laccases can oxidize a broad range of substrates, including phenolic and non-phenolic compounds. One of the main advantages of laccases is that they do not need the addition of cofactors, and use the readily available oxygen as oxidizing agent (Gianfreda, 1999).

## **1.2. MULTICOPPER OXIDASES**

The biological activation of molecular oxygen is a key reaction in biological systems. Enzymes involved in direct oxygen activation are oxygenases and oxidases. The first group transfers the oxygen atom(s) to a substrate, while the latter uses the oxygen as final electron acceptor by reducing it to water. Multicopper oxidases are an important class of oxidases reducing dioxygen in a



four-electron reduction to water with concomitant one-electron oxidation of the reducing substrate. These are a family that utilizes the unique redox properties of the copper ion in the catalytic centers (Giardina, et al., 2010; Nakamura and Go, 2005). MCO are characterized by having four copper ions that are classified into distinct copper centers (type 1, type 2 and type 3) (see below, section 1.2.2 for further details) (Stoj and Kosman, 2005). Two subfamilies of MCO can be distinguished based on their substrate specificity. Laccases are MCOs with higher specificity for different bulkier substrates and metallo-oxidases with higher catalytic efficiency towards low valence metal ions, such as  $\text{Cu}^+$ ,  $\text{Fe}^{2+}$  and  $\text{Mn}^{2+}$ . The natural occurring substrates of laccases is not known, however they are involved in different processes depending on the physiological organism. Currently, laccases are a subject of intense study towards its use in biotechnological processes mainly due to their wide range of reducing substrates. Prominent metallo-oxidases, such as human ceruloplasmin, yeast ferroxidase Fet3p and CueO from *Escherichia coli*, are known to be critically involved in metal homeostasis mechanisms. In aerobic metabolism, metals such as iron and copper, although essential for life, readily participate in reactions that result in the production of highly reactive oxygen species (Crichton and Pierre, 2001) which may be involved in cell damage.

### **1.2.1. OVERALL FOLD OF MULTICOPPER OXIDASES**

The MCO are enzymes that differ substantially in the amino acid sequence composition but have a similar three dimensional organization, composed of multiple cupredoxin domains. Three domain MCO include ascorbate oxidase, laccases, and metallo-oxidases such as CueO and Fet3p, whereas ceruloplasmin is a six domain protein. The cupredoxin fold is composed by an eight-stranded Greek key  $\beta$ -barrel. This fold is distinct from other Greek key  $\beta$ -barrels such as superoxide dismutase, the immunoglobulins, and fibronectin domains. The structural organization has changeable amounts of  $\alpha$ -helical that do not contribute to the core of the protein.

In evolutionary terms this protein family shows how a protein domain can be evolved towards a very specific function, in the case, copper binding. The evolution analysis makes possible to trace the stages through which proteins pass before acquiring a new structure and function. It is accepted that the domains of the multicopper oxidases were originated from a single-domain protein of the cupredoxin family (Ryden and Hunt, 1993). The first X-ray crystal structure of a cupredoxin domain was obtained from poplar plastocyanin (Colman, 1978). Various subsequent crystallographic studies on cupredoxins have been published (Figure 1.3). The increasing number of modifications in cupredoxin domains, like the creation of copper-binding sites and substrate binding pockets, led to the formation of multicopper oxidases. The key evolutionary intermediates are the two domain ancestral proteins (Lawton, et al., 2009; Murphy, et al., 1997; Ryden and Hunt, 1993). The two domain proteins are hypothesized to result from a single domain duplication event and to have architectures resembling the homotrimeric nitrite reductases. These nitrite reductases contain a T1 site in both domains and a T2 at the interface (Lawton, et al., 2009). According to Hunt and Ryden (1993) the three domain multicopper oxidases are formed by addition of one domain to a two domain protein. The structural similarity of the trinuclear (T2/T3 copper centers) interdomain copper-binding site in laccase, ascorbate oxidase and ceruloplasmin, suggests that it is not possible to postulate independent evolutionary routes for each one of these proteins. It was assumed that multicopper enzymes develop one from another; i.e., the ceruloplasmin loses three middle domains and forms a laccase-like protein or the duplication of the laccase-like domain results in the formation of the ceruloplasmin (Zhukhlistova, 2008).

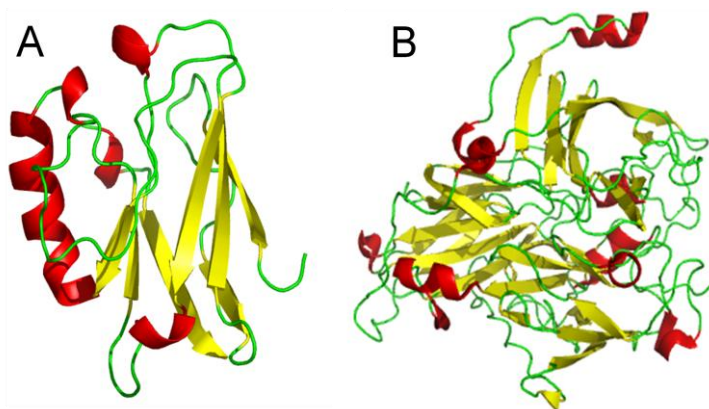
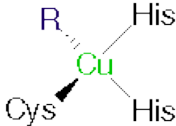
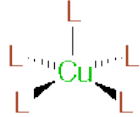
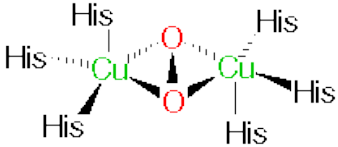


Figure 1.3: A) Cupredoxin fold from Azurin (PDB accession 1JOI). (B) Overall fold of CotA-laccase from *B. subtilis* (PDB accession code 1GSK) drawn with Pymol (DeLano, 2003).  $\beta$ -sheets are represented in yellow, and  $\alpha$ -helices represented in red.

### 1.2.2. COPPER CENTERS IN MULTICOPPER OXIDASES

The copper-containing centers of MCO were divided into three classes according to their spectroscopic features, reflecting the geometric and electronic structure of the active center (Table 1.1) (Lindley, 2001; Solomon, 1992). The mononuclear copper of MCO is composed by type 1 copper (T1) and involved in the substrate oxidation. The T2 copper together with the binuclear T3 coppers form the trinuclear cluster involved in the reduction of dioxygen to water using the electrons shuttled from T1.

Table 1.1: Classification of copper sites. Adapted from PROMISE database (Degtyarenko, et al., 1998).

Copper center	Protein class/family
<b>Type I (blue copper proteins)</b>	
 $\text{Cu}(\text{N}_{\text{His}})_2\text{S}_{\text{Cys}}\text{R}$ <p> <math>\text{R} = \text{S}_{\text{Met}}</math> (azurin, plastocyanin, laccase)  <math>\text{R} = \text{O}_{\text{Glu}}</math> (phytyocyanins)  <math>\text{R} = \text{H}_2\text{O}</math> (ceruloplasmin) </p>	<ul style="list-style-type: none"> <li>Small blue proteins <ul style="list-style-type: none"> <li>Auracyanin</li> <li>Azurin</li> <li>Phytyocyanin family</li> <li>Plastocyanin family</li> <li>Rusticyanin</li> </ul> </li> <li>Blue oxidases <ul style="list-style-type: none"> <li>Ascorbate oxidase</li> <li>Ceruloplasmin</li> <li>Laccase</li> </ul> </li> <li>Nitrite reductase</li> </ul>
<b>Type II</b>	
 $\text{Cu}(\text{N}_{\text{His}})_m\text{R}_n$ <p> <math>\text{L} = \text{N}, \text{O}</math> or S ligands; <math>\text{R} = \text{O}</math> or S ligands  <math>m = 1</math> to 4; <math>n = 0</math> to 3; <math>m+n = 4</math> or 5 </p>	<ul style="list-style-type: none"> <li>Cu, Zn superoxide dismutase</li> <li>Dioxygenases</li> <li>Monoxygenases <ul style="list-style-type: none"> <li>Dopamine Bhydroxylase</li> <li>Methane monooxygenase</li> <li>Peptidylglycine <math>\alpha</math>-hydroxylating monooxygenase</li> <li>Phenylalanine hydroxylase</li> </ul> </li> <li>Nitrite reductase</li> <li>Non-blue oxidases <ul style="list-style-type: none"> <li>Amine oxidase</li> <li>Diamine oxidase</li> <li>Galactose oxidase</li> <li>Lysyl oxidase</li> </ul> </li> </ul>
<b>Type III</b>	
 $\mu\text{O}_2[\text{Cu}(\text{N}_{\text{His}})_3]_2$	<ul style="list-style-type: none"> <li>Catechol oxidase</li> <li>Haemocyanins</li> <li>Tyrosinase</li> </ul>
<b>Trinuclear center (type II + type III)</b>	
	<ul style="list-style-type: none"> <li>Blue oxidases <ul style="list-style-type: none"> <li>Ascorbate oxidase</li> <li>Ceruloplasmin</li> <li>Laccase</li> </ul> </li> </ul>

### 1.2.2.1. Type 1 copper center

The T1 copper center, or “blue” center, is usually coordinated in a distorted tetrahedral manner, with strong ligands provided by thiolate sulphur of a Cys and the imidazole nitrogens of two histidines. This active site is completed by a variable axial ligand, that commonly is a methionine residue in most of MCO (see Table 1.1 and Figure 1.4A) (Dennison, 2005; Lindley, 2001; Solomon, et al., 1996). The T1 copper center is characterized by a very strong absorption band with a molar extinction coefficient in the range from 3000 to 6000  $\text{M}^{-1}\text{cm}^{-1}$  at a wavelength of  $\sim 600$  nm, associated to the typical intense blue colour. This absorption band is associated with the ligand-metal charge transfer from the sulphur atom of the cysteine to the copper atom  $\text{S}(\pi) \rightarrow \text{Cu}(\text{d}_x^2 - \text{y}^2)$ . Furthermore, the EPR spectrum of the T1 center exhibits very weak parallel hyperfine splitting lines due to the strong bond in the copper site (since the unpaired electron is considerably displaced toward the cysteine ligand, the strength of its interaction with the spin of the copper nucleus is reduced substantially (Solomon, et al., 1996; Zhukhlistova, 2008).

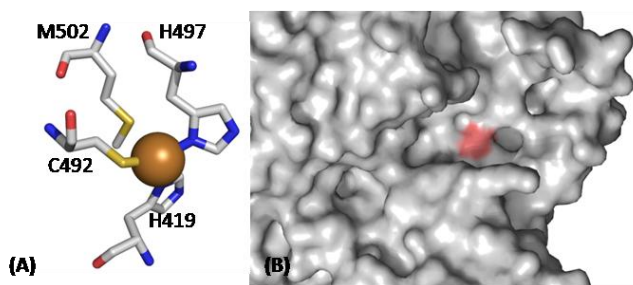


Figure 1.4: (A) CotA type 1 copper ligands. Two His and a Cys coordinate the T1 copper, and a Met is present as axial ligand. (B) Close-up of the active-site (T1 Cu center) region of CotA, using surface representation, highlighting (in magenta) the region of the most exposed histidine ligand of the copper, which is the residue that interacts with substrates.

This copper is near the protein surface to interact with the reducing substrate. In fact in CotA laccase, one of the His that coordinates T1 center is solvent exposed, and therefore it facilitates the electron transfer between the substrate

and the copper ion (see Figure 1.4B) (Enguita, et al., 2003). The His2Cys equatorial ligand set is always maintained in MCO, but the residue present in the axial position variable. In related proteins different axial ligands can be present, such as in the stellacyanins where a Gln coordinates (Hart, et al., 1996; Koch, et al., 2005). The putative plantacyanins that have either a Val or Leu in the axial position (Dennison, et al., 2003; Kim, et al., 2003; Nersissian, et al., 1998; Nersissian and Shipp, 2002). The azurins the backbone carbonyl oxygen of Gly residue provides a second weak axial interaction resulting in trigonal bipyramidal geometry. In fungal laccases there is a Phe or Leu at the position of Met, which no longer coordinates T1 copper (Dennison, 2005; Ducros, et al., 1998; Kim, et al., 2003). These sites, with non-coordinating side-chain in the axial position, have trigonal active site geometries (Crowley, et al., 2001; Impagliazzo and Ubbink, 2004; Ubbink, et al., 1998). These subtle structural changes have a dramatic effect on the redox potential of the T1 center in MCO. The presence of a Leu or Phe tends to short the distance between the Cys residue and the copper atom, stabilizing the reduced state of the center originating a high redox potential. On the other hand, the presence of a Met residue as fourth ligand increases the distance between Cys and the copper atom, stabilizing the oxidized state of the center, causing a reduction of the redox potential of the center (Durao, et al., 2006; Durao, et al., 2008). The presence/absence of this fourth ligand may contribute, at least, in part to the variations of the redox potential although other elements of the protein matrix are known to affect this parameter in MCO (Kosman, 2009).

#### **1.2.2.2. Trinuclear center**

The three coppers that compose the trinuclear center (two T3 and one T2 copper) are arranged in a triangular manner, as consistently observed in MCO, and are coordinated by eight His residues, in a pattern of four His-X-His motifs (Messerschmidt, 1997). Histidine residues coordinate the T3 copper ion pair, whereas T2 center is coordinated by the remaining two His residues (see Figure 1.5) (Giardina, et al., 2010).

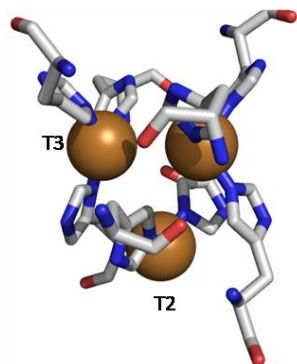


Figure 1.5: Typical trinuclear cluster containing the T2 site and the binuclear T3 site.

The T2, or “non-blue”, copper center is characterized by EPR signals similar to those observed for  $\text{Cu}^{2+}$  tetragonal complexes. The absorption spectra of these centers frequently have a low intensity. The T3 center is composed by two copper atoms bound to ligands and is called the binuclear site. The T3 coppers are paramagnetic which makes them “invisible” to EPR spectroscopy, but exhibit an absorption band at  $\sim 330$  nm. The trinuclear center acts in dioxygen binding and reducing it upon receiving four electrons forwarded from the mononuclear center T1. A more detailed description of the dioxygen reduction is done in the following section (section 1.2.3).

### 1.2.3. REACTION MECHANISM OF MULTICOPPER OXIDASES

One of the events involved in the reaction mechanism of MCO is the reduction of the T1 copper center by the electron transfer from the substrate. The rate of electron transfer depends on four factors: **1)** an interaction between donor and the acceptor with a probability and lifetime sufficient to allow the electron transfer to occur; **2)** the driving force for electron transfer; **3)** an overlap between the donor and acceptor orbital; and **4)** the change in the coordinates of the nuclei in the donor and acceptor as a result of their change in the redox state (Kosman, 2009). It is generally accepted that the rate limiting step in MCO is precisely the electron transfer between the reducing substrate and the T1 copper

which should occur via an outer sphere pathway. The exact mechanism of dioxygen reduction is still unknown; however several authors have been working on this issue, trying to understand the molecular basis the reduction of dioxygen to water. The different proposed mechanisms draw conclusions based on the results obtained by using different techniques such as X-ray crystal structures or spectroscopic data. We will present a more detailed description of the data obtained by Bento et al. (2005). The authors propose a reduction mechanism, by correlating the data obtained with different crystal structures of CotA-laccase. The differences in the crystal structures are in the trinuclear center where different oxygen species were modulated, a dioxygen, peroxide and a hydroxyl. The first event in this putative mechanism is the movement of molecular dioxygen to the trinuclear copper site where it binds to the type 3 copper atoms (Figure 1.6a).

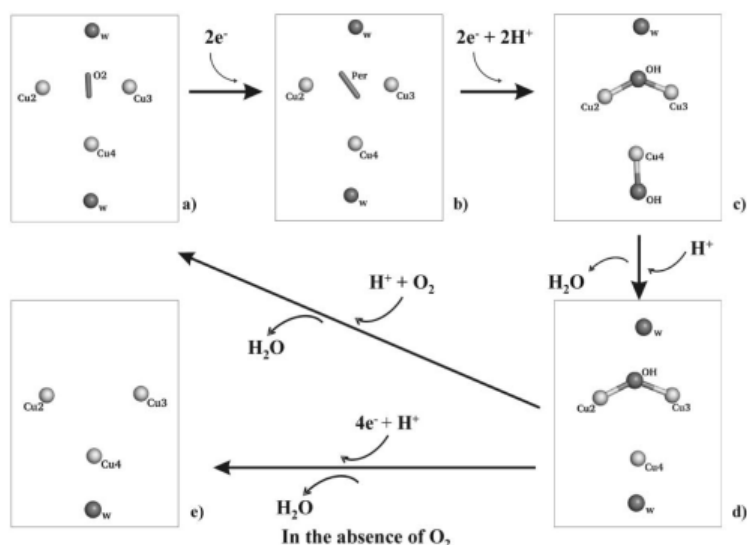


Figure 1.6: Putative mechanism of the reduction of dioxygen to water, proposed by Bento et al. 2005

The dioxygen access is provided by a well defined channel that normally is occupied with solvent molecules (Enguita, et al., 2004). Than both T3 copper ions can transfer one electron to one atom of oxygen of the dioxygen molecule forming peroxide intermediate, the diatomic O<sub>2</sub><sup>2-</sup> moiety that becomes inclined to the line between the T3 coppers. The possible pathway of electron transfer in



CotA involves substrate molecules reducing the T1 copper and then the transmission of these electrons through Cys492 and the adjacent histidines, His491 and His493 of T3 center (Figure 1.6b), which will dismember peroxide intermediate into two hydroxyl molecules (Figure 1.6c). One of these molecules will remain in a bridging position between both T3 coppers, and the other migrates to the opposite side of the T2 copper. The protons are most likely provided by the conserved acidic residues present in the access channel, like Glu498 (in the case of CotA laccase). The migration of one hydrogen peroxide to the T2 copper is difficult to explain only from the X-ray structures, once the amount of available space is limited and this phenomenon must involve a movement of the T2 copper and a local distortion of the protein geometry. However, the T2 is known to be more labile than the two T3 copper ions. It is possible that the T2 moves out the plane defined by the trinuclear cluster using the coordinating histidines as pivot points making it possible to bind a hydroxyl group and transfer it to the beginning position of the outlet solvent channel. Conformational changes in one residue coordinating the T2 copper ion were also reported for the laccase of *Coprinus cinereus* (Ducros, et al., 1998). After the separation of the two hydroxyl moieties between T2 and T3, the hydroxyl group in the T2 center is released as a water molecule after becoming protonated (Figure 1.6d). The remaining hydroxyl group that is bridging between the two T3 coppers then migrates to the far side of the T2 and after its protonation it will be released in the form of the second water molecule. When this turnover is complete the enzyme can then bind a second dioxygen molecule and re-enter the catalytic cycle, or in the absence of dioxygen the assimilation of four electrons (from the reducing substrate) will leave the coppers in the fully reduced state, ready to bind dioxygen as soon as it became available (Figure 1.6e). In the proposed mechanism of reduction of dioxygen to water, the T2 copper has two roles: 1) it helps to trap the dioxygen in the trinuclear cluster; 2) it temporarily binds the hydroxyl groups that arise from the reduction of the dioxygen immediately prior to their release in the form of water molecules. Therefore, T2 depleted enzymes should still be able to bind dioxygen molecule,

however its catalytic ability is compromised due to the inability to reduce dioxygen, as previously reported to the laccase of *Melanocarpus albomyces* (Hakulinen, et al., 2002).

A main issue that is still unsolved in the dioxygen reduction mechanism by MCO is to know the exact resting state of the enzymes. In CotA, this state seems to have a dioxygen moiety bound in the T3 center. However, contrarily to these results, the data obtained by Messerschmidt (1992) showed that the crystals of ascorbate oxidase have a hydroxyl group in the T3 binuclear center (Zaitseva, et al., 1996). Similar results were obtained in the structures of ceruloplasmin and for the laccases of *Trametes versicolor* (Piontek, et al., 2002), *Coprinus cinereus* (Ducros, et al., 1998), and for CueO from *E. coli* (Roberts, et al., 2002). Different authors, using different techniques, have also contributed to the elucidation of this reduction mechanism. A profit contribution has been made by Ed Solomon group, gaining insight into the reductive cleavage of the bond linking both oxygen atoms (Machonkin, et al., 2001; Palmer, et al., 2001; Solomon, et al., 2001). In many ways their proposals are similar to the mechanism described earlier. The data obtained for the peroxide adduct in CotA structure showed that an  $O_2^{2-}$  ion is bridging the T3 coppers in an inclined way. These results are similar to the ones obtained by Zoppellaro et al. (2001), where spectroscopic data sustains the possibility of a similar ion between these coppers. Moreover, the data provided by the spectroscopic measurements from Palmer and co-workers (2001) suggest that a hydroxyl group is always bridging the T3 coppers in every step of the catalytic cycle, with the only exception when the protein is in the fully reduced form. Apparently, a different number of factors may influence the “resting” state of the enzyme, factor such as, the method of purification, method of crystallization, pH, and redox potential of the copper ions and the availability of dioxygen. Taking into account the small differences reported the general guidelines of the reduction mechanism are the same.

#### 1.2.4. METALLO-OXIDASES SUBSTRATE SPECIFICITY

A small group of MCO, named metallo-oxidases, has a higher efficiency towards the oxidation of low valence metals ions such as,  $\text{Fe}^{2+}$ ,  $\text{Cu}^+$  and  $\text{Mn}^{2+}$ . Their physiologic role is far better understood and characterized than in laccases, even if it only represents a fraction of MCO family. The  $\text{Mn}^{2+}$  oxidation by these enzymes is still not well understood, when compared to the mechanism involved in the oxidation of  $\text{Cu}^+$  and  $\text{Fe}^{2+}$ . (Dick, et al., 2008; Francis and Tebo, 2002). For example, the CueO protein from *E. coli* plays a significant role in the homeostasis of  $\text{Cu}^+$  in this microorganism (Grass and Rensing, 2001; Hall, et al., 2008; Lee, et al., 2002). CueO is a cuprous, rather than ferrous oxidase and this specific activity is due to a unique motif in the protein. It has a Met-rich region that might block the access of bulky substrates and may provide a matrix for the electron transfer between the substrate and the T1 copper center. Binding of copper to this motif has been structurally characterized and structure-function studies have demonstrated that this is the “cuprous oxidase” motif, in metallo-oxidases related to bacterial copper resistance (Figure 1.7) (Kataoka, et al., 2007; Roberts, et al., 2002; Roberts, et al., 2003; Singh, et al., 2004).



Figure 1.7: View of the Met-rich segment in CueO from *E. coli*. Adapted from Roberts, et al., 2003.

An equivalent Met-rich sequence is found in several bacterial PcoA homologues indicating whatever are the function of this motif is highly conserved. Although the copper binding to this region has not been demonstrated spectrally, a ‘labile’ copper (rCu – Figure 1.7) is observed bound in CueO crystals soaked with  $\text{CuCl}_2$ . The binding of the copper atom is specific, involving ligation to two Met thioether S atoms and two Asp carboxylates. One of these carboxylates appears H-bonded to the (non-coordinating)  $\text{NH}\epsilon 2$  of H443 at the T1 copper in CueO. This H-bonding network provides an attractive electronic matrix coupling pathway for electron transfer into the T1. In fact, a very recent work suggests that this binding pocket is in fact where  $\text{Cu}^+$  binds to be oxidized to  $\text{Cu}^{2+}$  (Djoko, et al., 2010). Two of the four ligands to this labile copper atom come from the Met-rich motif, and the other two ligands come from a subsequent strand of  $\beta$ -sheet. Structure-function activity studies on CueO mutants confirm that the enzyme gets ‘activated’ most likely due to the binding of copper ions to this region. A model ferrous oxidase is the yeast Fet3p protein that contributes to the physiologic response to excess of  $\text{Fe}^{2+}$  in the cell (Shi, et al., 2003; Stoj and Kosman, 2003; Stoj, et al., 2007). In 2006 Stoj and co-workers presented some results that give a structural insight towards de  $\text{Fe}^{2+}$  specificity. The specificity of the ferric iron towards Fet3p is due to the presence of some acidic residues (Asp and Glu) in the protein surface (see Figure 1.8).

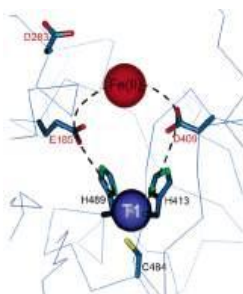


Figure 1.8: Proposed model of  $\text{Fe}^{2+}$  binding and electron-transfer to T1 Cu centre in Fet3p. The iron binding residues E185, D283, and D409 are shown relative to the T1 copper site. The dashed arrows indicate the electron-transfer pathways from the  $\text{Fe}^{2+}$  species to the T1 copper. The two carboxylate-imidazole H-bonds are essential components of these pathways. Illustration adapted from (Stoj, et al., 2006).

In fact, this binding site reduces the reduction potential of  $\text{Fe}^{2+}$  in comparison to the aqueous ferrous ion, providing a thermodynamically robust driving force for electron transfer. Furthermore, a Glu and an Asp of this binding site constitute parts of the electron transfer pathway from the bound  $\text{Fe}^{2+}$  to the protein T1 copper center. This electronic matrix coupling relies on H-bonds from the carboxylate of each residue to the NH group of the two His ligands of the T1 copper center. These acidic residues and its H-bond network appear to distinguish a ferroxidase from a laccase. Fet3p protein is also an essential component of the yeast high affinity iron uptake system that confers, on these opportunistic pathogens, a selective advantage in Fe-limited conditions; the AIDS related pathogen *Cryptococcus neoformans* illustrates this advantage in a particularly relevant fashion (Jung and Kronstad, 2008; Jung, et al., 2008; Jung, et al., 2006). This pathway involves the coupling of  $\text{Fe}^{2+}$  oxidation to  $\text{Fe}^{3+}$  by Fet3p with the uptake by a partner ferric iron permease (Kwok, et al., 2006; Kwok, et al., 2006; Singh, et al., 2006). The coupling of ferroxidation catalyzed by a specialized MCO to a subsequent  $\text{Fe}^{3+}$  trafficking event, e.g. uptake or efflux, transport, or storage, is a characteristic of the mechanism by which metazoan MCO ferroxidases contribute to their organism's iron metabolic pathways and is well illustrated by the mammalian protein ceruloplasmin (Cp).

Both these two type of MCO, cuprous and ferrous oxidase in humans and animal models, are linked to the molecular basis of disorders in iron and copper metabolism (Hellman and Gitlin, 2002; Jeong, et al., 2009; Madsen and Gitlin, 2007; Miyajima, 2002; Petrak and Vyoral, 2005). Free living organisms tend to be highly active to relatively precipitous changes in their environment. In bacteria this adaptation is often due to the acquisition of episomally encoded enzymatic activities. In *E. coli*, this, resistance is due in part to the *pco* metabolic pathway encoded on plasmid pRJ1004 (Brown, et al., 1995) while in *Pseudomonas syringae* the homologous *cop* system is encoded on plasmid pPT23D (Lee, et al., 2002). Among the enzymes found in this pathway is an MCO that in *E. coli* is known as the PcoA protein; a homologous CopA protein

is found in *P. syringae*. The *E. coli* bacterial chromosome also encodes an MCO linked to copper resistance, CueO (previously YacK), but similar MCO have been identified in different bacteria, *Campylobacter jejuni* (Hall, et al., 2008), *Pseudomonas aeruginosa* (Huston, et al., 2002), *Staphylococcus aureus* (Sitthisak, et al., 2005) *Rhodobacter capsulatus* (Wiethaus, et al., 2006) and *Legionella pneumophila* (Huston, et al., 2008). What is their physiological activity, however, has not been directly demonstrated. The hypothesis is that these proteins act as cuprous oxidases, reducing the steady-state level of the redox active,  $\text{Cu}^+$ , a known prooxidant.

### **1.2.5. DISTRIBUTION AND ROLE OF MULTICOPPER OXIDASES**

Multicopper oxidases are widely distributed in plants, fungi, bacteria and insects. Roles attributed to this enzyme include lignin synthesis by plants, pigmentation in bacteria, and morphogenesis in fungi (Baldrian, 2006; Hoegger, et al., 2006; Mayer and Staples, 2002; Nakamura and Go, 2005)

#### **1.2.5.1. Insect Laccases**

Several functions of insect laccases have been proposed. One of the first, suggested roles for an insect laccase was sclerotization of the egg case of a cockroach species, *Periplaneta americana* (Whitehead, et al., 1960). More recently, the insect laccases have been proposed to have a role in the exoskeleton formation. The exoskeleton or cuticle of insects has contributed greatly to their evolutionary success. It not only provides protection against the environment but also plays important roles in locomotion, respiration, and communication. The stabilization of the cuticle occurs in part when proteins in the procuticle become cross-linked by highly reactive quinones, a process known as sclerotization. The quinones are produced by the oxidation of catechols, mainly the derivatives of dopamine and dihydroxyphenylethanol (Sugumaran, et al., 1992). Oxidation may be carried out by two different types

of phenoloxidases present in the insect cuticle, tyrosinase and laccase. Laccases are able to oxidize both o- and p-diphenols. Yamazaki (1969) was the first author to establish its presence in the cuticle and to correlate its activity with the process of sclerotization. During the sclerotization process, diphenols such as N-acetyldopamine and N-b-alanyldopamine are oxidized by laccase and the quinones that are generated react with cuticular proteins to form cross-links between the proteins. Of the insect genomes that have been investigated, each contains at least two putative MCO genes, and some genomes contain more (Dittmer, et al., 2004). The genome of *Anopheles gambiae*, a species of mosquito, encodes five putative MCO genes (Dittmer, et al., 2004). At present, the function of just one type of insect MCO is known: cuticle tanning catalyzed by laccase 2 (Lac2) orthologs. The functions of laccase-1 type enzymes (Lac 1) and other insect MCO are still unknown. In *T. castaneum*, silencing of TcLac1 had no effect on cuticle tanning or viability. On the other hand, silencing TcLac2 had a profound impact in larvae (see Figure 1.9) (Arakane, et al., 2005).



Figure 1.9: The larval phenotype produced by injection of dsRNA for TcLac2. dsRNA for TcLac2 was injected into late larvae to observe the effect on larval cuticle tanning. (A) Last-instar, 1-d-old larvae, injected 3 d earlier with buffer or dsLac2. Adapted from (Arakane, et al., 2005).

The putative Lac1 ortholog in *Drosophila melanogaster* is expressed in Malpighian tubules (Wang, et al., 2004) and is slightly upregulated in unspecified tissues in response to immune challenge suggesting a possible immune function (De Gregorio, et al., 2001). Lac1 ortholog is expressed in the midgut and Malpighian tubules of feeding stage larvae but not in later, non-

feeding stage larvae or pupae. This expression pattern may indicate a role in detoxification of phenolic plant compounds or in metabolizing iron or copper in the larval diet (Dittmer, et al., 2004).

### **1.2.5.2. Plant Laccases**

Laccases are one of the oldest enzymes described and the first laccase was isolated from the lacquer tree *Rhus vernicifera* (Yoshida, 1883). The optional name of urushiol oxidase for this enzyme is related to the observation that the *R. vernicifera* laccase was responsible for the oxidation of urushiol, - a milky secretion of the lacquer tree, in the presence of oxygen by a process of polymerization and cross-linking producing lacquer, a hard and strong resin that has been used in traditional oriental artefacts. When the bark of the lacquer tree is wounded, it secretes a sap, a water-in-oil emulsion composed of urushiol [60–65% (w/w)], a catechol substituted with a long unsaturated aliphatic chain, carbohydrates (gums) [6.5–10% (w/w)], the enzyme laccase [0.1–1% (w/w)] and water [20–25% (w/w)] (Huttermann, et al., 2001). These ingredients have been used by East Asian artists and craftsman for the creation of lacquer works for more than 6,000 years. This mixture is excellently suited for plant defence against fungi, insects and phytophages. Urushiol is one of the most toxic compounds that have been discovered in the plant kingdom so far. In addition, the entire family of the *Anacardiaceae*, of which the lacquer tree is a member, appears to contain laccase in the resin ducts and in the secreted resin. Reports on the presence of laccase in other plant species are more limited. Cell cultures of *Acer pseudoplatanus* have been shown to produce and secrete laccase (Bligny and Douce, 1983; Tezuka, et al., 1993), and *Pinus taeda* tissue has been shown to contain eight laccases, all expressed predominantly in xylem tissue (Sato, et al., 2001). Other reports are those on the presence of a laccase in leaves of *Aesculus parviflora* and in green shoots of tea (Gregory and Bendall, 1966). Five distinct laccases have been shown to be present in the xylem tissue of *Populus americana* (Ranocha, et al., 1999). Other higher plant species also appear to contain laccases, although their characterization is less convincing



(Mayer and Staples, 2002). The laccase involvement in the plant lignification process is not a new idea, and it suffered, some turnaround along time. After the proposed role of laccases in lignification had been proposed and then discarded, in nowadays it is generally accepted that plant laccases may have a role in the early stages of lignification process in higher plants (Mayer and Staples, 2002)

### **1.2.5.3. Fungal Laccases**

As stated above the first laccase to be discovered was from plant origin, however a few years later it was also demonstrated in fungi (Bertrand, 1896). Laccase activity is present in many fungal species and it has already been purified from dozens of species (Baldrian, 2006). However, there are many taxonomic or physiological groups of fungi that do not produce significant amounts of laccase or where laccase is only produced by a few species. Laccases are particularly widespread in ligninolytic basidiomycetes (*Phanerochaete*, *Trametes*, *Pycnoporus*, *Nematoloma*, *Sporotrichum*, *Stropharia*, etc.), and more than 125 different basidiomycetous laccase genes have been described (Hoegger et al. 2006). It has become evident that laccases can play an important role in lignin degradation along with other extracellular enzymes such as lignin peroxidase and manganese peroxidase even though one of the strongest lignin degrading species, *Phanerochaete chrysosporium*, does not produce a typical laccase (Larrondo, et al., 2003; Lundell, et al., 2010). The precise function of the enzyme in this process, however, is still poorly understood. Besides delignification, fungal laccases have been associated with various organism interactions (intra and interspecific) and developmental processes such as fruiting body formation (Kues, 2000), pigment formation during asexual development (Clutterbuck, 1972; Tsai, et al., 1999), pathogenesis (Nosanchuk and Casadevall, 2003), competitor interactions (Iakovlev and Stenlid, 2000). Laccases of saprophytic and mycorrhizal fungi have also been implicated in soil organic matter cycling, e.g. degradation of soil litter polymers or formation of humic compounds (Burke and Cairney, 2002).

#### 1.2.5.4. Bacterial Multicopper Oxidases

Protein sequences that present similarity to laccases and despite the knowledge about the widespread occurrence of prokaryotic laccases, until now, the complete purification and characterization of bacterial multicopper oxidases is much reduced when compared to the ones from fungal origin. The majority of MCO in *Bacteria* are in fact metallo-oxidases which are thought to be involved in the homeostasis and detoxification of toxic metals. The first report of prokaryotic laccase is from the rhizospheric bacterium *Azospirillum lipoferum* (Givaudan, et al., 1993), where laccase occurs as a multimeric enzyme composed of a catalytic subunit and one or two large chains. The enzyme plays a role in cell pigmentation and utilization of plant phenolic compounds (Faure, et al., 1994). Another laccase has been reported from a melanogenic marine bacterium *Marinomonas mediterranea* producing two different polyphenol oxidases, able to oxidize substrates characteristic of both tyrosinase and laccase (Solano, et al., 1997). Laccase-like activity has also been found in other bacteria, e.g., CopA protein from *Pseudomonas syringae* (Mellano and Cooksey, 1988) and PcoA protein from *Escherichia coli* (Brown, et al., 1995). EpoA from *Streptomyces griseus* has been characterized biochemically as a laccase or related enzyme (Endo, et al., 2003) and has been expressed as recombinant rEpoA in *E. coli*. It occurs as a homotrimer of 114 kDa and has relatively narrow substrate specificity, as it does not oxidize a number of substrates including guaiacol and syringaldazine, which are known model laccase substrates. The enzyme appears to have a role in morphogenesis in *Streptomyces* spp (Endo, et al., 2003). The best studied bacterial laccase is the CotA, part of the endospore coat component of *Bacillus subtilis*. The *cotA* gene codes for a 65 kDa protein belonging to the outer spore coat. CotA participates in the biosynthesis of the brown spore pigment, which is also thought to be a melanin like product (Martins, et al., 2002) and seems to be responsible for most of the protection afforded by the spore coat against UV light and hydrogen peroxide. The protein exhibits a high thermal stability, and optimum

temperature of 75°C (Martins, et al., 2002). A laccase-like spore protein of a marine *Bacillus* strain SG1 has been shown to oxidize  $Mn^{2+}$ . Mutants in genes coding for multicopper oxidases have lost their metal-oxidizing activities. On polyacrylamide gels, laccase activity was present as complexes of enzymes from this bacterium (van Waasbergen, et al., 1996). Laccase-homologous sequences identified in thermophiles are very rare. Some of the recent reports include: laccase from *Streptomyces lavendulae* REN-7 (Suzuki, et al., 2003); a laccase like protein from the hyperthermophilic archaeon, *Pyrobaculum aerophilum* IM2 (Fitz-Gibbon, et al., 2002); a laccase like protein from the hyperthermophilic bacterium *Aquifex aeolicus* VF5 (Deckert, et al., 1998) and laccase from *Thermus thermophilus* HB27 (Miyazaki, 2005).

### **1.2.6. BIOTECHNOLOGICAL APPLICATIONS**

Laccases present an important potential for industrial applications, in sectors such as food technology, delignification of lignocellulosics, biosensor and analytical applications. Is not, therefore, surprising that his enzyme has been studied intensively and remains a topic of intense research today.

#### **1.2.6.1. Food Industry**

Wine stabilization is one of the main applications of laccase in food industry. The polyphenolic substances originated during wine production can be oxidized by laccases. This process is important to remove excess phenolic compounds that might be present in the wine. The excess of these phenolic compounds can react with other components present in the grape must causing changes in the sensorial aspects of the wine, in a process called madeirization (Minussi, et al., 2002). Laccases are also suitable for fruit juice stabilization procedures. Stutz (1993) proved that it is possible to produce clear and stable juices/concentrates with light colour by means of ultrafiltration and laccase addition without any large additional investment. Treatment with laccase at a compatible pH followed by “active” filtration or ultrafiltration improved colour and flavour

stability as compared to conventional treatments by addition of ascorbic acid and sulphites. Laccases are currently of interest in baking due to its ability to cross-link biopolymers. Thus, Flander et al. (2008) showed that a laccase from the white-rot fungus *Trametes hirsuta* has tightened wheat dough, indicating that the laccase treatment was beneficial to oat and oat-wheat bread. The laccase from *Trametes* spp. have been applied in the treatment of distillery waste waters and olive oil wastewaters, with some promising results concerning the phenolic compounds content of these waters (Madhavi and Lele, 2009).

#### **1.2.6.2. Delignification**

The industrial preparation of paper requires separation and degradation of lignin in wood pulp. Environmental concerns urge to replace conventional and polluting chlorine based delignification/bleaching procedures. The use of ligninolytic fungi or enzymes for the treatment of lignocellulosic raw material such as wood chips in pulping is referred to as biopulping (Burton, 2001). Biopulping is applicable to both mechanical and chemical procedures; its advantages include reduced refining energy or increased mill throughput in mechanical pulping, and enhanced paper strength properties, alleviated pitch problems, improved yield, and reduced environmental impact in papermaking. The improved strength properties of biomechanical pulp paper also allow the proportion of the more expensive reinforcement kraft pulp to be reduced in paper grades made from blends of mechanical and chemical pulps (Widsten and Kandelbauer, 2008). Although extensive studies have been performed to develop alternative bio-bleaching systems, few enzymatic treatments exhibit the delignification/brightening capabilities of modern chemical bleaching technologies. One of the few exceptions to this generalization is the development of laccase mediated systems (LMS) delignification technologies for kraft pulps. In fact, laccase is more readily available and easier to manipulate than lignin peroxidase (LiP) and manganese-dependent peroxidase (MnP) and LMS has already found practical applications such as the

Lignozym®-process (Bourbonnais, et al., 1998; Bourbonnais, et al., 1997; Carter, et al., 1997).

### **1.2.6.3. Decolorization of Dyes**

Annually the production of dyes and pigments can reach 800 000 tons, where at least 10% of the used dyestuff enters the environment through wastes (Palmieri, et al., 2005). Most of the dye molecules are very stable to light, temperature, and microbial attack, making them recalcitrant. These industrial effluents are toxic and are characterized by high chemical and biological oxygen demands, suspended solids and intense colour. White rot fungi are the most efficient ligninolytic organisms capable of degrading various types such as azo, heterocyclic, reactive, and polymeric dyes (Novotny, et al., 2000). The decolorization of dyes by white rot fungi was first reported by Glenn and Gold (1983), who developed a method to measure the lignolytic activity of *P. chrysosporium* based upon the decolorization of sulphonated polymeric dyes. The laccase enzymatic processes are considered environmental friendly since the degradation mechanisms proceeds through the release of molecular nitrogen which prohibits aromatic amines formation in contrast to anaerobic treatment that involves the activity of azoreductases, another class of dye degrading enzymes (Chivukula and Renganathan, 1995). Although there are several reports in the literature that shows the application of a few fungal laccases in the biotransformation of dyes, the first report of the use of a bacterial laccase towards the biotransformation of dyes is from our group. Pereira and co-workers (2009) had used CotA-laccase from *B. subtilis* to transform the azo dye Sudan Orange G. It was found that this enzyme does not require the addition of redox mediators for the decolorization of a wide range of structurally different dyes and presents optimal activity in the alkaline pH range, distinctive features when compared with fungal laccases. The enzymatic biotransformation of the azo dye Sudan Orange G (SOG) was addressed in more detail following a multidisciplinary approach. Biotransformation proceeds in a broad span of temperatures (30-80 °C) and more than 98% of Sudan Orange G is decolourised

within 7 h by using  $1\text{ U mL}^{-1}$  of CotA-laccase at  $37\text{ }^{\circ}\text{C}$ . Seven biotransformation products were identified using high-performance liquid chromatography and mass spectrometry and a mechanistic pathway for the azo dye conversion by CotA-laccase was proposed. The enzymatic oxidation of the Sudan Orange G resulted in the production of oligomers and, possibly polymers, through radical coupling reactions. A bioassay based on inhibitory effects over the growth of *Saccharomyces cerevisiae* showed that the enzymatic bioremediation process reduced 3-fold the toxicity of Sudan Orange G (Pereira, et al., 2009). CotA-laccase was also used to transform the commercial available anthraquinonic dye Acid Blue 62, and different spectroscopic and mass spec techniques were used to identify the intermediary and final products of the biotransformation. The main final product that was identified is the same to an intermediary product obtained when using crude fungal preparations. Some reaction products were found to be similar to the ones generated by other laccase, LAC3 from *Trametes* sp. C30, and is proposed that the intermediates formed undergo through coupling reactions. It was also shown that CotA-laccase was successful in reducing the toxicity of solutions containing Acid Blue 62 dye (Pereira, 2009).

#### **1.2.6.4. Biosensors**

During the past two decades, bioelectrochemistry has received increased attention. Progress on bioelectrochemistry has been integrated into analytical applications, e.g. in biosensors working as detectors in clinical and environmental analysis (Haghighi, et al., 2003). Due to the relatively broad substrate specificity, laccases hold great promises for many potential applications ranging from the development of oxygen cathodes in biofuel cells (Barton, et al., 2004) and biosensors. Moreover, biosensors for detection of morphine and codeine, catecholamines (Leite, et al., 2003), plant flavenoids and also for electroimmunoassay have been developed. Nanotechnology contributes to the development of smaller and more efficient biosensors through controlled deposition and specific adsorption of biomolecules on different types of surfaces, achieving micro and nanometer order. Immobilization has an

important influence on the biosensor sensitivity (Freire, et al., 2001). Micropatterning is an efficient method for the immobilization of laccases on a solid surface in order to develop a multi-functional biosensor (Martele, et al., 2003). Also, Roy et al. (2005) found that cross-linked enzyme crystals (CLEC) of laccase from *Trametes versicolor* could be used in biosensor applications with great advantage over the soluble enzyme. More recently, Cabrita et al. (2005) have immobilized laccase from *Coriolus versicolor* on N-Hydroxysuccinimide-terminated self-assembled monolayers on gold. This procedure could be useful for the further development of biosensors. In addition, an enzyme electrode based on the co-immobilization of an osmium redox polymer and a laccase from *T. versicolor* on glassy carbon electrodes has been applied to ultrasensitive amperometric detection of the catecholamine neurotransmitters dopamine, epinephrine and norepinephrine, attaining nanomolar detection limits (Ferry and Leech, 2005).

### **1.3. PROTEIN STABILITY**

Industrial enzymes need to stand harsh process conditions, namely, extreme pH values, high temperature, high pressure or salt concentrations, amongst others, while maintaining its catalytic properties. One of the general prerequisites for an enzyme to be applicable in industrial processes is a higher thermotolerance or thermostability. The folded conformations of proteins are only marginally stable under the best of conditions and can often be disrupted by an environmental change, such as rise in temperature, variation of pH, increase in pressure, or the addition of a variety of denaturants. Therefore, understanding the thermodynamic stability and molecular determinants of laccases is of utmost importance (Hilden, et al., 2009; Schmid, et al., 2001). The denaturation of a protein does not need to involve changes in covalent structure and is usually reversible, when it is clearly due to unfolding (Creighton, 1993). At equilibrium, unfolding transitions of single-domain proteins are usually two-state:



with only the native (N) and unfolded (U) states populated. The stability of a globular protein is quantified by the difference in Gibbs energy,  $\Delta G_u$ , between U and N. The properties of the U state, in terms of residual structure, extent of hydration, etc., remains a source of significant speculation and inquiry (Robertson and Murphy, 1997).

### 1.3.1. TECHNIQUES TO MEASURE PROTEIN STABILITY

The conformational stability of a protein can be studied by evaluating its unfolding by using different techniques. Spectroscopic methods, such as UV-Visible absorption, NMR, Raman, Fluorescence, CD, among others, are tools that easily characterize the unfolding of a protein. In order to use these spectroscopic measurements to evaluate the unfolding we need to use a spectroscopic property as probe to observe denaturation, such as Tarp fluorescence, metal centers absorption, secondary structure content, etc. To make these studies we need to control protein unfolding, for example by using different unfolding agents such as guanidine hydrochloride (GdnHCl), urea, temperature, pH, and others. From this analysis we can calculate important thermodynamic parameters of the protein; 1)  $\Delta G$  that is the free energy gap that separates the native from the unfolded state. Basically, this is the value of energy needed to unfold a protein. 2)  $m$  that is the cooperativity of the transition. This value evaluates the unfolding transition, if it is a cooperative process. 3)  $M$  that is the mid-point. This value represent the concentration where 50% of the proteins molecules are unfolded and depends on the nature of the denaturant agent that we are using, it can be i.e. a concentration of a chemical denaturant.

The equilibrium constant between the native and denatured states is defined as;

$$K = \frac{[U]}{[N]} \quad (1)$$



And is related to  $\Delta G_u$  as,

$$\Delta G_u = -RT \ln K \quad (2)$$

where  $R$  is the universal gas constant and  $T$  is the absolute temperature. Note that eqs 1 and 2 apply to the equilibrium between the native and unfolded states of a protein regardless of the possible presence of intermediate states. It has been found that  $\Delta G$  varies linearly with denaturant concentration (Greene and Pace, 1974) and consequently the conformational stability in the absence of denaturant ( $\Delta G^{H_2O}$ ) can be determined by linear extrapolation (Pace, 1986; Pace, et al., 1998).

$$\Delta G_u = \Delta G^{H_2O}_u - m_u [D] \quad (3)$$

where  $m_u$  is the dependence of  $\Delta G$  on denaturant concentration. The equations (2) and (3) equation (4) can be written,

$$\Delta G^{H_2O}_u = m_u [D]_{1/2} \quad (4)$$

where  $[D]_{1/2}$  is the denaturant concentration at the half point of denaturation.

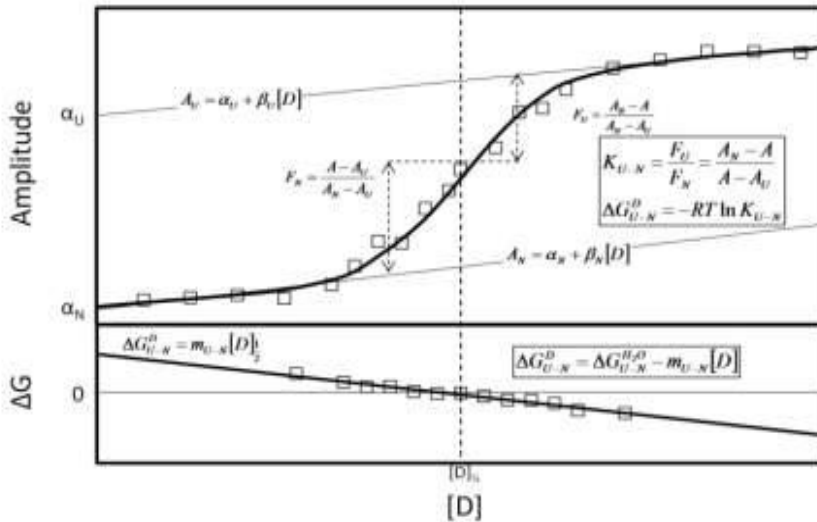


Figure 1.10: Upper panel, shows a typical denaturation curve where the transition can be monitored by an adequate spectroscopic measurement, as a function of denaturant concentration  $[D]$ . The pre and post unfolding baselines are shown in thin lines and the half-point of denaturation (where  $\Delta G=0$ ) is marked by vertical dashed line. The lower panel corresponds to the  $\Delta G$  value plotted as function of the denaturant concentration.

Figure 1.10, shows the typical unfolding profile for a monomeric protein. This type of transition is the typical one obtained for a two-state process. Partially-folded conformations, with thermodynamic properties distinctly different from either U or N, are energetically unstable relative to either U or N under all conditions. Multi-domain proteins can unfold step-wise, with the domains unfolding individually, either independently or with varying degrees of interactions between them (Brandts, et al., 1989; Griko Yu, et al., 1989). Multi-subunit proteins usually dissociate first, then the subunits unfold, unless domains are on the periphery of the aggregate where they can unfold independently (Jaenicke, 1987).

### **1.3.2. THERMAL STABILITY**

The protein stability can also be studied in terms of thermal stability, where the denaturing agent will be the temperature. As temperature increases, entropy of unfolding becomes higher and overcomes enthalpic forces ( $\Delta H$ ), that maintain the folded conformation. Since proteins are only marginally stable, even a small temperature increase can destabilize them. This is the reason why point mutations can often yield "temperature sensitive" proteins that denature with just a small increase in temperature. Proteins in thermophilic organisms are often seen to include more H-bonds and salt bridges (larger  $\Delta H$ ), as well as greater hydrophobic interactions (Robertson and Murphy, 1997). Two approaches are often used to evaluate the thermal stability of a protein, differential scanning calorimetry (where we can calculate thermodynamic parameters) and kinetic stability or long term stability, where we can simply determine the time that a protein maintains its catalytic activity when incubated at certain temperature.

### 1.3.2.1. Differential Scanning calorimetry

Differential scanning calorimetry (DSC) is a powerful technique for obtaining data on the thermodynamics of unfolding of globular proteins. DSC measures the excess heat capacity,  $C_p$ , of a protein in solution relative to buffer as a function of temperature. The  $C_p$  function can be analyzed to provide the thermodynamic data. The maximum in  $C_p$  occurs at the  $T_m$  of the protein. The area under the  $C_p$  curve gives the  $\Delta H_m$  of the transition, and the shift in the baseline yields  $\Delta C_p$  (see Figure 1.11) (Robertson and Murphy, 1997).

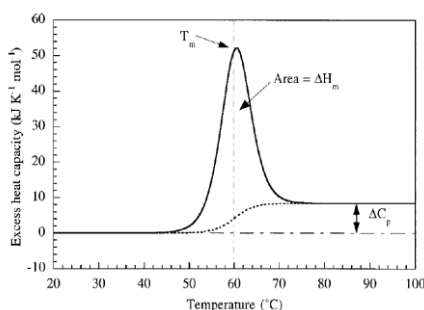


Figure 1.11: Simulated differential scanning calorimetry experiment for the two-state unfolding of a globular protein. Figure adapted from (Robertson and Murphy, 1997).

Thus, in principle, DSC can provide all of the thermodynamics of protein unfolding. In practice, it is difficult to obtain good data on the  $\Delta C_p$  from the baseline shift. Instead, several DSC experiments are performed in which the  $T_m$  of the protein is perturbed, usually by changing the pH. The difference in Gibbs energy is dependent on temperature according to,

$$\Delta G_u(T) = \Delta H_u(T) - T\Delta S_u(T) \quad (5)$$

where  $\Delta H_u$  and  $\Delta S_u$  are the differences in enthalpy and entropy at the same temperature at which  $\Delta G_u$  is being evaluated. The temperature dependence of  $\Delta H_u$  and  $\Delta S_u$  is defined by the heat capacity change,  $\Delta C_p$ , between the native and denatured states. The change in heat capacity reflects the amount of heat required to raise the temperature of a protein solution. This increase in heat capacity upon unfolding results primarily from restructuring the solvent (Robertson and Murphy, 1997). While  $\Delta C_p$  is itself slightly temperature

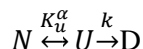
dependent, the assumption of a constant  $\Delta C_p$  does not lead to significant errors in any other parameter. The  $\Delta G_u$  can thus be described as,

$$\Delta G_u(T) = \Delta H_m \left( 1 - \frac{T}{T_m} \right) + \Delta C_p \left[ (T - T_m) - T \ln \left( \frac{T}{T_m} \right) \right] \quad (6)$$

where  $\Delta H_m$  is the value of  $\Delta H_u$  at  $T_m$ . Equation 6 is generally referred to as the modified Gibbs-Helmholtz equation (Fersht, 1998). The  $T_m$  (melting temperature) value is also a very important parameter, since it is the temperature where 50% of the protein population is unfolded.

### 1.3.2.2. Long term stability

The long term stability evaluates protein denaturation under controlled conditions. One of the typical assays is to incubate the protein at a point temperature and evaluate its irreversible denaturation. Irreversible protein denaturation is thought to involve at least two steps: (a) reversible unfolding of the native protein (N); (b) irreversible alteration of the unfolded protein (U) to yield a final state (D) that is unable to fold back to the native one. The long term stability of a protein quantifies the amount of enzyme that loses activity irreversibly during incubation at a certain temperature. Essentially, it quantifies the amount of enzyme that denatures irreversibly owing to events such as protein aggregation, misfolding and covalent changes such as the deamidation of asparagines and the oxidation of cysteines and methionines (Volkin and Klibanov, 1989). The two-step nature of irreversible denaturation is depicted in the following simplified scheme:



which is usually known as the Lumry and Eyring model (Lumry and Eyring, 1954). In this model the first stage involving the unfolding of N is characterized by  $K_u^\alpha$ , the equilibrium constant, and  $k$  is the rate constant. According to this model, the protein denaturation is considered to be a conjugated sequence of

equilibrium unfolding of the protein and of irreversible kinetically controlled conversion of the unfolded protein into a state incapable of renaturation. An important feature of the model is the assumption that the irreversible denaturation is a first order reaction (Sanchez-Ruiz, 1992). One important parameter that is calculated in these assays is the half-life time. This is inversely proportional to  $k$  and it will be representative of the time that a sample loses half of the activity at certain temperature of incubation.

### 1.3.3. PROTEIN FOLDING

Protein folding is the physical process by which a polypeptide folds into its characteristic and functional three-dimensional structure from random coil (Creighton, 1993). Each protein exists as an unfolded polypeptide or random coil when translated from a sequence of mRNA to a linear chain of amino acids. This polypeptide lacks any developed three-dimensional structure (see Figure 1.12 for an illustration). Amino acids interact with each other to produce a well-defined three dimensional structure, the folded protein, known as the native state. The resulting three-dimensional structure is determined by the amino acid sequence (Anfinsen, 1972).

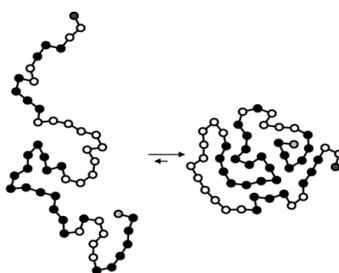


Figure 1.12: Protein folding. Example of a random coil polypeptide acquiring the final structure.

#### 1.3.3.1. Classical view

One of the greatest unsolved problems of science is the prediction of the three dimensional structure of a protein from its aminoacid sequence, the folding

problem. A denatured protein makes many interactions with solvent molecules. As the protein folds up, it exchanges those noncovalent interactions with others that it makes within itself: its hydrophobic side chains tend to pack with one another, and many of its hydrogen bond donors and acceptors pair with each other, especially those in the polypeptide backbone that form the hydrogen-bonded networks in helices and sheets (Fersht, 1998). The classical view of protein folding has emerged from the study of folding events at the macroscopic level, based on time resolved experiments, folding and unfolding kinetic data, which is explained by the simplest model giving the best fit of the observations (see Figure 1.13).

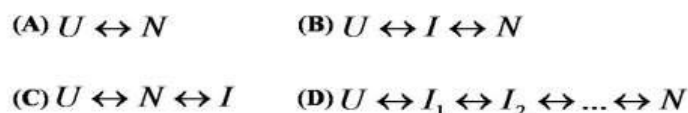


Figure 1.13: Folding models in the “classical view”. (A) Two state model; (B) On pathway intermediate model; (C) Off pathway intermediate; (D) Sequential model.

The early events in protein folding are important to understand it. The “classical studies” in protein folding propose a number of mechanisms (Fersht, 1997). In hierarchical models of protein folding, short range forces, for example backbone hydrogen bonding and torsion angle preferences, are dominant in the earlier stages of protein folding (see (Khan and Khan, 2002) for review).

- a) **Nucleation model** – presumes that the protein folding involves the formation of a cluster containing native residues that act as nucleus from which the native structure will propagate (Djikaev and Ruckenstein, 2007)
- b) **Nucleation condensation model** – postulates that localized sequence elements, serving as folding nucleus, can be responsible for protein secondary structure, whereas non localized sequence features, like hydrophobic and polar patterning could be responsible for protein

tertiary structure, based on hydrophobic collapse or condensation principle (Mohanraja, et al., 2003).

- c) **Framework model** – according to this model, protein folding is hierarchical, which during folding, the secondary structural elements are formed initially, which then constitute the framework for further formation of tertiary structure (Ptitsyn, 1995).
- d) **Hydrophobic collapse model** – in this model, globular proteins contain a hydrophobic core of nonpolar side chains, leaving the most of the polar and/or charged residues solvent exposed. The stabilization conferred by the sequestration of the hydrophobic side chains is thought to stabilize folding intermediates. This collapsed intermediate (molten globule) corresponds to a partially folded state (Khan and Khan, 2002).

#### 1.3.3.2. Levinthal Paradox

In 1969, Cyrus Levinthal noted that, because of the huge number of freedom degrees in an unfolded polypeptide chain, the molecule has an astronomical number of possible conformations (Levinthal, 1968). A polypeptide with 100 residues long will have 99 peptide bonds and so 198 different phi ( $\Phi$ ) and psi ( $\Psi$ ) bond angles. If each of these bond angles can be in one of three stable conformations the protein can fold in  $3^{198}$  different combinations. If a protein to fold correctly would sampling sequentially all the possible conformations, it would require a time longer than the age of the universe to arrive at its correct native conformation. This is true even if all these possible conformations are sampled at rapid (nanosecond or picosecond) rates. The "paradox" however is that most small proteins fold spontaneously on a millisecond or even microsecond time scale. This paradox is usually noted in the context of computational approaches to protein structure prediction (Zwanzig, et al., 1992). Levinthal himself knew that a polypeptide folds almost instantaneously, and that a random conformational search was therefore impossible. According to Levinthal, the protein structure could have a higher thermodynamic energy, this if the lower energy conformation was not kinetically accessible. An analogy

is a rock tumbling down a hillside that lodges in a gully rather than reaching the base (Hunter, 2006). Levinthal noted that protein folding is speeded and guided by the rapid formation of local interactions which then determine the further folding of the peptide (Durup, 1998; Sali, et al., 1994); this suggests local amino acid sequences which form stable interactions and serve as nucleation points in the folding process (Rooman, et al., 2002). More recent work on protein folding suggest that the folding is directed within funnel-like energy landscapes (Dill and Chan, 1997) that reduce the potential hyperspace (Durup, 1998; Sali, et al., 1994).

### **1.3.3.3. Folding funnel**

According, to Levinthal view, proteins would fold too slowly by undirected random searching of conformations. He concluded that protein folding must follow a pathway, which is a well defined sequence of events which follow one another so as to carry the protein from the unfolded random coil to a uniquely folded stable state (Levinthal, 1968). Anfinsen's dogma states that, at least for small globular proteins, the native structure is determined only by the protein's aminoacid sequence. This amounts to say that, at the environmental conditions (temperature, solvent concentration and composition, etc.) at which folding occurs; the native structure is a unique, stable and kinetically accessible minimum of the free energy (Anfinsen, 1973; Anfinsen, et al., 1961). These two lines of argument have led to the Levinthal paradox. How could folding be pathway dependent and pathway independent at the same time? However, according to the energy landscape perspective, there is no paradox because this "new" view recognizes that folding pathways are not the correct solution to the kinetic problem Levinthal posed. The landscape perspective readily explains the process of reaching a global minimum in free energy (satisfying Anfinsen's experiments) and doing so quickly (satisfying Levinthal's concerns) by multiple folding routes on funnel-like energy landscapes (Leopold, et al., 1992) (Figure 1.14).



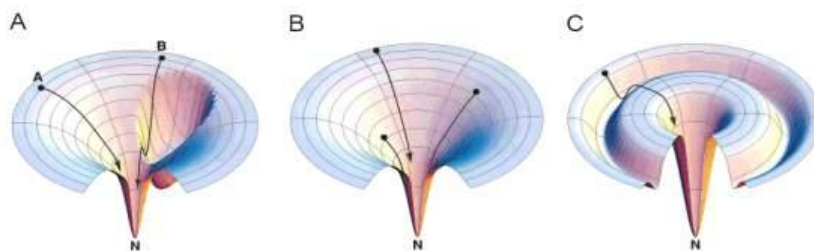


Figure 1.14: General shapes of landscapes: (A) The landscape is shown pictorially as having a kinetic trap, (a) is a throughway folding trajectory, whereas path (b) passes through a kinetic trap; (B) The landscape is smooth, unfolding paths are simply the reverses of the folding paths. (C) A landscape on which all folding molecules must pass through an obligatory folding intermediate, represented by the “moat” in the figure. Figure adapted from (Chan and Dill, 1998).

If we make an analogy to blindfolded golfer, stood at the edge of a very large driving range, and were told to hit the golf ball in a random direction, then the chances of sinking the ball in a single hole are infinitesimally small. However, if the driving range was sloped down from all directions to the hole, than the gravity would funnel the ball to the hole (Fersht, 1998). The folding funnel hypothesis is a specific version of the energy landscape theory of protein folding, which assumes that a protein's native state corresponds to its free energy minimum under the solution conditions usually encountered in cells. Although energy landscapes may be "rough", with many non-native local energy minima in which partially folded proteins can become trapped, the folding funnel hypothesis assumes that the native state is a deep free energy minimum with steep walls, corresponding to single well-defined tertiary structure. This has misled some to the idea that protein folding is a simple optimization problem with one minimum. In reality, free energy contains enthalpic (i.e. energetic) and entropic contributions which make a direct optimization impossible (Creighton, 1993). Obviously, that this theory, gets more complicated when dealing with larger proteins, due to the complexity of the folding. In lysozyme (using guanidine) Ikai and Tanford (1971), found that the folding pathway could be described by a two state-model ( $N \leftrightarrow U$ ). In other systems with more than one phase, the rates can vary by many orders of magnitude, being than the data interpreted in terms of folding intermediates (see (Chan and Dill, 1998) for a review). It is however; highly unlikely that there is a

unifying folding process that covers all proteins. Proteins have a huge variation in size, structure, residues composition and cofactors that there are bound to be many mechanisms of protein folding. On the other hand, the folding mechanisms of CI2, barstar and barnase, give some evidence of a unified system, variations of which could describe a large number of folding pathways (Fersht, 1997; Itzhaki, et al., 1995; Tan, et al., 1996). Whether protein folding is a concerted or stepwise process depends on the stability of individual protein substructures when considered in isolation or loosely complexed with one another (Fersht, 1998).

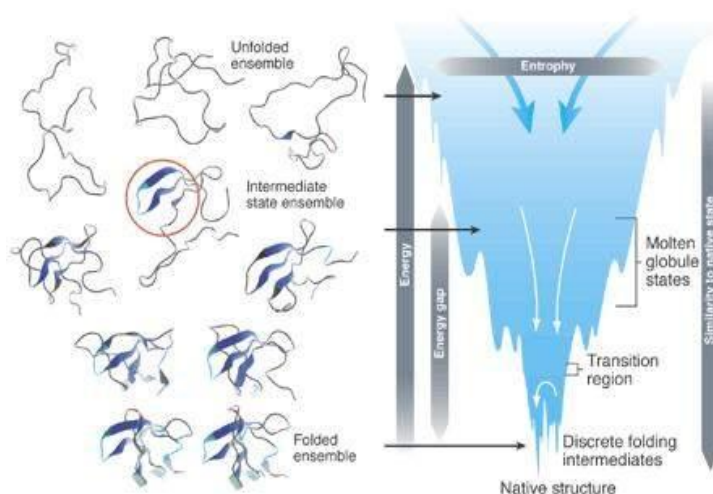


Figure 1.15: The free energy landscape for protein folding. Folding occurs through the progressive organization of ensembles of structures [shown here for the src-SH3 domain (left)] on a funnel-shaped free energy landscape (right). Conformational entropy loss during folding is compensated by the free energy gained as more native interactions are formed. Figure and caption adapted from (Brooks, et al., 2001).

In the last years the technological development enabled the construction of powerful informatics software (i.e. molecular dynamics simulation) and hardware (i.e. Blue Gene<sup>®</sup> computer from IBM<sup>®</sup>) that permit the study of folding from precise atomic analysis, through models involving simplified polymer chains, to completely abstract procedures. If we generalize and substitute the “classical view” of protein folding as a single stepwise pathway with different intermediates, the folding funnel theory should involve progressive association of an ensemble of partially native-like structures on a

free energy surface that resembles a rough funnel. Local free energy minima correspond to transient kinetic traps. The native state lies at the bottom of a set of convergent pathways (Figure 1.15).

#### 1.3.4. MOLECULAR DETERMINANTS OF STABILITY

The molecular basis for the stability of proteins is still a subject of intense study. Protein structures from thermophilic and mesophilic organisms have been compared, where different physico chemical factors are suggested to play a role in protein stability;

- a) **hydrophobicity**, hydrophobic interactions are the most important non-covalent forces that are responsible for different phenomena such as structure stabilization of proteins. Hydrophobicity provides stability to the protein structure, because it causes the non polar side chains to pack together in the interior of the protein to avoid contact with water (Rose and Wolfenden, 1993).
- b) **density of internal hydrogen bonds**, an increase of hydrogen bonding density at the protein surface aids in thermal stabilization. There is also a trend, albeit weaker, to increased secondary structure (especially helix) and decreased turn and coil conformations (Vogt and Argos, 1997)
- c) **distribution of charged residues on the surface**, polar atoms can act as hydrogen-bonding partners and are therefore energetically favourable at the water protein surface (Vogt and Argos, 1997)
- d) **proportion of certain amino acids**, among the principal residue substitutions associated with increased secondary structure are Gly→Ala and Lys→Arg (Argos, et al., 1979; Vogt and Argos, 1997)
- e) **presence of disulfide bridges**, role of disulfide bonds in protein structure and function is not limited to increasing thermodynamic stability, it may stabilize proteins more effectively at higher

temperatures. However, for extreme stability versus thermal denaturation, disulfides may be poor choices because cysteine may oxidize at high temperatures. The disulfide bridges may stabilize proteins by the reduction of conformational entropy in the denatured state (Betz, 1993; Matsumura, et al., 1989).

- f) **presence of metal centers**, structural metal-binding sites in proteins frequently achieve stability by binding metal ions in coordinately saturated ligand environments with idealized ligand metal bond geometries (Maglio, et al., 2003).
- g) **increased proline content**, the residue proline lacking an amide hydrogen is more rigid than other naturally occurring amino acids. Proline (similar to disulfide bonds) also reduces the conformational entropy in the denatured state. The main chain dihedral angle is constrained due to the presence of the pyrrolidene ring (Prajapati, et al., 2007).

In the majority of the thermophilic proteins so far studied, a general increase in the content of internal salt bridges and hydrogen bonds, as well as an enhanced proportion of amino acid residues in  $\alpha$ -helical conformation have been observed (Sternier and Liebl, 2001). The post-transcriptional modifications in proteins, like glycosylation are also suggested to have a general nonspecific effect on protein properties such as stability of the conformation (Wang, et al., 1996). Alan Fersht (1998), has compiled data about the effect of some residues and its effect in the structural properties in  $\alpha$ -helices (Table 1.2)

Table 1.2: Structural properties of aminoacids in  $\alpha$ -helices. Adapted from (Fersht, 1998).

Aminoacid	Effects relative to alanine
1. N-Cap	
Gly	Stabilizing. Exposes NH groups to solvent
Ser, Thr	Stabilizing. Hydrogen bonds with N+3
Asp	Stabilizing. Hydrogen bonds with N+3. Interacts with helix dipole
Asn	Stabilizing if the dihedral angles are appropriate
Gln	Hydrogen bonds with N+3
Glu	Weakly stabilizing. Hydrogen bonds with N+3. Loss of entropy
His	Weakly stabilizing. Hydrogen bonds with N+3. Loss of entropy
His(+), Lys, Arg	Destabilizing. Unfavourable interaction with helix
2. C-cap	
Gly	Stabilizing. Exposes terminal CO groups to solvent
Asn	Stabilizing. Makes hydrogen bonds with terminal CO groups
His(+), Lys, Arg	Weakly stabilizing. Make hydrogen bonds with terminal CO groups and interact favourably with helix dipole but lose entropy, especially in the case of Lys and Arg. More effective when side chains also interact elsewhere
Ser	Weakly destabilizing. Poor geometry for making hydrogen bonds with terminal CO groups.
Asp	Weakly destabilizing. Unfavourable interaction with helix dipole, cannot make hydrogen bonds with CO groups
3. Solvent exposed internal positions	
Met, Leu, Arg, Lys	Mildly destabilizing. Intrahelical interactions may be made
Ser	Destabilizing. OH group partly shielded from solvent
Cys	Destabilizing. The SH group prevents hydrogen bonding of water to the main chain CO and does not make as good as hydrogen bond.
Gln, Glu	Destabilizing. May form hydrogen bonds with polypeptide backbone in unfolded state
Thr, Val, Ile	Destabilizing because $\beta$ -branching allows only the <i>trans</i> conformation in folded state
Asp, Asn	Destabilizing. May form hydrogen bonds in the unfolded state and a probable reduction of the conformational freedom and salvation of the side chain
Phe, Tyr, His, Trp	Destabilizing. B-substitution reduces conformational freedom. His and Tyr may also form hydrogen bonds in the unfolded state.
Gly	Very destabilizing. Buries less hydrophobic surface area, makes less van der Waals contacts, and loses more conformational entropy on folding.
Pro	Very destabilizing. Loses two intrahelical hydrogen bonds

### **1.3.5. STABILITY IN METALLO-PROTEINS**

A number of proteins are stabilized by the addition of metal that bind specifically to the protein. The zinc finger motif is one example where the addition of zinc affects both the stability and the folding pathway (Cox and McLendon, 2000; Miura, et al., 1998). More examples are calmodulin and  $\alpha$ -lactalbumin which are calcium binding proteins that are significantly stabilized by  $\text{Ca}^{2+}$  binding (Masino, et al., 2000). The role of the metal in the folding process is not clear but for the proteins that are sufficiently stable to fold without the presence of the metal, the folding process is usually unaffected or slowed down by metal addition. The use of these metallo-enzymes to study the folding events enables the understanding of the role of the metal ion on the stability and on the folding process. The stability of the native conformation of metallo-proteins (like MCO) is the result of all noncovalent interactions between backbone and side chains atoms, the covalent bonds, disulfide bonds (if present), hydrogen bonds electrostatic forces of ion pairs, van der Waals interactions, also the hydrophobic effect, the coordinative bond between the metal ion and the protein side chains that act as ligands in all metallo-proteins. In general terms all the postulates for protein stability are also valid for multicopper oxidase together with the effect of the metal ion. The relative importance of each separate interaction and more importantly the ways, in which many of such interactions influence each other has been debated in detail and is still under consideration (Guzzi, et al., 1999).

#### **1.3.5.1. Small blue copper proteins**

More detailed studies concerning the stability, folding and unfolding of copper proteins were performed in small blue copper proteins like rusticyanin, azurin and plastocyanin. Alcaraz and Donaire (2004; 2005) found, by using stopped-flow spectroscopy, that rusticyanin can incorporate copper after protein folding, showing that copper binding can be subsequent to protein folding. These authors also show that the oxidized form of the copper ion ( $\text{Cu}^{2+}$ ) is more

effective in terms of stability to rusticyanin than the reduced form of the metal ( $\text{Cu}^+$ ). They made this observation by comparing the unfolding rates of the apo forms of the proteins incubated with both forms of the metal ion. A curious finding in this protein is that it aggregates in the presence of guanidinium chloride (Alcaraz and Donaire, 2004). This is quite an uncommon feature, formation of aggregates under chemical denaturing conditions. In azurin from *Pseudomonas aeruginosa*, it was found that the tight packing of the hydrophobic residues that characterize the inner structure of azurin is fundamental for the protein stability. This suggests that the proper assembly of the hydrophobic core is one of the most crucial event on the folding process (Mei, et al., 1999). Similar to the other copper proteins mentioned above, in azurin the copper ion also has a stabilizing effect on the protein structure (Leckner, et al., 1997). Furthermore, in a more recent work Pozdnyakova (2001), showed that introducing copper prior to protein folding does not speed up the polypeptide folding rate; nevertheless, it results in much faster ( $> 4000$ -fold) formation of the active center of azurin.

### **1.3.5.2. Studies in multicopper oxidases**

Dedicated studies on the stability of multicopper oxidases are just a few and with similar general conclusions. Agostinelli et al (1995) showed that the DSC from the laccase from *Rhus vernicifera*, of holo-laccase, type2 copper depleted and apo-laccase were deconvoluted into two independent two-state transitions, providing evidence for a domain structure of the protein. The correlation of the two transitions, with the bleaching of copper optical bands, show that the process involves the denaturation of copper sites. No detectable unfolding of secondary structure was observed, since the thermal transitions, characterized by low overall specific enthalpy, did not modify the CD spectra. This result suggests that the unfolding state of this laccase still has secondary structure, meaning that the unfolding is only due to the loss of the tertiary structure. A similar result, with three thermal transitions upon DSC study, in ascorbate oxidase also suggests a correlation between the structural domains and the

thermal unfolding profile. Furthermore, the authors showed that the copper ion has a stabilizing effect on the overall conformational stability (Agostinelli, et al., 1995; Savini, et al., 1990; Sedlak, et al., 2008). Korovleva et al (2001) showed that two fungal laccases from *Coriolus hirsutus* and *Coriolus zonatus* and their type2 copper depleted derivatives, also showed that the copper center are disrupted before the overall unfolding. In a multidomain MCO, human ceruloplasmin, Sedlak (2007), found that during unfolding there was the formation of a reversible intermediate which correlates with decreased secondary structure, exposure of aromatics, loss of two coppers, and reduced oxidase activity. Further additions of urea trigger complete protein unfolding and loss of all coppers. Attempts to refold this species result in an inactive apoprotein with molten-globule characteristics. However, the copper ions also have a stabilizing effect in this protein, since the apo-hCp also unfolds through a multistep reaction but the intermediate appears at slight lower denaturant concentrations (Sedlak and Wittung-Stafshede, 2007). In general terms, the stability studies in multicopper oxidases showed that the copper has a fundamental role in the overall conformational structure, and also that the thermal unfolding of these proteins is highly complex where no refolding was detected, and none of these proteins unfolded according to a single thermal domain. In fact, some authors suggest that the three thermal transitions determined by DSC may correspond to the three structural domains of these proteins.

The work presented in this dissertation focus on stability studies in multicopper oxidases. For this purpose two general strategies were adopted. First, we search in genome databases for uncharacterized hyperthermophilic multicopper oxidases. In this search, two microorganisms were identified as having coded in its genomes two multicopper oxidases, the hyperthermophilic *Aquifex aeolicus* (McoA) and the *Archaea*, *Pyrobaculum aerophilum* (McoP). Proteins from hyperthermophilic microorganisms have improved biochemical properties that enable a higher thermotolerance and thermostability, enhancing their



importance in these types of studies. These two genes were cloned in an expression vector, and the protein was overexpressed in *E. coli*. The recombinant proteins were purified and biochemically characterized. The second strategy, aimed on site directed mutagenesis in key residues of CotA from the mesophilic *B. subtilis*, and study its effect in the resulting proteins. The main advantage of this kind of strategy, is to evaluate the proteins that have intrinsic properties that enable their stability, or if there are some key residues that are fundamental for their overall stability. CotA is a particular protein since it is not part of the vegetative cell, and is instead part of the structure of the spore (reproductive structure that is adapted for dispersal and surviving for extended periods of time in unfavourable conditions) of *B. subtilis* (Martins, et al., 2002). CotA, among the three proteins studied is the only to have a disulfide bridge, which would be expected that this property could be related to the structural stability, therefore it was one properties studied. Other key mutation was in a ligand of a copper center, in the type 1 copper. The effect of copper in the proteins was also evaluated by thermal stability (using DSC) and by chemical stability (using stopped-flow spectroscopy). These studies give insights on the stabilizing effect of copper in the protein conformation



## 2 A ROBUST METALLO-OXIDASE FROM THE HYPERTHERMOPHILIC BACTERIUM *AQUIFEX* *AEOLICUS*

---

2.1.	INTRODUCTION.....	51
2.2.	EXPERIMENTAL PROCEDURES .....	53
2.3.	RESULTS AND DISCUSSION .....	59

### ABSTRACT

The gene, *Aquifex aeolicus* AAC07157.1, encoding a multicopper oxidase (McoA) and localized in the genome as part of a putative copper-resistance determinant, has been cloned, over-expressed in *Escherichia coli*, and purified to homogeneity. The isolated enzyme shows spectroscopic and biochemical characteristics typical of the well-characterized multicopper oxidase family of enzymes. McoA presents higher specificity ( $k_{\text{cat}}/K_m$ ) for cuprous and ferrous ions than to aromatic substrates and is therefore designated as a metallo-oxidase. Addition of copper is required for maximal catalytic efficiency. A comparative model structure of McoA has been constructed and a striking structural feature is the presence of a methionine-rich segment comparable to those present in copper homeostasis proteins. The kinetic properties of a methionine-rich deleted enzyme McoA $\Delta$ P321-V363 when compared to the wild type provide evidence for the key role of this region in the modulation of the catalytic mechanism. McoA has an optimal temperature of 75°C and presents remarkable heat stability at 80 and 90°C, with activity lasting up to 9 and 5h, respectively. McoA probably plays a role for *A. aeolicus* in copper and iron homeostasis.

**This chapter was published in the following scientific paper:**

André T. Fernandes, Cláudio M. Soares, Manuela M. Pereira, Robert Huber, Gregor Grass, Lígia O. Martins. 2007. A robust metallo-oxidase from the hyperthermophilic bacterium *Aquifex aeolicus*. FEBS J. 274: 2683-94

The genome DNA was kindly provided by Prof. Robert Huber. McoA homology model was derived by Prof. Cláudio M. Soares, Dr. Manuela Pereira carried the EPR measurements, and Dr. Gregor Grass evaluated the genomic context of the *mcoA* gene in *A. aeolicus* genome.

## **2.1. INTRODUCTION**

The multicopper oxidases (MCO) constitute a family of enzymes that present broad substrate specificity, oxidising numerous aromatic phenols and amines. The one-electron oxidation of these substrates occurs concomitantly with a four-electron reduction of molecular oxygen to water. The redox reactions catalyzed by these enzymes depend on the presence of three copper sites designated Cu types, 1, 2 and 3; a mononuclear T1 copper center that is the primary acceptor for electrons and a trinuclear center comprising one T2 and two T3 copper ions involved in dioxygen reduction to water (Lindley, 2001; Solomon, et al., 1996).

The laccases constitute a large subfamily of MCO and have been implicated in various biological activities related to lignolysis, pigment formation, detoxification and pathogenesis (Xu, 1999). Laccases have a great potential in various biotechnological processes mainly due to their high relative non-specific oxidation capacity, the lack of a requirement for cofactors, and the use of readily available oxygen as an electron acceptor. A few MCO members are able to oxidize, with high specificity, lower valence metal ions such as  $\text{Cu}^{1+}$ ,  $\text{Fe}^{2+}$  and  $\text{Mn}^{2+}$ , are thus designated as metallo-oxidases (Stoj and Kosman, 2005). Human ceruloplasmin (hCp), yeast ferroxidase Fet3p and CueO from *Escherichia coli* are known to be critically involved in cellular metal homeostasis mechanisms. The importance of these regulatory mechanisms is well known in aerobic metabolism, since metals such as iron and copper though essential for life, readily participate in reactions that result in the production of highly reactive oxygen species when allowed to accumulate in excess of cellular needs (Crichton and Pierre, 2001).

The catalytic and stability characteristics of bacterial laccases at the molecular level are of considerable interest and, as a model system, the CotA-laccase from *Bacillus subtilis* has been extensively studied (Bento, et al., 2005; Durao, et al., 2006; Enguita, et al., 2004; Enguita, et al., 2003; Martins, et al., 2002). The

main objectives of such studies are to dissect the catalytic mechanisms and to design laccases that better match biotechnological applications, using protein engineering techniques. Herein this investigation is extended to hyperthermophilic laccase-like enzymes since an understanding of the structure-function relationships in extremophilic enzymes is still limited and their use offers new opportunities for biocatalysis as a result of their superior stability (Egorova and Antranikian, 2005). In the genome databases very few thermo and hyperthermophiles microorganisms were found to contain homologous MCO. However, the *Aquifex aeolicus* genome revealed a 1,784-bp open reading frame (Accession No. AAC07157 .1 (Deckert, et al., 1998)), which on the basis of an amino acid sequence with a similarity of some 30% to the CotA-laccase from *B. subtilis*, and CueO from *E. coli*, was putatively assigned as a multicopper oxidase. *A. aeolicus* is a microaerophilic, hydrogen-oxidising, chemiolitoautotrophic bacterium that grows between 58-95°C and optimally at 89°C occupying the deepest branch of the bacterial phylogenetic tree (Eder and Huber, 2002). The present study reports the spectroscopic properties and biochemical characterization of the recombinant McoA (Multicopper oxidase from *Aquifex*). It is shown that McoA is a hyperthermostable copper-activated metallo-oxidase, with the features typical of the well-known MCO. However, one aspect of McoA is the presence of a Met-rich region that is absent in the “classic” MCO. A kinetic analysis of a variant enzyme deleted in this segment, McoA $\Delta$ P<sub>321</sub>-V<sub>363</sub>, indicates that this region occludes the substrate binding site, in agreement with the structural model proposed, and may be involved in the catalytic mechanism of the enzyme. The latter presumably involves copper binding and McoA is encoded within a copper-resistance determinant. The cuprous and ferrous oxidation competence of McoA offer a basis for proposing the expression of this activity *in vivo* and thereby a role in the suppression of copper and iron cytotoxicity.

## 2.2. EXPERIMENTAL PROCEDURES

**Construction of an expression-plasmid for the *mcoA* gene.** The *mcoA* gene was amplified by PCR using oligonucleotides: *mcoA*-182D (5'-ACTAAAGGAGGTAACATATGGACAGGC-3') and *mcoA*-1816R (5'-GACTTAGAATTCTCAACATATTGCACC-3'). The 1710 bp-long PCR product was digested with *Nde*I and *Eco*RI and inserted between the respective restriction sites of plasmid pET-21a(+) (Novagen) to yield pATF-1. An analysis of the *mcoA* gene reveals that it contains codons uncommon in *E.coli* including 25 for arginines, tRNA<sup>Arg</sup>(AGG/AGA/CGG/CGA), 18 for leucines, tRNA<sup>Leu</sup>(CTC) and 22 for isoleucines, tRNA<sup>Iso</sup>(ATA). These give limitations in its expression by ordinary *E. coli* strains. Rosetta (DE3) pLysS (Novagen) was used as the host strain since it possesses rare tRNA genes providing “universal” translation. Introduction of pATF-1 into Rosetta *E. coli* created strain LOM409, in which the McoA protein could be produced under the control of the T7lac promoter.

**Construction of an expression-plasmid for *mcoA* without the Met-rich segment.** Phosphorylated primers, *mcoA*-del322r (5'-GAAGTTGTAAAGCTTTATTACGTCATTTAC-3') and *mcoA*-del362d (5'-GTTATGGAGTTCAGGGTTACAAAGG-3') were used to amplify around plasmid pATF-1, excluding an internal fragment of *mcoA*. The PCR product was incubated with *Dpn*I, to digest template DNA, self-ligated and introduced into *E. coli* DH5 $\alpha$  by transformation. The resulting plasmid pATF-9 containing *mcoA*, with an in-frame deletion corresponding to codons 964 to 1087, was introduced into the Rosetta *E. coli* created strain LOM420, in which the McoA derivative protein McoA $\Delta$ P<sub>321-V363</sub> was produced under the control of the T7lac promoter.

**Overproduction and purification of McoA and McoA $\Delta$ P<sub>321-V363</sub>.** Strains LOM409 (wild type McoA) and LOM420 (McoA $\Delta$ P<sub>321-V363</sub>) were grown in Luria-Bertani (LB) culture medium supplemented with ampicillin (100  $\mu$ g/mL) and chloramphenicol (34  $\mu$ g/mL) at 37°C. Growth was followed until OD<sub>600</sub>=1,

at which time 100  $\mu\text{M}$  IPTG and 250  $\mu\text{M}$   $\text{CuCl}_2$  were added to the culture medium. Incubation was continued for a further 4 h. Cells were harvested by centrifugation (8000  $\times$  g, 15 min, 4°C). The cell pellet was suspended in 20 mM Tris-HCl buffer (pH 7.6), containing DNase I (10  $\mu\text{g}/\text{mL}$  extract),  $\text{MgCl}_2$  (5 mM) and a mixture of protease inhibitors (Complete™, mini-EDTA free protease inhibitor mixture tablets, Roche). Cells were disrupted in a French pressure cell (at 19000 psi), followed by a centrifugation (18 000  $\times$  g, 60 min, 4°C). Soluble protein was recovered from inclusion bodies based on a previously described method (Bollag, et al., 1996). In short, the inclusion bodies were washed with 20 mM Tris-HCl buffer (pH 7.6) containing 0.5% Triton X-100, and spun down by centrifugation (12 000  $\times$  g, 5 min, 4°C). Inclusion bodies were unfolded in 20 mM Tris-HCl (pH 7.6) buffer containing 8 M of urea, 2 mM of reduced glutathione and 0.2 mM of oxidized glutathione in a volume of 9 ml/g pellet (at final protein concentration below 2.5 mg/mL), for 1 h at room temperature. Refolding was performed by slowly adding 9 mL (for each ml of urea-protein solution) of working buffer containing 2 mM of reduced glutathione, 0.2 mM of oxidized glutathione and 50  $\mu\text{M}$  of  $\text{CuCl}_2$ , and waiting afterwards for 2-4 h at room temperature. Dialysis in a Diaflow (Amicon) with a 30 kDa membrane was performed to remove urea. Refolded protein was resuspended in 20mM Tris-HCl pH 7.6, centrifuged and the resulting soluble fraction was loaded onto an ion exchange Q-Sepharose column (bed volume 25 ml) equilibrated with Tris-HCl (20 mM, pH 7.6). Elution was carried out with a two-step linear NaCl gradient (0–0.5 and 0.5–1 M) in the same buffer. Fractions were collected and assayed for activity. Active fractions were pooled, concentrated by ultrafiltration (cut-off of 30 kDa), and equilibrated to 20 mM Tris-HCl (pH 7.6). The resulting sample was applied on a Superdex 200 HR 10/30 column (Amersham Biosciences) equilibrated with 20 mM Tris-HCl buffer, pH 7.6 containing 0.2 M NaCl. Active fractions were pooled, concentrated, incubated with 5 equivalents of  $\text{CuCl}_2$  per mole of McoA for 30 minutes. Excess copper was removed by passing the solutions through a Sephadex G-25 column (PD 10 columns, Amersham Biosciences). All



purification steps were carried out at room temperature in a fast protein liquid chromatography system (Åkta-FPLC, Amersham Biosciences).

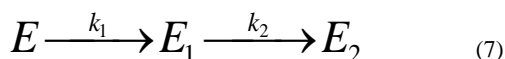
**UV/visible, EPR and CD spectra.** The UV/visible absorption spectra were obtained at room temperature in 20 mM Tris-HCl buffer, pH 7.6, using a Nicolet Evolution 300 spectrophotometer from Thermo Industries. Electron Paramagnetic Resonance (EPR) spectra were measured with a Bruker EMX spectrometer equipped with an Oxford Instruments ESR-900 continuous-flow helium cryostat. The spectra, obtained under non-saturating conditions (160  $\mu$ M protein content), were theoretically simulated using the Aasa and Vänngård approach (Aasa and Vänngård, 1975). CD spectra in the far-UV were measured on a Jasco-720 spectropolarimeter using a circular quartz cuvette with a 0.01-cm optical pathlength in the range of 190-250 nm. Protein content was 25  $\mu$ M in highly pure water (Mili-Q).

**Enzyme activities.** Cuprous oxidase activity were measured in terms of rates of oxygen consumption by using an oxygen electrode (Oxygraph, Hansatech, Cambridge UK) at 40°C, following the method described by Singh et al. (Singh, et al., 2004)). Stock solutions of  $[\text{Cu(I)(MeCN)}_4]\text{PF}_6$  (Sigma-Aldrich) were freshly prepared in argon-purged acetonitrile and subsequently diluted anaerobically by using gas-tight syringes. Reactions were initiated by adding the substrate to an air-saturated mixture containing enzyme, 100 mM acetate buffer, pH 3.5 and 5% acetonitrile. The buffer was chosen to provide the best stability for the substrate used and all reactions were corrected for background autoxidation rates of  $\text{Cu}^+$ . The oxidation of 2,2'-azinobis-(3-ethylbenzothiazoline-6-sulfonic acid) (ABTS), syringaldazine (SGZ), and ferrous ammonium sulphate were photometrically monitored at 40°C, unless otherwise stated, on either a Nicolet Evolution 300 spectrophotometer from Thermo Industries or at a Molecular Devices Spectra Max 340 microplate reader with a 96-well plate. Ferrous ammonium sulphate oxidation was monitored at 315 nm ( $\epsilon = 2,200 \text{ M}^{-1}\text{cm}^{-1}$ ) in 100 mM MES buffer at pH 5. The oxidation of ABTS and SGZ were followed at 420 nm ( $\epsilon = 36,000 \text{ M}^{-1}\text{cm}^{-1}$ ) and

530 nm ( $\epsilon = 65,000 \text{ M}^{-1}\text{cm}^{-1}$ ), respectively. Oxidations were determined using Britton-Robinson (BR) buffer (100 mM phosphoric acid, 100 mM boric acid and 100 mM acetic acid mixture titrated to the desired pH with 0.5 M NaOH). The standard reaction mixtures contained 1 mM of ABTS (pH 4) or 0.1 mM SGZ (pH 7). The effect of pH on the enzyme activity was determined at 40°C for ABTS and SGZ in BR buffer (pH 3-9). The optimal temperature for the activity was determined at temperatures ranging from 40 to 90°C by measuring ABTS oxidation at pH 4. Kinetic parameters were determined using reaction mixtures containing  $\text{Cu}^+$  (5-300  $\mu\text{M}$ , pH 3.5),  $\text{Fe}^{2+}$  (5-100  $\mu\text{M}$ , pH 5), ABTS (50-400  $\mu\text{M}$ , pH 4) and SGZ (1-100  $\mu\text{M}$ , pH 7). Kinetic constants  $K_m$  and  $k_{\text{cat}}$  were fitted directly to the Michaelis-Menten equation (OriginLab, Northampton, MA, USA). All enzymatic assays were performed at least in triplicate. The specific activity was expressed in  $\mu\text{mol}$  of substrate oxidized  $\text{min}^{-1}\text{mg}^{-1}$  of protein. The protein concentration was measured by using the absorbance band at 280 nm ( $\epsilon_{280} = 75,875 \text{ M}^{-1}\text{cm}^{-1}$ ) or the Bradford assay (Bradford, 1976) using bovine serum albumin as standard.

**Redox titrations.** Redox titrations were performed at 25°C, pH 7.6, under an argon atmosphere, and monitored by visible spectroscopy (300-900 nm) in a Shimadzu Multispec-1501 spectrophotometer. The reaction mixture contained 25-50  $\mu\text{M}$  enzyme in 20 mM Tris-HCl buffer, pH 7.6 and the following mediators each in a 10  $\mu\text{M}$  final concentration (reduction potential between brackets); p-benzoquinone [+240 mV], dimethyl-p-phenylenediamine [+344 mV], potassium ferrocyanide [+436 mV] monocarboxylic acid ferrocene [+530 mV], 1,1'-dicarboxylic acid ferrocene [+644 mV] and Fe(II/III)-Tris-(1,10-phenanthroline) [+1,070 mV]. Potassium hexachloroiridate (IV) was used as the oxidant and sodium dithionite as the reductant. The redox potential measurements were performed with a combined silver/silver chloride electrode, calibrated with a quinhydrone saturated solution at pH 7.0. The redox potentials are quoted against the standard hydrogen electrode.

**Kinetic Stability.** Kinetic thermostability was determined at 80 and 90°C by incubating an enzyme solution in 20mM Tris-HCl buffer, pH 7.6. At appropriated times samples were withdrawn, cooled and immediately examined for residual activity following the oxidation of ABTS. The activity decay was fitted according to a second-order exponential model. This assumes an initial deactivation first-order step that leads to an intermediate state ( $E_1$ ) displaying a fraction of the initial activity;  $\beta_1$  is the ratio of activities between  $E_1$  and the initial state, E. The state  $E_1$  deactivates also according to a first-order step to give state  $E_2$  with no activity in the case of McoA;  $\beta_2$  is the ratio of activities between  $E_2$  and the initial state. This deactivation model, previously used to describe the time-dependence deactivation of several other enzymes (Henley and Sadana, 1985), was used as McoA does not obey a more common first-order, single step deactivation mechanism. The following scheme describes the two-step series model:



Considering that at time zero all the protein shares the conformation E and that the residual activity is determined by the activity of each conformational state weighted by its content, equation (1) was obtained and used to fit the time-dependence of residual activity (Henley and Sadana, 1985):

$$f.act = \left(1 + \frac{\beta_1 k_1}{k_2 - k_1} - \frac{\beta_2 k_2}{k_2 - k_1}\right) e^{-k_1 t} - \left(\frac{\beta_1 k_1}{k_2 - k_1} - \frac{\beta_2 k_2}{k_2 - k_1}\right) e^{-k_2 t} + \beta_2 \quad (8)$$

**Structure of McoA by comparative modelling techniques.** The structure of the *A. aeolicus* McoA was derived on basis of the two bacterial laccases present in the PDB, CotA from *B. subtilis* ((Enguita, et al., 2003), PDB code: 1GSK) and CueO from *E.coli* ((Roberts, et al., 2002), PDB code: 1KV7), since these present considerably higher sequence identity (32.4% and 32.7% respectively) than the eukaryotic multicopper oxidases. The program MODELLER (Sali and Blundell, 1993), Version 6.1, was used for deriving the structure. The alignment was optimized through several modelling cycles until a good quality model for

the unknown structure was achieved. The quality was assessed by considering the restraint violations reported by MODELLER and a Ramachandran analysis performed by the program PROCHECK (Laskowski, et al., 1993). The final model (one of 60 structures with the lowest value of the MODELLER objective function) has 90.6% of the residues in the most favoured regions, 8.3% in the additional allowed regions, 1.1% in the generously allowed regions and no residues in the disallowed regions. Two large loops of the McoA could not be modelled on the basis of the two known structures. The two loops span from Ser 41 to Gly 60 and Phe321 to Val363. The latter is particularly long and presents considerable problems in the comparative modelling procedure. The decision was taken to model these two loops solely on the basis of stereochemical restraints and the general statistical preferences implemented in MODELLER.

**Other methods.** The McoA protein was identified by MALDI-TOF-MS after tryptic digestion using a mass spectrophotometer Voyager STR (Applied Biosystems), at Instituto de Tecnologia Química e Biológica. The molecular mass of the protein was determined on a gel filtration Superose 12 HR10/30 column (Amersham Biosciences) equilibrated with 20 mM Tris HCl pH 7.6 containing 0.2 M NaCl. Ribonuclease (13.7 kDa), chymotrypsinogen A (25 kDa), ovalbumin (43 kDa), albumin (67 kDa) and aldolase (158 kDa) were used as standards. The copper content was determined through the trichloroacetic acid/bicinchoninic acid (BCA) method of Brenner and Harris (Brenner and Harris, 1995) and confirmed by atomic absorption spectroscopy (Instituto Superior Técnico, Universidade Técnica de Lisboa, Chemical Analysis Facility). The isoelectric point was evaluated using IEF gels on a Phast System (Amersham Biosciences) with broad pI standards following the manufacturer's instructions.

### 2.3. RESULTS AND DISCUSSION

**McoA resembles CotA and CueO.** A sequence alignment of *A. aeolicus* McoA with CueO and CotA clearly indicates that the enzyme is a member of the multi-copper family of enzymes (Figure 2.1).

McoA	<u>MDRRKFIK</u> TSLSFALGFSVGLLSLSCGGGGTSSSSGQSGTISKOSINIPGYFLPDQORVSITAKWTTLEVIPGKSTMDLVYEIDNEYN....PVI	95
CueO	<u>MLRRDFLK</u> YSVALGASALPLWSRAAFARPALPIPDLLTADASN.....RMQLIVKAGQSTFAGKNATTWYNGNLLGPAV	78
CotA	.....MTLEKFVDALPIPDITLKPVOQSKEK.....TYEVTMEECTHQLHRDLPPTRLWGYNGLFPGPTI	60
Consensus	m r r f k ..... n p	
McoA	FLRKQGTFSADFVNNS.....GEDS.....IIHWHGFRAPWKS DGHPPYAVKDGETYSYDPFTIIDRSG.....TYFYHPPHGHRT	166
CueO	QLHKGKSVTDIHNQL.....AEDT.....TLHWHGLEIPGIVDGGPQGIIPAGSTR.TVFTFTPEQRAA.....TCWIHPHKGKT	148
CotA	EVKRNENYVKMNNLPSTHFLPIDHTIHSDSQHHEPEVKTVVHLHGGVTPDDSDGYPEAWFSKDFEQGTGPYFKREVYHYFNQQRGAILWYHDAHALT	160
Consensus	n ..... d ..... h h ..... dg ..... h h t	
McoA	GYQVYGLAGMIIEDEDEDNLKQALDLEYGVIDIPLIIQDKTFDSSGQLVYNP.....MGHMGWGDITILVNLTPNPMYDMVERKIYRFRILN	254
CueO	GRQVAMGLAGLVIED.DE.IRKLRLPKQWIGIDVPIIQDKRFSADQIDYQLDIM.....TAAVGWFGDTLLTNGAIYPQHSAPKGWLRILN	237
CotA	RLNVYAGLVGAYIIHDPEK...K.RLKLPSEYDVPLITDRTINEDGSLFYSPAPENPSPSLNPSIVPAFCGETILVNGKWPVLEVEPRKYRFRVIN	256
Consensus	g i d k ..... d i d ..... til n ..... r r i n	
McoA	GSNARPYRLALRGQRMRFWIGVEGGLDTPKEVNEILVAPGERIDILVDFRDASVNDVIKLYN..... <u>HPHNV</u>	325
CueO	GCNARSINIAASD.N..RPLYVIASDGLLAEPVKVTEPLLMGERFEVLVDISDGKAFDLVTLFVSQMGMAIPFDKPHPMRIQLPRITASGTLPTDL	334
CotA	ASNTRTYNLSLNGG...DFIQIGSDGGLLPKSVKLSFSLAPAERYDIIIDFT.AYEGESIILANSAG.....	321
Consensus	n r ..... i g g l l ..... e r d ..... l	
McoA	<u>TCGMGIMRGVGMERGVGVGNANMGVADNSEFEV</u> MEFRVTKDAYSIDKSIQPR...LSEVTPINTDGAQVQRITLGMRRMVFTINGETWEDGYANP	421
CueO	TTMPALPSLEGLTVRNLIK...MDPRITMGVGMIMKRYGAQMSGMDHDSMNAHMOGNGHGE...MDHGQNMDSGMNHGAMGNMNHGGKDFHNAFNGQV	434
CotA	.....CGGDVNPETDANIMQFRVTKPLAQKDESRRPKYLASYPSVQH.....ERIQN.....IRTLKLAGTQDEYGRPV	386
Consensus		
McoA	QDINN...PKVLEFQNNQGDVVIIEYVNNMTGYHHPMHIHGQFQVLER.....SL.....GPLRATDLGWKDTVIVAPMETVRIAVDMSPHYN	500
CueO	FDMNK...PMFAAQGRHERWISVG.G.DMMLHPFHIHGTFQFRILSE.....NG.....KAPAAHRTGAKDTVRVEG.GISEVLVKFHDAP	511
CotA	LLNNKRWHDVPTETPKVGTTEIWSIINPTRGTHPIHLHLVSVFVLDRRPFDIARYQESGELSYTGPAVPPPPSEKWKDTIQAHAGEVLRIATFG...P	483
Consensus	n ..... h h h ..... l ..... g w k d t	
McoA	EHQIYLLHCHILEHHDGMVNYRVN....	526
CueO	KEHAYMAHCHILEHEDTGMLGFTV....	536
CotA	YSGRYVWHCHILEHEDYDMRPMDDITDPHK	513
Consensus	h c h h m m	

Figure 2.1: Amino acid sequence alignment of McoA with CotA laccase from *B. subtilis* and with metallo oxidase CueO from *E. coli*. The alignment was generated using the primary sequence of the proteins. The consensus sequence shows the identity between amino acids residues. The consensus sequence of the twin-arginine translocation system is underlined for CueO and McoA. The copper ligands are all conserved (grey boxes), indicating that McoA is a multicopper oxidase. The two large loops spanning Ser 41 to Gly 60 and Phe 321 to Val 363 that have no counterparts of similar size on the templates are double underlined. The consensus sequence McoA protein in the NCBI database with the accession number NP-213770-1 was annotated as a putative periplasmic cell division protein from *A. aeolicus*.

The first 38 amino acid residues encoded by the *mcoA* gene most likely constitute a putative leader sequence for the twin-arginine translocation (Tat) system that signals the protein for the periplasmic space in an already folded state (Stanley, et al., 2000), in a similar manner to *E. coli* CueO (Grass and Rensing, 2001). Although there is, as yet, no experimental evidence for the role of this leader sequence, *A. aeolicus* does possess putative TAT genes and, in addition, the N-terminus of McoA “MDRRKFIK” significantly matches the TAT-consensus motif “S/TRRXFLK” (Figure 2.1, (Stanley, et al., 2000)).

Overall, most of the structure of the *A. aeolicus* McoA can be reasonably modelled using the CotA from *B. subtilis* and CueO from *E. coli* template structures, except for the two large loops spanning Ser 41 to Gly 60 and Phe 321 to Val 363; these loops have no counterparts in the template structures (Figure 2.1). The sequence segment Phe 321 to Val 363 is extensive and could be close to the T1 copper active site. If this is the case, the segment may control access to the binding site for aromatic substrates, a controlling factor for this enzyme's substrate specificity.

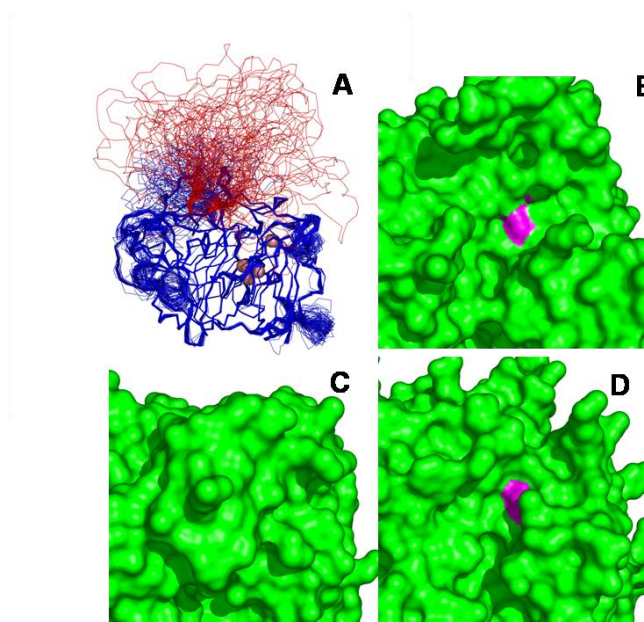


Figure 2.2: (A) Overlay of the 60 different models obtained in the final cycle of the comparative modelling procedure for McoA. The protein is represented by a thin ribbon and the copper atoms are represented by salmon coloured spheres, with the T1 Cu ion separated from the three nuclear centers constituted by T2 and T3 Cu ions. The loop spanning residues Phe 321 to Val 363 is coloured in red, while the rest of the protein is coloured in blue. (B) Close-up of the active-site (T1 Cu centre) region of CotA, using a surface representation, highlighting (in magenta) the region of the most exposed histidine ligand of the copper, which is the residue that interacts with substrates. (C) Same as (B), but for CueO. (D) Same as (B), but for McoA. In this case, the Phe321 to Val363 loop was excluded from the model. This figure was prepared with Pymol (DeLano, 2003).

Figure 2.2A shows a superposition of the 60 different structures obtained in the last cycle of the comparative modelling procedure, highlighting the Phe 321 to Val 363 loop in red. In Figure 2.2B, C and D, the active site (T1 Cu) zone of CotA, CueO and McoA multicopper oxidases are shown, respectively. The

molecular surface is marked in magenta in the zone of the most exposed histidine residues that bind copper, highlighting in this way, the active site accessibility. Note that for this analysis, the Phe 321 to Val 363 segment was excluded in McoA, since there is no reliable structural information concerning its conformation. Therefore, this accessibility comparison must be handled with care, given that this segment may occlude the active site. If this possibility is ignored here, we can see that the three multicopper oxidases present considerable differences on the active site zone. The most exposed active site is the one of CotA laccase, followed by McoA. Finally, the active site of CueO is buried (the histidine residue is not even exposed, since no magenta coloured zone is visible). While the conformation of the Met-rich 42 residue segment remains an open question requiring experimental structural characterisation, it is noteworthy that it contains 10 glycine and 12 methionines residues as follows;

PHNLIGMGMIGMRMGMGMERGMGMGNGMNMMDMGMDNSEFEV

The metallo-oxidase CueO, an essential component of the copper regulatory mechanism in *E.coli* under aerobic conditions (Grass and Rensing, 2001), contains a similar methionine rich region (14 Met and 6 Gly residues in a 42 amino acid segment (Roberts, et al., 2002)). The crystal structure of CueO with exogenous copper bound has been determined identifying a fifth copper-binding site in the Met-rich region, in a position to mediate electron transfer from substrates to the T1 copper center (Roberts, et al., 2003). Furthermore, Met-rich sequence motifs are found in a number of proteins involved in copper metabolism, such as PcoA and PcoC from *E.coli* (Huffman, et al., 2002) and numerous bacterial homologues, leading to the suggestion that such regions are involved in copper binding (Stoj and Kosman, 2005). It is therefore likely that Met-rich motif of McoA has a similar function. The *mcoA* gene is part of a putative copper-resistance determinant. *A. aeolicus* is a microaerophilic oxygen respiring organism that thrives in geothermally and volcanically heated habitats which are abundant in potentially toxic metals. In this regard it is interesting that the *mcoA* gene occurs in a determinant comprising seven putative genes of

which all but one, have strong similarities to orthologues from characterised copper-resistance systems from *E.coli* (Figure 2.3). All the genes are encoded on the *A. aeolicus* genome in the same direction of transcription.

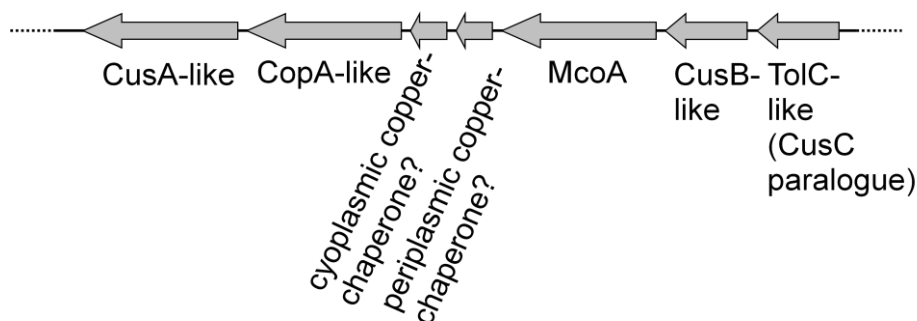


Figure 2.3: The *mcoA* gene from *Aquifex aeolicus* is part of a putative copper-resistance determinant. Six proteins with (and one without) similarity to known copper-detoxification systems are encoded by the *A. aeolicus* genome. The CopA-like copper-efflux ATPase transports  $\text{Cu}^+$  from the cytoplasm to the periplasm (34% identity to CopA from *E. coli*) whereas CusCBA-like tripartite transporter, detoxifies periplasmic  $\text{Cu}^+$  to the outside. The CusA-like pump protein of *A. aeolicus* shows 43% identity to CusA and the CusB-like membrane fusion protein 23% identity to CusB from *E. coli*. In contrast, the putative outer membrane efflux duct protein of the *A. aeolicus* copper-resistance determinant shows higher similarity to TolC, a paralogue of CusC from *E. coli*. Additionally, two putative copper chaperones (Accession No. AAC07166.1 and AAC07167.1) are present. The first bears similarity to the putative periplasmic copper chaperone CopG protein from several bacterial species. Each chaperone may be involved in binding and delivering of copper to the respective cytoplasmic or periplasmic efflux pumps, thereby preventing the accumulation of “free” redox-active  $\text{Cu}^+$ .

**Overproduction and purification of recombinant Wt McoA and McoAΔP321-V363.** The *mcoA* gene was amplified by PCR and inserted into the pET-21a(+) expression vector resulting in pATF-1. Attempts to express the protein in host *E. coli* BL21(DE3) or in Tuner (DE3) strains resulted in very low levels of protein production either in the soluble or insoluble fraction of cell lysates. This is most probably related to the higher number of amino acids with rare codon usage present in the *mcoA* gene sequence. Accordingly, the pATF-1 construct was transformed into *E. coli* Rosetta (DE3) pLysS (coding for rare tRNA's), resulting in strain LOM409. Upon induction with IPTG, a major band of around 59 kDa, absent in extracts prepared from uninduced LOM409,



appeared in the insoluble fraction of cell lysates, most probably in the form of inclusion bodies as visualised by SDS-PAGE (Figure 2.4A).

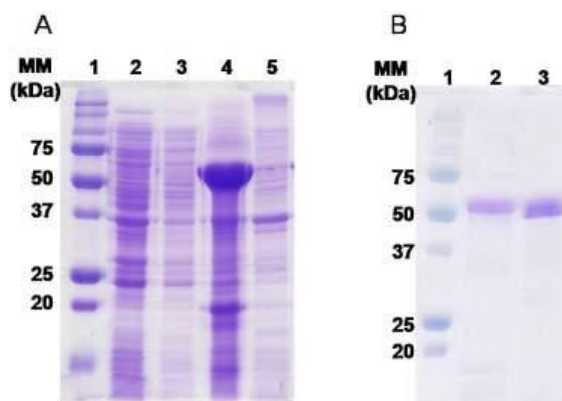


Figure 2.4: (A) SDS-PAGE analysis of McoA overproduction in *E. coli*. Lane 1, standard molecular mass markers, Lane 2, supernatant of a crude extract of an IPTG induced *E. coli* LOM409 culture, Lane 3, supernatant of a crude extract of non-induced *E. coli* LOM409 culture, Lane 4, insoluble fraction of a crude extract of an IPTG induced *E. coli* LOM409 culture, Lane 5, insoluble fraction of a crude extract of non-induced *E. coli* LOM409 culture. (B) SDS-PAGE analysis of purified McoA and McoAΔP321-V363. Lane 1, standard molecular mass marker, Lane 2, purified wild-type McoA protein, Lane 3, purified mutant McoAΔP321-V363 protein.

Attempts to produce the protein in the soluble form were unsuccessful. As a consequence, a protocol of unfolding and refolding was followed, as described in the 2.2 Experimental Procedures, and an enzyme solution with a blue colour (typical of blue multicopper oxidases) that exhibited enzymatic activity was successfully recovered. Dialysis and two chromatographic steps purified the protein to homogeneity (Figure 2.4B). The protein was identified by MALDI-TOF-MS after tryptic digestion with an identification score of 194 and sequence coverage of 46%. Gel filtration experiments gave a  $M_r$  value of 57.8 kD close to the theoretical value predicted for the monomer (59.5 kDa). The predicted isoelectric point (pI) of the enzyme was 5.33, whereas the measured pI of the purified enzyme was 4.12. To investigate the involvement of the Met-rich segment on McoA catalytic reaction a McoAΔP321-V363 mutant was constructed that lacks this region. The transformation and expression of the mutant enzyme was comparable to the wild type McoA. The molecular mass of the mutant

protein, as expected, is approximately 4.5 kDa lower than the wild type enzyme (Figure 2.4B).

**Spectroscopic characterisation.** McoA presents a typical UV-visible spectra for MCO (Figure 2.5A) with a the band at ~600 nm that corresponds to the Cu-Cys interaction at the T1 Cu center and a shoulder at 330 nm indicative of the presence of a hydroxyl group bridging the T3 copper ions (Solomon, et al., 1996).

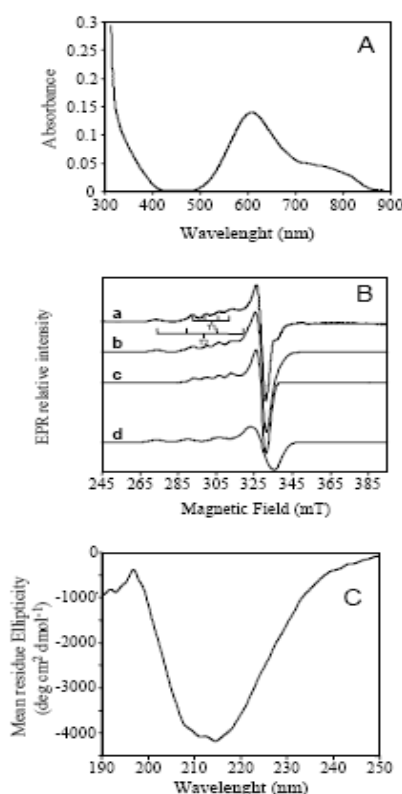


Figure 2.5: Spectroscopic properties of recombinant purified McoA. (A) UV-visible spectrum of McoA (70 $\mu$ M in 20mM Tris-HCl buffer, pH 7.6). (B) EPR spectrum. The T1 copper signal presents g values of 2.044, 2.044 and 2.221 and a hyperfine coupling constant  $A_1 = 68 \times 10^{-4} \text{cm}^{-1}$ , whereas the T2 copper center, the g and  $A_1$  values are 2.344, 2.055 and 2.269 and  $169 \times 10^{-4} \text{cm}^{-1}$ . Microwave frequency, 9.42 GHz; microwave power: 2.4 mW, modulation amplitude: 0.9 millitesla, temperature 95 K. (C) CD spectrum in the far UV reflecting a high  $\beta$ -sheet content.

A ratio of 2.5 mol copper/mol of protein was found for recombinant McoA. This finding is not completely surprising as a lower copper content has already been reported in other recombinant laccases such as the bacterial CotA-laccase (Martins, et al., 2002) and CueO from *E. coli* (Galli, et al., 2004). Indeed, copper incorporation in MCO has not been completely elucidated at the molecular level. The variant enzyme absorbance at 610 nm, relative to 280 nm, shows 40% less intensity (data not shown), than the wild type enzyme suggesting that the mutation has affected slightly the copper incorporation into the T1 Cu site. The EPR spectrum of the McoA protein presents resonances characteristic of copper center (Figure 2.5B). Spectrum simulation revealed the presence of two components integrated in the ratio 1:1. These components have g values and hyperfine coupling constants typical of T1 and T2 centers with g values of 2.044 and 2.222 and a hyperfine coupling constants,  $A_{\parallel}=68 \times 10^{-4} \text{ cm}^{-1}$  and 2.040, 2.055 and 2.260 and  $A_{\parallel}=169 \times 10^{-4} \text{ cm}^{-1}$ , respectively. The McoA variant enzyme was not different from the wild-type with regards to EPR spectroscopic characteristics (data not shown). The CD spectrum of McoA in the far-UV reflected the typical secondary structure found in MCO, rich in  $\beta$ -sheets with a negative peak at 213-214 nm (Figure 2.5C). Indeed, a secondary structure estimate based on the CDSSTR method yielded values of 6%  $\alpha$ -helical, 37%  $\beta$ -strand structure and more than 55% of turns and random coil structure (Sreerama, et al., 1999); these values are similar to those obtained by DSSP calculations based on the McoA model structure, namely 4%  $\alpha$ -helical and 32%  $\beta$ -strand structure (Kabsch and Sander, 1983). The CD spectrum of the variant McoA $\Delta$ P321-V363 (data not shown) showed a small increase in  $\alpha$ -helical and  $\beta$ -strand structure relatively to the wild type protein (from 6 to 8% and from 37 to 40%, respectively) and this correlates with the deletion of an unordered segment as proposed in the model structure. This also clearly indicates that deletion of the Met-rich segment did not cause any gross disruption or reorganization of the structure. The redox potential was measured by following the decrease in absorbance at 610 nm reflecting the reduction of

the T1 copper of McoA. The normalized amplitude of the absorbance at 610 nm and its dependence on the reduced potential is shown in Figure 2.6.

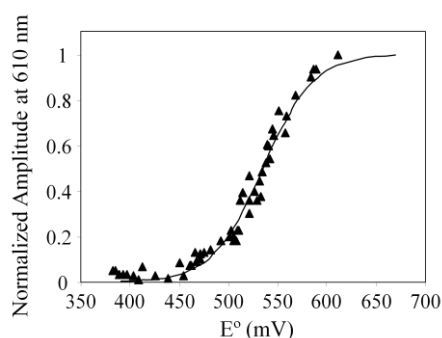


Figure 2.6: Redox titration of recombinant McoA. The solid line shows the best fit of the experimental data obtained using the Nernst equation, considering one electron transfer, with a reduction potential of 535mV.

The best fit was obtained using the Nernst equation, considering one electron transfer, with a redox potential of 535mV. The deletion of the Met-rich segment leads to redox potential of 494 mV (data not shown), only slightly lower than measured for the wild type enzyme. Redox potentials exhibited by MCO span a broad range of values, from 400 mV for plant laccases to 790 mV for some fungal laccases (Solomon, et al., 1996). McoA presents a high metal oxidative activity. The steady state kinetic parameters of purified *A. aeolicus* McoA were obtained for the metal ions  $\text{Fe}^{2+}$  and  $\text{Cu}^{+}$  and also for the substrates ABTS and SGZ in air saturated solutions, at 40°C (Table 2.1).

Table 2.1: Kinetic parameters for oxidation of the metal ions Cu(I), Fe(II) and the typical laccase substrates, ABTS (a non-phenolic compound) and SGZ (phenolic compound) of the recombinant purified wild-type McoA and its variant McoA $\Delta$ P<sub>321</sub>-V<sub>363</sub>, at 40°C.

	Substrates	$K_m$ ( $\mu$ M)	$K_m$ ( $\mu$ M) + Cu (II) <sup>a</sup>	$k_{cat}$ ( $\text{min}^{-1}$ )	$k_{cat}$ ( $\text{min}^{-1}$ ) + Cu (II) <sup>a</sup>	$k_{cat}/K_m$ ( $\text{min}^{-1}\mu\text{M}^{-1}$ )	$k_{cat}/K_m$ ( $\text{min}^{-1}\mu\text{M}^{-1}$ ) + Cu (II) <sup>a</sup>
Wild type	Cu (I) <sup>a</sup>	41 $\pm$ 2	46 $\pm$ 3	66 $\pm$ 5	165 $\pm$ 6	1.6	3.6
	Fe (II) <sup>b</sup>	5 $\pm$ 1	7 $\pm$ 2	17 $\pm$ 0.3	38 $\pm$ 0.6	3.4	5.4
	ABTS <sup>d</sup>	128 $\pm$ 8	59 $\pm$ 9	124 $\pm$ 5	114 $\pm$ 4	1.0	1.9
	SGZ <sup>e</sup>	38 $\pm$ 5	20 $\pm$ 3	29 $\pm$ 4	33 $\pm$ 6	0.8	1.7
McoA $\Delta$ P <sub>321</sub> -V <sub>363</sub>	Cu (I) <sup>a</sup>	39 $\pm$ 2	36 $\pm$ 5	8 $\pm$ 1	8 $\pm$ 0.3	0.2	0.23
	Fe (II) <sup>b</sup>	5 $\pm$ 2	9 $\pm$ 2	0.3 $\pm$ 0.01	0.2 $\pm$ 0.01	0.06	0.02
	ABTS <sup>d</sup>	57 $\pm$ 14	58 $\pm$ 11	0.41 $\pm$ 0.04	0.23 $\pm$ 0.05	0.005	0.004
	SGZ <sup>e</sup>	10 $\pm$ 3	12 $\pm$ 1	0.21 $\pm$ 0.02	0.11 $\pm$ 0.01	0.021	0.010

<sup>a</sup> optimal activity in the presence 100 $\mu$ M CuCl<sub>2</sub>

<sup>b</sup> in 100mM acetate buffer, pH 3.5 and 5% acetonitrile (optimal stability for the substrate).

<sup>c</sup> in 100mM MES buffer, pH 5 (optimal stability for the substrate).

<sup>d</sup> in Briton-Robinson buffer, pH 4 (optimal pH).

<sup>e</sup> in Briton-Robinson buffer, pH 7 (optimal pH).

The dependence of the enzymatic rates on substrate concentration followed Michaelis-Menten kinetics. The recombinant purified McoA exhibits higher enzyme specificity for the oxidation of the metal ions as compared to the typical laccase specificity for phenolic and non-phenolic substrates, and thus is designated as a metallo-oxidase. Maximal effectiveness ( $k_{cat}/K_m$ ) for the substrates tested was achieved upon addition of Cu<sup>2+</sup> to the reaction mixture. A 2-fold activation in the presence of exogenous Cu<sup>2+</sup> was observed at 100  $\mu$ M of CuCl<sub>2</sub> (concentration for optimal activity). Increased efficiency in the presence of cupric copper resulted for the metal substrates with an increase in the  $k_{cat}$  values (indicating activation in the electron transfer kinetics), while for the larger substrates there were decreased  $K_m$  values, indicating steric changes in the substrate binding pocket. Metal oxidase activities were also determined for purified human ceruloplasmin. With Fe<sup>2+</sup> as substrate, apparent  $K_m$  and  $k_{cat}$  values of 28  $\pm$  2  $\mu$ M and 8  $\pm$  2  $\text{min}^{-1}$  were determined. For Cu<sup>+</sup> oxidation the constants were 33  $\pm$  12  $\mu$ M and 15  $\pm$  1  $\text{min}^{-1}$ . These kinetic values are the same

order of magnitude as previous measurements for hCp (Stoj and Kosman, 2003). The  $k_{\text{cat}}/K_m$  value of McoA for  $\text{Cu}^+$  in the presence of exogenous copper is similar to that obtained for CueO from *E. coli* and two- to fourfold higher than for the yeast ferroxidase Fet3p and hCp (Singh, et al., 2004; Stoj and Kosman, 2003). McoA ferroxidase efficiency is three-fold higher compared with CueO and hCp and two-fold lower than for Fet3p (Singh, et al., 2004; Stoj and Kosman, 2003). All these data suggest that *A. aeolicus* McoA acts as a metallo-oxidase *in vivo*, acting as a cytoprotector and shifting the  $\text{Cu}^{2+}/\text{Cu}^+$  and  $\text{Fe}^{3+}/\text{Fe}^{2+}$  ratios towards the less toxic forms of copper and iron,  $\text{Cu}^{2+}$  and  $\text{Fe}^{3+}$  respectively, presumably in the periplasm of *A. aeolicus*, as predicted from the gene DNA sequence. Indeed, there is a growing indication of a link between periplasmic MCO and metal metabolism in bacteria that emerges from recent genetic, physiology and biochemical studies in *E. coli* (Grass, et al., 2004), *Pseudomonas aeruginosa* (Huston, et al., 2002), *Staphylococcus aureus* (Sitthisak, et al., 2005) and *Rhodobacter capsulatus* (Wiethaus, et al., 2006). McoA has maximal activity at pH 4 and 7 for ABTS and SGZ, respectively (data not shown), consistent with those exhibited by a number of laccases (Xu, 1999). The catalytic activity of McoA, for ABTS as substrate, was found to increase from a value of 2.3 to 7.2  $\mu\text{mol min}^{-1} \text{mg protein}^{-1}$  at 40°C and 75°C, respectively (data not shown). The optimal temperature ca. 75°C is identical to that observed for the CotA-laccase of *B. subtilis* (Martins, et al., 2002), but lower than the 92°C determined for the laccase of the thermophilic bacteria *Thermus thermophilus* (Miyazaki, 2005).

**Met-rich region is involved in the catalytic mechanism of McoA.** The deletion of the Met-rich segment resulted in a severe decrease in catalytic effectiveness for all the substrates tested (Table 2.1). The difference in the enzymatic efficiency in the variant McoA $\Delta$ P321-V363 compared with the wild type enzyme relies essentially in the  $k_{\text{cat}}$  term, suggesting that the presence of the Met-rich motif and its conformational arrangement is a key factor of the catalytic mechanism. In addition, no enzyme activation upon addition of  $\text{Cu}^{2+}$

was observed in the variant, showing that this segment most probably modulates the participation of exogenous  $\text{Cu}^{2+}$  in the catalytic mechanism, presumably through binding, in analogy with what happens in CueO. In the structure of a CueO crystal soaked in  $\text{CuCl}_2$  a labile  $\text{Cu}^{2+}$  ion is bound by two aspartates, two methionines, and a solvent molecule in the Met-segment near the T1 center, providing a possible electronic matrix coupling pathway for electron transfer into this center (Roberts, et al., 2003). The mutagenesis of these four copper ligands resulted in the loss of oxidase activity and copper tolerance, confirming a regulatory role for this site (Roberts, et al., 2003). In the variant enzyme, decreased  $K_m$  values were found for the larger aromatic substrates while these values remain basically unchanged for the smaller metal substrates when compared with the wild type enzyme. This may suggest that the Met-segment impairs the binding efficiency of larger substrates to the substrate binding site due to steric effects. This data supports a structure in which the Met-rich region masks the zone of the substrate binding site near the T1 Cu center, as observed in simulations of the McoA model structure. Interestingly, the  $K_m$  values for larger substrates in the Met-rich deleted enzyme are similar to values obtained in the wild type enzyme in the presence of copper. The presence of copper and its likely binding to this region could lead to a conformational change causing an enlargement of the substrate binding cavity. Clearly more structural studies are required.

**McoA is a hyperthermostable enzyme.** The kinetic stability of an enzyme is relevant not only in the evaluation of its thermostability, but also in the study of the pathway that leads to the formation of irreversible inactivated states of the enzyme. McoA activity decay can be fitted only through a sum of two exponentials (Figure 2.7A).

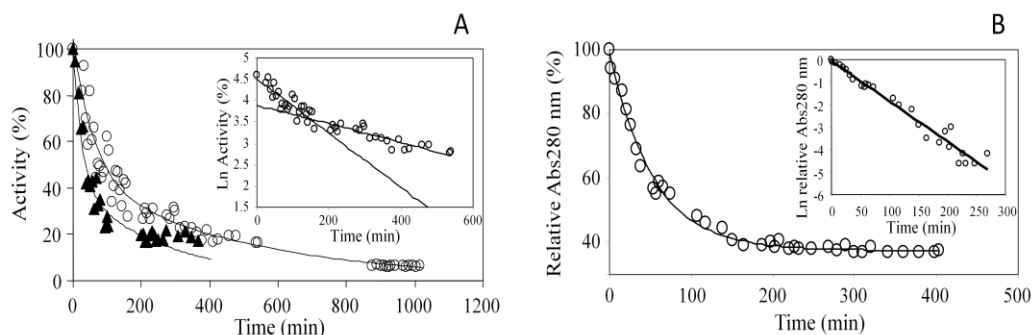


Figure 2.7: (A) Kinetic stability of McoA. Stabilities at 80°C (open circles) and 90°C (black triangles) was fitted accurately through a sum of two exponentials (the solid line shows the fit) according to scheme 1 shown in material and methods. The lifetime of the initial state E is 60 and 25min at 80 and 90°C, respectively. The intermediate state E1 with 50% of activity has a lifetime of 490 and 269min at 80 and 90°C, respectively, before giving the final state E2 with no activity. The inset shows clearly that the activity decay of McoA at both temperatures (data not shown for 90°C) cannot be fitted by a single first-order process as the logarithm of activity does not display an inverse linear relationship with time. (B) Amount of McoA soluble at 80°C measured by the absorbance at 280nm. The solid line shows a single-exponential fit with a rate constant of 0.019min<sup>-1</sup> (lifetime is 53±2min), an amplitude of 0.61 and an off-set value of 0.38 (the off-set value is the relative amount of McoA that remains soluble after completion and stabilization of the aggregates). The inset shows clearly that aggregation of McoA can be accurately fitted by a single exponential as proved by the inverse linear relationship between the logarithm of the relative absorbance at 280nm (after discounting the off-set value) and time.

This is clearly shown in a semilogarithm plot with two time range defining different linear relationships (insert of Figure 2.7B). A series-type mechanism is commonly used to describe deactivation pathways composed by two steps and this approach was used in the characterization of the kinetic stability of McoA (see Scheme (7), Experimental Procedures). The decay of McoA at 80°C is characterized by a first deactivation step that lasts 60 min resulting in an intermediate state with 50% of the initial activity. This intermediate deactivates slowly (lifetime of 490 min) to the final state that presents no activity. The same pathway describes McoA decay at 90°C but the rate constants of the two steps are higher as expected (lifetimes of 25 and 269 min for the first and second steps, respectively). By measuring the amount of soluble McoA at the different times of thermal incubation it was possible to assign the first phase of the activity decay to an aggregation process (Figure 2.7B). The amount of McoA soluble at 80°C decays accordingly to a single-exponential, giving a linear



relationship when plotted as a semi-logarithm graph (inset in Figure 2.7B). A lifetime of 53 min for the soluble species, very similar to the value of 60 min calculated for the first-phase of the activity decay, was calculated. Therefore, the 50% decay of initial activity was shown to be due to an aggregation process followed by a slow first-order step, as observed previously in other enzymes (Baptista, et al., 2003). The values obtained here indicate the extreme robustness of the McoA enzyme. However, the *T. thermophilus* laccase with a half-life of 868 min at 80°C is the most thermostable laccase reported so far (Miyazaki, 2005). The relative lower thermostability of the McoA in comparison to the *T. thermophilus* enzyme confirms a previous analysis described by Miyazaki (2005) of some parameters known to affect protein thermostability such as the proline content (10% and 5% for *Tth*-laccase and McoA, respectively) and the aliphatic index values, defined as the relative volume of the protein occupied by aliphatic chains of alanine, valine, isoleucine, and leucine (96.39 and 79.32 for *Tth*-laccase and McoA, respectively).



# 3 THE HYPERTHERMOPHILIC NATURE OF THE METALLO-OXIDASE FROM *AQUIFEX AEOLICUS*

---

3.1.	INTRODUCTION.....	75
3.2.	EXPERIMENTAL PROCEDURES.....	77
3.3.	RESULTS .....	80
3.4.	DISCUSSION.....	94

## ABSTRACT

The stability of the *Aquifex aeolicus* multicopper oxidase (McoA) was studied by spectroscopy, calorimetry and chromatography to understand its thermophilic nature. The enzyme is hyperthermostable as deconvolution of the differential scanning calorimetry trace shows that thermal unfolding is characterized by temperature values at the mid-point of 105, 110 and 114 °C. Chemical denaturation revealed however a very low stability at room temperature (2.8 kcal mol<sup>-1</sup>) because copper bleaching/depletion occur before the unfolding of the tertiary structure and McoA is highly prone to aggregate. Indeed, unfolding kinetics measured with the stopped-flow technique quantified the stabilizing effect of copper on McoA (1.5 kcal mol<sup>-1</sup>) and revealed quite an uncommon observation further confirmed by light scattering and gel filtration chromatography: McoA aggregates in the presence of guanidinium hydrochloride, i.e., under unfolding conditions. The aggregation process results from the accumulation of a quasi-native state of McoA that binds to ANS and is the main determinant of the stability curve of McoA. Kinetic partitioning between aggregation and unfolding leads to a very low heat capacity change and determines a flat dependence of stability on temperature.

**This chapter was published in the following scientific paper:**

André T. Fernandes, and Lígia O. Martins and Eduardo P. Melo. 2009. The hyperthermophilic nature of metallo-oxidase from *Aquifex aeolicus*. *Biochimica et Biophysica Acta*. 1794: 75-83.

### **3.1. INTRODUCTION**

The multi-copper oxidases (MCO) constitute a family of enzymes whose principal members are ceruloplasmin (Fe(II) oxygen oxidoreductase, EC 1.16.3.1), ascorbate oxidase (L-ascorbate oxygen oxidoreductase, EC 1.10.3.3) and laccase (benzenediol oxygen oxidoreductase, EC 1.10.3.2) (Lindley, 2001; Solomon, et al., 1996). This family of enzymes is widely distributed throughout nature and members are encoded in the genomes of organisms in all three domains of life - Bacteria, Archaea and Eukarya (Enguita, et al.). MCO that contain ~500 amino acid residues are composed of three Greek key  $\beta$ -barrel cupredoxin domains (domains1, 2 and 3) that come together to form three spectroscopically distinct types of Cu sites, i.e. type 1 (T1), type 2 (T2), and type 3 (T3) (Lindley, 2001; Solomon, et al., 1996). The T1 Cu site is characterized by an intense Cys-S  $\pi$  to  $\text{Cu}^{2+}$  charge transfer absorption at about 600 nm responsible for the blue color of these enzymes. The T2 Cu site is characterized by the lack of strong absorption features. The T3 Cu site is composed of two Cu atoms typically antiferromagnetically coupled, for example, through a hydroxide bridge. It is characterized by an intense transition at 330 nm originating from the bridging ligand that is apparent as a shoulder on the protein absorbance band at 280 nm. T1 mononuclear copper site is the primary acceptor site for electrons derived from the reducing substrate while the T2 and T3 sites form a trinuclear center that is the site for  $\text{O}_2$  reduction (Lindley, 2001; Solomon, et al., 1996; Stoj and Kosman, 2005). Multi-copper oxidases have broad substrate specificity and oxidize numerous aromatic phenols and amines. Only a few members present higher specificity to lower valent metal ions such as  $\text{Mn}^{2+}$ ,  $\text{Fe}^{2+}$  or  $\text{Cu}^+$ , being thus designated as metallo-oxidases (Stoj and Kosman, 2005). The best studied metallo-oxidases are human ceruloplasmin, yeast Fet3p and bacterial CueO which are suggested to play an in vivo catalytic role in the maintenance of both copper and iron homeostasis in their respective organisms.

We had recently cloned, overproduced, purified and characterized a recombinant metallo oxidase (McoA) from *Aquifex aeolicus*, a hydrogen-oxidising, chemolithoautotrophic bacterium that grows between 58 and 95 °C and optimally at 89 °C, occupying the deepest branch of the bacterial phylogenetic tree (Eder and Huber, 2002; Fernandes, et al., 2007). We found that McoA is a copper-activated metallo-oxidase with spectroscopic properties typical of MCO. However one particular aspect of McoA is the presence of a methionine rich region segment (residues 321–363) evidenced in the comparative model structure, reminiscent of those found in copper homeostasis proteins. Reaction kinetic analysis of the wild type enzyme and the deletion mutant (McoAΔP321-V363) without the methionine rich segment indicates that this region is near the T1 Cu catalytic center and is most probable involved in the catalytic mechanism through copper binding (Fernandes, et al., 2007).

The study of the hyperthermophilic nature of *A. aeolicus* McoA offers an opportunity to get insight into protein general mechanisms of thermostability and into stability mechanisms of this particular family of enzymes. Studies on the stability of MCO have focused mainly on thermal stability measured by differential scanning calorimetry (Agostinelli, et al., 1995; Durao, et al., 2006; Durao, et al., 2008; Koroleva, et al., 2001; Savini, et al., 1990). The study of unfolding pathways using chemical denaturants has been mostly performed for the small blue copper proteins which only have a T1 copper center (Alcaraz and Donaire, 2004; Alcaraz, et al., 2005; Bonander, et al., 2000; Mei, et al., 1999; Pozdnyakova, et al., 2001) besides a recent report with human MCO ceruloplasmin (Salgueiro, et al., 1997; Sedlak and Wittung-Stafshede, 2007). The stability of McoA was assessed in this work by using spectroscopic techniques, differential scanning calorimetry (DSC) and gel-filtration chromatography. Stopped-flow kinetics was performed to obtain additional information regarding the mechanism of unfolding and the role of copper in the stabilization of McoA. To our knowledge this is the first report on studies of MCO based on unfolding kinetics. Their measurement quantified the increase in

McoA stability due to copper binding and revealed the importance of aggregation processes on McoA stability. Among the different possible mechanisms responsible for its high thermostability McoA features an extremely flat dependence of stability on temperature.

### **3.2. EXPERIMENTAL PROCEDURES**

**Protein expression and purification.** Purification of recombinant McoA from *A. aeolicus* was performed as described before (Fernandes, et al., 2007). Apo-McoA was obtained by incubating McoA in 20 mM Tris HCl buffer, pH 7.6 in the presence of EDTA (5 mM) for 1 h followed by dialysis. Protein copper content of McoA forms was determined using the trichloroacetic acid/bicinchoninic acid method of Brenner and Harris (Brenner and Harris, 1995) and confirmed by atomic absorption spectroscopy (Instituto Superior Técnico, Universidade Técnica de Lisboa).

**UV-Vis Spectra.** UV–visible spectra were acquired using a Nicolet Evolution 300 spectrophotometer from Thermo Industries.

**Enzyme assays.** The enzymatic activities were routinely assessed at 40 °C using syringaldazine (SGZ) as substrate. The assay mixtures contained 0.1 mM SGZ, 20 mM Tris–HCl buffer pH 7.6 and the reactions were followed at 530 nm ( $\epsilon_{530}=65,000 \text{ M}^{-1} \text{ cm}^{-1}$ ). The protein concentration was measured by using the absorption band at 280 nm ( $\epsilon_{280}=75,875 \text{ M}^{-1} \text{ cm}^{-1}$ ).

**Equilibrium unfolding studies.** Steady-state fluorescence was measured in a Cary Eclipse spectrofluorimeter using 2  $\mu\text{M}$  of McoA and 296 nm as excitation wavelength. Increased guanidinium hydrochloride (GdnHCl) concentrations were used to induce proteins unfolding at pH 7.6 (20 mM Tris-HCl buffer) and pH 3 (50 mM glycine buffer). To monitor unfolding of McoA, a combination of fluorescence intensity and emission maximum was used as described by Durão et al. (2006). Unfolding of McoA was difficult to quantify through total emission (by integrating the fluorescence emission at different wavelengths) or

single wavelength fluorescence emission as the difference between the emission from folded and unfolded states is not very significant. The combination of fluorescence intensity and emission maximum decreases data scatter and gives very similar stability parameter values compared to the ones obtained from total fluorescence emission. The thermodynamic stability of McoA monitored by fluorescence was analyzed according to a two-state process using the following equations:

$$(9) \quad y = y_F f_F + y_U f_U$$

$$(10) \quad K_{(U-F)} = f_U / f_F$$

$$(11) \quad \Delta G_{(U-F)} = -RT \ln K_{(U-F)}$$

$$(12) \quad \Delta G_{(U-F)} = \Delta G_{(U-F)}^{water} - m_{(U-F)} [GdnHCl]$$

$$(13) \quad [GdnHCl]_{50\%} = \Delta G_{(U-F)}^{water} / m_{(U-F)}$$

where F and U are folded and unfolded states of McoA, respectively, y is the fluorescence signal, f is the fraction of McoA molecules with a given conformation, K is the equilibrium constant,  $\Delta G$  is the standard free energy,  $m_{(U-F)}$  is the linear dependence of  $\Delta G$  on GdnHCl concentration and  $[GdnHCl]_{50\%}$  is the GdnHCl concentration for  $\Delta G=0$ .  $y_F$  and  $y_U$  were calculated directly from the pre- and post-transition regions according to a linear dependence. Copper bleaching/depletion and loss of activity induced by GdnHCl were performed at 40 °C as described by Durão et al. (2006) and quantified by using Eqs. (9-13) but assuming an equilibrium that describes copper bleaching/depletion from the folded state. Copper bleaching resulting from reduction of the T1 Cu site cannot be distinguished from copper depletion and were used indistinctly.

**Quenching of fluorescence by acrylamide.** Quenching of tryptophyl fluorescence was carried out by titrating a McoA solution with a stock solution of acrylamide at room temperature in 20 mM Tris–HCl, pH 7.6 with 200 mM



NaCl. Excitation was at 296 nm and total fluorescence emission (F) was integrated from 305 to 420 nm. The total fluorescence was then corrected to account for acrylamide absorbance as described elsewhere (Andrade and Costa, 2002). Data was fitted to the Stern–Volmer equation:

$$(14) \quad F_0 / F = 1 + K_{SV} [Q]$$

where  $F_0$  and  $F$  are the total fluorescence emission in the absence and presence of quencher, respectively,  $K_{SV}$  is the Stern–Volmer quenching constant and  $[Q]$  is the acrylamide concentration.

**Thermal denaturation.** DSC was carried out in a VP-DSC from MicroCal at a scan rate of 60 °C/h. The experimental calorimetric trace was obtained with 0.3 mg/ mL of protein at pH 3 (50 mM glycine buffer) and a baseline obtained with buffer alone was subtracted from the experimental trace. The resulting McoA DSC trace was analyzed with the DSC software built within Origin spreadsheet to obtain the transition excess heat capacity function (a cubic polynomial function was used to fit the shift in baseline associated to unfolding). The excess heat capacity can only be accurately fitted using a non two-state model with three transitions (equation in the data analysis software).

**Gel filtration chromatography.** Gel filtration chromatography was carried out in a Superose 12 HR10/30 column (GE Healthcare) using 20 mM Tris-HCl, pH 7.6, 200 mM NaCl as eluent. For runs in the presence of GdnHCl the column was previously equilibrated with the same buffer containing the desired concentration of GdnHCl. Samples of McoA at 0.5 mg/mL concentration were incubated in 0–4 M GdnHCl for 1 h at room temperature before injection. Ribonuclease (13.7 kDa), chymotrypsinogen A (25 kDa), ovalbumin (43 kDa), albumin (67 kDa), aldolase (158 kDa) and catalase (232 kDa) were used as standards.

**Stopped-flow kinetics.** Kinetic experiments were carried out on an Applied Photophysics Pi-Star 180 instrument with fluorescence intensity detection. The

McoA and GdnHCl solutions both at pH 7.6 (20 mM Tris-HCl buffer) were mixed at a 1:10 ratio to give a final protein concentration between 2 and 0.05  $\mu\text{M}$  and the desired denaturant concentration and at least 6 shots were averaged for each denaturant concentration. Excitation was always at 296 nm and emission detected above 315 nm using a glass filter. Kinetics followed through fluorescence of ANS (8-anilino-1-naphthalenesulfonic acid) were recorded using excitation at 390 nm and emission detection above 455 nm (cut-off filter). The volumetric mixing ratio was of 1:10 and ANS (4  $\mu\text{M}$ ) was present in the GdnHCl solution only leading to a final ANS concentration of 3.6  $\mu\text{M}$  (final McoA concentration was 2  $\mu\text{M}$ ). To measure light scattering during a stopped-flow experiment the mixed ratio was kept at 1:10 but excitation was set at 500 nm and no filter was used in the emission photomultiplier. Protein concentrations in the optical cell of the stopped-flow were increased up to 9  $\mu\text{M}$  in the light scattering experiment. Kinetics of unfolding measured by fluorescence emission was analyzed according to a multi-exponential fit using the Pro-Data Viewer software provided by Applied Photophysics. The dependence of the logarithm of the rate constants on GdnHCl concentration was fitted using Origin software according to the following equation:

$$(15) \quad \ln k_{obs} = \ln k_U^{water} + m_U [GdnHCl]$$

where  $k_U^{water}$  is the rate constant of unfolding in water and  $m_u$  is the constant reflecting the linear dependence of the rate constant on GdnHCl concentration. The values of  $m_U$  are directly proportional to amino acid exposure to solvent upon unfolding (Fersht, 1998).

### 3.3. RESULTS

**Thermal stability.** Thermal stability of McoA tertiary structure was probed by DSC (Figure 3.1). The endothermic peak for thermal unfolding at pH 3 (higher pH values lead to protein precipitation before significant unfolding could be observed) displays a complex process. First, aggregation after unfolding was

observed leading to 100% irreversibility (no peak in the second scan). Secondly, the excess heat capacity can only be accurately fitted by considering three independent transitions. As expected, McoA is hyperthermostable exhibiting  $T_m$  values (temperature at which 50% of the molecules are unfolded) of 105 ( $\pm 1.5$ ), 110 ( $\pm 0.7$ ) and 114 ( $\pm 0.8$ ) °C. Each transition is actually a non-two state process as the calorimetric molar enthalpy is significantly smaller than the van't Hoff enthalpy, ( $\Delta H_{cal}/\Delta H_{vH}=0.71$ , 0.37 and 0.20, respectively for the first, second and third thermal transitions). DSC scans of apo-McoA did not give accurate results as apo-McoA aggregates (revealed by an exothermic shift in the baseline) before detection of an endothermic peak.

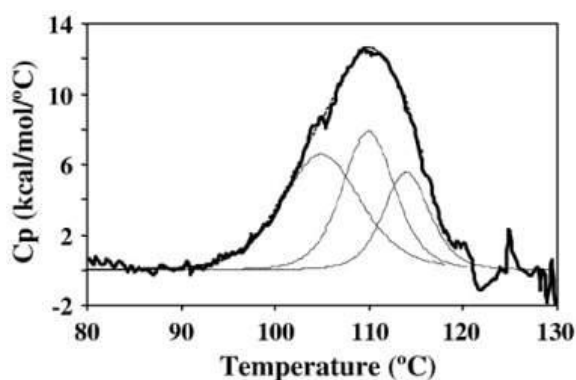


Figure 3.1: Excess heat capacity obtained from a DSC scan of McoA at pH 3 (thick line) fitted with three independent transitions shown separately in dashed lines as one or two transitions could not fit accurately the experimental trace. The dashed line under the DSC trace is the resulting sum of the three independent transitions.

**Thermodynamic stability and importance of copper.** The thermodynamic stability of McoA was studied by probing the tertiary structure, (fluorescence intensity), the copper binding at T1 center (absorbance at 610 nm) and also the enzyme activity in the presence of the chemical denaturant GdnHCl. Figure 3.2 shows the unfolding of the tertiary structure of McoA induced by increasing GdnHCl concentrations.

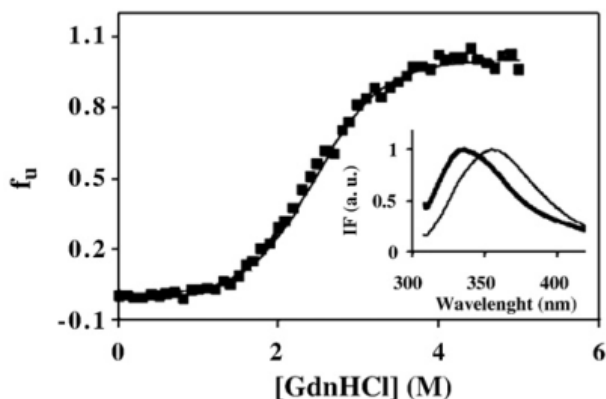


Figure 3.2: Fraction of McoA unfolded ( $f_U$ ) by GdnHCl at pH 7.6 as measured by fluorescence emission at 25 °C. The solid line is the fit according to the equation  $f_U = \frac{e^{(-\Delta G^0/RT)}}{1 + e^{(-\Delta G^0/RT)}}$  which was derived from Eqs. (11-15) and assumes the equilibrium  $F \leftrightarrow U$ . The inset shows the normalized emission spectra of folded (thick solid line) and unfolded McoA in the presence of 5 M GdnHCl (thin solid line). Stability at pH 3.0 is very similar (see Table 3.1).

With selective excitation of tryptophan residues at 296 nm, the wavelength at the emission maximum shifted from around 336 to around 355 nm upon unfolding reflecting the exposure of tryptophan residues at the protein surface (inset in Figure 3.2). McoA has seven tryptophan residues and their degree of exposure ranges from 0 to 56% in the model structure (Fernandes, et al., 2007), as compared to the exposure of Trp in a standard Gly-Trp-Gly extended peptide (Clothier, 1976). The unfolding of McoA induced by GdnHCl is apparently described by a two-state process where the folded and unfolded states seem to be the only states that accumulate at significant amounts. McoA tertiary structure unfolded with a mid-point of 2.7 M (GdnHCl concentration where 50% of the protein molecules were unfolded) and in water the folded state was more stable than the unfolded state by 2.8 kcal/mol at pH 7.6 (Table 3.1).

Table 3.1: Thermodynamic stability of apo- and as-isolated McoA at pH 7.6 and pH 3 in the absence and presence of copper in solution assessed by fluorescence emission (tertiary structure), activity and absorbance at 610 nm.

	$\Delta G^{\text{water}}$ (kcal mol <sup>-1</sup> )	[GdnHCl] <sub>50%</sub> (M)	$m$ (kcal mol <sup>-1</sup> M)
<b>Tertiary structure<sup>a</sup></b>	2.8 ± 0.6 (3.2 ± 0.2)	2.66 ± 0.32 (2.5 ± 0.1)	-1.0 ± 0.1 (-1.2 ± 0.1)
<b>Tertiary structure<sup>a</sup> (apoMcoA)</b>	2.3 ± 0.1 (3.3 ± 0.3)	2.32 ± 0.34 (2.4 ± 0.2)	-1.0 ± 0.2 (-1.4 ± 0.0)
<b>Tertiary structure<sup>a</sup> (McoA:copper 1:4)</b>	2.7 ± 0.4 (3.5 ± 0.3)	2.62 ± 0.29 (2.3 ± 0.1)	-1.0 ± 0.0 (-1.5 ± 0.1)
<b>Activity<sup>b</sup></b>	-1.3 ± 0.0	<sup>c</sup>	-13.9 ± 6.3
<b>Activity<sup>b</sup> (McoA:copper 1:4)</b>	0.12 ± 0.02	0.01	8.2 ± 0.1
<b>Abs 610 nm<sup>b</sup></b>	0.11	0.16	-0.7

Stability parameters of McoA at pH 3.0 are shown between brackets.

a Assuming the equilibrium  $F \leftrightarrow U$ .

b Assuming the equilibrium  $F \leftrightarrow F_{\text{copper bleached/depleted}}$ .

c At 0 M GdnHCl copper is bleached/depleted in more than 50% of the molecules ( $\Delta G_{U-F}^{\text{water}}$  is negative) and therefore the mid-point cannot be defined.

This low free energy gap at 25 °C in water is not associated to a specific set of titrating groups (notice that similar values were obtained at pH 7.6 and 3.0) but should mainly reflect the low cooperativeness of the transition as evaluated by the  $m_{(U-F)}$  parameter. We have found that the copper content of McoA does not affect the stability of the tertiary structure (Table 3.1). The as isolated enzyme is partially copper depleted (2.5:1, Cu/McoA) but addition of exogenous copper up to a final ratio of 4:1 (Cu/protein) has no influence in the conformational stability parameters. Moreover, the stability of apo-McoA (0.02:1, Cu:McoA) is only slightly lower than the exhibited by the as-isolated enzyme in the absence or presence of exogenous copper. Equilibrium refolding experiments carried out by dilution of McoA in 5 M GdnHCl have shown that unfolding induced by guanidinium is mostly but not totally reversible (data not shown). This statement is based on two observations: The refolding curve is shifted to lower guanidinium concentrations (around 1 M) and the fluorescence emission peak does not reach the value observed for native McoA (has reached 339 nm instead of 336 nm). A low degree of irreversibility can decrease slightly the absolute

values measured for the stability of McoA if the irreversible pathway shifted the equilibrium between folded and unfolded McoA within the transition region. By probing different levels of protein structure and function it is possible to get further insight on protein stability and unfolding pathways. Therefore, decays of activity and absorbance at 610 nm (signal from T1 Cu center) were also followed at increasing GdnHCl concentrations (Figure 3.3).

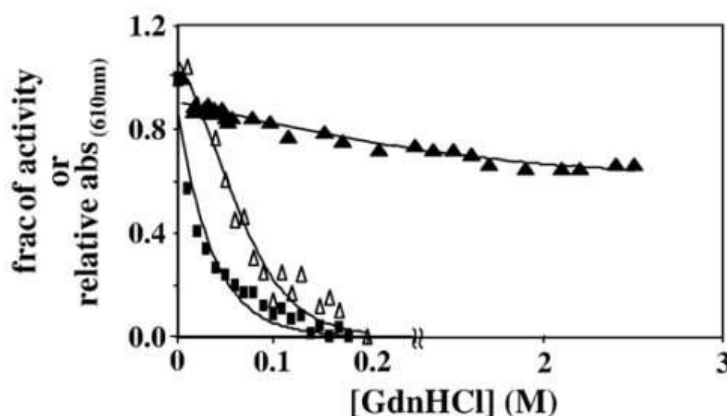


Figure 3.3: Change in activity in the absence (■) and presence of copper (Δ) (copper:McoA ratio is 4:1) and relative absorbance of McoA at 610 nm(▲) in the presence of increasing concentrations of GdnHCl, at 40 °C. The solid lines are the fits according to the equation  $y = y_F + y_{F(\text{copper bleached/depleted})} e^{(-\Delta G^\circ/RT)} / (1 + e^{(-\Delta G^\circ/RT)})$  which was derived also from Eqs. (11–15) and assumes the equilibrium  $F \leftrightarrow F_{(\text{copper bleached/depleted})}$ . The parameters  $y_F$  and  $y_{F(\text{copper bleached/depleted})}$  are the fraction of activity or the relative absorbance at 610 nm of folded McoA and folded McoA with copper bleached/depleted, respectively.

As absorbance at 610 nm and enzymatic activity are dependent on the presence of oxidised Cu atoms in the catalytic centers, both decays were described by a two-state process assuming an equilibrium between the folded state and the folded state with bleached copper as previously shown to occur in the CotA laccase (Durao, et al., 2006). The process of copper bleaching from T1 and the concomitant loss of activity are not related with the unfolding of tertiary structure as this only occur at higher GdnHCl concentrations. However, in contrast with CotA, in McoA the activity decay should not be mainly caused by the bleaching of T1 copper as it occurred at lower GdnHCl concentrations than the drop of the absorbance at 610 nm (Figure 3.3). In particular, the  $m$

parameter which represents the dependence of free energy change associated to copper bleaching on denaturant concentration is significantly different for the transition assessed by activity or absorbance at 610 nm (Table 3.1). This indicates that the T2/T3 Cu sites of McoA are affected at lower GdnHCl concentrations than the T1 Cu center. Indeed, in most MCO structures, T2 Cu appears to be the most labile center showing many times severe copper depletion, followed by the T3 center also showing some copper depletion (Bento, et al., 2005; Savini, et al., 1990). Additionally we show that activity decay of McoA is delayed in the presence of exogenous copper (Figure 3.3). This probably indicates that copper added exogenously binds to the protein and shifted the equilibrium towards the folded state of the enzyme with bound copper (the increase in the free energy gap, from  $-1.3$  to  $0.12$  kcal mol<sup>-1</sup> shown in Table 3.1 reflects this shift). In fact, the mid-point (GdnHCl concentration where 50% of the molecules are active) could only be determined in the presence of exogenous copper reflecting this shift in the equilibrium. Lower concentrations of denaturant than those required for the unfolding of the overall structure should lead to McoA copper bleaching/depletion. This would explain the similar stability of the tertiary structure of the different McoA forms; as-isolated in the absence or presence of exogenous copper and apo-enzyme (Table 3.1).

#### **Kinetics of chemically induced unfolding and aggregation of McoA.**

Kinetics of unfolding and refolding was measured using the stopped-flow technique. The kinetics of folding of McoA is complex with a lag phase before refolding dependent on enzyme and GdnHCl concentration (data not shown). The lag phase dependence on protein concentration indicates protein aggregation of the unfolded state when suddenly placed under native conditions in the dead-time of the stopped-flow experiment (Silow, et al., 1999). Therefore, kinetics of refolding was not analyzed in detail due to its complexity. Kinetics of unfolding was analyzed at different GdnHCl concentrations and at different McoA concentrations (Figure 3.4). For a final concentration of 2  $\mu$ M

protein (22  $\mu\text{M}$  of McoA in the reservoir syringe before the mixture), unfolding can be accurately fitted by using three exponentials as shown in Figure 3.4A. However, if McoA concentration is decreased to 0.5  $\mu\text{M}$  or below, two exponentials were enough to fit the kinetic traces indicating that protein aggregation is responsible for at least one of the kinetic constants observed with 2  $\mu\text{M}$  (Figure 3.4B). Thus, the additional kinetic phase observed at high McoA concentrations was related to an aggregation process occurring when the folded state of McoA is suddenly placed under unfolding conditions. The aggregation process was additionally proved by measuring light scattering of protein samples in a stopped-flow shot (Figure 3.4C). Light scattering increases with increasing McoA concentrations during the first 100 ms upon exposition to unfolding conditions.



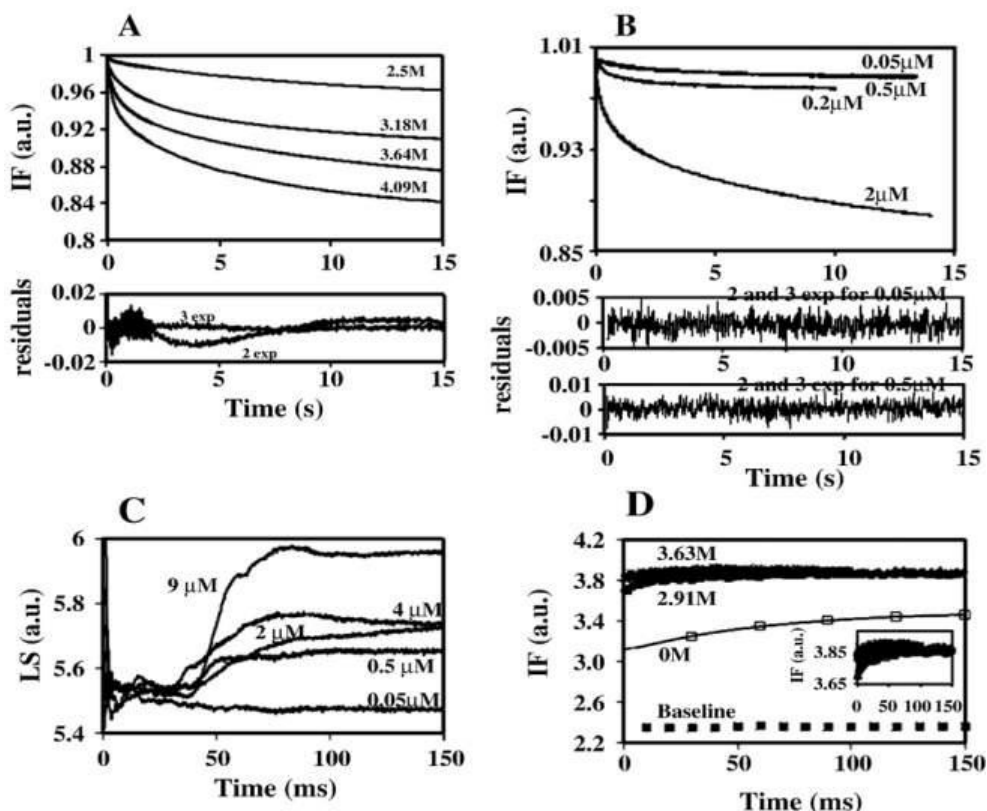


Figure 3.4: (A) Kinetic traces of 2 μM of McoA at pH 7.6 obtained at different GdnHCl concentrations. Kinetic traces had to be fitted according to a triple exponential equation independently of GdnHCl concentration. A double exponential equation cannot fit accurately the data as shown in the residuals plot. (B) Kinetic traces of McoA at different protein concentrations were measured at 3.64 M GdnHCl and were accurately fitted by using a double exponential equation up to 0.5 μM McoA concentration as residuals did not decrease from a double to a triple exponential fit (residuals plots). (C) Kinetic traces of McoA at different protein concentrations measured by light scattering (LS) during the first 150 ms after the dead time of the stopped-flow upon mixture with 3.64 M GdnHCl. (D) Kinetic traces followed trough fluorescence of ANS (excitation at 390 nm) during the unfolding of 2 μM of McoA upon mixture with 3.63 or 2.91 M GdnHCl. Both traces were fitted accurately by a single exponential with rate constants of 99.7 and 39.5 s<sup>-1</sup>, respectively. The inset shows the first 150 ms of the two kinetic traces to highlight the amplitude of the trace which is large enough to be fitted accurately. The fluorescence of ANS alone in the absence of protein is show as the baseline and the binding of ANS to folded McoA (0M GdnHCl curve) could only be fitted by using a three exponential equation with rate constants of 18.3, 1.5 and 0.12 s<sup>-1</sup>.

Protein aggregation has been related to partial exposure of hydrophobic surfaces that may be probed through fluorescence of the dye ANS (De Felice, et al., 2004; Pedersen, et al., 2004; Plakoutsi, et al., 2004; Ricchelli, et al., 2006). Therefore, the fluorescence of ANS was used to probe the unfolding of McoA

induced by GdnHCl in a stopped-flow experiment (Figure 3.4D). Kinetic traces described by a single rate constant were obtained. The rate constants measured ( $39.5$  and  $99.7\text{ s}^{-1}$  at  $2.91$  and  $3.63\text{ M}$  GdnHCl) are faster than the fastest rate constant measured through McoA fluorescence and reports the formation of a species within the first  $10\text{--}25\text{ ms}$ , prior to the aggregation process. ANS fluorescence reveals thus the formation of a species that precede McoA aggregation. As expected, in the absence of GdnHCl, ANS binds significantly slower to McoA with kinetics that could only be fitted with three exponentials. These are most probably related to ANS binding to regions with different accessibilities in the folded McoA. Considering that the fastest rate constant ( $18.3\text{ s}^{-1}$ ) is smaller than those measured prior to aggregation this rate should describe binding to more exposed hydrophobic patches in the native protein.

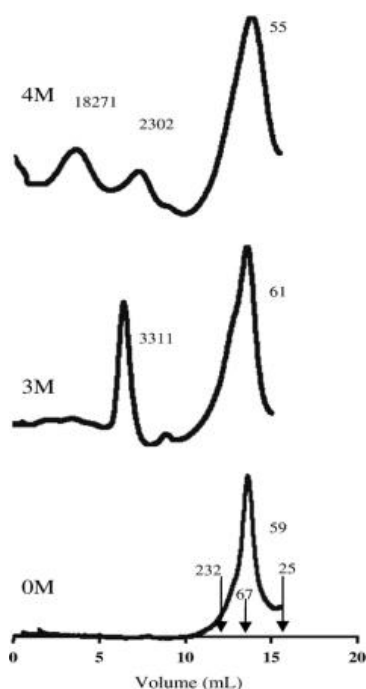


Figure 3.5: Gel filtration chromatography of McoA in the absence and presence of 3 and 4 M of GdnHCl. Arrows point to elution volumes of specific molecular weight standards and numbers assigned to peaks are the molecular weights calculated from the standards calibration curve.

The tendency of McoA for aggregation was also proved by gel filtration chromatography in the presence of guanidinium hydrochloride (Figure 3.5). At 0 M GdnHCl McoA elutes as a monomer according to its molecular weight of 59.5 kDa. In the presence of 3M and 4M GdnHCl where the protein is mostly or totally unfolded, large aggregates were detected in the chromatograms. Roughly, these aggregates can have from 40 to 300 McoA molecules according to the molecular weights extrapolated from standard calibration curves.

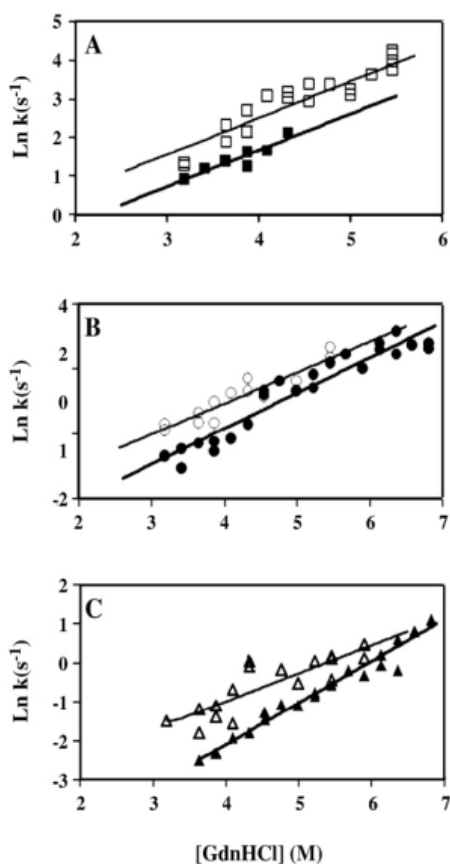


Figure 3.6: Logarithm of the three unfolding rate constants of as-isolated McoA (solid symbols) and apo-McoA (empty symbols) at different GdnHCl concentrations. The values of  $k_1$  (■, □) were shown in A,  $k_2$  (●, ○) in B and  $k_3$  (▲, △) in C and were fitted to Eq. (17).

The logarithm of the three rate constants of McoA unfolding at 2  $\mu$ M measured by stopped-flow were plotted in Figure 3.6 and describe the unfolding limb of a chevron plot. These were well fitted assuming a linear relationship with GdnHCl concentration, indicating that addition of higher amounts of

guanidinium hydrochloride causes a linear decrease of the free energy gap between the initial ground state and the transition state. This linear relationship also applies to the first phase assigned to the aggregation pathway (Figure 3.6A). The slope of this relationship, representing the  $m_u$  parameter, is directly proportional to amino acids exposure during the transition (Fersht, 1998). The ratio between  $m_u$  from kinetics and  $m_{(U-F)}$  from equilibrium experiments, also known as Brønsted  $\beta$  value, gives the fractional change in amino acid exposure in the transition state as compared to the final state (for an unfolding transition,  $\beta=1$  means a transition state as exposed as the unfolded state). These ratios are 0.63, 0.65 and 0.56 (calculated as  $m_u/RTm_{(U-F)}$ ) for the three transitions, showing that two out of three rate constants measured for 2  $\mu$ M of McoA result from parallel unfolding pathways that lead to protein aggregation. In fact, if all the measured rate constants resulted from a sequential unfolding pathway the transition state for the last unfolding step would have a  $\beta$  value of 1.84 and thus an improbably larger surface area exposed to solvent than the unfolded state which is assumed to be random coil and thus fully exposed. As mentioned above, the stabilizing effect of copper on McoA could not be quantified through equilibrium unfolding studies using GdnHCl as denaturant as copper should be depleted prior to the overall protein unfolding. The stabilization by copper was thus quantified through kinetic measurements. Kinetic measurements were used previously to quantify the increase in stability for the apo- to the holo-form of the small blue copper azurin which has only a T1 copper (Pozdnyakova, et al., 2001). Unfolding of apo-McoA (without copper) is faster compared with the as-isolated McoA (2.5:1, Cu/protein) due to the stabilizing effect of copper (Figure 3.6). Based on the differences between the rate constant in water ( $k_U$  water) for the as-isolated and apo-McoA it is possible to quantify the stabilizing effect of copper. The change induced by copper in the free energy gap between the ground state and the transition state can be calculated based on the following equation derived from the Arrhenius law:

$$\Delta\Delta G^\ddagger = RT (\ln k_{\text{no copper}} - \ln k_{\text{copper}})$$

Copper increases the free energy gap by 0.49, 0.79 and 1.5 kcal/mol for  $k_1$ ,  $k_2$  and  $k_3$ , respectively. The stabilizing effect of copper on the native state of McoA was 1.5 kcal mol<sup>-1</sup> when it is assumed that  $k_3$  reports the unfolding of monomeric McoA. Actually, as stated above, this value reports the free energy difference between the ground and the transition state and therefore reports the lower limit for the stabilizing effect of copper on the native state (it assumes no affinity of copper for the transition state).

**Dependence of stability on temperature.** The dependence of stability of McoA on temperature was also studied. Since direct measurement of  $\Delta C_p$  or measurements through changes of enthalpy by using DSC were not possible due to protein aggregation, a different approach was used to estimate the stability of McoA at different temperatures (Otzen and Oliveberg, 2004; Pace and Laurents, 1989). The apparent  $T_m$  value of 110 °C, corresponding to the peak of the excess heat capacity, as determined by DSC, and values of  $\Delta G^{\text{water}}$  measured at different temperatures using GdnHCl as denaturant were used to fit the temperature dependence of stability using the Gibbs–Helmholtz equation (Figure 3.7). Since its first proposal (Pace and Laurents, 1989), this methodology has been validated for other proteins (Otzen and Oliveberg, 2004; Pace and Laurents, 1989; Scholtz, 1995). However, combination of chemical and thermal stability has to be done with caution as the final unfolded state can be structurally different as clearly illustrated for human ceruloplasmin (Sedlak and Wittung-Stafshede, 2007; Sedlak, et al., 2008). Also for McoA, the final unfolded states should be structurally different as chemical unfolding is almost totally reversible compared to total irreversibility upon thermal unfolding. With this limitation in mind, the dependence of McoA stability on temperature was analyzed by combining chemical and thermal experiments. Stability of McoA plotted versus temperature at pH 7.6 and pH 3 shows that this enzyme presents an extremely flat dependence of stability on temperature. This can be explained by a change in the  $\Delta C_p$  upon unfolding of 0.11 and 0.27 kcal mol<sup>-1</sup> K<sup>-1</sup>, at pH 7.6 and 3, respectively.

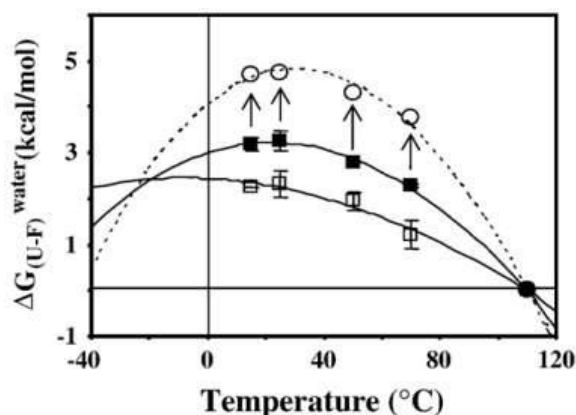


Figure 3.7: Temperature dependence of McoA stability at pH 7.6 (□) and pH 3 (■) built with an average  $T_m$  measured by DSC and chemical unfolding at different temperatures induced by GdnHCl. Experimental data was fitted (solid line) with the Gibbs–Helmholtz equation ( $\Delta G = \Delta H (1 - T/T_m) - \Delta C_p [(T_m - T) + T \ln(T/T_m)]$ ) using the Origin software to calculate the enthalpy change at  $T_m$  and the heat capacity change. Both, the  $\Delta C_p$  and the enthalpy change were allowed to change during the fit as the use a fixed value of  $\Delta H_{T_m}$  derived from the DSC scan prevents the convergence between the fit and experimental data (total enthalpy change derived from the DSC scan was  $167 \text{ kcal mol}^{-1}$  and that obtained from the fit was  $45 \text{ kcal mol}^{-1}$  at pH 3). Values of  $\Delta C_p$  are  $0.11 \pm 0.04$  and  $0.27 \pm 0.02 \text{ kcal mol}^{-1} \text{ K}^{-1}$  at pH 7.6 and pH 3, respectively. The dotted line is the fit obtained using the Gibbs–Helmholtz equation after adding  $1.5 \text{ kcal mol}^{-1}$  to the experimentally measured stability of McoA at pH 3 as illustrated by the arrows (see Results to rationalize this increase in stability which is due to the stabilizing effect of copper). Taking into account this stabilization by copper the  $\Delta C_p$  value increases to  $0.50 \pm 0.06 \text{ kcal mol}^{-1} \text{ K}^{-1}$ .

These values were significantly smaller than theoretically predicted from the amino acid sequence ( $8.9\text{--}9.4 \text{ kcal mol}^{-1} \text{ K}^{-1}$ , depending on the method used for calculation) (Myers, et al., 1995; Pace and Scholtz, 1997). Also, the use of a fixed enthalpy change measured by DSC to fit the Gibbs–Helmholtz equation prevents any convergence between experimental and fitted data. To obtain an accurate fit the enthalpy change calculated is around one fourth the enthalpy change measured experimentally by DSC (see values in the legend of Figure 3.7) reflecting the different nature of the chemical and thermal unfolding pathways. Considering that the equilibrium unfolding (as measured in Figure 3.2) quantifies the stability of apo-McoA, as copper is depleted at lower GdnHCl concentrations, the stabilizing effect of copper ( $1.5 \text{ kcal mol}^{-1}$ ) quantified by kinetics was added to the experimental equilibrium  $\Delta G^{\text{water}}$  values measured at pH 3. This addition resulted in a steeper stability curve (Figure 3.7)

and thus a larger  $\Delta C_p$  upon unfolding was determined ( $0.50 \text{ kcal mol}^{-1} \text{ K}^{-1}$ ) but still very far from the theoretically predicted value. To address the contribution of conformational dynamics to the uncommon  $\Delta C_p$  value of McoA, collisional quenching of fluorescence by an external quencher, such as acrylamide, was used. The exposure of tryptophan residues and protein conformational dynamics that may expose tryptophan residues periodically on a nanosecond time scale were probed by this technique (Eftink and Ghiron, 1976; Eftink and Ghiron, 1977). Exposed tryptophan residues also fluoresce at longer wavelengths as they sense the high polarity of water at the surface of the protein (Burstein, et al., 1973) and a correlation between the peak of emission and collisional quenching constants was previously observed (Eftink and Ghiron, 1976).

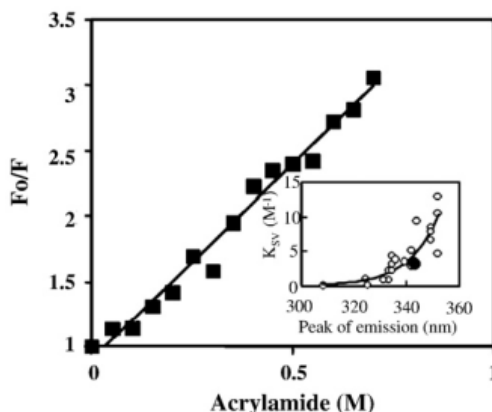


Figure 3.8: Collisional quenching of McoA WT (■) by acrylamide. The inset shows the correlation between the peak of emission and the Stern-Volmer quenching constant ( $K_{SV}$ ) for several proteins (○) (taken from (Eftink and Ghiron, 1976)) and for McoAWT (●).

The value of  $K_{SV}$  obtained for McoA was shown in Figure 3.8 and plotted versus the peak of fluorescence emission in comparison with other proteins in the inset of Figure 3.8. The  $K_{SV}$  value lie clearly within the range observed for other proteins indicating that McoA follows a general trend between peak position and degree of tryptophan exposure. McoA conformational dynamics, or at least those that may expose tryptophan residues, are not significantly larger. On the other hand, these results also point out to the fact that hyperthermophilic McoA does not present higher rigidity than other

characterized proteins. In fact, the common thought that thermal stability relies on enhanced conformational rigidity independently of the time scale selected to probe motion has been under dispute (Fitter and Heberle, 2000; LeMaster, et al., 2005; Wintrode, et al., 2003).

### **3.4. DISCUSSION**

Unfolding of McoA is a complex process. The DSC thermogram clearly shows that thermal unfolding of McoA is complex and three independent transitions have to be considered to fit the endothermic peak (Figure 3.2). Three transitions were previously used to describe DSC traces of plant ascorbate oxidase (Savini, et al., 1990), human ceruloplasmin (Bonaccorsi di Patti, et al., 1990) and CotA-laccase from *B. subtilis* (Duraio, et al., 2008) which apparently correlates with a structural organization in three cupredoxin- like domains for the ascorbate oxidase and CotA-laccase. Nevertheless, this hypothesis is not supported by the human ceruloplasmin structure which is comprised of six plastocyanin-like domains arranged in a triangular array (Zaitseva, et al., 1996). Disruption of copper sites previously to overall protein unfolding can lead to thermal transitions probed by DSC (Ma, et al., 2005). In addition, each transition induced by temperature is a non two-state process as the ratio  $\Delta H_{cal}/\Delta H_{vH}$  is bellow 1 (Stathopoulos, et al., 2006; Vassall, et al., 2006). In McoA these ratios are lower for the transitions with higher  $T_m$  values indicating the occurrence of protein aggregation. The aggregation of McoA leads to an asymmetrical DSC peak resulting in 100% irreversibility upon thermal unfolding. The long term stability of McoA has previously revealed that the majority of the activity decay was due to protein aggregation (Fernandes, et al., 2007). Decomposition of copper clusters may be another cause of irreversibility upon thermal unfolding (Moczygemba, et al., 2001).

**The role of copper on McoA stability.** McoA is a hyperthermostable enzyme with  $T_m$  values ranging from 105 to 114 °C but it has a low stability in water at room temperature (2.8 kcal mol<sup>-1</sup>, see Table 3.1). The stabilizing effect of



copper added exogenously was not detected in the chemically induced equilibrium unfolding of McoA because copper should be bleached or lost at lower GdnHCl concentrations, before the unfolding of the tertiary structure occurs (Figure 3.2 and Figure 3.3). This point is entirely supported by the equilibrium stability of apo-McoA which is only slightly lower than the as-isolated enzyme (Table 3.1). Moreover, a similar result was found in CotA-laccase from *B. subtilis* where the copper ions are also bleached before the unfolding of the tertiary structure of the protein (Durao, et al., 2006). Probably for the same reason the chemical stability of the *Rhus vernicifera* laccase is also independent of copper content, being similar in the apo- and holo-forms (Agostinelli, et al., 1995). Disruption of the T1 copper site also precedes global protein denaturation in other copper containing proteins (Stirpe, et al., 2005; Stirpe, et al., 2006). Like in McoA, copper-uptake in the presence of guanidinium hydrochloride by folded apo-azurin increase when exogenous copper is added to the solution (Pozdnyakova and Wittung-Stafshede, 2001). This indicates that the process of copper exchange between the protein and the bulk solution is easier (faster) in the presence of guanidinium hydrochloride probably due to increased conformational dynamics. Unfolding kinetics measured by stopped-flow was used to estimate the stabilizing effect of copper in McoA since the rate constants reflect the pre-equilibrium between the native with copper and without copper presumably formed during the dead-time of the stopped-flow. Using kinetics, the stabilizing effect of copper on the unfolding pathway was quantified to be 1.5 kcal mol<sup>-1</sup>. Copper also stabilizes McoA against thermal unfolding. This conclusion was taken up based on a DSC scan of a fully copper-loaded sample of McoA (4:1 instead of 2.5:1, Cu/McoA for the as-isolated protein) obtained by a new procedure (Durao, et al., 2008). The full copper-loaded McoA could not be thermally unfolded up to 130 °C, the maximum temperature attained by the DSC. The holoceruloplasmin is also 15-20 °C more stable than the apo-form against thermal unfolding (Sedlak, et al., 2008).

Aggregation is the main cause for the complexity of unfolding. The complexity of the unfolding pathway of McoA and the importance of aggregation effects even on chemically induced unfolding are entirely supported by kinetics measurements with the stopped-flow technique and by gel filtration chromatography. Unfolding kinetics at relatively high concentrations of McoA (2  $\mu$ M) was described by three exponentials (Figure 3.4A). The assignment of each rate constant to the unfolding of a single domain would be tempting but, kinetics of unfolding become double exponential when a lower McoA concentration was used indicating that at least one rate constant relates to protein aggregation (Figure 3.4B). Also, the Brønsted  $\beta$  value shows that the three rate constants cannot result from the sequential unfolding of each domain. The  $\beta$  value gives the fractional change in amino acid exposure in the transition state compared to that of the unfolded state ( $\beta=1$ ) (Fersht, 1998), and a value of 1.84 was measured for McoA. If the three rate constants resulted from the sequential unfolding of each domain, the transition state would have higher exposition to solvent in the transition state than in the unfolded state which clearly is not possible. Aggregates of McoA formed during the first 100 ms in the stopped-flow experiment reveal an extremely fast aggregation process (Figure 3.4C). In fact, as shown for the chymotrypsin inhibitor 2, the aggregation process is not always slow and irreversible but may take place transiently on a millisecond time scale (Silow, et al., 1999). Kinetics of unfolding of McoA in the presence of the dye ANS reveals the formation of a species within the first 10-25 ms, prior to aggregation (Figure 3.4D). This species is able to bind ANS having thus hydrophobic patches exposed to solvent that should mediate aggregation. McoA most probably aggregates from a quasi-native state, with the tertiary structure slightly distorted to expose hydrophobic patches as observed for other proteins (Pedersen, et al., 2004; Plakoutsi, et al., 2004). Accumulation of a quasi-native state was previously observed to be promoted at low pH values in the presence of salt for the S6 ribosomal protein (Pedersen, et al., 2004) or in the presence of trifluoroethanol for the acylphosphatase (Plakoutsi, et al., 2004). Multiple or heterogeneous transition

state ensemble that lead to both aggregation and unfolding should result from the accumulation of the quasi-native state. Kinetic partitioning between aggregation and other pathways seems to be more common than one would believe (Baptista, et al., 2003; Silow, et al., 1999; Zettlmeissl, et al., 1979). Interestingly, pathways that putatively lead to aggregation have slightly larger degrees of amino acid exposure in the transition state ( $\beta$  values are 0.63 and 0.65 for  $k_1$  and  $k_2$  compared to 0.56 for  $k_3$ ) reflecting the additional exposure acquired by the quasi-native relatively to the native state. Aggregation of the folded state in the presence of chemical denaturants, generally, quite uncommon among proteins, was further confirmed by gel filtration chromatography which has revealed the presence of several large and heterogeneous aggregates of McoA (Figure 3.5). These aggregates might cause some degree of irreversibility detected after chemically induced unfolding. Interestingly, the folded state of the blue copper rusticyanin was also shown to aggregate in the presence of GdnHCl (Alcaraz and Donaire, 2004). The slowest rate constant  $k_3$  most probably characterizes the unfolding of monomeric McoA and thus the transition state for unfolding ( $\beta=0.56$ ) should structurally resemble the unfolded state in contrast to the majority of small globular proteins which have a transition state close to the folded state (Dagget and Fersht, 2000). In conclusion, the complexity of unfolding of McoA reflects parallel pathways due to protein aggregation which is related to the accumulation of a quasi-native state with hydrophobic patches exposed to solvent.

Partition between unfolding and aggregation draws a flat dependence of stability on temperature. McoA exhibits a small difference in stability between the folded and unfolded states in a broad range of temperatures drawing a flat dependence of stability on temperature. Thermal unfolding of the blue copper plastocyanin shows a similar pattern with a low stability in water at room temperature (2-3.5 kcal mol<sup>-1</sup>) and a dependence on temperature flatter than that predicted from the primary structure. Actually, the flat dependence of  $\Delta G^{\text{water}}$  on temperature due to a low  $\Delta C_p$  is one of the mechanisms that leads to enhanced

thermal stability in proteins from thermophiles as it provides a suitable mechanism for balancing a high  $T_m$  with the optimal stability for protein function (Fitter and Heberle, 2000; Kumar, et al., 2000; Robic, et al., 2003; Zhou, 2002). The  $\Delta C_p$  value determined for this flat dependence of McoA,  $0.27 \text{ kcal mol}^{-1} \text{ K}^{-1}$ , is significantly lower than the one predicted theoretically ( $8.9\text{--}9.4 \text{ kcal mol}^{-1} \text{ K}^{-1}$ ) (Myers, et al., 1995; Pace and Scholtz, 1997). Interestingly, the hyperthermophilic ferredoxin from *A. ambivalens* which is a oxidase containing iron–sulphur centers, displays also a rather flat stability versus temperature due to a  $\Delta C_p$  value significantly lower than theoretically predicted (Moczygemba, et al., 2001). The curve for McoA becomes less flat ( $\Delta C_p=0.50 \text{ kcal mol}^{-1} \text{ K}^{-1}$ ) when the stabilizing effect of copper is taken into account but the folded state is still marginally more stable than the unfolded state even at room temperature (Figure 3.7). The low value of  $\Delta C_p$  is entirely in accordance with the low cooperativeness of the transition as evaluated by the equilibrium  $m_{(U-F)}$  parameter. Heat capacity and  $m$  values are both intrinsically related to changes in solvent exposure (Myers, et al., 1995; Otzen and Oliveberg, 2004). The low  $\Delta C_p$  value upon unfolding of McoA might be explained by different reasons. Firstly, an increased number of electrostatic interactions or hydrogen-bonding network around an ionised group in the core of the protein (Lee, et al., 2005; Spolar, et al., 1992; Zhou, 2002). Secondly, a high level of conformational dynamics of the folded state for solvent access as the heat capacity change is dominated by the non-polar surface area exposed to water (Jaenicke, et al., 1996). Thirdly, the presence of residual structure in the unfolded state whether aggregated or not (Robic, et al., 2003; Vieille and Zeikus, 2001). McoA has five additional totally buried (zero accessible surface area to water) ionisable residues than its mesophilic counterpart CueO from *E. coli* as it could be shown in the comparative structure model (Fernandes, et al., 2007). This might give some contribution to the low  $\Delta C_p$  value observed as the removal of three ionisable residues involved in a charge cluster in the thermophilic ribosomal protein L30e have increased the  $\Delta C_p$  value by  $0.4 \text{ kcal mol}^{-1} \text{ K}^{-1}$  (Lee, et al., 2005). Regarding the level of conformational dynamics of

the folded state, collisional fluorescence quenching studies point to common degrees of protein dynamics. A mutant enzyme lacking a methionine rich segment involved in the modulation of the catalytic mechanism by copper binding displays a 2-3 fold larger  $\Delta C_p$  value than wild type McoA, despite some uncertainty in the measurements. This segment should display large conformational dynamics to mediate the role of copper in the catalytic mechanism and its structure could not be modelled by homology. Therefore, any significant contribution of large conformational dynamics of the folded state to the low  $\Delta C_p$  value should be restricted to the methionine-rich segment. The aggregation of McoA upon chemically unfolding conditions as proved by gel filtration chromatography and kinetic measurements, undoubtedly will confer residual structure to the final state at equilibrium contributing to the low  $\Delta C_p$  value observed. An unusual low  $\Delta C_p$  value determined for a thermophilic ribonuclease H (35% lower than the mesophilic counterpart) was also assigned to residual structure in the unfolded state and the authors have raised the hypothesis that residual structure in the unfolded state might be an important and novel mechanism for tuning protein energetic and function (Robic, et al., 2003). The aggregation of McoA also explains the low cooperativeness of the unfolding process ( $m$  value) which relates to changes in solvent exposure. The low enthalpy change calculated using the Gibbs-Helmholtz equation when compared to the calorimetric enthalpy might reflect the formation of the quasi-native state and its aggregation in the presence of guanidinium in contrast with the putative aggregation of the unfolded state after thermal unfolding. Molecules of the quasi-native state that aggregate do not contribute to the total enthalpy change as much as those that unfold thermally, even if they aggregate after thermal unfolding as indicated by the irreversibility of the DSC scan. Kinetic partitioning between unfolding and aggregation should be the main factor behind the unusual low chemical stability and thermodynamic parameters observed for McoA. The results reported in this study revealed interesting features on the hyperthermostable nature of McoA such as (i) the hyperthermostable character of McoA with very high  $T_m$  values as probed by

DSC, (ii) the role of copper as a determinant of the thermodynamic stability, (iii) a fast aggregation process of the folded state under unfolding conditions due to the accumulation of a quasi-native state that binds ANS and (iv) an extremely flat dependence of stability on temperature due to a very small  $\Delta C_p$  value upon unfolding. We were able to show that aggregation of the quasi-native state upon unfolding conditions is the main cause for the small  $\Delta C_p$  value determined for this enzyme.

# 4 THE MULTICOPPER OXIDASE FROM THE ARCHAEON *PYROBACULUM AEROPHILUM* SHOWS NITROUS OXIDE REDUCTASE ACTIVITY

---

4.1.	INTRODUCTION.....	103
4.2.	EXPERIMENTAL PROCEDURES.....	105
4.3.	RESULTS .....	110
4.4.	DISCUSSION.....	124
4.5.	SUPPLEMENTARY MATERIAL .....	127

## ABSTRACT

The multicopper oxidase from the hyperthermophilic archaeon *Pyrobaculum aerophilum* McoP was overproduced in *Escherichia coli* and purified to homogeneity. The enzyme consists of a single 49.6-kDa subunit and the combined results of UV-visible, CD, EPR and resonance Raman spectroscopies showed the characteristics features of the multicopper oxidases. The analysis of McoP sequence allowed deriving its structure by comparative modelling methods. This model provided a criterion for designing meaningful site-directed mutants of the enzyme. McoP is a hyper-thermoactive and thermostable enzyme with optimum reaction temperature of 85°C, a half-life of inactivation of around 6 h at 80°C and, temperature values at the mid-point from 97 to 112°C. McoP is an efficient metallo-oxidase that catalyzes the oxidation of Cu(I) and Fe(II) ions with turnover rate constants of 356 and 128 min<sup>-1</sup>, respectively, at 40°C. Noteworthy, McoP follows a ping-pong mechanism with a 3-fold higher catalytic efficiency when using nitrous oxide as electron acceptor as compared with dioxygen, the typical oxidizing substrate of multicopper oxidases. This finding led us to propose that McoP represents a novel archaeal nitrous oxide reductase most probably involved in the final step of the denitrification pathway of *P. aerophilum*.

**This chapter was published in the following scientific paper:**

André T. Fernandes, João M. Damas, Smilja Todorovic, Robert Huber, M. Camilla Baratto, Rebecca Pogni, Cláudio M. Soares, and Lígia O. Martins. 2010. The Multicopper Oxidase from the Archaeon *Pyrobaculum aerophilum* shows Nitrous Oxide Reductase Activity. FEBS J. 277: 3176-3189

The genome DNA was kindly provided by Prof. Robert Huber. McoP homology model was derived by João M. Damas and Prof. Cláudio M. Soares, M. Camilla Baratto and Prof. Rebecca Pogni carried the EPR measurements, and Dr. Smilja Todorovic carried the RR spectroscopy.



## 4.1. INTRODUCTION

Multicopper oxidases (MCO) are a large family of enzymes that couple the one-electron oxidation of substrates with the four-electron reduction of molecular oxygen to water (Lindley, 2001; Solomon, et al., 1996). This family is unique among copper proteins since its members contain one of each of the three types of biologic copper sites, type 1 (T1), type 2 (T2) and the binuclear type 3 (T3). Type 1 (T1) Cu is characterized by an intense  $S(\pi) \rightarrow Cu(d_{x^2-y^2})$  charge transfer (CT) absorption band at around 600 nm, responsible for the intense blue colour of these enzymes, and a narrow parallel hyperfine splitting [ $A_{\parallel} = (43-90) \times 10^{-4} \text{ cm}^{-1}$ ] in the electron paramagnetic resonance (EPR) spectra. This is the site of substrate oxidation and in this respect the MCO family can be separated into two classes; enzymes that oxidize aromatic substrates with high efficiency, i.e. laccases, and those that oxidize metal ion substrates, or metallo-oxidases. The trinuclear center, where dioxygen is reduced to water, is comprised of two type 3 (T3) and one type 2 (T2) copper ions. The two T3 Cu ions, which are usually antiferromagnetically coupled through a bridging ligand and therefore EPR silent, show a characteristic absorption band at 330 nm. The T2 Cu copper site lacks strong absorption bands and exhibits a large parallel hyperfine splitting in the EPR spectra [ $A_{\parallel} = (150-201) \times 10^{-4} \text{ cm}^{-1}$ ]. MCO are widely distributed throughout the nature and play essential roles in the physiology of almost all aerobes.

In recent years we have focused our attention onto the study of prokaryotic members of MCO, the CotA-laccase from *Bacillus subtilis* and the metallo-oxidase McoA from *Aquifex aeolicus*, due to their potential for biotechnological applications (Enguita, et al., 2003; Fernandes, et al., 2009; Fernandes, et al., 2007; Martins, et al., 2002; Pereira, et al., 2009; Pereira, 2009). Several structure-function relationship studies have been performed revealing redox properties of the T1 copper site and giving structural insights into the principal stages of the mechanism of dioxygen reduction at the trinuclear center (Bento,

et al., 2005; Chen, et al., 2010; Durao, et al., 2006; Durao, et al., 2008). Enzymes from extremophiles and thermophiles, in particular, are promising for industrial applications as they have a high intrinsic thermal and chemical stability. The search for multicopper oxidases, among genomes of hyperthermophilic *Archaea* sequenced so far, revealed that the *Pyrobaculum aerophilum* is the only microorganism that possesses a multicopper oxidase like enzyme coded by the PAE1888 gene (Fitz-Gibbon, et al., 2002). Therefore, in this work we set out to fully characterize this archaeal enzyme. An additional interest for this enzyme came from a recent report on the transcriptional patterns of *P. aerophilum* upon cultivation in the presence of oxygen, nitrate, arsenate and ferric ions that suggested its putative involvement in the last step of the denitrification pathway of this microorganism (Cozen, et al., 2009). This would represent a completely new function among the MCO. *P. aerophilum* is a microaerophilic, chemioautotrophic microorganism, recognized for its respiratory versatility being capable of using several organic, as well as inorganic compounds as substrates during aerobic or anaerobic respiration (Cozen, et al., 2009; Feinberg and Holden, 2006; Feinberg, et al., 2008). It is the only hyperthermophilic denitrifier that has thus far been characterized (Afshar, et al., 1998; de Vries, et al., 2003; Volkl, et al., 1993). The reduction of nitrate to dinitrogen gas is accomplished by different types of metalloenzymes in four subsequent steps: nitrate is reduced to nitrite, then to nitric oxide, followed by reduction to nitrous oxide and by final reduction to dinitrogen (Tavares, et al., 2006; Zumft, 1997). The nitrate and nitric oxide reductases of *P. aerophilum* have been isolated and biochemically characterized and the gene coding for a heme O-containing nitric oxide reductase was identified in its genome (Afshar, et al., 2001; de Vries, et al., 2003; Fitz-Gibbon, et al., 2002). However, no recognizable homolog of *nosZ*, which encodes for nitrous oxide reductase (N<sub>2</sub>OR) in bacteria, has been found in the genome of this archaeon indicating the existence of an alternative and unknown N<sub>2</sub>OR. This hypothesis was also raised for other bacterial and archaeal strains that reduce nitrous oxide and lack identified N<sub>2</sub>OR genes (Zumft and Kroneck, 2007).

This study describes the purification, biochemical and structural characterization (based on the comparative model) of the first hyperthermophilic archaeal-type metallo-oxidase designated McoP (Multicopper oxidase from *P. aerophilum*). Indeed, while in eukaryotes and bacteria multicopper oxidases, both laccases and metallo-oxidases are well-characterized, only one archaeal laccase has been described so far (Uthandi, et al., 2010). Whereas the recombinant purified McoP is similar in several aspects to other well-characterized MCO, it is unique in terms of being the first multicopper oxidase that uses more efficiently nitrous oxide than dioxygen as an oxidizing substrate. Overall, our results reinforce the prediction raised by Cozen et al. (2009) that McoP is involved in the denitrification pathway of *P. aerophilum*, thus representing, a novel N<sub>2</sub>OR.

## 4.2. EXPERIMENTAL PROCEDURES

**Cloning *mcoP* in *Escherichia coli*.** The *mcoP* gene was amplified by PCR using oligonucleotides mcoP-191D (5'-CTCAGCCAT ATGATCACTAGAAGG-3') and mcoP-15R (5'-CTCTTCCTCGAGCGGATTATTTAAC-3'). The 1543 bp-long PCR product was digested with NdeI and XhoI and inserted between the same restriction sites of plasmid pET-15b (Novagen, Darmstadt, Germany) to yield pATF-20, allowing the expression of *mcoP* gene with a six histidine tag fusion to the N-terminal. The expression strain *E. coli* Tuner (DE3) (Novagen, Darmstadt, Germany) was freshly transformed with pG-KJE8 (*Cm<sup>r</sup>*) (from Takara Bio Inc., Kyoto, Japan) before being transformed with the recombinant plasmid pATF-20. In pG-KJE8 the L-arabinose inducible promoter (*araB*) was used to express the *dnak/dnaJ/grpE* chaperones and the *Pzt-1* (tet) promoter regulates the expression of *groES/groEL* chaperones. The co-expression of chaperones with *mcoP* enables the overproduction of soluble McoP.

**Site Directed Mutagenesis.** Single amino acid substitutions in McoP protein were created using the QuikChange site-directed mutagenesis kit (Stratagene,

Santa Clara, CA, USA). Plasmid pATF-20 (containing the wild-type *mcoP* sequence) was used as template and primers *mcoPM297Ad* (5'-CCCATGCATT TAGAAGCGGGCCACGG-3') and *mcoPM297Ar* (5'-CCGTGGCCCGCTTCTAAA TGCATGGG-3') were used to generate the M297A, primers *mcoPM389Ad* (5'-CAAGG CGTCTGCGCCCCACCCTATC-3') and *mcoPM389Ar* (5'-GATAGGGTGGGGCGCAG ACGCCTTG-3') were used to generate the M389A mutation, primers *mcoPE296Qd* (5'-CCCATGCATTTACAAATGGGCCACGGG-3') and *mcoPE296Qr* (5'-CCCGTGGCCCA TTTGTAAATGCATGGG-3') were used to generate the E296Q mutation, and primers *mcoPW355Ad* (5'-GGAATGCAGGCGACGA TAAACGGC-3') and *mcoPW355Ar* (5'-GCCGTTTATCGTCGCCTGCATTCC-3') were used to generate the mutant W355A. The presence of the desired mutations in the resulting plasmids, pATF-27 (carrying the M297A point mutation), pATF-28 (bearing the E296Q point mutation), pATF-33 (carrying the mutation M389A) and pATF-34 (carrying the mutation W355A) and the absence of unwanted mutations in other regions of the insert, were confirmed by DNA sequence analysis. These plasmids were introduced into *E.coli* Tuner expression strain, along with plasmid pG-KJE8, as mentioned above.

***Overproduction and purification of recombinant proteins.*** The expression strains were grown in Luria-Bertani culture medium supplemented with ampicillin (100 µg/mL), chloramphenicol (34 µg/mL), arabinose (1 mg/mL) and tetracycline (1 ng/mL) at 30°C. Growth was followed until  $D_{600}=0.6$ , at that point 100 µM IPTG and 250 µM CuCl<sub>2</sub> were added to the culture medium and the temperature lowered to 25°C. Incubation was continued for further 4h when a change to microaerobic conditions was achieved (Durao, et al., 2008). Cells were harvested by centrifugation (8000 x g, 10 min, 4°C) after a further 20 h of growth. The cell sediment was suspended in 20 mM phosphate buffer (pH 7.4) with 100 mM of NaCl, containing DNase I (10 µg/mL extract), MgCl<sub>2</sub> (5 mM) and a mixture of protease inhibitors, antipain and leupeptin (2 µg/mL extract).

Cells were disrupted in a French press cell (at 19000 psi) and centrifuged (18 000 x g, 60 min, 4°C) to remove cell debris. The cell lysate was then loaded onto a 1 mL HisTrap HP column (GE Healthcare, Waukesha, WI, USA) equilibrated with 20 mM phosphate buffer, pH 7.4 supplemented with 100 mM NaCl. Elution was carried out with a one-step linear imidazole (500 mM) gradient of 40 mL in the same buffer. The active fractions were pooled out and concentrated before applied on a Superdex 75 HR 10/30 column (GE Healthcare) equilibrated with 20 mM Tris-HCl buffer, pH 7.6 with 0.2 M NaCl. All purification steps were carried out at room temperature in an AKTA-purifier (GE Healthcare). The His-tag was subsequently removed by using the Thrombin Digestion kit (Novagen, Darmstadt, Germany).

***Spectroscopic analysis.*** The spectroscopic analysis of the protein samples were routinely performed after incubation with the oxidizing agent potassium iridate followed by dialysis. The UV-Visible spectra were recorded at room temperature in 20 mM Tris-HCl buffer, pH 7.6, in the presence of 200 mM NaCl. CD in the far-UV was measured on a Jasco-815 spectropolarimeter using a protein content of 25  $\mu$ M in highly pure water (Mili-Q), as described previously (Fernandes, et al., 2007). RR spectra were measured as previously described with 568 nm excitation (Durao, et al., 2008). The fitted band intensities and frequencies were used for determination of the intensity weighted frequency  $\langle \nu_{\text{Cu-S}} \rangle$ . CW-X-band (CW - continuous wave) EPR measurements were carried out with a Bruker E500 Eleksys Series using the Bruker ER 4122 SHQE cavity and an Oxford helium continuous flow cryostat (ESR900). EPR samples were prepared by adding increasing quantity of exogenous-copper ( $\text{CuCl}_2$ ) to the enzyme solution, in a final concentration of 196  $\mu$ M. Recombinant McoP was also incubated with exogenous copper to yield a final ratio protein:copper of 1:5, and a final concentration of 122  $\mu$ M of protein. The EPR spectra of McoP were recorded at 70 K with 0.5 mT modulation amplitude, 100 KHz modulation frequency, 2 mW microwave power  $\nu = 9.396$  GHz. The EPR spectra were baseline-corrected and simulated

using software for fitting EPR frozen solution spectra that is a modified version of a program written by J.R. Pilbrow (Cusimne) (Rakhit, et al., 1985).

**Redox titrations.** Redox titrations performed at 25°C, pH 7.6, under an argon atmosphere, were monitored by visible spectroscopy (300-900nm) in a Shimadzu Multispec-1501 spectrophotometer. The reaction mixture contained 25-50  $\mu$ M enzyme in 20 mM Tris-HCl buffer, pH 7.6 and the following mediators in 10  $\mu$ M final concentration each (reduction potential between brackets): 1,2 -naphthoquinone-4-sulfonic acid (+215 mV), dimethyl-p-phenylenediamine (+344 mV), monocarboxylic acid ferrocene (+530 mV), 1,1'-dicarboxylic acid ferrocene (+644 mV) and Fe(II/III)-Tris-(1,10-phenantroline) (+1,070 mV). Potassium hexachloroiridate (IV) was used as oxidant and sodium dithionite as reductant. The redox potential measurements were performed with a combined silver/silver chloride electrode, calibrated with a quinhydrone saturated solution at pH 7.0. The redox potentials are quoted against the standard hydrogen electrode.

**Substrate specificities and kinetics.** The catalytic properties of McoP were measured in the presence of oxygen using four different reducing substrates; two aromatic, the non-phenolic ABTS and the phenolic SGZ, and two metals, cuprous and ferrous ions. This was done at 40 °C, as technical limitations prevented cuprous oxidation measurements at higher temperatures. The effect of pH on the enzyme activity was determined for ABTS and SGZ in Britton–Robinson buffer (100 mM boric acid, 100 mM phosphoric acid, 100mM acetic acid mixture titrated to the desired pH with 0.5M NaOH) as previously described (Durao, et al., 2006). For measurements with metal ions, the pH was chosen in accordance with the metal ions stability in solution; pH 3.5 for Cu(I) and pH 5 for Fe(II). The oxidation of ABTS, SGZ and ferrous ammonium sulphate were spectrophotometrically monitored on either a Nicolet Evolution 300 spectrophotometer (Thermo Industries, Waltham, MA, USA) or on a Sinergy 2 microplate reader with a 96-well plate (BioTek, Winooski, VT, USA). Cuprous oxidase activity was measured in terms of oxygen consumption

rates by using an oxygraph as previously described (Fernandes, et al.). The optimal temperature for the activity was determined for ABTS at temperatures ranging from 30 to 90 °C. Apparent kinetic parameters were determined using reaction mixtures containing  $\text{Cu}^+$  (10–300  $\mu\text{M}$ , pH 3.5),  $\text{Fe}^{2+}$  (5–70  $\mu\text{M}$ , pH 5), ABTS (10–200  $\mu\text{M}$ , pH 3) and SGZ (1–100  $\mu\text{M}$ , pH 7). The apparent kinetic constants  $K_m$  and  $k_{\text{cat}}$  were fitted directly to the Michaelis–Menten equation (Origin Lab software, Northampton, MA, USA). All enzymatic assays were performed at least in triplicate. The second-order kinetic analysis by using Fe(II) (as reducing substrate) and  $\text{N}_2\text{O}$  and  $\text{O}_2$  (as oxidizing substrate) was spectrophotometrically assayed by monitoring the oxidation of  $\text{Fe}^{2+}$  at 315 nm. The cuvettes (1 mL) containing 100 mM of Britton–Robinson buffer at pH 5 and 300  $\mu\text{M}$  of Fe(II) were sealed with rubber stoppers and made anaerobic with argon bubbling. A saturated solution of  $\text{O}_2$  (1 mM) and  $\text{N}_2\text{O}$  (25 mM) was prepared by bubbling mili-Q water in a sealed serum bottle with  $\text{O}_2$  or  $\text{N}_2\text{O}$  gas (Kristjansson and Hollocher). The kinetic constants for  $\text{N}_2\text{O}$ ,  $\text{O}_2$  and  $\text{Fe}^{2+}$  were determined by varying the concentrations of the reducing and oxidizing substrate as described elsewhere (Bukh, et al., 2006).

**Thermal stability.** Kinetic stability was performed as previously described by Martins and co-workers (Martins, et al.). Briefly, the enzyme was incubated at 80°C, and tested for activity at 40°C using ABTS as the substrate at fixed time intervals. DSC was carried out in a VP-DSC instrument from MicroCal at a scan rate of 60°C h<sup>-1</sup>. The experimental calorimetric trace was obtained at pH 3 (50 mM glycine buffer) after baseline correction (buffer alone). The resulting DSC trace was analyzed with the DSC software built within the Origin spreadsheet to obtain the transition excess heat capacity function (a cubic polynomial function was used to fit the shift in baseline associated with unfolding).

**Comparative modelling.** The structure model of *P. aerophilum* McoP was derived using comparative modelling methods through the program MODELLER (Sali, 1995), release 9v3. For that, both *E. coli* CueO (Roberts, et

al., 2002) (PDB code: 1KV7) and *B. subtilis* CotA (Enguita, et al., 2003) (PDB code: 1GSK) structures that show 29.0% and 23.1% sequence identity, respectively, were chosen as templates. These templates were first structurally aligned, providing a profile against which the McoP sequence was aligned with the ALIGN2D feature of MODELLER. This sequence alignment, together with the two known structures, was the basis for deriving an initial structural model of McoP. Then, the alignment was changed in an iterative process and new structural models were derived until its quality, assessed using the program PROCHECK (Laskowski, et al., 1993), was found satisfactory. After loop refinement, the final model presented 89.1% of the residues in the most favoured regions of the Ramachandran plot, 10.9% in the additional allowed regions and no residues in the generously allowed or disallowed regions.

**Other methods.** The copper content was determined through the trichloroacetic acid/bicinchoninic acid (BCA) method (Brenner and Harris, 1995). The protein concentration was measured by using the absorbance band at 280 nm ( $\epsilon_{280} = 57\,750\text{ M}^{-1}\text{ cm}^{-1}$ ) or the Bradford assay (Bradford, 1976) using bovine serum albumin as standard.

### 4.3. RESULTS

**Biochemical, spectroscopic and structural characterization of recombinant McoP.** Sequence alignment of *P. aerophilum* McoP with CueO from *E. coli* and CotA-laccase from *B. subtilis* clearly indicates that this enzyme is a member of the multicopper oxidase family of enzymes (Figure 4.1). The MCO sequence motif pattern, which contains the four elements that together comprise the copper-binding sites in the protein, is conserved in McoP, including a methionine residue corresponding to the axial position of the type 1 copper in other MCO. Furthermore, McoP has in its sequence a predicted TAT-dependent putative signal peptide, indicating that this protein should be exported to the space between the cytoplasmatic membrane and the external protein surface layer (S-layer) (Volkl, et al., 1993).



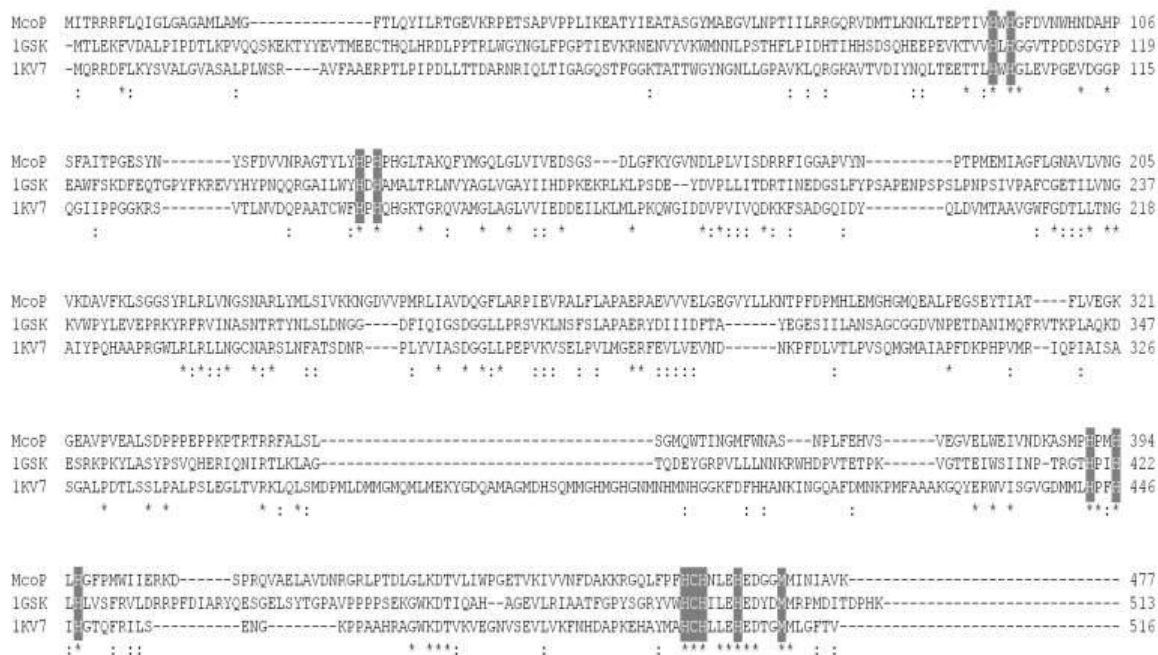


Figure 4.1: Sequence alignment of McoP with CotA-laccase from *B. subtilis* (1GSK) and CueO from *E. coli* (1KV7). The alignment was generated by using the primary sequence of the respective proteins. The copper ligands of multicopper oxidases (grey boxes) are all conserved in McoP. Two dots indicate similarity, whereas an asterisk indicates identity.

The *mcoP* gene encodes a protein with 477 amino acids with a predicted molecular mass of 52.9 kDa. The gene was cloned into the expression vector pET-15b to make pATF-20 and the final construct was transformed into *E. coli* Tuner (DE3). The recombinant McoP was purified to homogeneity by using metal affinity and exclusion chromatography, showing a single band of around 52 kDa in SDS-PAGE (see supplementary material Table 4.S4 and Figure 4.S4). Size-exclusion chromatography yielded a native molecular mass of 49.6 kDa. The as-isolated enzyme was found partially copper depleted, containing 3.2 mol of copper per mol of protein instead of the expected 4:1 ratio. The UV-Vis spectrum of McoP shows the spectroscopic characteristics of the MCO with a charge transfer (CT) absorption band at approximately 600 nm, originating from the type 1 Cu-S(Cys) bond, and a small shoulder at 330 nm, characteristic

of a bridging ligand between the type 3 copper ions (Figure 4.2A). The circular dichroism (CD) spectrum of McoP reflected the typical secondary structure of MCO, rich in  $\beta$ -sheets, with a negative peak at  $\sim 213$  nm (see supplementary material Figure 4S.10). A secondary structure estimate based on the CDSSTR method yielded values of 6% in  $\alpha$ -helices, 30% in  $\beta$ -sheets and more than 60% in turns and random coils (Sreerama, et al., 1999). The resonance Raman (RR) spectrum (Figure 4.2B) reveals a number of vibrational modes in the low frequency region, originating from the coupling of the Cu-S(Cys) stretch with the S-C $_{\beta}$ -C $_{\alpha}$ (Cys) bond, as typically observed in copper proteins containing a T1 Cu center (Blair, 1985; Durao, et al., 2008; Green, 2006). The intensity-weighted frequency  $\langle \nu_{\text{Cu-S}} \rangle$  of all Cu-S stretching modes, which is inversely proportional to the Cu-S (Cys) bond length in the T1 site, was  $406 \text{ cm}^{-1}$  (Blair, 1985; Durao, et al., 2008; Green, 2006).

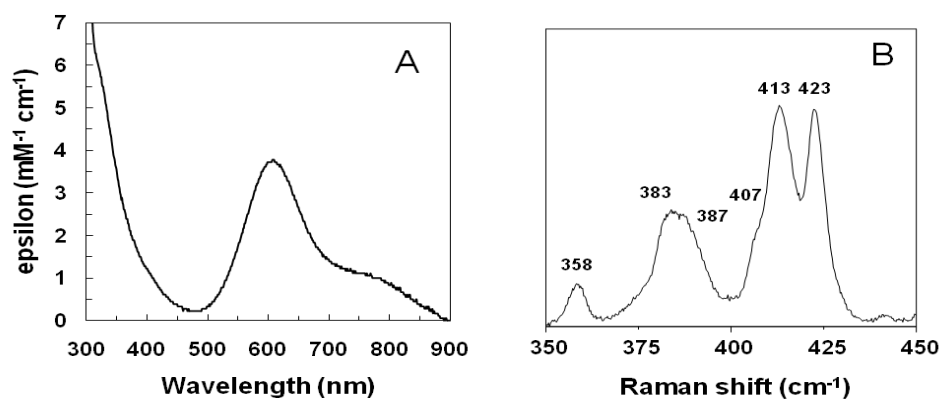


Figure 4.2: (A) UV-visible spectrum of the as-isolated recombinant McoP. (B) Resonance Raman spectrum of 2mM McoP, measured with 568 nm excitation, 5 mW laser power and 40 s accumulation time, at 77K.

Relatively small value of  $\langle \nu_{\text{Cu-S}} \rangle$  correlates well with the low redox potential of the T1 Cu center ( $E^0(\text{T1})=398 \text{ mV}$ ) (Blair, 1985; Durao, et al., 2008; Green, 2006), determined by the disappearance of the CT absorption band in the 500-800 nm region (Figure 4.3).

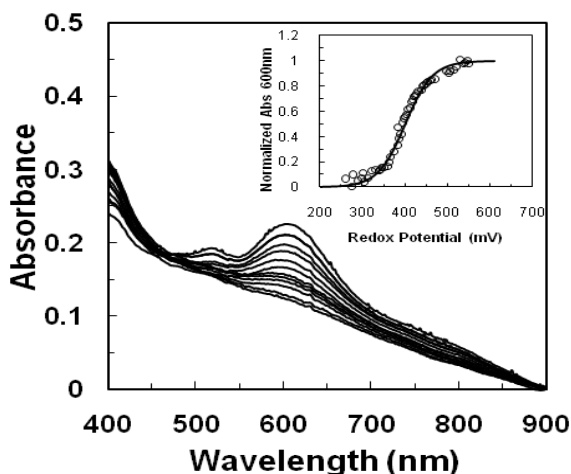


Figure 4.3: Redox potential determination. UV-visible spectra of McoP (50  $\mu$ M) in 20 mM Tris-HCl buffer, pH 7.6 obtained along the redox titration. Inset: Titration curve followed at 600 nm. The line corresponds to a fitting to the sequential equilibrium of one electron step.

The X-band electron paramagnetic resonance (EPR) spectrum of the as-isolated McoP paired to its simulation (Figure 4.4A) reveals the values of the magnetic parameters  $g_{\parallel} = 2.224 \pm 0.001$  and  $A_{\parallel} = (71.6 \pm 1) \times 10^{-4} \text{ cm}^{-1}$  that fall within the range of the type 1 copper contribution. No evidence for the characteristic resonances of type 2 copper center are present in the spectrum (Pogni, 2007; Solomon, 1992).

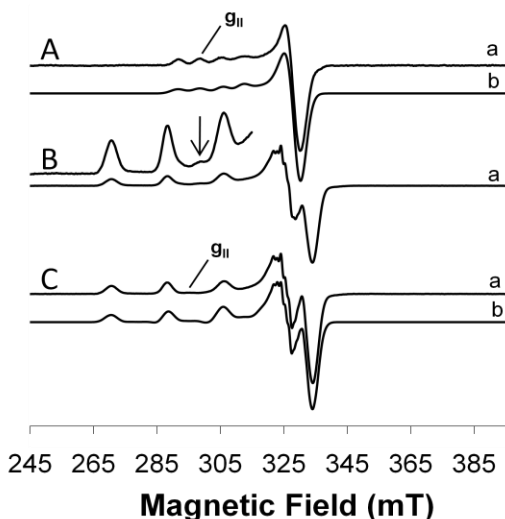


Figure 4.4: X-band EPR spectrum of (A) the as-isolated McoP (a) paired to its simulation (b) and (B) after incubation with 5 equivalents of Cu(II). The contribution of type 1 copper is present in both spectra, as pointed out with an arrow. (C) Experimental spectrum of the McoP incubated with Cu(II) subtracted from the as-isolated McoP (a) paired to its simulation (b), where the contribution of type 2 copper is evident.

A new set of resonances with spin Hamiltonian magnetic parameters typical for a type 2 copper center ( $g_{\parallel} = 2.258 \pm 0.001$  and  $A_{\parallel} = (183.4 \pm 1) \times 10^{-4} \text{ cm}^{-1}$ ) appears in the spectrum after addition of exogenous copper (Figure 4.4B-C). Overall, the analysis of EPR spectra suggests that McoP is in a T2-depleted form, which is in accordance with the lower copper:protein ratio measured in the as-isolated protein and the requirement for exogenous copper to achieve full activity (see below). The crystal structures of CueO from *E. coli* and CotA from *B. subtilis* were used to derive a structural model for McoP by comparative modelling techniques (Figure 4.5A). As expected, the model reveals the same overall fold of MCO, assembled from three cupredoxin domains, as the structures used as templates. The active sites of MCO are highly conserved and include a His-Cys-His triad, which forms a Cys-His bridging the T1 and T3 copper ions, this triad is likely to provide the route of the intramolecular electron transfer from the T1 Cu to the T3 binuclear cluster during substrate turnover (illustrated in Figure 4.5B).

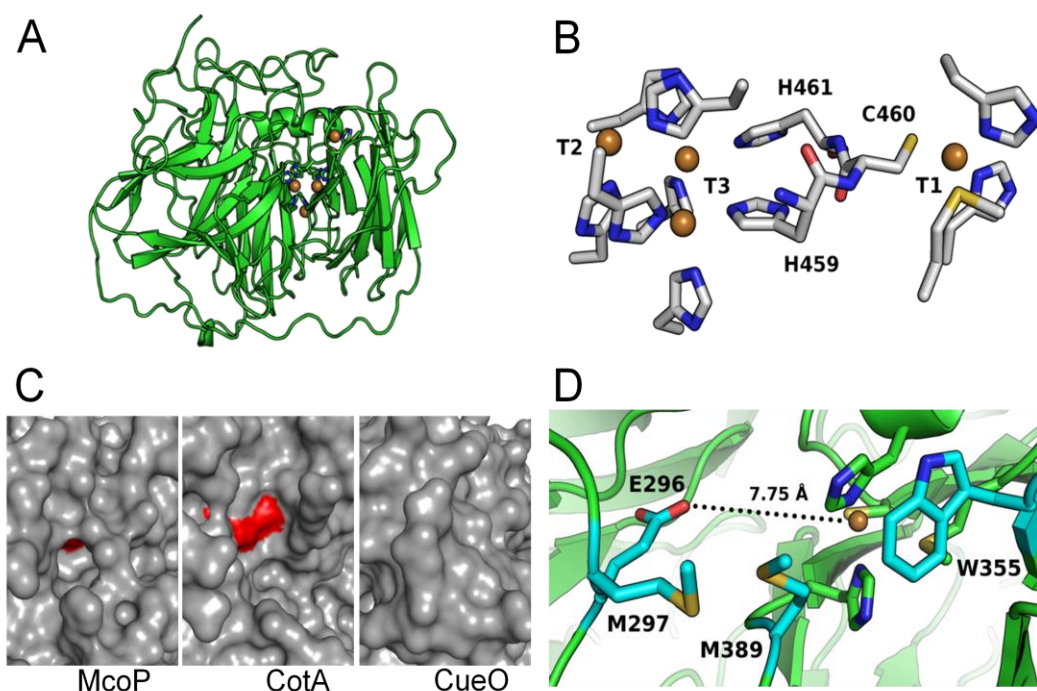


Figure 4.5: (A) Overall fold and copper centers of McoP. The protein is represented in cartoon with the copper coordinating residues in stick and the copper ions in sphere representation. (B) T1 and T2-T3 centers coordinating residues. The side chain residues of copper centers are in stick representation. The H459-C460-H461 triad bridges the T1 and T3 copper centers. (C) Comparison of binding pocket of McoP model with CotA and CueO structures. The proteins are in surface representation. The T1 copper center contribution to that surface is highlighted in red. (D) Close-up on the binding pocket near the T1 copper center of McoP. The T1 copper binding residues side chains are in stick representation. The occluding M297, M389 and W355 as well as the semi-buried E296 are also in stick representation and highlighted in cyan. This figure was prepared with PYMOL (DeLano, 2003).

The analysis of the model suggests that T1 center in McoP is less exposed than in the CotA laccase (Enguita, et al., 2003), but not so buried as the CueO, which is occluded by a Met-rich helix and loop in the latter (Figure 4.5C) (Roberts, et al., 2002). The residues contributing to the semi-occlusion of this site in McoP are W355 (which substitutes N408 in CueO and L386 in CotA), M389 (structurally equivalent to M441 of CueO) and M297 (in a similar position to M303 of CueO) (Figure 4.5D). Furthermore, there is a negatively charged residue in the neighbourhood of the T1 center, E296 (in a similar position to

Q302 of CueO), which is semi-buried into the binding pocket and at 7.75 Å distance of the T1 copper atom (Figure 4.5D).

***McoP is a thermoactive and hyperthermostable enzyme.*** As expected for a hyperthermophilic enzyme, McoP showed a reaction optimum temperature around 85°C (Figure 4.6) which is comparable to that of the *Thermus thermophilus* laccase (Miyazaki, 2005) and *A. aeolicus* metallo-oxidase (Fernandes, et al., 2007) and close to the optimal temperature for *P. aerophilum* growth (Volkl, et al., 1993).

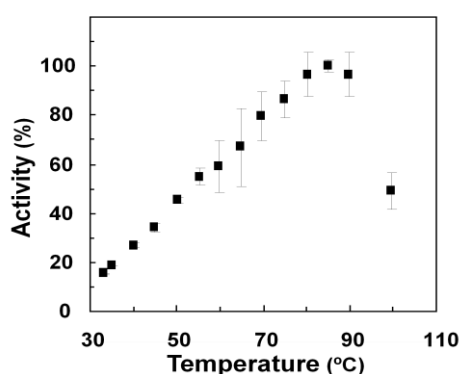


Figure 4.6: Temperature dependence of recombinant McoP activity.

McoP reveals intrinsic hyperthermostability, as shown by kinetic stability measurements at 80°C that allow determination of the amount of enzyme that loses activity irreversibly. The enzyme deactivates according to the first order kinetics and a half-life of inactivation of 330 min (5.5 hours) was calculated (Figure 4.7A and insert). This shows that McoP is a robust catalyst, although to lower extent than McoA from *A. aeolicus* and the laccase from *T. thermophilus* (Fernandes, et al., 2007; Miyazaki, 2005).

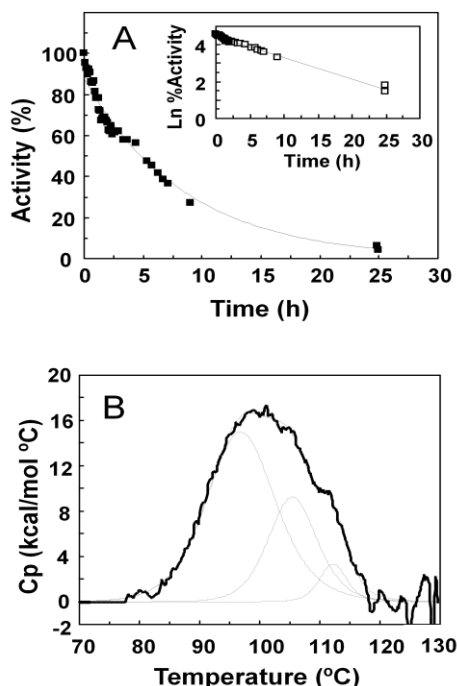


Figure 4.7: (A) Kinetic stability of McoP. The activity decay at 80°C was fitted accurately considering an exponential decay (the solid line shows the fit) with a half-life time of 330 minutes. The inset clearly shows that the activity decay of McoP can be fitted to a single first-order process, as the logarithm of activity displays an inverse linear relationship with time. (B) Differential scanning calorimetry of McoP. Excess heat capacity obtained from the DSC scan (at pH 3) of McoP. The thick line (experimental data) was fitted with three independent transitions shown separately in thin lines with melting temperatures of 96.6, 101.5 and 112.2°C.

The first-order deactivation kinetics can be described by the classical Lumry-Eyring model ( $N \leftrightarrow U \rightarrow D$  where N, U and D are the native, the reversibly unfolded and the irreversibly denatured enzyme), pointing to a simple pathway of unfolding and deactivation. The thermal stability was further probed by differential scanning calorimetry (DSC). The DSC thermogram (Figure 4.7B) reveals a complex process as the excess heat capacity profile can only be fitted using a non-two-state model with three independent transitions (Fernandes, et al., 2009). The mid-point temperatures at each transition clearly reflect the high stability of McoP: 96.6°C ( $\pm 0.7$ ), 101.5°C ( $\pm 0.4$ ) and 112.2°C ( $\pm 0.4$ ). Similarly, three transitions were previously used to describe unfolding profiles of plant ascorbate oxidase (Savini, et al., 1990), human ceruloplasmin

(Bonaccorsi di Patti, et al., 1990), CotA-laccase from *B. subtilis* (Duraio, et al., 2008) and McoA from *A. aeolicus* (Fernandes, et al., 2009) and they apparently correlate with a structural organization in three cupredoxin-like domains for the ascorbate oxidase, CotA-laccase and McoA, and six cupredoxin domains organized into three pairs in human ceruloplasmin (Lindley, 2001).

***McoP is a metallo-oxidase.*** The catalytic properties of McoP were measured with standard substrates in the presence of oxygen, i) two aromatic reducing substrates (2,2'-azinobis-(3-ethylbenzothiazoline-6-sulfonic acid) (ABTS) and the phenolic syringaldazine (SGZ) and ii) two metal reducing substrates,  $\text{Cu}^+$  and  $\text{Fe}^{2+}$  ions. The activity tested in the presence of various concentrations of exogenous copper (10-1000  $\mu\text{M}$   $\text{CuCl}_2$ ) revealed that 100  $\mu\text{M}$   $\text{CuCl}_2$  enhanced 2-fold the enzymatic rates and thus, all activities were measured in the presence of this copper concentration. Overall, the pH profiles for aromatics are similar to those of other characterized MCO (Xu, 1997), displaying the typical monotonically decrease for ABTS with maximal activity at pH 3 and a bell-shaped profile with optimum at pH 7 for SGZ oxidation (data not shown). The enzyme showed Cu(I)/Fe(II) oxidation kinetics that follow the Michaelis-Menten model with 2-10 higher efficiencies for  $\text{Cu}^+$  and  $\text{Fe}^{2+}$  as compared with the tested aromatic compounds, with ferrous ion being the favourite substrate (Table 4.1).

Table 4.1: Steady-state apparent kinetic parameters of McoP. Reactions were performed in the presence of 0.1 mM  $\text{CuCl}_2$  and at 40°C (30% of the maximal activity (see Figure 4.6)).

Substrate	$K_m^{\text{app}}$ ( $\mu\text{M}$ )	$k_{\text{cat}}^{\text{app}}$ ( $\text{min}^{-1}$ )	$k_{\text{cat}}/K_m$ ( $\text{M}^{-1}\text{s}^{-1}$ )
<b>Cu(I)</b>	124 $\pm$ 22	354 $\pm$ 30	4.8 x 10 <sup>4</sup>
<b>Fe(II)</b>	22 $\pm$ 2	126 $\pm$ 6	9.6 x 10 <sup>4</sup>
<b>ABTS</b>	133 $\pm$ 8	72 $\pm$ 6	0.9 x 10 <sup>4</sup>
<b>SGZ</b>	14 $\pm$ 5	24 $\pm$ 0	2.9 x 10 <sup>4</sup>



The metal oxidation efficiencies ( $k_{\text{cat}}/K_m$ ), measured at 40°C, are equivalent to those reported for other members of the MCO family (Fernandes, et al., 2007; Hall, et al., 2008; Singh, et al., 2004; Stoj and Kosman, 2003). Nevertheless, considering that at 40°C, only 30% of the maximal activity is achieved (Figure 4.6), McoP can be considered quite a remarkable catalyst at the optimum temperature with efficiencies of  $1.6 \times 10^5 \text{ M}^{-1}\text{s}^{-1}$  and  $3.2 \times 10^5 \text{ M}^{-1}\text{s}^{-1}$ , for  $\text{Cu}^+$  and  $\text{Fe}^{2+}$ , respectively.

Since substrate oxidation occurs via the T1 Cu center, substrate specificity is conferred by structure-activity relationships near this site (Kosman, 2009). Guided by the structure obtained by comparative modelling, site-directed mutagenesis was used to replace W355, M297 and M389 (Figure 4.5D) by alanine to test the hypothesis that these residues could i) hinder the access of bulky substrates or, ii) in the case of Met residues, provide a pathway for electron transfer from the metal substrates to the T1 center, as shown for CueO (Roberts, et al., 2002). We show that these mutations resulted in proteins exhibiting similar biochemical and spectroscopic properties as compared with wild-type (Table 4.2).

Table 4.2: Copper content, molar coefficients and reduction potentials ( $E^0$ ) of the T1 copper center of McoP and mutants. The  $E^0$  (T1) is determined using the Nernst equation.

Enzyme	Copper :protein	$\epsilon$ 600 nm ( $\text{mM}^{-1} \text{cm}^{-1}$ )	Redox potential (mV)
Wild-type	$3.2 \pm 0.1$	3.7	398
M297A	$3.1 \pm 0.3$	3.6	400
M389A	$3.4 \pm 0.3$	3.4	405
W355A	$3.0 \pm 0.1$	3.8	ND*
E296Q	$3.1 \pm 0.2$	3.8	435

For the Met and E296 mutants slight differences in the enzymatic efficiencies (2-3 fold lower), were found for the larger aromatic compounds, whereas these values remain basically unchanged for the smaller metal substrates (Table 4.3).

Table 4.3: Steady-state apparent kinetic constants for Cu<sup>+</sup> and ABTS for the different site-directed mutants. Reactions were performed at 40°C in the presence of 0.1 mM CuCl<sub>2</sub>.

Enzyme	$K_{m \text{ app}}$ ( $\mu\text{M}$ )		$k_{\text{cat app}}$ ( $\text{min}^{-1}$ )		$k_{\text{cat}} / K_{\text{m}}$ ( $\text{M}^{-1} \text{s}^{-1}$ )	
	Cu(I)	ABTS	Cu(I)	ABTS	Cu(I)	ABTS
Wild-type	124 $\pm$ 22	133 $\pm$ 8	356 $\pm$ 32	72 $\pm$ 5	4.8 $\times 10^4$	0.9 $\times 10^4$
M297A	101 $\pm$ 5	106 $\pm$ 6	272 $\pm$ 4	23 $\pm$ 4	4.5 $\times 10^4$	0.4 $\times 10^4$
M389A	100 $\pm$ 27	100 $\pm$ 4	299 $\pm$ 13	20 $\pm$ 1	5.0 $\times 10^4$	0.3 $\times 10^4$
W355A	87 $\pm$ 7	100 $\pm$ 10	256 $\pm$ 9	52 $\pm$ 7	4.9 $\times 10^4$	0.9 $\times 10^4$
E296Q	110 $\pm$ 17	136 $\pm$ 18	300 $\pm$ 20	28 $\pm$ 2	4.5 $\times 10^4$	0.4 $\times 10^4$

These changes are most probably associated with minor alterations in the neighbourhood of the T1 center. Overall we concluded that the mutated residues individually are not contributing appreciably for the substrate specificity of McoP.

McoP displays one of the lowest redox potential values (Figure 4.3) among MCO, ranging from 340 mV for ascorbate oxidase to 790 mV for some fungal laccases (Solomon, et al., 1996). We show by site-directed mutagenesis that this value is at least partially correlated with the proximity of E296 (Figure 4.5D) since its replacement by a glutamine resulted in an increase of the redox potential by 30 mV (Table 4.2). Therefore, the presence of this negative charge in the T1 neighbourhood most likely contributes to the stabilization the positive oxidized state of T1 Cu, in contrast with the neutral reduced state, leading to a lower redox potential. Interestingly, ascorbate oxidase also exhibits a negatively

charged residue close to the T1 Cu center and a relatively low redox potential (see above) (Quintanar, et al., 2007).

***McoP uses N<sub>2</sub>O as well as O<sub>2</sub> as electron acceptor.*** Considering the recent hypothesis raised by Cozen and co-workers (2009) that McoP could play a role in the denitrification pathway of *P. aerophilum*, we have tested the catalytic reduction of dioxygen, nitrous oxide and nitrite, using Fe<sup>2+</sup> as electron donor. McoP is unable to reduce NO<sub>2</sub><sup>-</sup> under the tested conditions, but it does reduce N<sub>2</sub>O and O<sub>2</sub> at the rates of 6.8 (± 0.5) and 3.8 (± 0.7) μmol·min<sup>-1</sup>·mg<sup>-1</sup>, respectively. Therefore we conclude that McoP is kinetically competent to reduce nitrous oxide to nitrogen and water, as well as dioxygen to water. In order to get further insight into the catalytic features of McoP, the reaction mechanisms for the reduction of nitrous oxide and dioxygen, were addressed under steady-state conditions. Primary plots of 1/V<sub>0</sub> versus 1/[S] for the oxidation of McoP by nitrous oxide or dioxygen (Figure 4.8A, B) reveal parallel lines that are consistent with a ping-pong mechanism that is in accordance with the previous findings reported for the laccases of the lacquer tree *Rhus vernicifera* and the fungus *Trametes villosa* (Bukh, et al., 2006; Petersen and Degn, 1978).

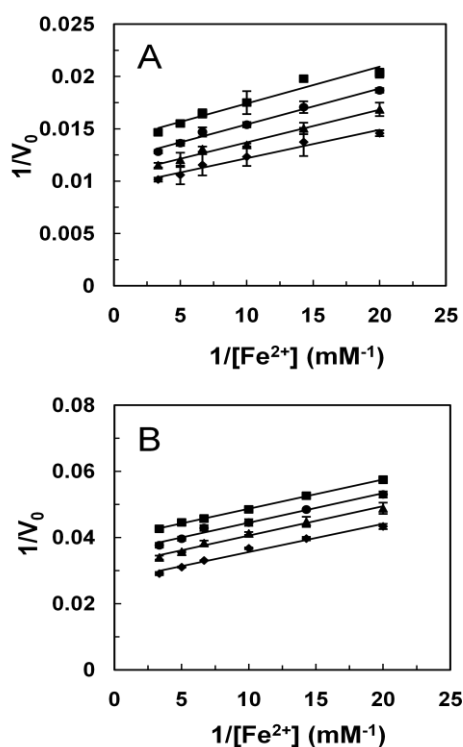


Figure 4.8: Primary plots of  $1/V_0$  against  $1/[S]$  for McoP. Oxidation of ferrous ion (Fe(II)) at different concentrations of (A)  $N_2O$  and (B)  $O_2$  (50  $\mu M$  ■, 70  $\mu M$  ●, 120  $\mu M$  ▲ and 250  $\mu M$  ◆).  $V_0$  and  $[Fe^{2+}]$  are the initial rate of oxidation and concentration of reducing substrate, respectively. Error bars show sample standard deviation.

The kinetic parameters of McoP towards  $N_2O$  and  $O_2$  were deduced using the secondary plots of the line intercepts versus  $1/[B]$  and slopes versus  $1/[B]$  for which the following equations were used:

$$(16) \quad \frac{1}{V_o} = \frac{K_{mB}}{V_{max}} \frac{1}{B} + \frac{1}{V_{max}}$$

$$(17) \quad \frac{K_{mappA}}{V_o} = \frac{K_{mA}}{V_{max}}$$

$V_o$  is the enzyme activity,  $K_m$  is the affinity constant, either for A (reducing) or B (oxidizing) substrate. The obtained  $K_m$  values are similar for  $O_2$  ( $31 \pm 0.2 \mu M$ ) and  $N_2O$  ( $33 \pm 4 \mu M$ ,

Table 4.4). As expected, the  $K_m$  values for  $Fe^{2+}$  remain the same, in reactions using either electron acceptor. However, the turnover rates are around 3-fold higher for  $N_2O$  as substrate than for  $O_2$  and a higher efficiency was measured for  $N_2O$  reduction as compared to the  $O_2$  reduction

Table 4.4: Steady-state kinetic parameters for recombinant enzymes McoP from *P. aerophilum* and CotA-laccase from *B. subtilis* measured at 40°C. Reactions were performed using either  $N_2O$  or  $O_2$  as reducing substrate. Due to the different specificity for reducing substrates, Fe(II) was used in assays with the metallo-oxidase McoP, and ABTS in reactions using CotA-laccase.

Enzyme	Substrates	$K_m$ ( $\mu M$ )	$k_{cat}$ ( $s^{-1}$ )	$k_{cat}/K_m$ ( $M^{-1} s^{-1}$ )
<b>McoP</b>	Fe(II)/ $O_2$	$O_2$	$31 \pm 0.2$	$0.9 \times 10^5$
		Fe(II)	$35 \pm 0.2$	$0.9 \times 10^5$
	Fe(II)/ $N_2O$	$N_2O$	$32 \pm 1.0$	$3.0 \times 10^5$
		Fe(II)	$33 \pm 4.0$	$3.0 \times 10^5$
<b>CotA</b>	ABTS/ $O_2$	$O_2$	$37 \pm 1.0$	$58 \times 10^5$
		ABTS	$109 \pm 1.0$	$20 \times 10^5$
	ABTS/ $N_2O$	$N_2O$	$168 \pm 0.3$	$1.3 \times 10^5$
		ABTS	$126 \pm 2.0$	$1.7 \times 10^5$

Therefore, McoP shows a preference to nitrous oxide as substrate. In analogous assays, we tested the nitrous oxide reductase activity of the recombinant enzymes McoA from *A. aeolicus* and CotA-laccase from *B. subtilis*. The metalloxidase McoA under the tested conditions is unable to use nitrous oxide as electron acceptor. Notably, CotA-laccase is able to use  $N_2O$  as electron acceptor although with a 10-fold lower  $k_{cat}$  than the one determined for  $O_2$  (in a reaction where ABTS was used instead of  $Fe^{2+}$  as the electron donor), clearly showing that dioxygen is its favourite substrate (Table 4.4).

#### 4.4. DISCUSSION

The hyperthermophilic archaeon *P. aerophilum* can use diverse respiratory pathways which suggest that this organism is capable to respond to geochemical fluctuations within its native environments. Unlike most hyperthermophilic *Archaea* this archaeon can withstand the presence of oxygen, growing efficiently under microaerobic conditions. This fact explains the presence of an open reading frame in its genome, putatively assigned to a multicopper oxidase, which is not found among its anaerobic close relatives. The dissimilatory nitrate reduction to dinitrogen in *P. aerophilum* is relatively well studied; enzymatic activities of the denitrification pathway were detected in cellular fractions, and  $\text{NO}_3^-$  and NO reductases purified and characterized (Afshar, et al., 2001; Afshar, et al., 1998; de Vries, et al., 2003; Fitz-Gibbon, et al., 2002; Volkl, et al., 1993). Noteworthy, no recognizable homolog of *nosZ*, which encodes for nitrous oxide reductase ( $\text{N}_2\text{OR}$ ) in bacteria, has been found in the genome of this archaeon, indicating the existence of an alternative type of microbial  $\text{N}_2\text{O}$  reductase (Zumft and Kroneck, 2007). Interestingly, as in the case of *P. aerophilum*, the genomes of denitrifying microorganisms *Nitrosomonas europaea*, *Nitrosomonas eutropha*, *Haloferax volcanii* and *Haloarcula marismortui* lack the typical bacterial genes for  $\text{N}_2\text{O}$  reduction (Zumft and Kroneck, 2007). Recently, DNA microarrays were used to compare genome expression patterns of *P. aerophilum* cultures supplemented with oxygen, nitrate, arsenate or ferric iron-citrate as terminal electron acceptors (Cozen, et al., 2009). These studies revealed an upregulation of gene PAE1888 coding for McoP during nitrate respiration suggesting a role for this MCO as a  $\text{N}_2\text{OR}$ . The present study provides experimental evidence that McoP is kinetically competent to use  $\text{N}_2\text{O}$  as electron acceptor providing further evidences in support of a role in the denitrification pathway of *P. aerophilum*. The specific activity of the recombinant McoP measured *in vitro* ( $6.8 \text{ U mg}^{-1}$  at  $40^\circ\text{C}$  which corresponds to  $26 \text{ U mg}^{-1}$  at  $85^\circ\text{C}$ , the optimal reaction temperature) lies in the middle of the range of values found for other  $\text{N}_2\text{ORs}$  from *Achromobacter*

*cycloclastes*, *Pseudomonas nautica*, *Geobacillus thermodenitrificans* or *Paracoccus denitrificans*, that show activities from 1.2 to 157 U mg<sup>-1</sup> (Dell'acqua, et al., 2008; Fujita, et al., 2007; Kristjansson and Hollocher, 1980; Liu, et al., 2008). Nevertheless, higher *in vivo* catalytic efficiency can be anticipated as a result of the interaction with the putative physiological redox partner(s). McoP is most probably localized in the “periplasmic” space between the cytoplasmic membrane and the S-layer of *P. aerophilum*, as its sequence contains a putative TAT-dependent signal peptide. The activities of the remaining denitrification pathway enzymes are localized in the membrane of *P. aerophilum* (Afshar, et al., 1998; de Vries, et al., 2003), therefore various small mobile electron carriers (e.g. cytochromes or cupredoxins) that could possibly act as physiological electron donors for McoP are expected to be present in the membrane vicinity (Dell'acqua, et al., 2008). *P. aerophilum* does not have polyhemic *c*-type cytochromes but its genome sequence contains two ORFs that encode for putative *c*-type monohemic, cytochrome-containing proteins (Feinberg and Holden, 2006). Nevertheless, as the substrate specificity of MCO is quite broad and thus the nature of physiological reductant of McoP is not clear at this point. For example, over 50 substrates have been identified in the reaction catalyzed by human ceruloplasmin, a mammalian MCO that is abundant in the serum and in interstitial fluid (Frieden and Hsieh, 1976; Hellman and Gitlin, 2002; Young and Curzon, 1972).

In spite of being promiscuous regarding the reducing substrates, dioxygen has been described as their sole oxidant of MCO (Bento, et al., 2005; Kosman, 2009; Lindley, 2001; Solomon, et al., 2008; Solomon, et al., 1996). The main electron transfer steps in the reaction mechanism of MCO are: i) the reduction of the T1 copper center by the substrates, ii) the electron shuttle, through the Cys-His electron transfer pathway, to the trinuclear center, and iii) the dioxygen reduction by the trinuclear cluster (Bento, et al., 2005; Chen, et al., 2010; Solomon, et al., 2008). The trinuclear center is primed to bind dioxygen and generate bridged intermediates, but it also binds other exogenous ligands such

as, nitric oxide, cyanide, fluoride and azide (Bento, et al., 2005; Solomon, et al., 1996; Wilson and Torres, 2004). The finding that McoP, as well as CotA laccase from *B. subtilis*, are able to couple the  $4e^-/4H^+$  reduction of  $O_2$  to  $H_2O$  as well as the  $2e^-/2H^+$  reduction of  $N_2O$  to  $N_2$  and  $H_2O$ , is quite interesting from the point of view of the MCO enzymology and raises new questions regarding the reaction mechanisms taking place at the trinuclear site of these enzymes. Coincidentally, the microbial  $N_2O$  reductases, whose kinetic and structural characteristics have been studied in most detail in bacteria of the genera *Pseudomonas*, *Paracoccus* and *Achromobacter* are homodimeric multi-copper proteins (Solomon, et al., 2007; Zumft and Kroneck, 2007). The crystal structures of  $N_2OR$  revealed that the copper ions are organized in two centers, a di-copper electron transfer and storage cluster,  $Cu_A$ , and the tetra-copper-sulphide center,  $Cu_Z$ ; the former resembles the  $Cu_A$  found in cytochrome oxidases and the latter is a novel mixed-valent copper center ( $Cu_4S$ ) with a sulphide ion bridging a distorted tetrahedron of copper atoms (Brown, et al., 2000; Haltia, et al., 2003; Paraskevopoulos, et al., 2006). This cluster is coordinated by seven histidines and a water-derived ligand is proposed to bridge two of the copper ions ( $Cu_I$  and  $Cu_{IV}$ ), where substrate binds to the enzyme. It was proposed on the basis of the crystal structures that electrons enter at the mixed valent binuclear  $Cu_A$  center of one subunit and are transferred over a 10 Å super exchange pathway to the  $Cu_Z$  cluster of a second subunit where  $N_2O$  reduction occurs (Brown, et al., 2000; Paraskevopoulos, et al., 2006; Zumft and Kroneck, 2007). Interestingly, copper nitrite reductases contain both T1 and T2 Cu sites in their catalytic centers (Tavares, et al., 2006).

The efficiency of cuprous and ferrous ion oxidation by McoP is up to 10-fold higher than those observed for other metallo-oxidases, such as *E. coli* CueO, human ceruloplasmin or yeast Fet3p (Kosman, 2009; Stoj and Kosman, 2005). These are reported to play a critical role in the maintenance of metal ion homeostasis in the respective organisms (Kosman, 2009; Lindley, 2001; Stoj and Kosman, 2005). The analysis of the *P. aerophilum* genome shows that



*mcoP* is not part of a putative metal-resistant determinant, as it is the case of *cueO* in *E. coli* or *mcoA* in *A. aeolicus* (Fernandes, et al., 2007; Stoj and Kosman, 2005), however McoP could probably act *in vivo* as a cytoprotector since it has the catalytic competence to shift Cu(I) or Fe(II) towards the less toxic oxidised forms. Moreover, the enzymes from the MCO family are known as “moonlighting” proteins, which are able to change their functions in response to changes in concentration of their ligand/substrate, differential localization and/or differential expression (Bielli and Calabrese, 2002). As an example, plausible physiological function(s) of human ceruloplasmin include copper transport, iron homeostasis, biogenic amine metabolism and defence against oxidative stress (Bielli and Calabrese, 2002).

In conclusion, this work provided the spectroscopic, biochemical and kinetic characterization of a unique hyperthermostable MCO that exhibits a higher specificity for nitrous oxide than for dioxygen, representing a novel N2OR. *P. aerophilum* thrives in geothermally and volcanically heated habitats, in which potentially cytotoxic metals are usually abundant. In accordance with this, McoP is a thermoactive and thermostable metallo-oxidase showing high efficiency in the oxidation of toxic transition metals. Work is in progress to determine the crystallographic structure of this enzyme, which will help in the dissection of its unusual properties.

#### 4.5. SUPPLEMENTARY MATERIAL

Table 4.S5: Purification of recombinant McoP produced in *Escherichia coli*

Purification step	Protein (mg)	Total Activity (μmol/min.mL)	Specific Activity (μmol/min.mg)	Yield (%)	Purification (fold)
CrudeExtract	242	12.0	0.050	100	-
Histrap	6	10.2	1.7	84.5	34.9
Superdex	1.2	3.0	2.2	25.0	43.6

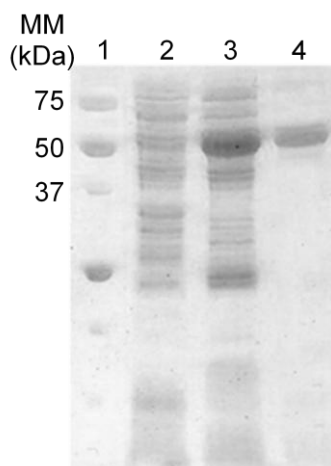


Figure 4.S4.9: SDS-PAGE analysis of McoP overproduction and purification. Lane 1, standard molecular mass markers. Lane 2, crude extract of an IPTG-induced *E. coli* culture. Lane 3, sample after the His-Trap chromatography. Lane 4, sample after the Superdex-75 chromatography.

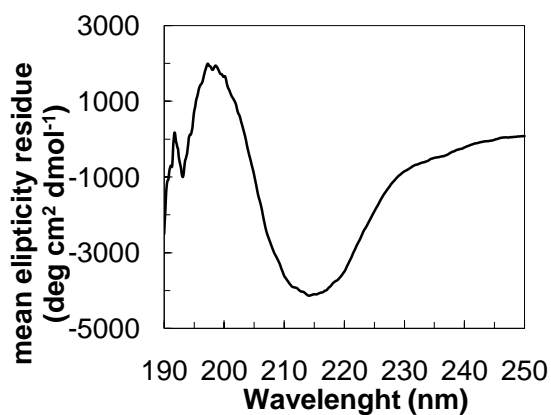


Figure 4.S10: CD spectrum in the far-UV region, reflecting the typical secondary structure of multicopper oxidases, rich in  $\beta$ -sheets, with a negative peak at 213-214 nm.

# 5 STABILITY STUDIES IN COTA-LACCASE FROM *BACILLUS SUBTILIS*

---

5.1.	REPLACEMENT OF THE AXIAL LIGAND IN COTA.....	132
5.2.	EFFECT OF COPPER CONTENT IN THE STABILITY OF COTA...	143
5.3.	THE REMOVAL OF A DISULFIDE BRIDGE OF COTA .....	155

## ABSTRACT

CotA-laccase has the dual advantage of being both thermostable ( $t_{1/2}$  (80°C) = 2h) and thermoactive ( $T_{\text{opt}} = 75^\circ\text{C}$ ) and is able to oxidise a variety of substrates including non-phenolic and phenolic compounds, and also a range of synthetic azo and anthraquinonic dyes, thus having a potential use for diverse biotechnological applications. Furthermore, chemical denaturation studies, as assessed by trp fluorescence, revealed that CotA unfolds according to a two-state transition ( $N \leftrightarrow U$ ), with a midpoint of GdnHCl concentration as high as 4.6 M and a free-energy exchange in water of 10 kcal mol<sup>-1</sup>. We have also found that, copper depletion from type 1 copper site is a key event in the inactivation of the enzyme and thus a determinant of its thermodynamic stability. In fact, mutations in the axial ligand of T1 Cu that subtly perturbed its coordination lead to dramatic effects on the thermodynamic stability of the enzyme. The use of a multidimensional approach that measures changes at the level of tertiary structure (fluorescence), secondary structure (circular dichroism in the far-UV), function (activity) and copper binding/coordination (absorbance at 600 nm) provided information on the heterogeneity of protein population in equilibrium. It was found that the copper content of CotA-laccase has a profound impact in the kinetic and thermal stability of CotA as assessed by long term stability (at 80°C) and differential scanning calorimetry (DSC). Indeed, holoCotA, produced in recombinant *Escherichia coli* under microaerobic conditions, is a very stable enzyme, followed by apoCotA reconstituted in vitro with Cu<sup>+</sup>, and by apoCotA reconstituted with Cu<sup>2+</sup>. Therefore, Cu incorporation into the protein seems to occur more effectively during the *in vivo* folding and is dependent on its oxidation state, a higher Cu:protein ratio is achieved with Cu<sup>+</sup> than with Cu<sup>2+</sup> form.

**This chapter was published in the following scientific papers:**

Paulo Durão, Isabel Bento, André T. Fernandes, Eduardo P. Melo, Peter F. Lindley, Lígia O. Martins. 2006. Perturbations of the T1 copper site in the CotA-laccase from *Bacillus subtilis*: structural, biochemical, enzymatic and stability studies. J. Biol. Inorg. Chem. 11: 514-526\*

Paulo Durão, Zhenjia Chen, André T. Fernandes, Peter Hildebrandt, Daniel H. Murgida, Smilja Todorovic, Manuela M. Pereira, Eduardo P. Melo, Lígia O. Martins. 2008. Copper incorporation into recombinant CotA-laccase from *Bacillus subtilis*: characterization of fully copper loaded enzymes. J. Biol. Inorg. Chem. 13:183-93\*

André T. Fernandes, Manuela M. Pereira, Catarina I. Silva, Isabel Bento, Peter F. Lindley, Eduardo Pinho Melo, Lígia O. Martins. 2010. The removal of a disulfide bridge of CotA-laccase changes the slower motion dynamics involved in copper binding but has no effect on the thermodynamic stability. J. Biol. Inorg. Chem. DOI: 10.1007/s00775-011-0768-9.

\* I have performed the stability measurements in the papers

CotA-laccase is a MCO and is an integral protein of the outer layer matrix of the spore of the Gram positive bacterium *Bacillus subtilis*. The spores are structures designated to resist to a wide range of physical-chemical extremes such as wet and dry heat, desiccation, radiation, UV light and oxidizing agents, which would destroy vegetative cells. In *B. subtilis* the dehydrated spore core, which contains a copy of the chromosome, is surrounded by a thick layer of a modified peptidoglycan called the cortex, which is delimited by two layers. The inner coat layer is in direct contact with the cortex with a fine lamellar appearance and mainly composed by proteins. The outer coat layer is thicker and is also composed by proteins, including CotA-laccase (Driks, 1999). The structure of the coat results from a multistep assembly process that involves more than 30 different protein components ranging in size from about 6 to 70 kDa. A CotA null mutant ( $\Delta cotA$ ) has no detectable effect on lysozyme resistance or germination, but it does prevent the appearance of a brown pigment characteristic of colonies in the late stages of sporulation, which should protect spores against UV light (Martins, et al., 2002). The gene coding for CotA-laccase was cloned, the protein was produced in *E. coli* purified and characterized. X-ray studies have shown that the enzyme has the typical 3-domain fold of laccase (Enguita, et al., 2003) with a T1 mononuclear copper center in domain 3 and a trinuclear copper cluster (two T3 ions and a T2 copper ion) located between domains 1 and 3, and have given insights regarding the role of ABTS as an oxidative mediator (Enguita, et al., 2004). Moreover, studies involving structural intermediates of O<sub>2</sub> reduction have provided a new model mechanism for the dioxygen reduction in multicopper oxidases (Bento, et al., 2005). We have used CotA-laccase as a model system in our lab, and have performed several different structure-function studies. In the frame of these studies, the kinetic and thermodynamic stability of the enzyme and variants was assessed as well as the effect of copper incorporation.

### 5.1. EFFECT OF THE REPLACEMENT OF THE AXIAL LIGAND IN THE REDOX PROPERTIES OF COTA

The catalytic rate-limiting step in MCO is considered to be the oxidation of substrate at the T1 site, most probably controlled by the difference of the redox potential between this site and the substrate (Xu, 1996). Redox potentials exhibited by laccases span a broad range of values from 400 mV for plant laccases to 790 mV for some fungal laccases (Solomon, et al., 1996). The conserved coordinating amino acids for the T1 copper site are two histidines and a cysteine, and natural variations occur in the so called axial position with a single interaction from a methionine being the most common arrangement (Figure 5.1)

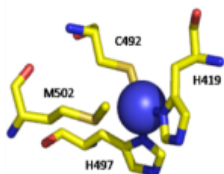


Figure 5.1: Insight into the T1 copper center of CotA-laccase. Figure prepared with Pymol (DeLano, 2003)

Fungal laccases have non-coordinating phenylalanine or leucine at this position and these may contribute, at least in part, to the high  $E^0$  observed in these enzymes (Karlin, et al., 1997). This high redox potential should be a direct consequence of the nature of the axial ligand, which influences the stabilization of the reduced, versus the oxidised, state of the copper atom. However, other parameters are known to influence the redox potential, such as the solvent accessibility of the metal site, the charge dipole distribution around the copper, and the hydrogen bonds with the Cys sulphur atom.

Axial ligand mutations at T1 copper sites in other enzymes (such as the blue copper enzymes) have been studied and it has been recognized the importance of the nature of these residues in modulating the redox potential in a range of ~100-200 mV (Kataoka, et al., 2005; Palmer, et al., 2003; Xu, 1996; Xu, et al., 1999). The present study utilized site-directed mutagenesis to examine how the

replacement of a weakly coordinating methionine of the T1 mononuclear copper by the non-coordinating residues, phenylalanine and leucine, affects the protein regarding structure, redox potential, the enzymatic properties,  $k_{\text{cat}}$  and  $K_{\text{m}}$ , and its overall thermodynamic stability. This information will assist the development of strategies targeted at the improvement of laccases as biocatalysts.

The reduction potential of the T1 copper was 455 mV, 548 mV and 515 mV for the wild-type, M502L and M502F mutants, respectively. Thus the replacement of the axial methionine residue by a leucine and phenylalanine in the CotA-laccase led to an increase of the redox potential by ca. 100 mV and 60 mV, respectively. However, this increase in  $E^0$  was accompanied by significant changes in the catalytic properties for both mutants. The M502L mutant exhibits a 2-4 fold decrease in the  $k_{\text{cat}}$ , compared with the wild-type enzyme towards the oxidation of all the non-phenolic and phenolic substrates tested, while M502F presents a 10-fold decrease in the  $k_{\text{cat}}$  towards the oxidation of the non-phenolics and an 1840- and 665-fold decrease in the  $k_{\text{cat}}$  towards the oxidation of the phenolic substrates.

The higher reduction potential determined for both mutants would appear to favour an increased reaction velocity, however, no direct correlation was found between the reduction potentials calculated for the M502L and M502F enzymes and the oxidation rates of several non-phenolic and phenolic substrates tested when compared with the wild-type enzyme. This leads us to hypothesize that mutations could have affected the electronic tunnelling and/or the reorganization energy (which is dependent on the dynamics of the protein) of the two electron-transfer processes (from the reducing substrate to the T1 center and/or from this to the trinuclear site). In alternative, it cannot be ruled out an effect of the mutations on the binding pocket the enzyme. In fact, the oxidation of substrates by laccases at the T1 site is considered to be a “outer-sphere” electron transfer, described by Marcus theory (Marcus and Sutin, 1985). Outer-sphere electron transfer (ET) refers to an ET event that occurs between two

species that remain separate before, during, and after the ET event, forcing the electron to move through space from one redox center to the other (Moser and Dutton, 1996). According to Marcus theory, an “outer-sphere” ET rate ( $k_{ET}$ ) is mainly determined by three factors: the donor-acceptor electronic coupling, the redox potential, and the reorganization energy (Moser and Dutton, 1996).

Interestingly, the structural comparison of both mutants with the wild-type CotA showed no major alterations in the overall fold of the enzyme. The exception is a region positioned close to the mutated residue. Indeed, the slight movement of the mutated residue towards the protein surface, and away from the T1 copper atom, leads to a concerted movement of this region, pushing it away towards the solvent, and slightly increasing the exposure of the copper center (Figure 5.2).

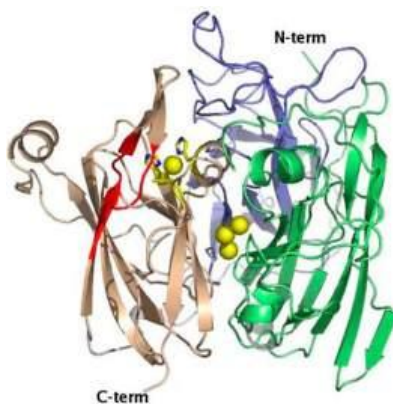


Figure 5.2: Representation of the three-dimensional structure of CotA with the cupredoxin domains coloured differently (domain 1 green, domain 2 slate, domain 3 wheat) and the variant region in red (M502L residues 371–377, 386–399; M502F residues 375–376, 387–389).

### 5.1.1. EXPERIMENTAL PROCEDURES

Steady-state fluorescence was measured in a Carry Eclipse spectrofluorimeter using 280nm as excitation wavelength. CotA-laccase and single mutants were in Tris-HCl buffer 20mM at pH 7.6 with 200mM NaCl. Several fluorescence signals can be used to monitor the unfolding transitions of proteins such as steady-state fluorescence intensity, emission maximum and fluorescence



anisotropy. Currently fluorescence intensity (total intensity by integrating the emission at different wavelengths or intensity at a specific wavelength) is mostly used and appropriately measured as it is directly related to the mole fraction of states of the protein (Eftink, 1994). For some cases such as the enzymes under study, fluorescence intensity can not be used because there is no significant discernible difference between the signals from macroscopic states that characterize unfolding transitions. Although, fluorescent intensity changes can not be used, the emission maximum shifts to longer wavelengths upon unfolding when tryptophan residues become exposed to the high polarity of water molecules (the enzyme emission maximum shifts from 330 to 354 nm upon unfolding). To monitor unfolding of the enzymes under study using fluorescence, a combination of two signals was used: fluorescence intensity and emission maximum. The use of the emission maximum might skew slightly the tracking of the population of states towards the more intensely emitting state (Eftink, 1994; Monsellier and Bedouelle, 2005), but the use of these two signals was the only approach able to provide accurate data within the transition region. Firstly, the spectra were normalized (dividing by the intensity at the maximum of emission) to reflect clearly the shift in the emission maximum. Secondly, the wavelength at which the relative fluorescence intensity (intensity relative to the maximum) changes more significantly was selected (370nm for CotA-laccase and mutants) and the relative fluorescence intensity at this wavelength was used to monitor unfolding of CotA-laccase and single mutants. Further details are given in the Durão et al., 2006.

The thermodynamic stability was also evaluated based on enzymatic activity and absorbance at 600 nm in the presence of different concentrations of guanidinium hydrochloride (GdnHCl). Absorbance at 600 nm was measured in the presence of different GdnHCl concentrations (0-3M), by using 123  $\mu$ M CotA in 20 mM Tris-HCl pH 7.6 buffer with 200 mM NaCl. Enzymatic activity was measured in the same GdnHCl concentration range, following the oxidation of SGZ at 530 nm in the same buffer by using 0.015, 0.29, 0.30  $\mu$ M of CotA,

M502L and M502F, respectively. These measurements were done in a 96 well plate spectrophotometer Spectra Max 384 from Molecular Devices.

### 5.1.2. THERMODYNAMIC STABILITY OF M502 MUTANTS

The thermodynamic stability and characterization of the unfolding of CotA induced by GdnHCl was achieved by using different spectroscopic techniques and activity measurements. Figure 5.3A shows the thermodynamic stability of the tertiary structure of CotA wild type as assessed by fluorescence. The wavelengths at the emission maxima reflect clearly the exposure of tryptophan residues to the high polarity of water at the surface of the protein upon unfolding (Lakowicz, 1999).

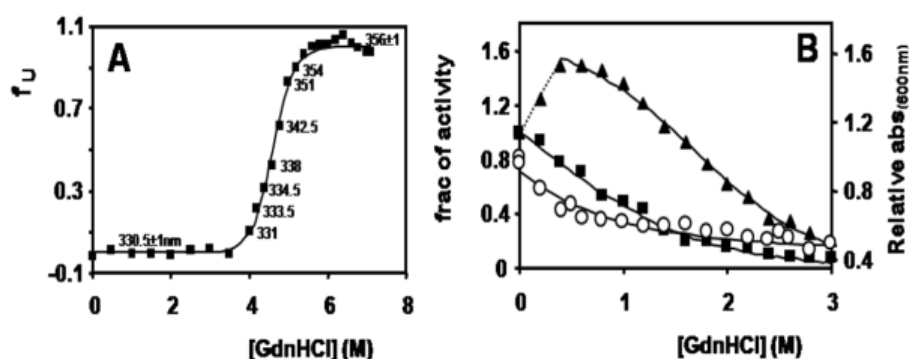


Figure 5.3: (A) Fraction of wild-type CotA laccase unfolded ( $f_U$ ) by guanidinium hydrochloride (GdnHCl) as measured by fluorescence emission. The solid line is the fit according to the equation  $f_U = \exp(\Delta G^0/RT) / (1 + \exp(\Delta G^0/RT))$ , and the numbers are the wavelengths at the emission maximum. (B) Change in activity in the absence (squares) and presence (triangles) of copper (copper-to-CotA ratio 4:1) and change in absorbance at 600 nm (circles) at increasing GdnHCl concentrations. The solid lines are the fits according to the equation  $y = y_N + y_{N(\text{no copper})} \exp(\Delta G^0/RT) / (1 + \exp(\Delta G^0/RT))$ , which assumes the equilibrium  $N \leftrightarrow N_{\text{no copper}}$  (Durao, et al., 2006). In the presence of exogenous copper, an initial increase in activity which cannot be fitted according to the process of copper loss is highlighted by a dashed line to help visual inspection.

The CotA tertiary structure unfolding, was fitted according to a two state transition which assumes the equilibrium  $N \leftrightarrow U$  (Figure 5.3A). (Durao, et al., 2006). The thermodynamic data shows that CotA-laccase is very stable,

displaying a GdnHCl concentration of 4.6 M at the midpoint (where 50% of the molecules are unfolded), and the native state is more stable than the unfolded state by 10 kcal mol<sup>-1</sup> at 25 °C (Table 5.1).

Table 5.1: Thermodynamic stability of the tertiary structure of CotA wild-type as assessed by fluorescence spectroscopy

	$\Delta G_{1st}^{\circ \text{ water (a)}}$ (kcal/mol)	$m_{1st}$ (kcal/mol)	Mid-point <sub>1st</sub> (M)
<b>CotA wt</b>	10.0±0.1	2.2±0.0	4.6±0.1

Far-UV circular dichroism was also used to assess the unfolding of the secondary structure (data not shown). The CotA secondary structure unfolds at the same GdnHCl concentration as unfolding of the tertiary structure was observed (4-6 M) but accurate quantification was not possible. CotA has a relatively low content of the secondary structure, mostly  $\beta$ -sheets (3.5% of  $\alpha$ -helixes and 37% of  $\beta$ -sheets, PDB entry 1GSK) which display a low mean residue ellipticity (Kelly and Price, 1997).

Thermodynamic stability was also assessed by activity measurements and absorbance at 600 nm to probe CotA function and copper binding at T1, respectively (Figure 5.3B). The data can be described assuming the equilibrium  $N \leftrightarrow N_{\text{no copper}}$  which relates the native population of the protein with (N) and without copper ( $N_{\text{no copper}}$ ) (Durao, et al., 2006). Since both the activity and the absorbance at 600 nm depend on copper binding to T1 center and they follow approximately the same trend upon increased GdnHCl concentrations, the decays of activity and absorbance at 600 nm were accurately fitted according to a two-state process describing an equilibrium between the native state with copper and the native state with no copper at T1 ( $N \leftrightarrow N_{\text{no copper}}$ ). Parameters describing this equilibrium assessed by activity are shown in Table 5.2.

Table 5.2: Thermodynamic stability of CotA wild-type as assessed by activity. Activity was measured in the absence and presence of copper (1:4 ratio protein:copper).

	$\Delta G^{\circ}1^{st}water$ (a) (kcal/mol)	m1 <sup>st</sup> (kcal/mol)	Mid-point1 <sup>st</sup> (M)
<b>CotA wt</b>	0.2±0.0	0.7±0.1	0.3±0.1
<b>CotA wt + copper (1:4)</b>	1.4±0.4	0.9±0.1	1.5±0.3

(a) 1<sup>st</sup> states for first transition, which is from N with copper (N) to N without copper (N<sub>no Cu</sub>) for the wt.

The process of copper depletion from T1 and the concomitant loss of activity seem not to be related to the unfolding of secondary and tertiary structures as they occur at much lower GdnHCl concentrations, 0.3 M compared with 4.6 M. Therefore, copper depletion is the key event in the enzyme inactivation and thus in the thermodynamic stability of CotA wild-type. Even in buffer (at 0 M GdnHCl), the native state with copper is only marginally more stable than the native state without copper at the T1 (0.2 kcal mol<sup>-1</sup>), leading to the accumulation of around 43% of CotA molecules without copper. This observation is fully supported by measuring the equilibrium between N and N<sub>no copper</sub> in the presence of copper in solution (Figure 5.3B, Table 5.2). CotA wild-type is able to incorporate copper with an initial increase in GdnHCl concentration up to 0.4 M, leading to an increase in activity. The parameters obtained from the fit also reflect copper uptake as the equilibrium is shifted towards N in the presence of copper and the energy gap between N and N<sub>no copper</sub> increases to 1.4 kcal mol<sup>-1</sup>. Clearly, the loss of the CotA enzymatic activity correlates to T1 copper depletion, and not with global unfolding of secondary and tertiary structures.

These results appear to contradict previous results where it was observed that the unfolding of three fungal laccases coincides with their inactivation (Kelly and Price, 1997), but are in accordance with results obtained for the thermal denaturation of the plant *Rhus vernicifera* laccase (Agostinelli, et al., 1995) and in the fungal *Coriolus hirsutus* and *Coriolus zonatus* laccases (Koroleva, et al.,

2001), where copper is lost at relatively low temperatures and where global unfolding of secondary and tertiary structures could not still be detected.

The mutations M502L and M502F have a profound impact on the stability of CotA. Only the stability of M502L is shown in Figure 6.4 but the mutant M502F shows basically the same behaviour (Table 5.2).

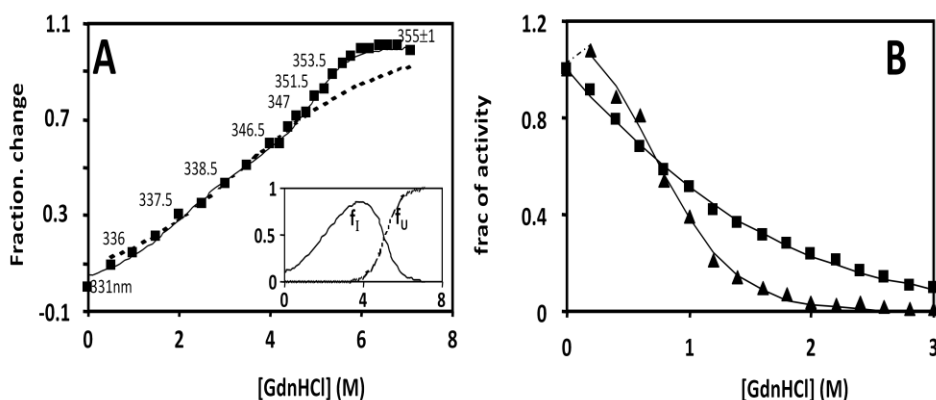


Figure 5.4: (A) Fractional change of the fluorescence signal from M502L mutant induced by GdnHCl as measured by fluorescence emission. The dashed line is the fit according to a two-state model ( $N \leftrightarrow U$ ), and the solid line is the fit according to a three-state model ( $N \leftrightarrow I \leftrightarrow U$ ) (Durao, et al., 2006). Numbers are the wavelengths at the emission maximum showing that M502L mutant initiate unfolding (accumulation of I) at very low GdnHCl concentrations. The inset shows precisely the accumulation of I and its disappearance to give the unfolded state with the increase in GdnHCl concentration, calculated according to equation. (B) Change in activity of CotA M502L mutant in the absence (■) and presence of copper (▲) (ratio 4:1 copper:CotA) at increasing GdnHCl concentrations. The solid lines are the fits according to the equation  $y = y_N + y_{N(\text{no copper})} e^{(-\Delta G^0/RT)} / (1 + e^{(-\Delta G^0/RT)})$  (Durao, et al., 2006) where  $y_N$  and  $y_{N(\text{no copper})}$  are the relative activity for the native and native state without copper, respectively. In the presence of copper, a small increase in activity which cannot be fitted according to the process of copper loss was highlighted by a dashed line to help visual inspection.

The accumulation of an intermediate state (I) in-between N and U that occurs at low GdnHCl concentration (at 1.9 M GdnHCl, 50% of molecules are in the I state) allows the accurate fit of the unfolding process. The I state accumulates at low GdnHCl concentration because the native state is more stable than the I state by only 1.4 kcal mol<sup>-1</sup> (Table 5.3).

Table 5.3: Thermodynamic stability of the tertiary structure of CotA wt and mutants M502L and M502F as assessed by fluorescence spectroscopy

	$\Delta G_{1st}^{o, \text{water}}$ (kcal/mol)	$m_{1st}$ (kcal/mol)	Mid-point <sub>1st</sub> (M)	$\Delta G_{2nd}^{o, \text{water}}$ (b) (kcal/mol)	$m_{2nd}$ (kcal/mol)	Mid-point <sub>2nd</sub> (M)
<b>CotA wt</b>	10.0±0.1	2.2±0.0	4.6±0.1	—	—	—
<b>M502L</b>	1.4±0.0	0.7±0.1	1.9±0.2	7.1±0.6	1.4±0.1	5.0±0.0
<b>M502F</b>	1.4±0.1	0.9±0.1	1.6±0.0	6.2±0.5	1.3±0.2	4.8±0.2

(a) 1<sup>st</sup> states for first transition, meaning from N to U for wt and from N to I for mutants

(b) 2<sup>nd</sup> states for second transition, meaning from I to U, which exists only for mutants

Tryptophan residues are partially exposed to water in the I state as shown by the wavelength of the emission maximum, indicating that the I state is a partially unfolded state. As the stability of the I state is close to that of the native state, the conversion from I to U occurs only at high GdnHCl concentrations and is thermodynamically similar to the conversion of N to U in the wild-type protein. The term  $m$ , which is the cooperativeness of the transition, contains interesting information as it is a measure of the degree of unfolding for a given transition (Table 5.3) (Fersht, 1998). The global unfolding of the wild-type protein is characterized by an  $m$  value of 2.2 kcal mol<sup>-1</sup> M<sup>-1</sup>, which is equal to the overall unfolding transition from N to U for the mutants ( $m_{1st}+m_{2nd}$  is 2.1 and 2.2 kcal mol<sup>-1</sup> M<sup>-1</sup> for M502L and M502F, respectively). This indicates that the structure of N is basically the same for wild-type and mutant proteins at the level of exposure to the solvent (as it is not expected that the U state will change upon mutation).

This observation is fully supported by the invariant three-dimensional structures obtained for both mutants and by the invariant emission maximum of tryptophan residues (approximately 331 nm). Nevertheless, our results indicate that the native overall structure of the mutant enzyme is less stable when compared with the structure of the wild-type enzyme. In fact, global unfolding of the wild type is characterized by a  $\Delta G^0$  water of 10 kcal mol<sup>-1</sup>, but the free-energy gap between N and U for the mutants (given by  $\Delta G_{1st}^{o, \text{water}} + \Delta G_{2nd}^{o, \text{water}}$ ) is lower for M502L (8.5 kcal mol<sup>-1</sup>) and even lower for M502F (7.6 kcal mol<sup>-1</sup>),

the most destabilized structure. The mutant M502L also loses activity at very low GdnHCl concentrations in exactly the same way as the wild-type (the midpoints are 0.4 and 0.3 M, respectively; Table 5.3).

Copper uptake however was not significant at low GdnHCl concentrations and only a very small increase in the activity was observed (Figure 5.4B). Probably, the I state that accumulates at low GdnHCl concentration cannot incorporate copper from the solution. For the mutant M502F, copper uptake was even more compromised and the equilibrium was further shifted to  $N_{\text{no copper}}$ , leading to  $\Delta G^0_{\text{water}}$  being negative and more than 50% of the protein molecules having no copper at T1 (Table 5.4).

Table 5.4: Thermodynamic stability of CotA wt and mutants M502L and M502F as assessed by activity. Activity was measured in the absence and presence of copper (1:4 ratio protein:copper) for wt and M502L and in the presence of two copper concentrations (1:8 and 1:70 ratios protein:copper) for M502F mutant.

	$\Delta G^0_{1st \text{ water}}$ (a) (kcal/mol)	$m_{1st}$ (kcal/mol)	Mid-point <sub>1st</sub> (M)
<b>CotA wt</b>	0.2±0.0	0.7±0.1	0.3±0.1
<b>CotA wt + copper (1:4)</b>	1.4±0.4	0.9±0.1	1.5±0.3
<b>M502L</b>	0.3±0.7	0.7±0.1	0.4±0.9
<b>M502L + copper (1:4)</b>	1.0±0.4	1.5±0.5	0.7±0.1
<b>M502F + copper (1:8)</b>	-0.1±0.8	0.8±0.1	(b)
<b>M502F + copper (1:70)</b>	0.8±0.3	1.2±0.1	0.6±0.1

(a) 1<sup>st</sup> states for first transition, which is from N with copper ( $N$ ) to N without copper ( $N_{\text{no Cu}}$ ) for the wt. For mutants the intermediate I accumulate at very low GdnHCl concentration and the first transition might be from N to  $I_{\text{no Cu}}$ .

(b) At 0M GdnHCl more than 50% of the molecules have no copper at T1 ( $\Delta G^0_{\text{water}}$  is negative) and therefore the mid-point cannot be defined.

It appears that the mutations M502L and M502F have destabilized the conformation of the T1 site without causing gross structural changes in the tertiary structure. These mutations may have created a “hot spot” where partial unfolding that leads to accumulation of the I state is probably initiated. The

slight movement of the mutated residues towards the protein surface, and away from the type 1 copper atom, leads to a concerted movement of the region positioned close to the mutated residues (see above), pushing it away towards the solvent, and opening the copper center. The loss of stability observed for the mutant proteins may be correlated with this structural change. Indeed, the weakening of the copper coordination and subtle alterations in the interconnections of the residues could lead to decreasing stabilization of the center and thus of the whole structure.

### **5.1.3. CONCLUDING REMARKS**

In this study we have evaluated the effect of the replacement of the axial ligand (Met) by two non coordinating residues (Leu and Phe). A raise of the potential redox of the both mutant enzymes by as much as 100 mV has been attributed to the weakening in the T1 Cu coordination. Nevertheless, no direct correlation has been found between the redox potentials calculated for the M502L and M502F enzymes and the oxidation rates of non-phenolic and phenolic substrates tested, as lower turnover rates were calculated for both mutants when compared with the wild-type enzyme. Furthermore, the mutations in the axial ligand have a profound impact on the thermodynamic stability of the enzyme; the accumulation of an intermediate state in between the native and unfolded states occurs at low concentrations of denaturant contrasting with the two-state unfolding process of the wild-type enzyme.

Mutant M502F is more severely compromised in its biological function than the M502L mutant, probably due to its higher molecular mass. This resulted in a higher local instability of the structure as shown by the smaller free energy gap calculated between the native and unfolded states and also on the decreased ability to incorporate copper from solution as compared with the wild-type or the M502L mutant.



Additionally, these results indicate that copper depletion is a key event in the inactivation and thus in the thermodynamic stability of CotA-laccase. The enzyme loses copper from the T1 site and the activity decreases abruptly at very low GdnHCl concentrations, compared with those needed to unfold secondary and tertiary structure, indicating that copper is the first event affecting the enzyme thermodynamic stability. In the present work it has been shown that subtle rearrangements in the coordination sphere of the T1 copper result in major loss of function regarding the catalytic as well as the overall stability of the enzyme, launching new questions regarding our understanding of the structure and function of the oxidative copper site of the blue multicopper oxidases.

## **5.2. EFFECT OF COPPER CONTENT IN THE STABILITY OF COTA-LACCASE**

Studies involving the overproduction of bacterial laccases in the heterologous *E. coli* host have shown that the attainment of enzymatically active recombinant laccases is dependent on the addition of exogenous copper to the growth media and/or the reaction mixture assays (Galli, et al., 2004; Martins, et al., 2002; Sanchez-Amat, et al., 2001). The absence of copper in the culture media does not affect the yield of laccases production; it resulted in the production of an apo-protein that is devoid of oxidase activity (Martins, et al., 2002). This is, most probably, related to the fact that overproduction of copper full loaded MCO in the cytoplasm of *E. coli* is limited by the availability of free copper at the intracellular environment.

It is known that *E. coli* uses different copper homeostasis systems to maintain a cellular copper quota within a narrow range, around 10  $\mu$ M when in aerobic conditions (Changela, et al., 2003; Rensing and Grass, 2003). However, switching *E. coli* cultures grown in the presence of copper from aerobic to microaerobic growth conditions, was reported to affect the overall metal ion physiology and the regulation of the homeostasis mechanisms (Outten, et al.,

2001). While the mechanism of copper toxicity is fundamentally unsolved it is known that during anaerobic growth the alterations in the regulation of copper homeostasis systems (*cue* and *cus*) results in increased copper accumulation and copper toxicity (Macomber, et al., 2007; Outten, et al., 2001). The increased toxicity in *E.coli* was proposed to result from a shift in total copper from the  $\text{Cu}^{2+}$  to  $\text{Cu}^{+}$  oxidation state, a more noxious form (Beswick, et al., 1976; Outten, et al., 2001).

The copper incorporation in MCO is still a poorly understood process and remains an important issue of discussion in the literature (Blackburn, et al., 2000; Davis-Kaplan, et al., 1998; Galli, et al., 2004; Hellman, et al., 2002; Palmer, et al., 2003). The understanding of this mechanism is important from biochemical, spectroscopic and structural viewpoints and also from a biotechnological perspective. In this work we have identified growth conditions that allow for the production of a fully copper loaded recombinant enzyme in the cytoplasm of *E. coli*. In addition, several spectroscopic techniques, including UV–Vis, EPR and RR, as well as kinetic and thermal stability assays were used to characterize the different variants of the protein obtained, through different metal-incorporation procedures (Durao, et al., 2008).

### 5.2.1. EXPERIMENTAL PROCEDURES

Kinetic stability was performed as described by Martins et al. (2002). In brief, the enzyme was incubated at 80°C and at fixed time intervals samples were withdrawn and tested for activity at 37°C using ABTS as substrate. DSC was carried out in a VP-DSC from MicroCal at a scan rate of 60 deg h<sup>-1</sup>. The experimental calorimetric trace was obtained with 0.3 mg mL<sup>-1</sup> of protein at pH 3 (50 mM glycine buffer) and a baseline obtained with buffer alone was subtracted from the experimental trace. The resulting DSC trace was analyzed with the DSC software built within the Origin spreadsheet to obtain the transition excess heat capacity function (a cubic polynomial function was used

to fit the shift in baseline associated to unfolding). The excess heat capacity could only be accurately fitted using a non two-state model with three transitions (equation in the data analysis software).

### 5.2.2. COPPER INCORPORATION INTO COTA-LACCASE

Crude extracts of *E. coli* cells grown under microaerobic conditions had two-fold lower total protein content (in agreement with lower cellular yield), but remarkably a nearly 100-fold higher enzymatic activity for ABTS, when compared with crude extracts of cells grown under aerobic conditions. Purified protein samples from microaerobic cultures were more intensely blue when compared with protein preparations purified from cells grown under aerobic conditions, correlating with a stronger band intensity of the T1 Cu as monitored by the absorption at 600 nm (Figure 5.5)

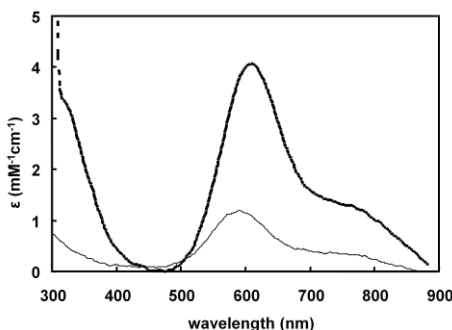


Figure 5.5: UV-vis spectra of the as-isolated CotA species produced in aerobic (*thin* line) and in microaerobic (*thick* line) conditions

The shoulder at 330 nm, indicative of a ligand bridging the T3 Cu ions, was also present with an absorption intensity nearly equivalent to that of the absorption band with a maximum at 600 nm. The purified enzyme from aerobic cultures exhibited an incomplete metal incorporation (0.5:1 Cu to protein), also observed in previous studies with CotA-laccase (Durao, et al., 2006). In contrast, copper content measurements revealed a Cu-to-protein stoichiometry close to 4 for the protein purified from cells grown under microaerobic

conditions, ensuring that all four copper ions required for enzyme activity were incorporated into the active sites.

The cells from microaerobic cultures showed clearly enhanced copper content as measured by atomic absorption (data not shown) these cells accumulated up to a 80-fold higher copper than cells aerobically. The rise in copper concentration (presumably in the more toxic cuprous form) in anaerobic conditions was previously related to limitations in the *cue* primary copper export system (Outen et al., 2001).

To further elucidate copper incorporation in MCOs, we have incubated aliquots of an apoCotA form, (from cells grown in unsupplemented-Cu medium), with increasing molar equivalents of  $\text{Cu}^+$  or  $\text{Cu}^{2+}$ . These experiments showed that copper incorporation is a sequential process, with T1 Cu being the first to be reconstituted, followed by the T2 and T3 Cu centers (Figure 5.6), which in accordance with data obtained for CueO, Fet3p and bilirubin oxidase where partial copper intermediates were observed (Blackburn et al., 2000, Galli et al., 2004, Kataoka et al., 2005). The maximum copper content of the apoCotA reconstituted with  $\text{Cu}^{2+}$  was never higher than 2.5 copper equivalents per protein, while the apoenzyme reconstituted with  $\text{Cu}^+$  exhibits a full complement with four Cu ions. These results suggest that recombinant CotA-laccase is synthesized in the cytoplasm *E. coli*, through an incorporation of  $\text{Cu}^+$ . This is consistent with evidence that cuprous is the valence state of intracellular copper accumulating under anaerobic conditions (Outten et al., 2001, Beswick et al., 1976).

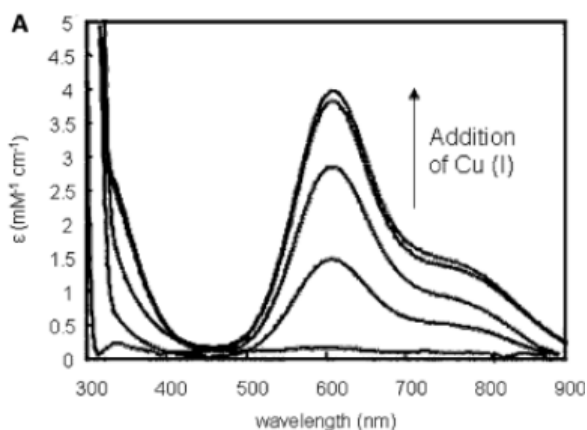


Figure 5.6: Reconstitution of apoCotA with  $\text{Cu}^+$  measured by UV-Vis absorption.

The reconstitution of the holoCotA derivatives, resulting from EDTA-depletion of holoenzyme, followed an identical sequential incorporation pattern. Interestingly, and in clear contrast with reconstitution of apoCotA (synthesized and folded in *E. coli* in the absence of Cu) the copper full occupancy was reached after addition of 4 equivalents of either  $\text{Cu}^+$  or  $\text{Cu}^{2+}$ . These holo derivatives *in vitro* findings show that the competent-state of CotA required for copper insertion is critically dependent of the apoenzyme preparations.

The enzymes as-isolated, the partially Cu loaded and the holoCotA, exhibited, as expected, enormous differences with regard to the  $k_{\text{cat}}$  values, as large as 200-fold. Noteworthy, the reconstituted holoCotA derivatives with either  $\text{Cu}^{2+}$  or  $\text{Cu}^+$ , seems to complete recover the native conformation and the structure of the copper-containing sites, as the  $k_{\text{cat}}$  values calculated are similar to as-isolated holoCotA (Table 5.5).

Table 5.5: Steady-state kinetic constants for 2,20-azinobis(3-ethylbenzthiazoline-6-sulfonic acid) (ABTS) and syringaldazine (SGZ) for different CotA laccase forms

CotA species	ABTS		SGZ	
	$K_m$ ( $\mu\text{M}$ )	$k_{\text{cat}}$ ( $\text{s}^{-1}$ )	$K_m$ ( $\mu\text{M}$ )	$k_{\text{cat}}$ ( $\text{s}^{-1}$ )
<b>partially Cu loaded-CotA</b>	$101 \pm 22$	$1.5 \pm 0.2$	$16 \pm 1$	$0.4 \pm 0.0$
<b>holoCotA</b>	$124 \pm 17$	$322 \pm 20$	$18 \pm 3$	$80 \pm 4$
<b>apoCotA reconstituted with <math>\text{Cu}^{2+}</math></b>	$87 \pm 10$	$22 \pm 1$	$10 \pm 1$	$18 \pm 0.4$
<b>apoCotA reconstituted with <math>\text{Cu}^+</math></b>	$105 \pm 6$	$82 \pm 2$	$10 \pm 2$	$74 \pm 9$
<b>holoCotA treated with EDTA and reconstituted with <math>\text{Cu}^{2+}</math></b>	$126 \pm 11$	$242 \pm 15$	$17 \pm 2$	$67 \pm 5$
<b>holoCotA depleted with EDTA and reconstituted with <math>\text{Cu}^+</math></b>	$134 \pm 10$	$294 \pm 15$	$22 \pm 3$	$85 \pm 7$

The apoCotA reconstituted with  $\text{Cu}^{2+}$ , showed 10 to 25% catalytic activity for the different substrates when compared with the as-isolated holoCotA. This suggest that a small fraction (10-25%) of the protein is fully loaded and redox active, whereas the remaining of the protein molecules were incompletely loaded, not contributing to the protein turnover. Unexpectedly, the apoCotA reconstituted with cuprous ions ( $\text{Cu}^+$ ) and exhibiting a full complement of Cu ions, have lower  $k_{\text{cat}}$  values towards the oxidation of the substrates compared to the as-isolated holoCotA. The difference in the turnover rates could differ as much as 2 to 5-fold. The kinetic analysis of the different variants of CotA-laccase has shown that no major alterations were observed regarding the  $K_m$  for the different substrates (Table 5.5).

This data points to the fact that apoCotA, synthesized by *E.coli* in the absence of copper, is unable to be reconstituted *in vitro* either with  $\text{Cu}^+$  or  $\text{Cu}^{2+}$  to the native conformation of the protein molecule. Presumably folding in the

presence of copper is indispensable for the correct structure of the copper-containing sites (Durao, et al., 2008).

### 5.2.3. THERMAL STABILITY OF COTA VARIANTS

As shown above, the different variants of CotA-laccase have different catalytic properties. These differences, apparently, are not only related to the copper content in the protein, but are also related to the timing of copper incorporation.

This ‘timing’ refers to the fact that the incorporation *in vivo*, during or before folding inside the cell, is different of the incorporation *in vitro*. In fact, only the enzyme produced in the holo form, after EDTA treatment can recover, all the catalytic properties of the wild-type, showing that the copper incorporation is dependent on the *in vivo* conditions. To further characterize the different forms of CotA we have performed stability studies, involving kinetic stability and DSC measurements.

For the analysis of the kinetic stability at 80 °C we have used only the active forms, since the apo forms do not have the catalytic centers, and thus impossible to evaluate its long-term stability (Figure 5.7).

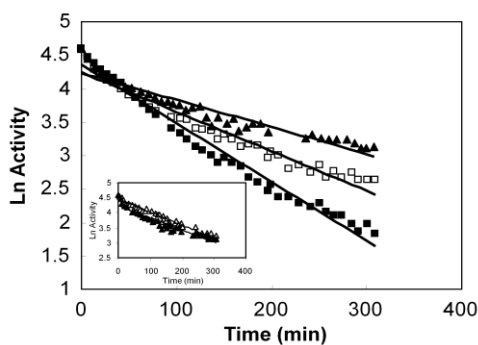


Figure 5.7: Kinetic stability of the as-isolated Holo-CotA ( $\blacktriangle$ ), apoCotA reconstituted with  $\text{Cu}^+$  ( $\square$ ) and reconstituted apoCotA with  $\text{Cu}^{2+}$  ( $\blacksquare$ ) at 80°C. Deactivation obeys first-order kinetics ( $\ln \text{act.} = \ln \text{act.}(t=0) - k_d t$ , where  $k_d$  is the rate constant of deactivation) and the calculated half-life time ( $t_{1/2} = \ln 2 / k_d$ ) for the as isolated holoCotA (full loaded *in vivo*) was 172 min ( $R^2 = 0.91$ ), for the reconstituted holoCotA (full loaded *in vitro*) was 117 min ( $R^2 = 0.95$ ) and for the reconstituted depleted-CotA was 79 min ( $R^2 = 0.98$ ).

The different species of CotA deactivate according to a first-order process, which can be described by the classical Lumry–Eyring model applied to the majority of enzymes ( $N \leftrightarrow U \rightarrow D$ , where N, U and D are the native, the reversible unfolded and the irreversible denatured enzyme), pointing to a simple pathway of unfolding and deactivation.

HoloCotA is the most stable, retaining 50% of activity after 172 min at 80 °C. Although apoCotA reconstituted with  $\text{Cu}^+$  contains roughly the same copper content as holoCotA, it is less stable, having a half-life of 117 min, showing once again the importance of the presence of copper during the folding process inside the cell. The least stable species is apoCotA reconstituted with  $\text{Cu}^{2+}$ , containing 2.5 Cu per protein, which takes 79 min to lose 50% of its initial activity, showing the fundamental role of copper in the stability of these enzymes. The reconstituted holoCotA derivatives, after EDTA treatment, (reconstituted with either  $\text{Cu}^+$  or  $\text{Cu}^{2+}$ ) have a half-life of 178 min and are therefore as stable as holoCotA, showing the recovery of the physico-chemical properties responsible for the thermal stability of CotA-laccase.

The thermal stability of the different CotA species was also probed by DSC to gather additional insight into the specificity of copper incorporation, through its effect on protein stability. The DSC thermograms of these proteins reveal a complex process similar to the ones obtained earlier for McoA and McoP (Figure 5.8). Similar aggregational effects were detected, leading to 100% of irreversibility and also the fitting, of the experimental data, requires three independent transitions. Three thermal transitions were previously used to describe DSC traces of ascorbate oxidase (Savini, et al., 1990) and ceruloplasmin (Bonaccorsi di Patti, et al., 1990).



Interestingly, the temperature at the mid-point of each transition clearly reflects the stability of each species of CotA ( $T_m$  values in Figure 5.8). The as-isolated holoCotA is around 2 °C more stable than the apoCotA reconstituted with  $\text{Cu}^+$ , independently of the transition under consideration. This latter species is in turn more stable than the apoCotA reconstituted with  $\text{Cu}^{2+}$ , but the differences in  $T_m$  values depend on the transition, being 7.1, 4.6 and 3.6 °C for the first, second and third transition, respectively.

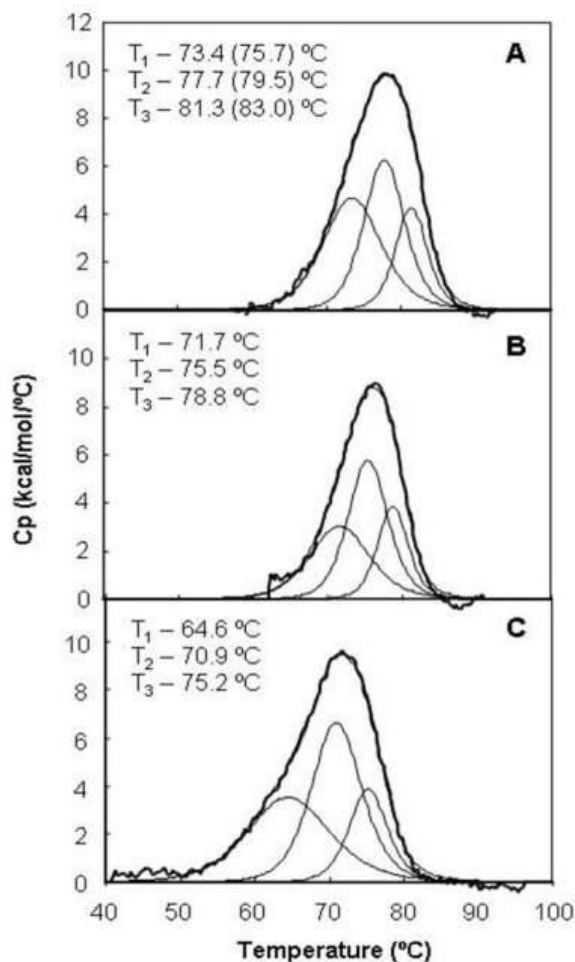


Figure 5.8: Excess heat capacity obtained from a DSC scan (at pH3) of as isolated Holo-CotA (A), apoCotA reconstituted with Cu<sup>+</sup> (B) apoCotA reconstituted with Cu<sup>2+</sup> (C). The thick line (experimental data) was fitted with three independent transitions shown separately in dashed lines. The dashed line under the DSC trace is the resulting sum of the three independent transitions.

The reconstituted holoenzyme derivatives (reconstituted either with Cu<sup>+</sup> or with Cu<sup>2+</sup>) are even slightly more stable than the holoCotA (T<sub>m</sub> values in parentheses in Figure 5.8, scan A). In addition, each transition measured by DSC is a non-two-state process as the calorimetric molar enthalpy is significantly smaller than the van't Hoff enthalpy. The behaviour is similar for the three species of CotA, with the ratio  $\Delta H_{cal}/\Delta H_{vH}$  taking the values of 0.94, 0.52 and 0.18 for the first, second and third transition of as-isolated holoCotA, respectively. Ratios

$\Delta H_{\text{cal}}/\Delta H_{\text{vH}}$  smaller than 1 indicate protein aggregation (Vassall, et al., 2006) and explain why thermal unfolding of CotA leads to irreversibility even at pH 3.

Interestingly, both kinetic and thermal stability data for the different Cu-loaded forms of CotA reflect a clear pattern. HoloCotA is the most stable, followed by apoCotA reconstituted with  $\text{Cu}^+$ , and the least stable is apoCotA reconstituted with  $\text{Cu}^{2+}$ . These results show, as referred before, that copper content as well as copper incorporation (*in vivo* vs. *in vitro*) has a direct impact on the stability of the enzyme. If holoCotA is depleted with EDTA and then reconstituted with copper, it becomes as stable as the original species.

Copper binding to MCO is well known to stabilize the enzyme (Agostinelli, et al., 1995; Ragusa, et al., 2002) and indeed we have observed this stabilizing effect both for kinetic and for thermal stability. Stabilization by copper depends on the type of coordination involved (T1, T2 or T3) (Agostinelli, et al., 1995; Koroleva, et al., 2001; Milardi, et al., 2003) but probably also on subtle changes of each coordination geometry, as pointed out by the differences in stability between apoCotA reconstituted with  $\text{Cu}^+$  and the as-isolated holoCotA and its reconstituted derivatives which have the same copper content.

#### 5.2.4. CONCLUDING REMARKS

The copper content of the recombinant CotA-laccase, heterologous produced in *E. coli* is shown to be strongly dependent on the presence of copper and oxygen in the culture media. In copper-supplemented media, a switch from aerobic to microaerobic conditions leads to the synthesis of a recombinant holo-enzyme, while the maintenance of aerobic conditions results in the synthesis of a copper-depleted population.

Although, the precise role of copper in protein folding is not well understood our kinetic and stability data in the full copper loaded enzymes suggests variations in the incorporation of Cu in the catalytic centers as it proceeds *in*

*vivo* or *in vitro*. The reconstituted apoCotA with  $\text{Cu}^+$ , though presenting a similar copper content as compared to the as-isolated holoCotA, showed a slight lower oxidation rates ( $k_{\text{cat}}$ ) for the substrates that were tested.

Interestingly, kinetic stability shows the same trend of  $k_{\text{cat}}$  value which is also lower for the reconstituted (either with  $\text{Cu}^+$  or  $\text{Cu}^{2+}$ ) than for the as-isolated holoCotA. Furthermore, the behaviour observed for the three species of CotA regarding thermal stability measured by DSC is exactly the same as the observed for the kinetic stability and  $k_{\text{cat}}$  values showing that efficiency of copper incorporation has a direct impact on the catalytic performance as well on the thermal stability of the enzyme.

DSC data confirmed that copper incorporation *in vivo* (as-isolated holoCotA) should be more effective as compared with copper incorporation *in vitro* (reconstituted apoCotA with  $\text{Cu}^+$ ) since the as-isolated holoenzyme exhibited higher stability even if the copper content is similar for both samples. This effect might be associated with unspecific *in vitro* copper binding at other sites rather than at the copper centers or, at least, a less effective coordination of copper at the catalytic sites. Furthermore, this phenomenon seems to be independent on the protein since similar results (concerning copper content) were obtained also for McoA (for details please consult section 8.1).

However, none of these possibilities can be clearly investigated here and further work will be needed to elucidate the structural mechanisms of the copper incorporation in MCO.

### **5.3. THE REMOVAL OF A DISULFIDE BRIDGE OF COTA-LACCASE CHANGES THE SLOWER MOTION DYNAMICS INVOLVED IN COPPER BINDING BUT HAS NO EFFECT ON THE THERMODYNAMIC STABILITY**

#### **5.3.1. ABSTRACT**

The contribution of the disulfide bridge in CotA-laccase from *Bacillus subtilis* is assessed with respect to the enzyme's functional and structural properties. The removal of the disulfide bond by site directed mutagenesis, creating the C322A mutant, does not affect the spectroscopic or catalytic properties and, surprisingly, neither the long-term or thermodynamic stability parameters of the enzyme. Furthermore, the crystal structure of C322A mutant indicates that the overall structure is essentially the same as the wild-type with only slight alterations evident in the immediate proximity of the mutation. In the mutant enzyme, the loop containing the C322 residue becomes less ordered, suggesting perturbations to the substrate binding pocket. Despite the wild-type and C322A mutant showing similar thermodynamic stability in equilibrium, the holo or apo-forms of the mutant unfolds at faster rates as compared with the wild-type enzyme. The ps-ns time range dynamics of the mutant enzyme was not affected as shown by acrylamide collisional fluorescence quenching analysis. Interestingly, copper uptake or copper release as measured by stopped-flow technique occurs also more rapidly in the C322A mutant as compared to the wild-type enzyme. Overall the structural and kinetic data presented here suggest that the disulfide bridge in CotA-laccase contributes to the conformational dynamics of the protein at the  $\mu$ s-ms time-scale with implications for the rates of copper incorporation and release from the catalytic centres.

#### **5.3.2. INTRODUCTION**

The family of multicopper oxidases (MCOs), that includes the functional classes of metallo-oxidases and laccases, is mostly constituted by proteins that contain approximately 500 amino acid residues and are composed of three Greek key  $\beta$ -barrel cupredoxin domains (domains 1, 2 and 3) that come together to form three spectroscopically distinct types of Cu sites, i.e. type 1 (T1), type 2 (T2), and type 3 (T3) (Lindley, 2001; Messerschmidt, 1997). The T1 Cu centre

is the site of substrate oxidation and a wide range of compounds, such as polyphenols, diamines and even some inorganic metals are electron donor substrates. The trinuclear centre comprises two T3 and one T2 copper ions that functionally cooperate in the reduction of dioxygen to water. Laccases have a high potential for biotechnological applications, mainly due to their wide range of oxidizing substrates, the use of readily available oxygen as final electron acceptor and the lack of requirement for expensive cofactors. In the past few years many studies have enabled the elucidation of a significant number of structural and functional aspects of these enzymes, but many questions still remain. One of these involves the understanding of the molecular determinants of enzyme long-term and conformational stability. However, using an enzyme in an industrial environment requires a high stability, since most of the industrial activities are carried out at high temperatures, extreme pH values, and high pressures among other physico-chemical adverse conditions. Therefore understanding the molecular mechanisms involved in the stability properties of laccases is of utmost importance and may lead to the generation of improved biocatalysis by proteins.

In these last year's our attention has focused on the study of thermo and hyperthermostable prokaryotic MCOs, the CotA-laccase from *Bacillus subtilis*, and the metallo-oxidases, McoA from *Aquifex aeolicus* and McoP from *Pyrobaculum aerophilum* (Fernandes, et al., 2010; Fernandes, et al., 2007; Martins, et al., 2002). These enzymes are all thermoactive ( $T_{opt} > 75^{\circ}\text{C}$ ) and remarkably thermostable with melting temperatures between 80 and 114 °C (Durao, et al., 2008; Fernandes, et al., 2010; Fernandes, et al., 2009; Martins, et al., 2002). Copper was identified as a major determinant of the long-term and thermodynamic stability of the CotA-laccase and McoA (Durao, et al., 2008; Fernandes, et al., 2009), in agreement with previous studies performed with the eukaryotic MCOs ascorbate oxidase, human ceruloplasmin (hCp), yeast Fet3p and the laccases from *Rhus vernicifera*, and *Coriulus hirsutus* highlight (Agostinelli, et al., 1995; Koroleva, et al., 2001; Savini, et al., 1990; Sedlak and

Wittung-Stafshede, 2007; Sedlak, et al., 2008). Unfolding kinetics measured by the stopped-flow technique revealed that McoA aggregates under unfolding conditions, an uncommon feature among proteins and this was further confirmed by light scattering, gel filtration and ANS binding (Fernandes, et al., 2009). The kinetic partitioning between aggregation and unfolding should be the main factor behind the low chemical stability of McoA at room temperature ( $2.8 \text{ kcal mol}^{-1}$ ) and for its low heat capacity change ( $\Delta C_p = 0.27 \text{ kcal mol}^{-1} \text{ K}^{-1}$ ) (Fernandes, et al., 2009). These lead to a flat dependence of stability on temperature and explain the hyperthermostable nature of this enzyme. On the other hand, CotA laccase, despite the narrower dependence of stability on temperature, shows a remarkable chemical stability towards chemical denaturation (an energy gap of approximately  $10 \text{ kcal mol}^{-1}$  at room temperature) (Durao, et al., 2006) and therefore is more thermodynamically stable in the thermophilic temperature range (unpublished data). Furthermore, point mutations close to the T1 copper centre of CotA-laccase have a profound impact on the thermodynamic stability of the enzyme without causing major structural changes in the tertiary structure (Durao, et al., 2006; Durao, et al., 2008).

In the present study the long standing topic of the role of disulfide bonds in protein stability is revisited for the CotA-laccase. Disulfide bridges, according to the classical theories confer stability by reducing the conformational entropy of the unfolded relative to the native state, thereby decreasing the entropy gain upon unfolding (Brockwell, 2007; Pace, et al., 1998; Radestock, 2008; Zhou, et al., 2008). The single intra-domain disulfide bridge of the enzyme CotA-laccase from *Bacillus subtilis* was disrupted, and the mutant C322A was characterized by using spectroscopic methodologies and fast kinetics of unfolding and of copper binding or release. Most of the studies on copper proteins using stopped-flow kinetics are confined to the simplest T1 copper proteins azurin and rusticyanin (Alcaraz, et al., 2005; Pozdnyakova and Wittung-Stafshede, 2001; Wittung-Stafshede, 2004). Overall, the data presented shows that the disulfide

bridge has no significant effect on the three-dimensional structure, catalytic properties and thermodynamic stability of CotA but contributes to its conformational dynamics in the  $\mu$ s-ms time-scale with implications in the rates of copper incorporation and release from the catalytic centres. This study contributes to our understanding of the mechanisms of copper incorporation in multicopper oxidases.

### 5.3.3. EXPERIMENTAL PROCEDURES

**Construction of C322A mutant.** Single amino acid substitution in one of the cysteines (C322A) involved in the disulfide bridge of CotA-laccase was created using the QuikChange site-directed mutagenesis kit (Stratagene). Plasmid pLOM10 (containing the wild-type *cotA* sequence) was used as a template and the primers forward 5'- GCA AAC AGC GCG GGC AAC GGC GGT GAC GTC AAT C - 3' and reverse 5'- GAT TGA CGT CAC CGC CGT TGC CCG CGC TGT TTG C -3' were used to generate the C322A mutant. The presence of the desired mutation in the resulting plasmid and the absence of unwanted mutations in other regions of the insert were confirmed by DNA sequence analysis. The recombinant plasmid was transformed into *Escherichia coli* Tuner (DE3) strain (Novagen) to obtain strain AH3551.

**Overproduction and purification.** Strains AH3551 (containing the gene *cotA* with the point mutation C322A) and AH3517 (containing the wild-type *cotA* gene (Martins, et al., 2002)) were grown in Luria-Bertani medium supplemented with ampicillin (100 mg mL<sup>-1</sup>) at 30°C. Growth was monitored until OD<sub>600</sub> = 0.6, at which time 0.1 mM isopropyl- $\beta$ -D-thiogalactopyranoside and 0.25 mM CuCl<sub>2</sub> were added to the culture medium and the temperature lowered to 25°C. Incubation was continued for further 4 h when a change to microaerobic conditions was achieved (Duraó, et al., 2008). Cells were harvested by centrifugation (8000 x g, 10 min, 4°C) after a further 20h. For the overproduction of the apoCotA forms no copper was added to the culture medium (Duraó, et al., 2008). Proteins were purified by using a two-step



purification procedure as previously described (Bento, et al., 2005; Martins, et al., 2002).

**UV–Vis, EPR and CD spectra.** Protein samples were routinely oxidised using potassium iridate followed by dialysis. UV–Vis spectra were recorded using a Nicolet Evolution 300 spectrophotometer from Thermo Industries. The EPR spectra were measured with a Bruker EMX spectrometer equipped with an Oxford Instruments ESR-900 continuous flow helium cryostat. The spectrum obtained under non-saturating conditions was theoretically simulated using the Aasa and Vänngård approach (Aasa and Vanngard, 1975). A circular dichroism (CD) spectrum in the far-UV region was measured on a Jasco-720 spectropolarimeter (Tokyo, Japan) using a circular quartz cuvette with a 0.01-cm optical path length in the range of 190–250 nm.

**Enzymatic assays.** The oxidation reactions of 2,2'-azinobis-(3-ethylbenzo-6-thiazolinesulfonic acid) (ABTS) and syringaldazine (SGZ) were photometrically monitored with either a Nicolet Evolution 300 spectrophotometer from Thermo Industries or a Molecular Devices Spectra Max 340 microplate reader with a 96-well plate. All procedures were carried out as previously described (Durao, et al., 2006).

**Crystallization and structure solution.** Crystals of the C322A mutant protein were obtained from a crystallization solution containing 12 % of PEG MME5k, 0.1 M sodium citrate at pH 5.5 and 16 % of isopropanol, using the vapour diffusion method. Crystals were harvested after six days and cryo-protected in a solution containing the crystallisation solution plus 22 % of ethylene glycol. Data collection, from a flash cooled crystal, was undertaken on beam line ID13-EH1, at the ESRF in Grenoble, France, and a data set with 2.25Å resolution was obtained. Diffraction data was processed and scaled using MOSFLM (Leslie, 1992; Leslie, 2006) and SCALA, from CCP4 suite (CCP4, 1994), respectively. The three-dimensional structure of the mutant protein was solved by the molecular replacement method using the program MOLREP (Vagin and Teplyakov, 1997) and as a search model, the structure of the native CotA

(1W6L) (Bento, et al., 2005), from which the solvent molecules as well as the copper ions had been removed. Refinement of the structural model was undertaken with the program REFMAC (Murshudov, et al., 1999) and model building and improvement with the program COOT (Emsley and Cowtan, 2004). Isotropic refinement of the atomic displacement parameters was performed for all atoms. The occupancies of the copper ions were adjusted so that their isotropic thermal vibration parameters refined approximately to those observed for the neighbouring atoms. Solvent molecules were positioned after a few cycles of refinement as well as several molecules of ethylene glycol. In order to model the species observed in between the type 3 copper sites, careful analysis of the omit and standard difference Fourier syntheses, as well as of thermal vibration coefficients was undertaken, and a diatomic species was identified at this site (see for example (Bento, et al., 2010)). The model giving the best refinement corresponded to a dioxygen moiety with the O-O distances constrained to target value of 1.204Å. Such a moiety could be an  $\text{O}_2^{2-}$  species, a partially protonated version or a mixture of such states.

**Stability.** Long-term thermostability was determined at 80°C for an enzyme solution in 20 mM Tris-HCl buffer, pH 7.6. At appropriated times samples were withdrawn, cooled and immediately examined for residual activity following the oxidation of ABTS as previously described (Martins, et al., 2002). The thermodynamic stability assessed by steady-state fluorescence was measured in a Cary Eclipse spectrofluorimeter using 296 nm as the excitation wavelength. All proteins were in 20 mM Tris-HCl buffer at pH 7.6 and increasing concentrations of GuSCN were used to induce unfolding at 25°C. Unfolding was measured by a combination of fluorescence intensity and emission maximum and quantified using two-state equations (Durao, et al., 2006). The stability of the tertiary structure was assessed by differential scanning calorimetry (DSC) as previously described (Durao, et al., 2008).

**Stopped-flow kinetics.** Kinetic experiments were carried out on an Applied Photophysics Pi-Star 180 instrument with absorption and fluorescence intensity

detection. A mixing ratio of 1:1 to give a final protein concentration of 2  $\mu\text{M}$  and 20  $\mu\text{M}$  for fluorescence and absorption detection, respectively, was used. The unfolding or refolding of proteins was followed by fluorescence with an excitation wavelength of 296 nm, and emission detected above 320 nm using a glass filter. For the unfolding experiments the proteins in 20 mM Tris-HCl, pH 7.6, were mixed with 100 mM Britton-Robinson, pH 1.6, to a final pH of 1.8. Copper release and binding was measured by absorption at 600 and 330 nm, to probe the T1 and T3 copper ions, respectively. For copper binding experiments, the apo forms of proteins in 20 mM of Tris-HCl, pH 7.6, were mixed with solutions ranging from 20 to 240  $\mu\text{M}$  of  $\text{CuCl}_2$  in the same buffer. All kinetic traces were analysed according to a multi-exponential fit using the Pro-Data Viewer software provided by Applied Photophysics.

**Other methods.** Copper content of proteins was determined by the trichloroacetic acid/bicinchoninic acid (BCA) method (Brenner and Harris, 1995). The protein concentration was measured using the CotA absorption band at 280 nm ( $\epsilon_{280}=84,739 \text{ M}^{-1} \text{ cm}^{-1}$ ). Redox titrations were performed at 25 °C, and pH 7.6, under an argon atmosphere, and were monitored by visible absorbance (300–900 nm) as described previously (Durao, et al., 2006).

#### 5.3.4. RESULTS AND DISCUSSION

**Spectroscopic analysis.** The recombinant C322A mutant shows the same chromatographic pattern during purification as the wild-type CotA-laccase. Protein samples were judged to be homogeneous by the observation of a single band on Coomassie Blue-stained SDS/PAGE. Each holoprotein “as isolated” contained approximately 4 moles of Cu per 1 mole protein. The UV-visible spectra of wild-type and C322A mutant are very similar presenting an intense absorption band at 600 nm ( $\epsilon = 4000 \text{ M}^{-1} \text{ cm}^{-1}$ ) due to the charge transfer transition characteristic of the T1 Cu centre (Figure 5.9A). The EPR spectrum of C322A mutant resembles that of wild-type protein (i.e. the spin Hamilton

parameters for the wild-type and mutant proteins for both the T1 and T2 Cu are similar (Figure 5.9B)). The CD spectrum of the mutant in the far-UV region reveals minimal changes in the secondary structure as compared to that of the wild type – the signal is dominated by  $\beta$ -sheets, turns and random coils and a small percentage of  $\alpha$ -helix (Figure 5.9C). Overall it seems that the C322A mutation results only in very subtle differences in the electronic structure of the copper centres.

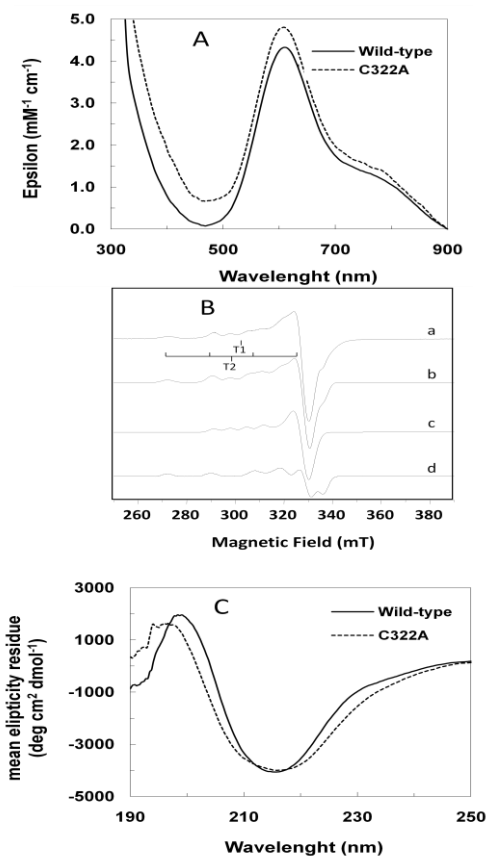


Figure 5.9: (A) UV-Visible spectra of CotA wild-type and C322A mutant in 20 mM Tris-HCl with 200 mM NaCl, pH 7.6. (B) EPR spectrum of C322A mutant obtained at 10 K (a). Microwave frequency, 9.39 GHz 2.4 mW; modulation amplitude: 0.9 mT. Simulation of the total spectrum (b) and deconvolution of the different components (c and d). The parameters used are: for T1  $g_{min}=2.042$ ,  $g_{med}=2.046$ ,  $g_{max}=2.228$  and  $A_{max}=70 \times 10^{-4} \text{ cm}^{-1}$  and for T2  $g_{min}=2.035$ ,  $g_{med}=2.094$ ,  $g_{max}=2.250$  and  $A_{max}=187 \times 10^{-4} \text{ cm}^{-1}$ . The contribution of T1 and T2 components is 1:1 in the simulation of the total spectrum. The hyperfine splitting  $A_{max}$  of T1 and T2 Cu centres are indicated. (C) CD spectra in the far-UV region.

**Redox and catalytic properties.** The reduction of the T1 copper centre was monitored by the decrease of the  $S(\pi) \rightarrow Cu(d_{x^2-y^2})$  charge transfer (CT) absorption band at around 600 nm. The replacement of C322 by an alanine resulted in a decrease of the redox potential of the T1 Cu centre ( $E_{T1}^0$ ) by ~70 mV (Table 5.6).

Table 5.6: Activation energy ( $\Delta G^\ddagger$ ), redox potential of the T1 copper and steady-state kinetic constants for ABTS and SGZ for wild-type and C322A mutant. Activation energy was determined using ABTS as substrate

	$\Delta G^\ddagger$ (kcal/mol)	$E^0$ (mV)	ABTS		SGZ	
			$K_m$ ( $\mu M$ )	$k_{cat}$ ( $s^{-1}$ )	$K_m$ ( $\mu M$ )	$k_{cat}$ ( $s^{-1}$ )
<b>wild-type</b>	$2.9 \pm 0.1$	$525 \pm 10$	$102 \pm 1$	$264 \pm 9$	$8 \pm 2$	$79 \pm 4$
<b>C322A</b>	$4.2 \pm 0.9$	$457 \pm 5$	$105 \pm 9$	$238 \pm 17$	$8 \pm 0.3$	$73 \pm 1$

The lower  $E_{T1}^0$  can reflect the variation of several factors, including the solvent accessibility and the electrostatic interactions between the metal centre and the protein (Solomon, et al., 1996). The enzymatic kinetic constants ( $k_{cat}$  and  $K_m$ ) measured for the C322A mutant are similar to those exhibited by the wild-type enzyme (Table 5.6). The lower  $E_{T1}^0$  determined for the mutant enzyme would appear to favour a decreased reaction velocity as the rate of an electron transfer reaction ( $k_{ET}$ ), is a major component of  $k_{cat}$ , and directly dependent on the  $E^0$  (Moser and Dutton, 1996). However, accordingly to the Marcus theory, two other factors, affects the rate of an electron transfer reaction ( $k_{ET}$ ): the electronic tunnelling, that depends on the exact geometry of the protein matrix and the reorganization energy that depends on the structure and dynamics of the protein (Moser and Dutton, 1996; Solomon, et al., 1996). Therefore, possible reasons for discrepancies in the reaction rate in relation to the redox potential of C322A must lie in the interplay among different and complex factors that are present in the catalytic mechanism of multicopper oxidases.

**Thermodynamic stability characterization.** The stability of CotA upon chemical induced unfolding was evaluated by tryptophan fluorescence. The

equilibrium curves at increasing concentrations of GuSCN shows that the native state is more stable than the unfolded state by 5.5 and 5.4 kcal mol<sup>-1</sup> for the wild-type and C322A, respectively showing that the overall stability is maintained in the mutant despite the disruption of the disulfide bridge.

Table 5.7: Thermodynamic stability of the tertiary structure of wild-type CotA and C322A mutant

	<b>Wild-type</b>	<b>C322A</b>
<b><math>\Delta G^{\circ}</math> (kcal/mol)</b>	5.5 $\pm$ 0.8	5.4 $\pm$ 1.3
<b><math>m</math> (kcal/mol)</b>	-3.4 $\pm$ 0.6	-3.4 $\pm$ 0.8
<b>Mid point (M)</b>	1.6 $\pm$ 0.1	1.6 $\pm$ 0.1

Moreover, the other parameters that characterize the structural stability, namely the concentration of GuSCN at which 50% of the molecules are unfolded (mid-point) and the cooperativity of unfolding ( $m$ ), are similar for the wild-type and mutant proteins (Figure 5.10A and Table 5.7).

.

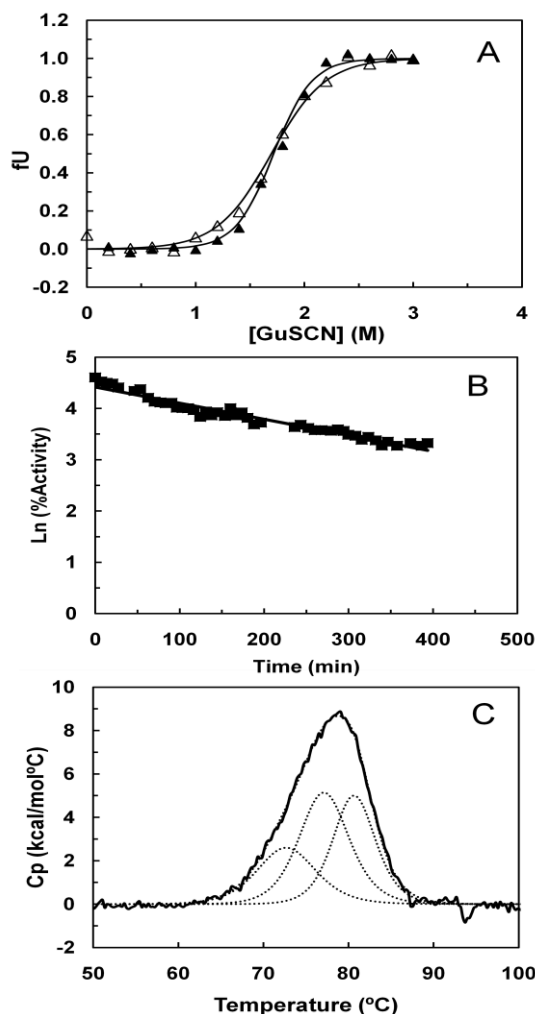


Figure 5.10: (A) Fraction of CotA wild-type (closed symbols) and C322A mutant (open symbols) unfolded ( $f_U$ ) by guanidine thiocyanate (GuSCN) as measured by trp fluorescence emission. The solid lines are the fits according to the equation  $f_U = \exp(-\Delta G^0/RT) / (1 + \exp(-\Delta G^0/RT))$ , which assumes the equilibrium  $N \leftrightarrow U$ . (B) Long-term stability of the C322A mutant protein at 80°C. (C) Differential scanning thermogram of the C322A mutant protein (solid line) fitted by three thermal transitions (dotted line).

The thermal stability was further probed by DSC (Figure 5.10C). The transitions obtained for the C322A mutant are as complex as previously reported for wild-type and other MCOs, because aggregation occurs after the first scan, leading to 100 % irreversibility in the process (Durao, et al., 2008; Fernandes, et al., 2010; Fernandes, et al., 2009). Moreover, the excess heat

capacity could only be fitted using three calorimetric transitions, supporting sequential domain unfolding. The overall thermal stability of C322A is comparable to the wild type with mid-point temperatures ( $T_m$ ) at each transition of 73°C, 78°C and 81°C. Overall these results show that the disulfide bridge does not have a major contribution for the thermodynamic or the thermal stability of CotA-laccase.

**Structural characterization.** The three dimensional structure of the C322A mutant was solved and the overall fold is very similar to the wild-type (the rms deviation of the  $C_\alpha$  trace is 0.618Å). Similarly to the wild-type holo-structure, the copper centres in C332A show full occupancies and a diatomic oxygen species was modelled in the trinuclear centre (Figure 5.11A). Interestingly, in the mutant enzyme the loop that comprises residues 90 to 97, which is usually very poorly defined in previous CotA structures (Bento, et al., 2005; Enguita, et al., 2003), became less disordered and it was possible to model into the electron density maps residues 90 to 92 and 95 to 97. In the structure of C322A mutant the Cys229 residue become exposed to the solvent and appears to be chemically modified and a methyl thio-cysteine moiety has been modelled at this position. A similar modification of exposed cysteine residues into oxy-cysteines has already been observed in other CotA structures where the protein was produced following the microaerobic expression protocol (Durao, et al., 2008). In the wild-type, the loop where Cys322 is involved in the disulfide bridge with Cys229 is well ordered and defined. In contrast, the most significant difference in the mutant structure is observed in the position of this loop that becomes less ordered and moves some 8Å away towards the solvent side (Figure 5.11B). As the disulfide bridge is located at one of the edges of the substrate binding pocket, the mutation induces a slight change in the configuration of the binding pocket, and changing the substrate binding surface. This, in turn, may influence the incorporation of copper into the mononuclear T1 copper centre. This observation could contribute to the decreased  $E^0_{T1}$ , determined for the C322A mutant (Karlin, et al., 1997). Indeed, substitutions of hydrophobic residues with



an alanine residue in the vicinity of the T1 Cu of CotA-laccase in a previous study have shown to increase the solvent accessibility and causing a decrease of the redox potential of the metal centre of the mutants (Durao, et al., 2008).

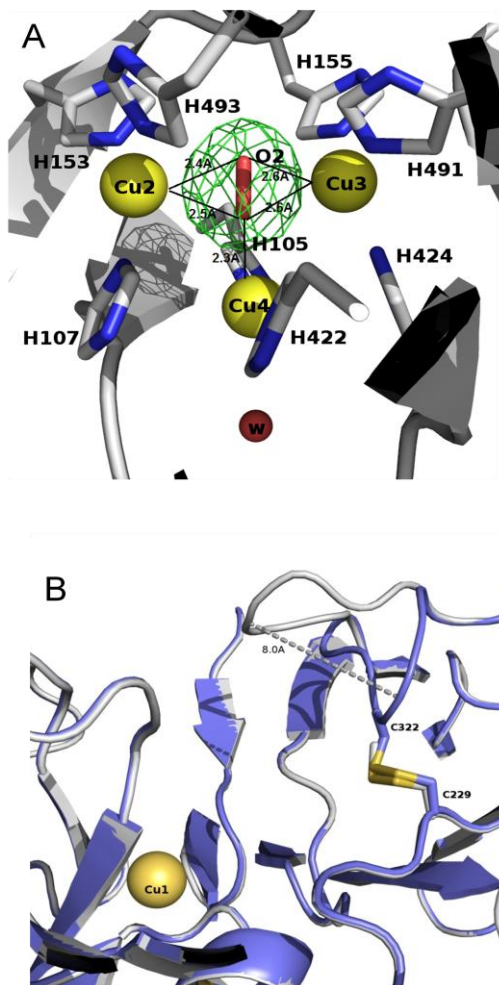


Figure 5.11: (A) Close-up view of the trinuclear centre in the C322A mutant structure. A different Fourier synthesis contoured at the 4 sigma level. (B) Superposition of the C $\alpha$  tracing of the C322A mutant protein and holoCotA. The loop that contains residue 322 is coloured in orange for the wild type and in grey for the mutant. Residue 229 in the C322A mutant protein is coloured by atom type.

**Collisional quenching by acrylamide.** In order to address possible modifications in the mutant protein dynamics, the accessibility of the tryptophan fluorophores was studied by using acrylamide as a fluorescence quencher (Figure 5.12).

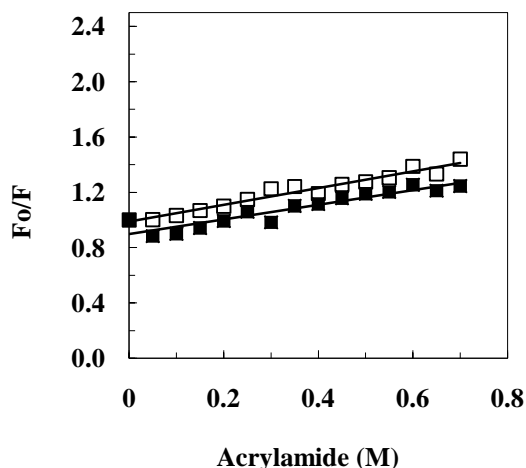


Figure 5.12: Stern-Volmer plot. Collisional quenching of CotA wild-type (closed symbols) and of C322A mutant (open symbols).

The Stern-Volmer plots for wild-type and C322A mutant are very similar, showing that the accessibility of tryptophan residues to acrylamide is similar in both proteins. The quenching of a fluorophore depends upon its “exposure” to the quencher. Indeed, a buried residue may occasionally expose itself to collisions with the quencher as a result of local or large scale conformational fluctuations in the protein. Quenching of tryptophan fluorescence has to occur during the lifetime of the excited state and therefore only protein dynamics within this ps-ns time range may allow acrylamide collision to tryptophan residues. Therefore, collisional quenching also probes motion dynamics within the ps-ns scale of fluorescence lifetimes (Eftink and Ghiron, 1977; Somogyi, et al., 1994) at least for tryptophan residues that are partially exposed at the protein surface (Calhoun, et al., 1986). The results obtained show that the disruption of the disulfide bridge in the CotA-laccase, does not affect protein dynamics in the ps-ns time scale, which is generally defined as the faster time scale of protein motions.

**Kinetics of the acid-unfolding reaction.** Unfolding kinetics as assessed by trp fluorescence, using the stopped-flow technique were measured using in the apo

and holo-forms of the enzymes under study. Acidification was used to promote protein unfolding and, interestingly, it was observed that unfolding of the apo-forms is characterized by a decrease in fluorescence whilst those of the holo forms are characterized by an increase in fluorescence (Figure 5.13). This inversion of the fluorescence signal is most probably due to the assigned role of copper as a quencher of fluorescence (Lakowicz, 1999).

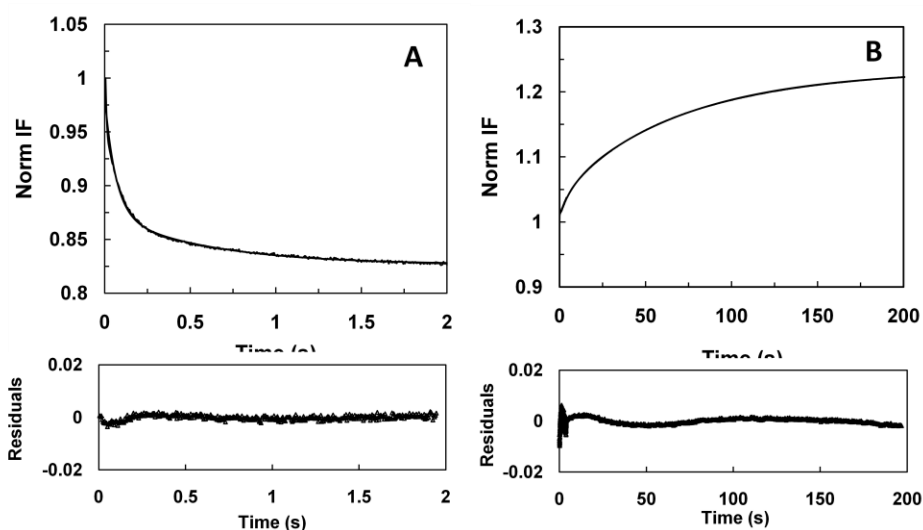


Figure 5.13: Unfolding induced by acid and assessed by tryptophan fluorescence. (A) Total fluorescence intensity variation of apo-CotA wild-type. (B) Total fluorescence intensity variation of holo-CotA wild-type. Kinetic traces were fitted with a double-exponential for the apo-form and a triple exponential for the holo form as shown in the residuals plot.

The conformational unfolding of apo-forms was fitted with a second order exponential, while the unfolding of the holo forms could only be accurately fitted by using a triple exponential (Table 5.8). This is most probably related to a higher complexity of the unfolding pathway in the holo-forms which certainly, reflects the presence of copper ions at the catalytic centres. A lower number of unfolding phases, in apo-forms, is also observed in other metallo proteins (Zhang and Matthews, 1998). In the blue copper azurin an unfolding pathway of higher complexity, caused by a redox active copper ion that remains bound to the protein in the unfolded state was observed (Leckner, et al., 1997).

Table 5.8: Values for the  $k_1$ ,  $k_2$  and  $k_3$  constants obtained from the fitting of kinetic traces reporting the variation in fluorescence intensity upon acid-induced unfolding.

	$k_1$ (s <sup>-1</sup> )	$k_2$ (s <sup>-1</sup> )	$k_3$ (s <sup>-1</sup> )
<b>Apo-CotA</b>	16.95 ± 1.09	1.81 ± 0.09	-
<b>Apo-C322A</b>	22.1 ± 0.07	1.59 ± 0.05	-
<b>Holo-CotA</b>	0.12 ± 0.01	0.02 ± 0.00	0.002 ± 0.001
<b>Holo-C322A</b>	0.38 ± 0.01	0.10 ± 0.01	0.03 ± 0.01

The unfolding rates of the apo-forms are almost 100-fold higher than the holo-forms (Table 5.8) highlighting the effect of copper in stabilizing the protein three-dimensional structure. This stabilizing effect of copper could not be quantified through the most classical approaches, such as equilibrium unfolding studies using chemical denaturants, because the enzymes become copper depleted at low concentrations of denaturant prior to the overall unfolding (Durao, et al., 2006; Fernandes, et al., 2009). In consequence, the stabilizing effect of copper ion was calculated applying the Arrhenius law (that accounts for the unfolding rates of the apo and holo forms) to each unfolding phase, for the mutant and wild type enzyme (Table 5.8) (Pozdnyakova, et al., 2001). For these enzymes no major differences were observed as the stabilizing effect for phase 1 ( $k_1$ ) is 1.6 and 1.8 kcal mol<sup>-1</sup> and for phase 2 ( $k_2$ ) is 0.2 and 0.3 kcal mol<sup>-1</sup> for CotA wild-type and C322A mutant, respectively. These values are in the lower limit for the stabilizing effect of copper in the native state, i.e. assuming absence of copper affinity in the transition state during unfolding and are also in agreement with the spectroscopic and structural analysis, which revealed no major differences in the properties of the copper centres. Overall, the present results show that the mutant C322A globally unfolds faster than the wild-type enzyme. This suggests that the mutant most likely refold also faster as compared with the wild-type, given that at the equilibrium the stability is not affected by the mutation (see above). However, due to the occurrence of protein aggregation, the folding kinetics of these proteins could not be investigated here.

**Kinetics of copper depletion and binding.** The rates of copper release from the T1 Cu site were monitored upon acid-induced unfolding of the wild-type and C322A mutant holo-forms. The kinetic traces measured at 600 nm were accurately fitted according to a double exponential (not shown), pointing to a complex process which might be a consequence of the centre reorganization, preceding the copper release from T1 Cu site (Table 5.9).

Table 5.9: Values for the  $k_1$  and  $k_2$  constants obtained from the fitting of kinetic traces reporting the decay of absorbance at 600 nm upon acid-induced unfolding.

	$k_1$ (s <sup>-1</sup> )	$k_2$ (s <sup>-1</sup> )
<b>Holo-CotA</b>	$3.37 \pm 0.71$	$0.38 \pm 0.08$
<b>Holo-C322A</b>	$7.43 \pm 0.97$	$2.71 \pm 0.90$

The 2-fold higher decay rates at 600 nm in the C322A mutant as compared to the wild-type indicate a faster removal of the T1 copper ion in the mutant enzyme.

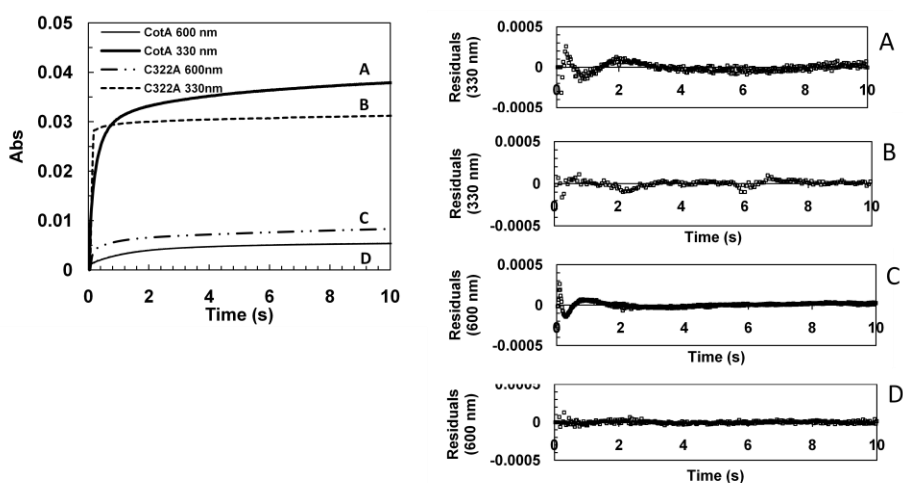


Figure 5.14: Copper binding to apo-forms of wild-type (solid line) and C322A (dotted line). Kinetic traces measured by the absorbance at 600 nm (A) and at 330 nm (B). Residuals are from triple exponential fits (upper residuals for CotA and lower residuals for C322A).

The kinetic traces describing copper binding to the T1 and T3 of the apo-forms, measured at 600 and 330 nm, respectively, required a triple-exponential to be accurately fitted, despite the attempt to use pseudo-first order conditions, (i.e. copper:apo-protein in a 10:1 ratio; Figure 5.14 and Table 5.10). These multiple rate constants might result from the presence of non-pseudo first order conditions or from binding followed by protein reorganization. Indeed, it has been recognized that metal binding to proteins may involve complex pathways with at least one intermediate during the binding process (Bah, et al., 2006; Cawthorn, et al., 2009; Choi, et al., 2006; Taniguchi, et al., 1990).

Table 5.10: Values for the  $k_1$ ,  $k_2$  and  $k_3$  constants obtained from the fitting of kinetic traces reporting copper binding to T1 and T3 sites (absorbance at 600 nm and 330 nm, respectively).

	$\lambda$	$k_1$ (s <sup>-1</sup> )	$k_2$ (s <sup>-1</sup> )	$k_3$ (s <sup>-1</sup> )
<b>Apo-CotA</b>	600 nm	20.12 ± 6.05	0.78 ± 0.02	0.09 ± 0.004
	330 nm	4.93 ± 0.11	0.75 ± 0.04	0.06 ± 0.001
<b>Apo-C322A</b>	600 nm	26.6 ± 6.2	1.7 ± 0.8	0.12 ± 0.02
	330 nm	10.4 ± 0.15	1.4 ± 0.02	0.08 ± 0.008

For example, in human ceruloplasmin it has been proposed that copper binding *in vitro* is a cooperative process presumably mediated by conformational changes transmitted within the protein upon copper binding (Hellman, et al., 2002). On the other hand, copper binding to Sco from *Bacillus subtilis*, a protein involved in the assembly of the Cu<sub>A</sub> centre in cytochrome *c* oxidase, is described by a two-step binding mechanism where the first step is a bimolecular process producing an intermediate that undergoes an isomerisation step to yield the final holo-form (Cawthorn, et al., 2009). The fast rate constant  $k_1$  measured in the wild-type and mutant enzymes was assigned to the first bimolecular step of copper binding (Table 5.10). This rate was shown to be dependent on the copper concentration (data not shown). The C322A mutant presents slightly faster rates of copper binding followed at both 600 and 330 nm (Table 5.10).

Interestingly, the rates of copper binding to the T1 centre are faster as compared to the rates measured to the T3 centre. This is in accordance to our previous results that pointed to a sequential process of copper incorporation into CotA-laccase, with the T1 Cu centre being the first to be reconstituted, followed by the T2 and T3 Cu centres (Durao, et al., 2008), similarly to what occurs in CueO from *E. coli*, yeast Fet3P and human ceruloplasmin (Blackburn, et al., 2000; Galli, et al., 2004; Kataoka, et al., 2005). The differences observed in the rates of Cu incorporation and release in the mutant enzymes as compared to the wild-type should reflect subtle alterations in the protein dynamics with consequences in structural unfolding rates and in the rates of copper release and incorporation. Only this slower motion regime and not the ps-ns time range dynamics was affected as shown by acrylamide collisional fluorescence quenching analysis. The higher dynamics observed seems not to affect copper coordination in the catalytic centres. In fact, and as shown above, the stabilizing effect of copper is similar for both enzymes as well as the spectroscopic and catalytic properties of the enzymes. Binding sites in proteins have a dual stability character, and are often characterized by the presence of regions with low and with high structural stability, in an overall arrangement that contributes for an optimized binding affinity (Luque, et al., 2002). In most cases the low-stability regions are loops that become stabilised upon ligand binding and covered a significant portion of the ligand after binding, while catalytic residues of enzymes, are usually located in regions with higher structural stability. Copper has a pivotal role in CotA-laccase stability as well as in other multicopper oxidases (Agostinelli, et al., 1995; Durao, et al., 2008; Koroleva, et al., 2001; Sedlak and Wittung-Stafshede, 2007; Sedlak, et al., 2008) as shown here by the 100-fold faster unfolding rates of apo-forms relative to the holo-forms, as measured by fluorescence intensity. Copper incorporation in multicopper oxidases is however a poorly understood process at the molecular level (1999; Blackburn, et al., 2000; Davis-Kaplan, et al., 1998; Galli, et al., 2004; Kataoka, et al., 2005; Kwok, et al., 2006; Sedlak and Wittung-Stafshede, 2007; Sedlak, et al., 2008; Shi, et al., 2003). The results presented in this study

indicate that the disulfide bridge in CotA-laccase should contribute to the stabilization of the loop in the vicinity of the T1 Cu centre, highlighted in Figure 5.11, providing the necessary frame for the incorporation of the copper ions at the catalytic sites.



## 6 GENERAL DISCUSSION

---



## 6.1. DISCUSSION

The family of multicopper oxidases, that includes the functional classes of metallo-oxidases and laccases, is constituted by proteins that catalyze the oxidation of a variety of aromatic compounds, in particular phenolic substrates, coupled to the four-electron reduction of molecular dioxygen to water. This family of enzymes is distributed in all branches of Life and in recent years there is an increasing interest, from the scientific community, to isolate and study these biocatalysts due to their physiological roles as well as their biotechnological potential. The broad substrate specificity of laccases and the use of readily available dioxygen as reducing substrate make them very interesting biocatalysts for various industrial processes, such as food technology, delignification of lignocellulosics, biosensor and analytical applications. However, to use enzymes in industry, low production costs and high enzymatic efficiency and also a high stability toward denaturation are required, to properly work under the typical harsh conditions, in which industrial processes occur.

In this work we focused our attention into the study of molecular determinants involved in the stability of multicopper oxidases. To achieve these objectives two main strategies were outlined;

- i) To clone in heterologous hosts and characterize MCOs from hyperthermophilic sources. The characterization of enzymes naturally thermostable is expected to provide clues on the kinetic and thermodynamic properties involved in the maintenance of the proper fold under different denaturant conditions.
- ii) Identify, through the use of site-directed mutagenesis, key residues involved in protein stabilization in CotA-laccase. The use of SDM in a well characterized enzyme can elucidate the key role of certain residues, namely residues involved

in metal coordination and disulfide bridges, putatively determinants of protein stability.

### **Hyperthermophilic McoA from *Aquifex aeolicus* and McoP from *Pyrobaculum aerophilum***

The first part of this thesis focuses on the identification, cloning, expression, purification and characterization of two new hyperthermophilic multicopper oxidases, McoA from *Aquifex aeolicus* and McoP from *Pyrobaculum aerophilum*.

McoA and McoP are multicopper oxidases that show all the typical spectroscopic properties of other well known enzymes of the same family. The UV-Vis spectra shows the typical T1 absorbance at 600 nm, the EPR spectra shows the typical T1 and T2 parameters and the CD spectra shows the common secondary structure of these proteins, rich in  $\beta$ -sheets. A higher kinetic efficiency towards the oxidation of low valence metal ions than to aromatic substrates was observed for both enzymes, showing that they belong, to the functional class of metallo-oxidases among MCOs. Furthermore, the two enzymes are thermoactive, with optimal temperatures around 80°C, and also hyperthermostable with melting temperatures near 100°C as evaluated by DSC.

*A. aeolicus* and *P. aerophilum* thrive in geothermally and volcanically heated habitats, which are abundant in potentially toxic metals. The *mcoA* gene is located close to six genes, of which all but one, codes for putative proteins with strong similarities to orthologues from characterized copper-resistance systems from *E. coli*. All these genes are encoded on the *A. aeolicus* genome in the same direction of transcription, and even if it is not clear if it represents a single operon or several independent transcriptional units it is most likely that they share a similar regulation. In this regard, even if the *mcoP* gene in *P. aerophilum* is not part of a metal-resistance determinant, like *mcoA*, we suggest that both enzymes have a probable physiologic function of cytoprotection against toxic forms of low valence metals such as  $\text{Cu}^+$  or  $\text{Fe}^{2+}$ , based on their

catalytic properties, showing the highest efficiency towards the oxidation of metal ions. Free low valence metals, such as copper, zinc, iron and manganese, may be toxic due to the generation of reactive oxygen species that can damage lipids, proteins, and DNA. However the trace presence of these metals is fundamental for the cells metabolism as they play important roles in electron transport and redox reactions as cofactors of many enzymes such as cytochrome *c* oxidase and superoxide dismutase (Pesci and Pickett, 1994; Pitcher and Watmough, 2004). Therefore the concentrations of these metals are highly regulated in the cell and the lack of this regulation has implications in several diseases (Arnesano, et al., 2002; Crichton and Pierre, 2001). In *E. coli*, three systems for copper tolerance have been identified, *cus* (for Cu-sensing) systems, and the plasmid-encoded *pco* (for plasmid-borne copper resistance) and the chromosomally encoded *cueo* (for Cu efflux) (Brown, et al., 1995; Franke, et al., 2003; Lee, et al., 2002; Outten, et al., 2001). Other microorganisms have similar systems, e.g. *Enterococcus hirae* have also a copper-responsive promoter that are part of a series of chromosomally linked genes arranged as operons that allow maintaining the correct metal homeostasis (Harris, et al., 1998).

McoP from *P. aerophilum* shows a new feature among this family of MCO, has it uses more efficiently nitrous oxide (N<sub>2</sub>O) as final electron acceptor, than the typical oxidizing of MCOs dioxygen (O<sub>2</sub>). The dissimilatory reduction of nitrate to dinitrogen (N<sub>2</sub>) by *P. aerophilum* is relatively well studied; enzymatic activities of the denitrification pathway were detected in cellular fractions, and nitrate and nitric oxide reductases purified and characterized (Afshar, et al., 2001; Afshar, et al., 1998; Fitz-Gibbon, et al., 2002; Tavares, et al., 2006; Volkl, et al., 1993; Zumft, 1997). It is worth mentioning that no recognizable homolog of *nosZ*, which codes for N<sub>2</sub>OR in bacteria, has been found in the genome of this archaeon, suggesting the presence of other enzyme, responsible for the last step of the denitrification pathway (Zumft and Kroneck, 2007). *P. aerophilum* is not the only microorganism that is able to produce N<sub>2</sub> without the

presence of the typical recognizable *nosZ* gene; *Nitrosomonas europea*, *Nitrosomonas eutropha*, *Haloferax volcanii* and *Haloarcula marismortui* also lack the typical bacterial NosZ enzyme (Zumft and Kroneck, 2007), therefore it is possible that MCOs from these organisms also share this putative physiological function of nitrous oxide reductase.

Both McoA and McoP are dependent on the exogenous addition of copper to the reaction mixture to achieve full kinetic efficiency in contrast to what happen with CotA-laccase from *Bacillus subtilis*. In McoP ‘copper activation’ is most probably related to the apparent labile nature of the T2 copper (Fernandes, et al., 2010). Indeed, the EPR spectroscopy analysis suggests that this copper should be in constant exchange with the solvent, and therefore the addition of exogenous copper should dislocate the equilibrium towards the enzyme with copper in the T2 site.

In McoA, the comparative model structure showed the presence of a striking structural feature, a methionine-rich region (residues 321–363) reminiscent of those found in copper homeostasis proteins. This Met-rich region showed to be involved in the enzyme modulation, and a possibility is that it blocks the access of bulkier substrates to the binding pocket, or act, as an electron transfer matrix between the reducing substrate and the T1 copper center. The deletion of the Met-rich region segment in McoA resulted in severe decrease in catalytic efficiency towards all the substrates. Indeed, the differences observed between the wild type protein and the McoA $\Delta$ P321-V363 mutant relies essentially in the  $k_{cat}$  term, which decreases between 8 for Cu<sup>+</sup> to 300 times for ABTS, suggesting that the presence of this region and its conformational arrangement is a key factor in the catalytic mechanism. In addition, copper activation was abolished in the mutant enzyme, reinforcing the importance of this region in the catalytic mechanism, probably by modulating the participation of the exogenous copper in the enzyme mechanism. This data support conformations for the methionine rich region masking the zone of the substrate binding site near the T1 center as observed in simulations of the McoA model structure (Fernandes et al. 2007).

In CueO from *E. coli*, it was showed that a fifth copper bind to residues in a loop similar to the one found in McoA, modulating the catalytic activity (Roberts, et al., 2003). In fact, this Met-motifs are found in several proteins involved in copper trafficking and homeostasis, including Crt (from *Yeast*) Pco, Cop and CueO from *E. coli* (Jiang et al, 2005; Roberts et al 2002). These methionine rich regions can be arranged in MXXM motifs containing 3-5 methionines residues and, some proteins involved in copper transport utilize multiple methionines sites for copper binding (Roberts et al, 2002).

### **Thermal stability of MCOs**

The stability of the MCOs studied in this work was evaluated by their kinetic stability and by differential scanning calorimetry that allowed measuring the proteins melting temperatures. With regard to the results obtained in the long-term stability, McoA is the most stable with a half-life time of around 9 hours at 80 °C, whereas McoP activity lasts for around 6 hours and, CotA-laccase that takes 3 hours to lose 50% of its activity when incubated at that temperature. Comparing the data obtained by DSC for the three enzymes we can observe that the thermogram of McoA, McoP and CotA-laccase, revealed a complex process, due to aggregation after unfolding leading to 100% of irreversibility (no peak in the second scan) and also an excess heat capacity, which can only be accurately fitted by considering three independent transitions. The same three thermal transitions were previously used to describe DSC traces of ascorbate oxidase (AO) and human ceruloplasmin (hCp) (Bonaccorsi di Patti et al. 1990, Savini et al. 1990). These three thermal transitions, apparently, correlate with the structural organization of three cupredoxin-like domains for most of the proteins studied and the six cupredoxin domains organized into three pairs in hCp. In addition, each transition measured by DSC is a non-two-state process, as the calorimetric molar enthalpy is significantly smaller than the van't Hoff enthalpy (Durão et al. 2008; Fernandes et al. 2009). The analysis of the DSC thermal unfolding data shows that McoA is the most stable with an average  $T_m$  of 110 °C, followed by McoP with a  $T_m$  of 104 °C and CotA is the

less stable with an average melting temperature of 77 °C. The data obtained by these studies clearly show the hyperthermophilic behaviour of both McoA and McoP when compared with their thermophilic counterpart CotA-laccase. In fact, these data clearly correlates with the physiological temperatures of the host microorganisms.

Even considering that MCOs are widespread among all branches of Life, the homologous from thermo and hyperthermophilic sources are relatively scarce. In fact, besides the enzymes that we mentioned on this thesis, there is just one more homologous protein from *Thermus thermophilus* (Miyazaki, 2005). In fact, this is the most thermostable laccase characterized so far, with a half-life time of 870 min at 80 °C. According, to Miyazaki (2005) the primary sequence of *Tth*-laccase presents the highest aliphatic index (96%, compared to 78, 79 and 89% for CotA, McoA and McoP, respectively) and also the highest proline content (10% compared to 9, 8 and 5 for CotA, McoP and McoA, respectively) which are known factors that might contribute to a higher thermostability. However, the characterization of the protein did not involve other techniques besides the evaluation of the long-term stability and it is fragile to draw final explanations based only in theoretical analysis of the primary sequence.

### **Copper Stabilizing effect**

Metal-binding sites in proteins are stabilized by binding the metal ions in coordinately saturated ligand environments with optimized bond geometries (Maglio, et al., 2003). We have used an expression protocol that allowed us to isolate CotA-laccase, and also other recombinant MCOs with all the coppers in the active center, with obvious positive implications in the catalytic efficiency and stability. Recombinant *E. coli* microaerobically cultures are able to produce, in the cytoplasmic space, a full loaded recombinant enzyme, while in aerobic conditions a Cu-depleted population of proteins is produced. We have shown that Cu physiology in *E. coli* is dependent on the oxygen availability; under microaerobic growth conditions in Cu-supplemented media, cells



accumulate higher amounts of Cu than when grown under aerobic conditions. Therefore, the heterologous expression of a fully Cu loaded enzyme under aerobic conditions by *E. coli* is likely to be impaired by the presence of low cellular concentrations of this transition metal ion.

The reconstitution with cuprous or cupric ions of apoCotA, synthesized by *E. coli* in the presence of oxygen in unsupplemented-Cu media, showed that a fully Cu loaded reconstituted enzyme is obtained only when the incorporation occurs in the presence of  $\text{Cu}^+$  as compared with results of incorporation with  $\text{Cu}^{2+}$ . These observations suggest that the CotA laccase is synthesized *in vivo* through incorporation of the copper in +1 oxidation state. Nevertheless, the apoCotA reconstituted with  $\text{Cu}^+$ , even with its full complement of Cu ions, possesses slight lower catalytic ability and thermal stability when compared with the as-isolated holoCotA. These results point to a critical role of Cu in the correct folding of recombinant CotA laccase in the cytoplasm of *E. coli*.

In fact, the DSC thermograms of different variants of CotA-laccase, with variable copper content, allowed to identify a trend in the  $T_m$  obtained (Durao et al., 2008). The data showed that holoCotA is the most stable, followed by apoCotA reconstituted with  $\text{Cu}^+$ , and the least stable is apoCotA reconstituted with  $\text{Cu}^{2+}$ . These results show that Cu content as well as Cu incorporation (*in vivo* vs. *in vitro*) have a direct impact on the overall stability of the enzyme. If holoCotA is depleted with EDTA and then reconstituted with Cu, it becomes as stable as the original holoCotA, meaning that the protein fold acquired *in vivo* and the correct Cu coordination are crucial for maximum stability. The effect of copper in stability was also evaluated under chemical induced unfolding, but it could not be quantified through equilibrium unfolding studies, using GdnHCl as denaturant, as copper is depleted prior to overall protein unfolding (Durao, et al., 2006; Fernandes, et al., 2009). In fact, the T1 copper, at least, in both CotA and McoA is bleached at lower GdnHCl concentrations compared to the unfolding of the tertiary structure and therefore no strong stabilization towards chemical denaturation, by copper is expected at equilibrium (Fernandes, et al.,

2009; Durao, et al., 2006). The stabilization by copper was thus quantified through unfolding kinetic measurements of the apo and holo-forms of the enzymes by monitoring changes in tryptophan emission.

The unfolding rate constants of the apo-forms are 50 to 100-fold faster as compared with the corresponding holo-forms, as a result of the copper stabilizing effect in the protein structures. The change induced by copper in the free energy gap between the ground state and the transition state was calculated based on the Arrhenius law ( $\Delta\Delta G^\ddagger = RT (\ln k_{apo} - \ln k_{holo})$ ). The values calculated were 2.7 and 1.5 kcal mol<sup>-1</sup> for CotA and McoA, respectively. These results show that the copper stabilizes both proteins by a considerable increase in the free energy gap, showing that the copper ions are in fact a fundamental factor in the thermodynamic stability of these proteins. Most of studies on the stabilizing effect of copper in proteins have been performed in the small blue copper oxidase azurin from *Pseudomonas aeruginosa* (Milardi, et al., 2003). Metal binding and unfolding studies have shown that the copper ion stabilizes the azurin structure by ~5.5 kcal mol<sup>-1</sup> (Pozdnyakova and Wittung-Stafshede, 2001). However, it should be noted that this is a smaller protein only 128 residues.

### **Thermodynamic Stability**

The chemical stability of the tertiary structure of the enzymes was measured by fluorescence intensity upon increasing concentrations of a chemical denaturant. With selective excitation of tryptophan residues at 296 nm, the fluorescence spectra changed upon unfolding, reflecting the exposure of tryptophan residues at the protein surface. Both unfolding profiles, of CotA and McoA, could be accurately fitted according to a two state process ( $N \leftrightarrow U$ ) where the folded and unfolded states seems to be the only states that accumulate at significant amounts.

CotA has nine tryptophan residues with percentages of exposure to water between 0 and 8% compared to a Trp residue in a standard Gly-Trp-Gly extended peptide (Chothia, 1976). Upon unfolding the wavelengths at the emission maxima shifted to the red, clearly reflecting the exposure of Trp residues to the high polarity of water at the surface of the protein. The CotA structure is very stable, displaying a GdnHCl concentration of 4.6 M at the midpoint (where 50% of the molecules are unfolded) and the native state is more stable than the unfolded state by 10 kcal mol<sup>-1</sup>. CotA-laccase has a higher chemical stability as compared with McoA; the GdnHCl midpoint is almost two-fold higher (4.6 M as compared to 2.8 M) than the one calculated for McoA, while the free energy gap in water, between the native and unfolded states is 3-times higher for CotA (10 kcal mol<sup>-1</sup> as compared to 2.7 kcal mol<sup>-1</sup>). The low  $\Delta G^{\text{water}}$  of McoA should mainly reflect the low cooperativeness of the transition as evaluated by the *m* parameter.

Contrarily to CotA wild-type, where the unfolding profile could be accurately fitted according to a two state transition, in M502L and M502F mutants, where the axial ligand of the T1 Cu was replaced by the residues Leu and Phe with higher redox potentials in the T1 Cu centers but with low activities, the chemical unfolding profile data could only be fitted using a three state transition. The accumulation of an intermediate (I) in-between N and U that occurs at low GdnHCl concentration (at around 1.9M GdnHCl, 50% of molecules are in the I state) allows the accurate fit of the unfolding process. The native state is only ~1.4 kcal mol<sup>-1</sup> more stable than the I state explaining its accumulation at low GdnHCl concentration. Tryptophan residues are partially exposed to water in the I state indicating that is a partially unfolded state. The conversion from I to the unfolded state occurs only at high GdnHCl concentrations and is thermodynamically similar to the conversion of N to U in the wild type. To gather further insight into the I state, we have analyzed the collisional quenching by acrylamide for both mutants, M502L and M502F. Assuming that acrylamide quenching is dynamic, as it seems from the linear

Stern-Volmer plots, the  $K_{SV}$  constant reflects the accessibility of tryptophan residues to collisions with acrylamide. A linear Stern-Volmer plot is generally, also indicative of a single class of tryptophan residues, all equally accessible to acrylamide. The values of  $K_{SV}$  reported for the wild type ( $0.56 \text{ M}^{-1}$ ) and mutant M502L ( $0.24 \text{ M}^{-1}$ ) are small, reflecting the buried position of tryptophan residues (Melo, et al., 2007). The most distinctive feature of acrylamide quenching is clearly the identification of the intermediate I revealed during guanidinium denaturation experiments. In the presence of 2 M of GdnHCl where the intermediate I accumulates, the  $K_{SV}$  value increase  $\sim 4$  fold for the mutants compared to a  $\sim 1.5$  fold increase for the wild-type protein. Quenching by acrylamide indicates that the intermediate state I is partially unfolded, exposing tryptophan residues to collisions with acrylamide in accordance with the red-shift observed for the wavelengths at the emission maximum.

These observations are fully supported by the invariant three-dimensional structures obtained for both mutants and by the same emission maximum of tryptophan residues ( $\sim 331 \text{ nm}$ ) in the native state. However, it appears that the mutations M502L and M502F have destabilized the conformation of the T1 site without causing gross structural changes in the tertiary structure.

It is well known that stabilization by Cu depends on the type of coordination involved (T1, T2 or T3) (Agostinelli, et al., 1995; Koroleva, et al., 2001; Milardi, et al., 2003) but probably also on subtle changes of each coordination geometry. The T1 axial ligand mutations may have created a “hot-spot” where partial unfolding that leads to accumulation of the I state is probably initiated. Truly, the  $\text{C}^{\delta 2}$  Leu502 atom is located further way from the T1 copper and no longer coordinates it, as observed in other laccases which have a leucine at that position. In the M502F mutant the phenylalanine residue is positioned even further away from the copper atom and does not coordinate to it. The slight movement of the mutated residue towards the protein surface, and away from the T1 copper atom, leads to a concerted movement of this region, pushing it away towards the solvent, and slightly increasing the exposure of the copper

center. The lower stability of the M502 mutants may be correlated with this subtle structural change. Indeed, the weakening of the copper coordination, and the slight alterations in the residues interconnections could lead to a decreasing stabilization of the center and thus of the whole structure.

Actually the T1 copper center and its vicinity seem to have a fundamental role in the overall stability, and dynamics of CotA-laccase. We have disrupted the single disulfide bridge of CotA-laccase, which is located at one of the edges of the substrate binding pocket. Remarkably, the removal of this S-S bridge did not affect the protein stability under equilibrium conditions. Furthermore, the crystal structure of C322A indicates that the overall structure is essentially the same as the wild-type with slight alterations evident only in the immediate proximity of the mutation. Indeed, in the mutant enzyme, the loop containing the C322 residue becomes less ordered, leading to a putative increase in the solvent accessibility of the T1 Cu center. The maintenance of the catalytic parameters in the C322A mutant suggest also that the reduction potential should be the same, however the reduction of approximately 70 mV determined for the C322A, suggests that the T1 copper ion should have higher solvent accessibility in accordance with X-ray data.

In order to get more insight on the role of the S-S bridge in the protein dynamics we have measured the rates of copper bleaching/binding and structural unfolding of CotA wild-type and of C322A mutant using the stopped-flow technique. Despite the same thermodynamic stability in equilibrium conditions, the C322A mutant shows a faster unfolding as compared with the wild-type enzyme for both the holo and the apo-forms. Kinetics of acid-induced unfolding have shown also the essential role of copper in stabilizing the protein structure where the apo-forms exhibit around 100-fold faster unfolding rates relative to the holo forms. Furthermore, the kinetics of copper binding to apo-forms showed that C322A mutant binds copper at faster rates as compared to

the wild-type enzyme suggesting that the S-S bridge is somehow involved in the maintenance of slow dynamics of the copper at the T1 center.

Overall our results show that the S-S removal affects the protein dynamics in the lower,  $\mu$ s-ms time regime and not in the fast ps-ns time-scale as previously shown, by using acrylamide as a collisional quencher, and thus having consequences at the ms time-range accessible through stopped-flow kinetics. In fact, it is known that protein dynamics in the so-called slower motion regime ( $\mu$ s-ms) occur at significant levels in loops, such as the one displaced by the removal of the disulfide bridge and, seem to be particularly sensitive to bond ligands, even when no major differences are detected in the structure of un-bond and bond forms (Boehr, et al., 2006). The data also shows that this increased dynamics also favours, in acidic conditions, the unfolding rates and therefore should also affect refolding rates, (not measured due to aggregation), to keep the thermodynamic stability constant.

### **Mechanism for thermostability**

The study of the hyperthermophilic nature of an enzyme offers an opportunity to get insight into protein general mechanisms of thermostability. The study of unfolding pathways, in copper proteins, using chemical denaturants has been mostly performed for the small blue copper proteins which only have a T1 copper center (Alcaraz and Donaire, 2004; Alcaraz, et al., 2005; Bonander, et al., 2000; Mei, et al., 1999) besides a study with human MCO ceruloplasmin (Sedlak and Wittung-Stafshede, 2007). The complexity of the unfolding of the larger MCOs, is therefore a challenge that remains to be fully understood.

Therefore we have analyzed in more detail the hyperthermophilic nature of McoA. The unfolding kinetics measured for McoA reflects parallel pathways (due to the aggregation) which are related to the formation of a quasi native state prior to unfolding, as evaluated by gel filtration, UV-vis spectroscopy and ANS binding (Fernandes, et al., 2009). The formation of these aggregates

reduces the hydration in the surface of the molecule causing a decrease in the protein heat capacity ( $\Delta C_p$ ). An increased number of electrostatic interactions or hydrogen-bonding network around an ionized group in the core of protein, a high level of conformational dynamics and the presence of residual structure in the unfolded state (either aggregates or not) are also known contributors to a low  $\Delta C_p$  (Lee, et al., 2005; Spolar, et al., 1992; Zhou, 2002) (Jaenicke, et al., 1996) (Robic, et al., 2003; Vieille and Zeikus, 2001).

In order to elucidate the hyperthermophilic nature of McoA we have measured its stability curve ( $\Delta G$  vs.  $T$ ) and compared it to its mesophilic counterpart, CotA-laccase. We evaluated the chemical stability at different temperatures, and the experimental data was fitted according with the Gibbs-Helmholtz equation ( $\Delta G = \Delta H_{T_m}(1 - T/T_m) - \Delta C_p [(T_m - T) + T \ln(T/T_m)]$ ) (Figure 6.1). The data shows that McoA exhibits a flatter dependence of stability on temperature than CotA. In fact, the stability curve of McoA is characterized by heat capacity five-fold lower than CotA (0.5 and 2.6 kcal mol<sup>-1</sup> K<sup>-1</sup> for McoA and CotA, respectively), which allows the protein to remain folded over a wider range of temperatures as compared with CotA.

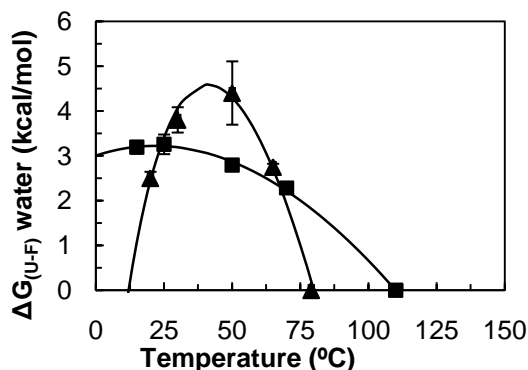


Figure 6.1: Protein stability curves of McoA (squares) and CotA (triangles) at pH 3, fitted according with the Gibbs-Helmholtz equation (Fernandes, et al., 2009).

Actually, the strategy shared by hyperthermophilic proteins to maintain their fold, and to have the flexibility necessary to its catalytic activity at high temperatures can be divided into three main strategies; i) the stability curves ( $\Delta G$  vs.  $T$ ) can be shifted toward a higher  $\Delta G$  values; ii) it can be shifted toward higher temperatures; or iii) it can be flattened, due to a smaller difference in partial molar heat capacity between protein's folded and unfolded states ( $\Delta C_p$ ) (Vieille and Zeikus, 2001). Proteins that function at high temperatures may thus employ various strategies to fold and function at the required temperature, being the most common contribution to attain a higher  $T_m$ , a raise in the stability curve to higher values of  $\Delta G$  (Razvi and Scholtz, 2006). Moreover, it was found that some proteins can even use combinations of the three proposed mechanism to reach their superior thermostability (Vieille and Zeikus, 2001). McoA is part of a group of thermophilic enzymes that balances their high  $T_m$  values with the optimal conformational stability for function, at high temperatures, through a low heat capacity ( $\Delta C_p$ ).



## Research Highlights

The work described on this thesis has allowed the gathering of important information about MCOs. The isolation and characterization of two new hyperthermophilic enzymes, with really interesting properties shows that much still needs to be studied in order to elucidate the different roles of MCOs. The importance of the Met-rich segments, and the exact mechanism underlying the electron transfer by these motifs is still under debate, where many questions remain to be answered, namely regarding the residues that do bind the fifth copper and consequently the electron pathway from the reducing substrate to the T1 copper center. McoP uses more efficiently  $\text{N}_2\text{O}$  as oxidizing agent than the typical  $\text{O}_2$  for MCO. This new feature is highly interesting from the fundamental point of view, but still needs further elucidation, especially concerning the way that the trinuclear centers can accommodate different molecules besides the typical dioxygen.

Site directed mutagenesis in the axial ligand of CotA, showed a dramatic effect, either in the kinetics of the enzyme as well as in the thermodynamic stability of the protein. The single S-S bridge of CotA is not involved in the stability but the structural and kinetic data suggest that this S-S bond contributes to the conformational dynamics of the protein at the  $\mu\text{s}$ -ms time-scale with implications in the rates of copper incorporation and release from the catalytic centers. The use of SDM to elucidate specific roles of point residues has been widely used in protein science, with some success, even besides its time consuming. Also, small perturbations, apparently innocuous, at a point location in a structure of a protein may have dramatic side effects in some biophysical/biochemical parameters has observed in the CotA M502 mutants. A possible way to overcome these limitations is to use laboratory forced evolution in order to generate thousands of variants, with a selected characteristic, before proceeding to more detailed studies.

A more detailed study concerning the thermodynamic nature of McoA revealed that the high thermal stability of McoA relies essentially in a low heat capacity that flattens the dependence of  $\Delta G$  on temperature, enabling McoA to maintain its fold over a wide range of temperatures. CotA has a lower thermal stability but a higher chemical stability, which is explained by a higher heat capacity and consequently a higher  $\Delta G$  of the protein, with the drawback of having a higher dependence on temperature (less thermostable). Work concerning the folding kinetics can be performed and the data will permit to better understand the folding mechanism of these enzymes. Furthermore, such studies can also reveal the fundamental role of copper during the folding of the polypeptide chain.

In fact, we have shown that the copper incorporation during folding of CotA-laccase is fundamental to achieve full thermostability. The exact mechanism by which copper influences the folding *in vivo* in MCOs is still unknown. If copper binds to the polypeptide promoting the folding and consequently the formation of functional biomolecules, or if it binds after the proper folding of the polypeptide is still an answered question. We have been able to show that  $\text{Cu}^+$  does bind to the apo form of the protein yielding a final ratio of 4 coppers per molecule.

## 7 REFERENCES

---



(1999) Nomenclature committee of the international union of biochemistry and molecular biology (NC-IUBMB), Enzyme Supplement 5 (1999), *Eur J Biochem*, **264**, 610-650.

Aasa, R. and Vanngard, T. (1975) EPR signal intensity and powder shapes: A reexamination, *Journal Magnetic Resonance*, **19**, 308-315.

Afshar, S., Johnson, E., de Vries, S. and Schroder, I. (2001) Properties of a thermostable nitrate reductase from the hyperthermophilic archaeon *Pyrobaculum aerophilum*, *J Bacteriol*, **183**, 5491-5495.

Afshar, S., Kim, C., Monbouquette, H.G. and Schroder, I.I. (1998) Effect of tungstate on nitrate reduction by the hyperthermophilic archaeon *pyrobaculum aerophilum*, *Appl Environ Microbiol*, **64**, 3004-3008.

Agostinelli, E., Cervoni, L., Giartosio, A. and Morpurgo, L. (1995) Stability of Japanese-lacquer-tree (*Rhus vernicifera*) laccase to thermal and chemical denaturation: comparison with ascorbate oxidase, *Biochem J*, **306** ( Pt 3), 697-702.

Alcaraz, L.A. and Donaire, A. (2004) Unfolding process of rusticyanin: evidence of protein aggregation, *Eur J Biochem*, **271**, 4284-4292.

Alcaraz, L.A., Jimenez, B., Moratal, J.M. and Donaire, A. (2005) An NMR view of the unfolding process of rusticyanin: Structural elements that maintain the architecture of a beta-barrel metalloprotein, *Protein Sci*, **14**, 1710-1722.

Andrade, S.M. and Costa, S.M. (2002) Spectroscopic studies on the interaction of a water soluble porphyrin and two drug carrier proteins, *Biophys J*, **82**, 1607-1619.

Anfinsen, C.B. (1972) The formation and stabilization of protein structure, *Biochem J*, **128**, 737-749.

Anfinsen, C.B. (1973) Principles that govern the folding of protein chains, *Science*, **181**, 223-230.

Anfinsen, C.B., Haber, E., Sela, M. and White, F.H., Jr. (1961) The kinetics of formation of native ribonuclease during oxidation of the reduced polypeptide chain, *Proc Natl Acad Sci U S A*, **47**, 1309-1314.

Arakane, Y., Muthukrishnan, S., Beeman, R.W., Kanost, M.R. and Kramer, K.J. (2005) Laccase 2 is the phenoloxidase gene required for beetle cuticle tanning, *Proc Natl Acad Sci U S A*, **102**, 11337-11342.

- Argos, P., Rossmann, M.G., Grau, U.M., Zuber, H., Frank, G. and Tratschin, J.D. (1979) Thermal stability and protein structure, *UCLA Forum Med Sci*, 159-169.
- Arnesano, F., Banci, L., Bertini, I., Ciofi-Baffoni, S., Molteni, E., Huffman, D.L. and O'Halloran, T.V. (2002) Metallochaperones and metal-transporting ATPases: a comparative analysis of sequences and structures, *Genome Res*, **12**, 255-271.
- Bah, A., Garvey, L.C., Ge, J. and Di Cera, E. (2006) Rapid kinetics of Na<sup>+</sup> binding to thrombin, *J Biol Chem*, **281**, 40049-40056.
- Baldrian, P. (2006) Fungal laccases - occurrence and properties, *FEMS Microbiol Rev*, **30**, 215-242.
- Baptista, R.P., Chen, L.Y., Paixao, A., Cabral, J.M. and Melo, E.P. (2003) A novel pathway to enzyme deactivation: the cutinase model, *Biotechnol Bioeng*, **82**, 851-857.
- Barton, S.C., Gallaway, J. and Atanasov, P. (2004) Enzymatic biofuel cells for implantable and microscale devices, *Chem Rev*, **104**, 4867-4886.
- Bento, I., Martins, L.O., Gato Lopes, G., Armenia Carrondo, M. and Lindley, P.F. (2005) Dioxygen reduction by multi-copper oxidases; a structural perspective, *Dalton Trans*, 3507-3513.
- Bento, I., Silva, C.S., Chen, Z., Martins, L.O., Lindley, P.F. and Soares, C.M. (2010) Mechanisms underlying dioxygen reduction in laccases. Structural and modelling studies focusing on proton transfer, *BMC Struct Biol*, **10**, 28.
- Bertrand, G. (1896) Sur la presence simultanee de la laccase et de la tyrosinase dans le suc de quelques champignons, *Seances Acad Sci*, **123**, 463-465.
- Beswick, P.H., Hall, G.H., Hook, A.J., Little, K., McBrien, D.C. and Lott, K.A. (1976) Copper toxicity: evidence for the conversion of cupric to cuprous copper in vivo under anaerobic conditions, *Chem Biol Interact*, **14**, 347-356.
- Betz, S.F. (1993) Disulfide bonds and the stability of globular proteins, *Protein Sci*, **2**, 1551-1558.
- Bielli, P. and Calabrese, L. (2002) Structure to function relationships in ceruloplasmin: a 'moonlighting' protein, *Cell Mol Life Sci*, **59**, 1413-1427.
- Blackburn, N.J., Ralle, M., Hassett, R. and Kosman, D.J. (2000) Spectroscopic analysis of the trinuclear cluster in the Fet3 protein from yeast, a multinuclear copper oxidase, *Biochemistry*, **39**, 2316-2324.

- Blair, D.F., Campbell, G. W, Cho, W. K., English, A. M., Fry, H. A., Lum, V., Norton, K. A., Schoonover, J. R., Chan, S. I. (1985) Resonance Raman studies of blue copper proteins: effects of temperature and isotopic substitutions. Structural and thermodynamic implications, *J. Am. Chem. Soc.*, **107**, 5755-5766.
- Bligny, R. and Douce, R. (1983) Excretion of laccase by sycamore (*Acer pseudoplatanus* L.) cells. Purification and properties of the enzyme, *Biochem J*, **209**, 489-496.
- Boehr, D.D., Dyson, H.J. and Wright, P.E. (2006) An NMR perspective on enzyme dynamics, *Chem Rev*, **106**, 3055-3079.
- Bollag, D., Rozycki, M. and Edelstein, S. (1996) *Protein Methods*. John Wiley & Sons, New York.
- Bonaccorsi di Patti, M.C., Musci, G., Giartosio, A., D'Alessio, S. and Calabrese, L. (1990) The multidomain structure of ceruloplasmin from calorimetric and limited proteolysis studies, *J Biol Chem*, **265**, 21016-21022.
- Bonander, N., Leckner, J., Guo, H., Karlsson, B.G. and Sjolín, L. (2000) Crystal structure of the disulfide bond-deficient azurin mutant C3A/C26A: how important is the S-S bond for folding and stability?, *Eur J Biochem*, **267**, 4511-4519.
- Bourbonnais, R., Leech, D. and Paice, M.G. (1998) Electrochemical analysis of the interactions of laccase mediators with lignin model compounds, *Biochim Biophys Acta*, **1379**, 381-390.
- Bourbonnais, R., Paice, M.G., Freiermuth, B., Bodie, E. and Borneman, S. (1997) Reactivities of Various Mediators and Laccases with Kraft Pulp and Lignin Model Compounds, *Appl Environ Microbiol*, **63**, 4627-4632.
- Bradford, M.M. (1976) A rapid and sensitive method for the quantification of microgram quantities of protein utilizing the principle of protein-dye binding, *Anal. Biochem*, **72**, 248-254
- Bradford, M.M. (1976) A Rapid and Sensitive Method for the Quantitation of Microgram Quantities of Protein Utilizing the Principle of Protein-Dye Binding, *Anal. Biochem.*, **72**, 248-254.
- Brandts, J.F., Hu, C.Q., Lin, L.N. and Mos, M.T. (1989) A simple model for proteins with interacting domains. Applications to scanning calorimetry data, *Biochemistry*, **28**, 8588-8596.
- Brenner, A.J. and Harris, E.D. (1995) A quantitative test for copper using bicinchoninic acid, *Anal Biochem*, **226**, 80-84.

- Brockwell, D.J. (2007) Probing the mechanical stability of proteins using the atomic force microscope, *Biochem Soc Trans*, **35**, 1564-1568.
- Brooks, C.L., 3rd, Onuchic, J.N. and Wales, D.J. (2001) Statistical thermodynamics. Taking a walk on a landscape, *Science*, **293**, 612-613.
- Brown, K., Djinicovic-Carugo, K., Haltia, T., Cabrito, I., Saraste, M., Moura, J.J., Moura, I., Tegoni, M. and Cambillau, C. (2000) Revisiting the catalytic CuZ cluster of nitrous oxide (N<sub>2</sub>O) reductase. Evidence of a bridging inorganic sulfur, *J Biol Chem*, **275**, 41133-41136.
- Brown, N.L., Barrett, S.R., Camakaris, J., Lee, B.T. and Rouch, D.A. (1995) Molecular genetics and transport analysis of the copper-resistance determinant (pco) from *Escherichia coli* plasmid pRJ1004, *Mol Microbiol*, **17**, 1153-1166.
- Bukh, C., Lund, M. and Bjerrum, M.J. (2006) Kinetic studies on the reaction between *Trametes villosa* laccase and dioxygen, *J Inorg Biochem*, **100**, 1547-1557.
- Burke, R.M. and Cairney, J.W. (2002) Laccases and other polyphenol oxidases in ecto- and ericoid mycorrhizal fungi, *Mycorrhiza*, **12**, 105-116.
- Burstein, E.A., Vedenkina, N.S. and Ivkova, M.N. (1973) Fluorescence and the location of tryptophan residues in protein molecules, *Photochem Photobiol*, **18**, 263-279.
- Burton, S. (2001) Low-energy thermomechanical pulping process using an enzyme treatment of wood between refining zones.
- Cabrita, J.F., Abrantes, L.M. and Viana, A.S. (2005) N-Hydroxysuccinimide terminated self-assembled monolayers on gold for biomolecules immobilisation, *Electrochim Acta*, **50**, 2117-2214.
- Calhoun, D.B., Vanderkooi, J.M., Holtom, G.R. and Englander, S.W. (1986) Protein fluorescence quenching by small molecules: protein penetration versus solvent exposure, *Proteins*, **1**, 109-115.
- Carter, D.N., McKenzie, D.G., Johnson, A.P. and Idner, K. (1997) Performance parameters of oxygen delignification, *Tappi J*, **80**, 111-117.
- Cawthorn, T.R., Poulsen, B.E., Davidson, D.E., Andrews, D. and Hill, B.C. (2009) Probing the kinetics and thermodynamics of copper(II) binding to *Bacillus subtilis* Sco, a protein involved in the assembly of the Cu(A) center of cytochrome c oxidase, *Biochemistry*, **48**, 4448-4454.
- CCP4, C.C.P., Number 4 (1994) The CCP4 suite: programs for protein crystallography, *Acta Cryst.*, **D50**, 760-763.



- Chan, H.S. and Dill, K.A. (1998) Protein folding in the landscape perspective: chevron plots and non-Arrhenius kinetics, *Proteins*, **30**, 2-33.
- Changela, A., Chen, K., Xue, Y., Holschen, J., Outten, C.E., O'Halloran, T.V. and Mondragon, A. (2003) Molecular basis of metal-ion selectivity and zeptomolar sensitivity by CueR, *Science*, **301**, 1383-1387.
- Chen, Z., Durao, P., Silva, C.S., Pereira, M.M., Todorovic, S., Hildebrandt, P., Bento, I., Lindley, P.F. and Martins, L.O. (2010) The role of Glu498 in the dioxygen reactivity of CotA-laccase from *Bacillus subtilis*, *Dalton Trans*, **39**, 2875-2882.
- Chivukula, M. and Renganathan, V. (1995) Phenolic Azo Dye Oxidation by Laccase from *Pyricularia oryzae*, *Appl Environ Microbiol*, **61**, 4374-4377.
- Choi, D.W., Zea, C.J., Do, Y.S., Semrau, J.D., Antholine, W.E., Hargrove, M.S., Pohl, N.L., Boyd, E.S., Geesey, G.G., Hartsel, S.C., Shafe, P.H., McEllistrem, M.T., Kisting, C.J., Campbell, D., Rao, V., de la Mora, A.M. and Dispirito, A.A. (2006) Spectral, kinetic, and thermodynamic properties of Cu(I) and Cu(II) binding by methanobactin from *Methylosinus trichosporium* OB3b, *Biochemistry*, **45**, 1442-1453.
- Chothia, C. (1976) The nature of the accessible and buried surfaces in proteins, *J Mol Biol*, **105**, 1-12.
- Clutterbuck, A.J. (1972) Absence of laccase from yellow-spored mutants of *Aspergillus nidulans*, *J Gen Microbiol*, **70**, 423-435.
- Colman, P., Freeman, HC, Guss, JM, Murata, M, Norris, VA, Ramshaw, JAM, Venkatappa, MP. (1978) X-ray crystal structure analysis of plastocyanin at 2.7 Å resolution, *Nature*, **272**, 319 - 324
- Cox, E.H. and McLendon, G.L. (2000) Zinc-dependent protein folding, *Curr Opin Chem Biol*, **4**, 162-165.
- Cozen, A.E., Weirauch, M.T., Pollard, K.S., Bernick, D.L., Stuart, J.M. and Lowe, T.M. (2009) Transcriptional map of respiratory versatility in the hyperthermophilic crenarchaeon *Pyrobaculum aerophilum*, *J Bacteriol*, **191**, 782-794.
- Creighton, T. (1993) *Proteins - Structures and Molecular Properties*. W. H. Freeman and Company, New York.
- Crichton, R.R. and Pierre, J.L. (2001) Old iron, young copper: from Mars to Venus, *Biometals*, **14**, 99-112.

- Crowley, P.B., Otting, G., Schlarb-Ridley, B.G., Canters, G.W. and Ubbink, M. (2001) Hydrophobic interactions in a cyanobacterial plastocyanin-cytochrome f complex, *J Am Chem Soc*, **123**, 10444-10453.
- Dagget, V. and Fersht, A. (2000) Transition states in protein folding. In Pain, R. (ed), *Mechanism of Protein Folding*. Oxford University Press, Oxford, 175-211.
- Davis-Kaplan, S.R., Askwith, C.C., Bengtzen, A.C., Radisky, D. and Kaplan, J. (1998) Chloride is an allosteric effector of copper assembly for the yeast multicopper oxidase Fet3p: an unexpected role for intracellular chloride channels, *Proc Natl Acad Sci U S A*, **95**, 13641-13645.
- De Felice, F.G., Vieira, M.N., Meirelles, M.N., Morozova-Roche, L.A., Dobson, C.M. and Ferreira, S.T. (2004) Formation of amyloid aggregates from human lysozyme and its disease-associated variants using hydrostatic pressure, *FASEB J*, **18**, 1099-1101.
- De Gregorio, E., Spellman, P.T., Rubin, G.M. and Lemaitre, B. (2001) Genome-wide analysis of the *Drosophila* immune response by using oligonucleotide microarrays, *Proc Natl Acad Sci U S A*, **98**, 12590-12595.
- de Vries, S., Strampaad, M.J., Lu, S., Moenne-Loccoz, P. and Schroder, I. (2003) Purification and characterization of the MQH2:NO oxidoreductase from the hyperthermophilic archaeon *Pyrobaculum aerophilum*, *J Biol Chem*, **278**, 35861-35868.
- Deckert, G., Warren, P.V., Gaasterland, T., Young, W.G., Lenox, A.L., Graham, D.E., Overbeek, R., Snead, M.A., Keller, M., Aujay, M., Huber, R., Feldman, R.A., Short, J.M., Olsen, G.J. and Swanson, R.V. (1998) The complete genome of the hyperthermophilic bacterium *Aquifex aeolicus*, *Nature*, **392**, 353-358.
- Degtyarenko, K.N., North, A.C., Perkins, D.N. and Findlay, J.B. (1998) PROMISE: a database of information on prosthetic centres and metal ions in protein active sites, *Nucleic Acids Res*, **26**, 376-381.
- DeLano, W.L. (2003) *The PyMOL Molecular Graphics System*. DeLano Scientific, Palo Alto, CA, USA.
- Dell'acqua, S., Pauleta, S.R., Monzani, E., Pereira, A.S., Casella, L., Moura, J.J. and Moura, I. (2008) Electron transfer complex between nitrous oxide reductase and cytochrome c552 from *Pseudomonas nautica*: kinetic, nuclear magnetic resonance, and docking studies, *Biochemistry*, **47**, 10852-10862.
- Dennison, C. (2005) Ligand and loop variations at type 1 copper sites: influence on structure and reactivity, *Dalton Trans*, 3436-3442.

- Dennison, C., Harrison, M.D. and Lawler, A.T. (2003) Alkaline transition of phytocyanins: a comparison of stellacyanin and umecyanin, *Biochem J*, **371**, 377-383.
- Dick, G.J., Torpey, J.W., Beveridge, T.J. and Tebo, B.M. (2008) Direct identification of a bacterial manganese(II) oxidase, the multicopper oxidase MnxG, from spores of several different marine *Bacillus* species, *Appl Environ Microbiol*, **74**, 1527-1534.
- Dill, K.A. and Chan, H.S. (1997) From Levinthal to pathways to funnels, *Nat Struct Biol*, **4**, 10-19.
- Dittmer, N.T., Suderman, R.J., Jiang, H., Zhu, Y.C., Gorman, M.J., Kramer, K.J. and Kanost, M.R. (2004) Characterization of cDNAs encoding putative laccase-like multicopper oxidases and developmental expression in the tobacco hornworm, *Manduca sexta*, and the malaria mosquito, *Anopheles gambiae*, *Insect Biochem Mol Biol*, **34**, 29-41.
- Djikaev, Y.S. and Ruckenstein, E. (2007) Model for the nucleation mechanism of protein folding, *J Phys Chem B*, **111**, 886-897.
- Djoko, K.Y., Chong, L.X., Wedd, A.G. and Xiao, Z. (2010) Reaction mechanisms of the multicopper oxidase CueO from *Escherichia coli* support its functional role as a cuprous oxidase, *J Am Chem Soc*, **132**, 2005-2015.
- Driks, A. (1999) *Bacillus subtilis* spore coat, *Microbiol Mol Biol Rev*, **63**, 1-20.
- Ducros, V., Brzozowski, A.M., Wilson, K.S., Brown, S.H., Ostergaard, P., Schneider, P., Yaver, D.S., Pedersen, A.H. and Davies, G.J. (1998) Crystal structure of the type-2 Cu depleted laccase from *Coprinus cinereus* at 2.2 Å resolution, *Nat Struct Biol*, **5**, 310-316.
- Durao, P., Bento, I., Fernandes, A.T., Melo, E.P., Lindley, P.F. and Martins, L.O. (2006) Perturbations of the T1 copper site in the CotA laccase from *Bacillus subtilis*: structural, biochemical, enzymatic and stability studies, *J Biol Inorg Chem*, **11**, 514-526.
- Durao, P., Chen, Z., Fernandes, A.T., Hildebrandt, P., Murgida, D.H., Todorovic, S., Pereira, M.M., Melo, E.P. and Martins, L.O. (2008) Copper incorporation into recombinant CotA laccase from *Bacillus subtilis*: characterization of fully copper loaded enzymes, *J Biol Inorg Chem*, **13**, 183-193.
- Durao, P., Chen, Z., Silva, C.S., Soares, C.M., Pereira, M.M., Todorovic, S., Hildebrandt, P., Bento, I., Lindley, P.F. and Martins, L.O. (2008) Proximal mutations at the type 1 copper site of CotA laccase: spectroscopic, redox, kinetic and structural characterization of I494A and L386A mutants, *Biochem. J.*, **412**, 339-346.

Durao, P., Chen, Z., Silva, C.S., Soares, C.M., Pereira, M.M., Todorovic, S., Hildebrandt, P., Bento, I., Lindley, P.F. and Martins, L.O. (2008) Proximal mutations at the type 1 copper site of CotA laccase: spectroscopic, redox, kinetic and structural characterization of I494A and L386A mutants, *Biochem J*, **412**, 339-346.

Durup, J. (1998) On “Levinthal paradox” and the theory of protein folding, *Journal of Molecular Structure* **424**, 157-169.

Eder, W. and Huber, R. (2002) New isolates and physiological properties of the Aquificales and description of *Thermocrinis albus* sp. nov, *Extremophiles*, **6**, 309-318.

Eftink, M.R. (1994) The use of fluorescence methods to monitor unfolding transitions in proteins, *Biophys J*, **66**, 482-501.

Eftink, M.R. and Ghiron, C.A. (1976) Exposure of tryptophanyl residues in proteins. Quantitative determination by fluorescence quenching studies, *Biochemistry*, **15**, 672-680.

Eftink, M.R. and Ghiron, C.A. (1977) Exposure of tryptophanyl residues and protein dynamics, *Biochemistry*, **16**, 5546-5551.

Egorova, K. and Antranikian, G. (2005) Industrial relevance of thermophilic Archaea, *Curr Opin Microbiol*, **8**, 649-655.

Emsley, P. and Cowtan, K. (2004) Coot: model-building tools for molecular graphics, *Acta Crystallogr D Biol Crystallogr*, **60**, 2126-2132.

Endo, K., Hayashi, Y., Hibi, T., Hosono, K., Beppu, T. and Ueda, K. (2003) Enzymological characterization of EpoA, a laccase-like phenol oxidase produced by *Streptomyces griseus*, *J Biochem*, **133**, 671-677.

Enguita, F.J., Marcal, D., Martins, L.O., Grenha, R., Henriques, A.O., Lindley, P.F. and Carrondo, M.A. (2004) Substrate and dioxygen binding to the endospore coat laccase from *Bacillus subtilis*, *J Biol Chem*, **279**, 23472-23476.

Enguita, F.J., Martins, L.O., Henriques, A.O. and Carrondo, M.A. (2003) Crystal structure of a bacterial endospore coat component. A laccase with enhanced thermostability properties, *J Biol Chem*, **278**, 19416-19425.

EuropaBio (2003) White Biotechnology: Gateway to a More Sustainable Future. Brussels.

Faure, D., Bouillant, M.L. and Bally, R. (1994) Isolation of *Azospirillum lipoferum* 4T Tn5 Mutants Affected in Melanization and Laccase Activity, *Appl Environ Microbiol*, **60**, 3413-3415.

- Feinberg, L.F. and Holden, J.F. (2006) Characterization of dissimilatory Fe(III) versus NO<sub>3</sub><sup>-</sup> reduction in the hyperthermophilic archaeon *Pyrobaculum aerophilum*, *J Bacteriol*, **188**, 525-531.
- Feinberg, L.F., Srikanth, R., Vachet, R.W. and Holden, J.F. (2008) Constraints on anaerobic respiration in the hyperthermophilic Archaea *Pyrobaculum islandicum* and *Pyrobaculum aerophilum*, *Appl Environ Microbiol*, **74**, 396-402.
- Fernandes, A.T., Damas, J.M., Todorovic, S., Huber, R., Baratto, M.C., Pogni, R., Soares, C.M. and Martins, L.O. (2010) The multicopper oxidase from the archaeon *Pyrobaculum aerophilum* shows nitrous oxide reductase activity, *FEBS J*, **277**, 3176-3189.
- Fernandes, A.T., Martins, L.O. and Melo, E.P. (2009) The hyperthermophilic nature of the metallo-oxidase from *Aquifex aeolicus*, *Biochim Biophys Acta*, **1794**, 75-83.
- Fernandes, A.T., Soares, C.M., Pereira, M.M., Huber, R., Grass, G. and Martins, L.O. (2007) A robust metallo-oxidase from the hyperthermophilic bacterium *Aquifex aeolicus*, *FEBS J*, **274**, 2683-2694.
- Ferry, Y. and Leech, D. (2005) Amperometric detection of catecholamine neurotransmitters using electrocatalytic substrate recycling at a laccase electrode., *Electroanalysis*, **17**, 2113-2119.
- Fersht, A. (1998) *Structure and mechanism in protein science: a guide to enzyme catalysis and protein folding*. W. H. Freeman and Company, New York.
- Fersht, A.R. (1997) Nucleation mechanisms in protein folding, *Curr Opin Struct Biol*, **7**, 3-9.
- Fitter, J. and Heberle, J. (2000) Structural equilibrium fluctuations in mesophilic and thermophilic alpha-amylase, *Biophys J*, **79**, 1629-1636.
- Fitz-Gibbon, S.T., Ladner, H., Kim, U.J., Stetter, K.O., Simon, M.I. and Miller, J.H. (2002) Genome sequence of the hyperthermophilic crenarchaeon *Pyrobaculum aerophilum*, *Proc Natl Acad Sci U S A*, **99**, 984-989.
- Flander, L., Rouau, X., Morel, M.H., Autio, K., Seppanen-Laakso, T., Kruus, K. and Buchert, J. (2008) Effects of laccase and xylanase on the chemical and rheological properties of oat and wheat doughs, *J Agric Food Chem*, **56**, 5732-5742.
- Francis, C.A. and Tebo, B.M. (2002) Enzymatic manganese(II) oxidation by metabolically dormant spores of diverse *Bacillus* species, *Appl Environ Microbiol*, **68**, 874-880.

- Franke, S., Grass, G., Rensing, C. and Nies, D.H. (2003) Molecular analysis of the copper-transporting efflux system CusCFBA of *Escherichia coli*, *J Bacteriol*, **185**, 3804-3812.
- Freire, R.S., Durán, N. and Kubota, L.T. (2001) Effects of fungal laccase immobilization procedures for the development of a biosensor for phenol compounds, *Talanta*, **54**, 681-686.
- Frieden, E. and Hsieh, H.S. (1976) The biological role of ceruloplasmin and its oxidase activity, *Adv Exp Med Biol*, **74**, 505-529.
- Fujita, K., Chan, J.M., Bollinger, J.A., Alvarez, M.L. and Dooley, D.M. (2007) Anaerobic purification, characterization and preliminary mechanistic study of recombinant nitrous oxide reductase from *Achromobacter cycloclastes*, *J Inorg Biochem*, **101**, 1836-1844.
- Galli, I., Musci, G. and Bonaccorsi di Patti, M.C. (2004) Sequential reconstitution of copper sites in the multicopper oxidase CueO, *J Biol Inorg Chem*, **9**, 90-95.
- Gianfreda, L.X., F., B, J.M. (1999) Laccases: A Useful Group of Oxidoreductive Enzymes, *Bioremediation Journal*, **3**, 1-25.
- Giardina, P., Faraco, V., Pezzella, C., Piscitelli, A., Vanhulle, S. and Sannia, G. (2010) Laccases: a never-ending story, *Cell Mol Life Sci*, **67**, 369-385.
- Givaudan, A., Effosse, A., Faure, D., Potier, P., Bouillant, M.L. and Bally, R. (1993) olyphenol oxidase in *Azospirillum lipoferum* isolated from rice rhizosphere : evidence for laccase activity in nonmotile strains of *Azospirillum lipoferum*., *FEMS Microbiol Lett*, **108**, 205-210.
- Glenn, J.K. and Gold, M.H. (1983) Decolorization of Several Polymeric Dyes by the Lignin-Degrading Basidiomycete *Phanerochaete chrysosporium*, *Appl Environ Microbiol*, **45**, 1741-1747.
- Grass, G. and Rensing, C. (2001) CueO is a multi-copper oxidase that confers copper tolerance in *Escherichia coli*, *Biochem Biophys Res Commun*, **286**, 902-908.
- Grass, G. and Rensing, C. (2001) Genes involved in copper homeostasis in *Escherichia coli*, *J Bacteriol*, **183**, 2145-2147.
- Grass, G., Thakali, K., Klebba, P.E., Thieme, D., Muller, A., Wildner, G.F. and Rensing, C. (2004) Linkage between catecholate siderophores and the multicopper oxidase CueO in *Escherichia coli*, *J Bacteriol*, **186**, 5826-5833.

- Green, M.T. (2006) Application of Badger's rule to heme and non-heme iron-oxygen bonds: an examination of ferryl protonation states, *J Am Chem Soc*, **128**, 1902-1906.
- Greene, R.F., Jr. and Pace, C.N. (1974) Urea and guanidine hydrochloride denaturation of ribonuclease, lysozyme, alpha-chymotrypsin, and beta-lactoglobulin, *J Biol Chem*, **249**, 5388-5393.
- Gregory, R.P. and Bendall, D.S. (1966) The purification and some properties of the polyphenol oxidase from tea (*Camellia sinensis* L.), *Biochem J*, **101**, 569-581.
- Griko Yu, V., Venyaminov, S. and Privalov, P.L. (1989) Heat and cold denaturation of phosphoglycerate kinase (interaction of domains), *FEBS Lett*, **244**, 276-278.
- Guzzi, R., Sportelli, L., La Rosa, C., Milardi, D., Grasso, D., Verbeet, M.P. and Canters, G.W. (1999) A spectroscopic and calorimetric investigation on the thermal stability of the Cys3Ala/Cys26Ala azurin mutant, *Biophys J*, **77**, 1052-1063.
- Haghighi, B., Gorton, L., Ruzgas, T. and Jönsson, L.J. (2003) Characterization of graphite electrodes modified with laccase from *Trametes versicolor* and their use for bioelectrochemical monitoring of phenolic compounds in flow injection analysis, *Anal Chim Acta*, **487**, 3-14.
- Hakulinen, N., Kiiskinen, L.L., Kruus, K., Saloheimo, M., Paananen, A., Koivula, A. and Rouvinen, J. (2002) Crystal structure of a laccase from *Melanocarpus albomyces* with an intact trinuclear copper site, *Nat Struct Biol*, **9**, 601-605.
- Hall, S.J., Hitchcock, A., Butler, C.S. and Kelly, D.J. (2008) A Multicopper oxidase (Cj1516) and a CopA homologue (Cj1161) are major components of the copper homeostasis system of *Campylobacter jejuni*, *J Bacteriol*, **190**, 8075-8085.
- Haltia, T., Brown, K., Tegoni, M., Cambillau, C., Saraste, M., Mattila, K. and Djinovic-Carugo, K. (2003) Crystal structure of nitrous oxide reductase from *Paracoccus denitrificans* at 1.6 Å resolution, *Biochem J*, **369**, 77-88.
- Harris, E.D., Qian, Y., Tiffany-Castiglioni, E., Lacy, A.R. and Reddy, M.C. (1998) Functional analysis of copper homeostasis in cell culture models: a new perspective on internal copper transport, *Am J Clin Nutr*, **67**, 988S-995S.
- Hart, P.J., Nersissian, A.M., Herrmann, R.G., Nalbandyan, R.M., Valentine, J.S. and Eisenberg, D. (1996) A missing link in cupredoxins: crystal structure of cucumber stellacyanin at 1.6 Å resolution, *Protein Sci*, **5**, 2175-2183.

- Hellman, N.E. and Gitlin, J.D. (2002) Ceruloplasmin metabolism and function, *Annu Rev Nutr*, **22**, 439-458.
- Hellman, N.E., Kono, S., Mancini, G.M., Hoogeboom, A.J., De Jong, G.J. and Gitlin, J.D. (2002) Mechanisms of copper incorporation into human ceruloplasmin, *J Biol Chem*, **277**, 46632-46638.
- Henley, J. and Sadana, A. (1985) Characterization of enzyme deactivation using a series type mechanism, *Enzyme Microb Technol*, **7**, 50-60.
- Hilden, K., Hakala, T.K. and Lundell, T. (2009) Thermotolerant and thermostable laccases, *Biotechnol Lett*, **31**, 1117-1128.
- Hoegger, P.J., Kilaru, S., James, T.Y., Thacker, J.R. and Kues, U. (2006) Phylogenetic comparison and classification of laccase and related multicopper oxidase protein sequences, *FEBS J*, **273**, 2308-2326.
- Huffman, D.L., Huyett, J., Outten, F.W., Doan, P.E., Finney, L.A., Hoffman, B.M. and O'Halloran, T.V. (2002) Spectroscopy of Cu(II)-PcoC and the multicopper oxidase function of PcoA, two essential components of *Escherichia coli* pco copper resistance operon, *Biochemistry*, **41**, 10046-10055.
- Hunter, P. (2006) Into to the fold, *EMBO Rep*, **7**, 249-252.
- Huston, W.M., Jennings, M.P. and McEwan, A.G. (2002) The multicopper oxidase of *Pseudomonas aeruginosa* is a ferroxidase with a central role in iron acquisition, *Mol Microbiol*, **45**, 1741-1750.
- Huston, W.M., Naylor, J., Cianciotto, N.P., Jennings, M.P. and McEwan, A.G. (2008) Functional analysis of the multi-copper oxidase from *Legionella pneumophila*, *Microbes Infect*, **10**, 497-503.
- Huttermann, A., Mai, C. and Kharazipour, A. (2001) Modification of lignin for the production of new compounded materials, *Appl Microbiol Biotechnol*, **55**, 387-394.
- Iakovlev, A. and Stenlid, J. (2000) Spatiotemporal Patterns of Laccase Activity in Interacting Mycelia of Wood-Decaying Basidiomycete Fungi, *Microb Ecol*, **39**, 236-245.
- Ikai, A. and Tanford, C. (1971) Kinetic evidence for incorrectly folded intermediate states in the refolding of denatured proteins, *Nature*, **230**, 100-102.
- Impagliazzo, A. and Ubbink, M. (2004) Mapping of the binding site on pseudoazurin in the transient 152 kDa complex with nitrite reductase, *J Am Chem Soc*, **126**, 5658-5659.



Itzhaki, L.S., Otzen, D.E. and Fersht, A.R. (1995) The structure of the transition state for folding of chymotrypsin inhibitor 2 analysed by protein engineering methods: evidence for a nucleation-condensation mechanism for protein folding, *J Mol Biol*, **254**, 260-288.

Jaenicke, R. (1987) Folding and association of proteins, *Prog Biophys Mol Biol*, **49**, 117-237.

Jaenicke, R., Schurig, H., Beaucamp, N. and Ostendorp, R. (1996) Structure and stability of hyperstable proteins: glycolytic enzymes from hyperthermophilic bacterium *Thermotoga maritima*, *Adv Protein Chem*, **48**, 181-269.

James, J. and Lee, B. (1997) Glucoamylases: Microbial sources, Industrial Applications and Molecular Biology - A Review, *J Food Biochem*, **21**, 1-52.

Jeong, S.Y., Rathore, K.I., Schulz, K., Ponka, P., Arosio, P. and David, S. (2009) Dysregulation of iron homeostasis in the CNS contributes to disease progression in a mouse model of amyotrophic lateral sclerosis, *J Neurosci*, **29**, 610-619.

Jung, W.H. and Kronstad, J.W. (2008) Iron and fungal pathogenesis: a case study with *Cryptococcus neoformans*, *Cell Microbiol*, **10**, 277-284.

Jung, W.H., Sham, A., Lian, T., Singh, A., Kosman, D.J. and Kronstad, J.W. (2008) Iron source preference and regulation of iron uptake in *Cryptococcus neoformans*, *PLoS Pathog*, **4**, e45.

Jung, W.H., Sham, A., White, R. and Kronstad, J.W. (2006) Iron regulation of the major virulence factors in the AIDS-associated pathogen *Cryptococcus neoformans*, *PLoS Biol*, **4**, e410.

Kabsch, W. and Sander, C. (1983) Dictionary of protein secondary structure: pattern recognition of hydrogen-bonded and geometrical features, *Biopolymers*, **22**, 2577-2637.

Karlin, K.D., Zhu, Z.Y. and Karlin, S. (1997) The extended environment of mononuclear metal centres in protein structures, *Proc. Natl. Acad. Sci.*, **94**, 14225-14230.

Kataoka, K., Kitagawa, R., Inoue, M., Naruse, D., Sakurai, T. and Huang, H.W. (2005) Point mutations at the type I Cu ligands, Cys457 and Met467, and at the putative proton donor, Asp105, in *Myrothecium verrucaria* bilirubin oxidase and reactions with dioxygen, *Biochemistry*, **44**, 7004-7012.

Kataoka, K., Komori, H., Ueki, Y., Konno, Y., Kamitaka, Y., Kurose, S., Tsujimura, S., Higuchi, Y., Kano, K., Seo, D. and Sakurai, T. (2007) Structure and function of the engineered multicopper oxidase CueO from *Escherichia*

coli--deletion of the methionine-rich helical region covering the substrate-binding site, *J Mol Biol*, **373**, 141-152.

Kelly, S.M. and Price, N.C. (1997) The application of circular dichroism to studies of protein folding and unfolding, *Biochim Biophys Acta*, **1338**, 161-185.

Khan, R.H. and Khan, F. (2002) Models for protein folding and nature's choice of protein as catalyst, *Biochemistry (Mosc)*, **67**, 520-524.

Kim, S., Mollet, J.C., Dong, J., Zhang, K., Park, S.Y. and Lord, E.M. (2003) Chemocyanin, a small basic protein from the lily stigma, induces pollen tube chemotropism, *Proc Natl Acad Sci U S A*, **100**, 16125-16130.

Koch, M., Velarde, M., Harrison, M.D., Echt, S., Fischer, M., Messerschmidt, A. and Dennison, C. (2005) Crystal structures of oxidized and reduced stellacyanin from horseradish roots, *J Am Chem Soc*, **127**, 158-166.

Koroleva, O.V., Stepanova, E.V., Binukov, V.I., Timofeev, V.P. and Pfeil, W. (2001) Temperature-induced changes in copper centers and protein conformation of two fungal laccases from *Coriolus hirsutus* and *Coriolus zonatus*, *Biochim Biophys Acta*, **1547**, 397-407.

Kosman, D.J. (2009) Multicopper oxidases: a workshop on copper coordination chemistry, electron transfer, and metallophysiology, *J Biol Inorg Chem*.

Kristjansson, J.K. and Hollocher, T.C. (1980) First practical assay for soluble nitrous oxide reductase of denitrifying bacteria and a partial kinetic characterization, *J Biol Chem*, **255**, 704-707.

Kues, U. (2000) Life history and developmental processes in the basidiomycete *Coprinus cinereus*, *Microbiol Mol Biol Rev*, **64**, 316-353.

Kumar, S., Tsai, C.J. and Nussinov, R. (2000) Factors enhancing protein thermostability, *Protein Eng*, **13**, 179-191.

Kwok, E.Y., Severance, S. and Kosman, D.J. (2006) Evidence for iron channeling in the Fet3p-Ftr1p high-affinity iron uptake complex in the yeast plasma membrane, *Biochemistry*, **45**, 6317-6327.

Kwok, E.Y., Stoj, C.S., Severance, S. and Kosman, D.J. (2006) An engineered bifunctional high affinity iron uptake protein in the yeast plasma membrane, *J Inorg Biochem*, **100**, 1053-1060.

Lakowicz, J.R. (1999) *Principles of fluorescence spectroscopy*. Kluwer/Plenum, New York.

- Larrondo, L.F., Salas, L., Melo, F., Vicuna, R. and Cullen, D. (2003) A novel extracellular multicopper oxidase from *Phanerochaete chrysosporium* with ferroxidase activity, *Appl Environ Microbiol*, **69**, 6257-6263.
- Laskowski, R.A., MacArthur, M.W., Moss, D.S. and Thornton, J.M. (1993) Procheck - a Program to Check the Stereochemical Quality of Protein Structures, *Journal of Applied Crystallography*, **26**, 283-291.
- Laskowski, R.A., MacArthur, M.W., Moss, D.S. and Thornton, J.M. (1993) PROCHECK: a program to check the stereochemical quality of protein structures, *J. Appl. Crystallog.*, **26**, 283-291.
- Lawton, T.J., Sayavedra-Soto, L.A., Arp, D.J. and Rosenzweig, A.C. (2009) Crystal structure of a two-domain multicopper oxidase: implications for the evolution of multicopper blue proteins, *J Biol Chem*, **284**, 10174-10180.
- Leckner, J., Bonander, N., Wittung-Stafshede, P., Malmstrom, B.G. and Karlsson, B.G. (1997) The effect of the metal ion on the folding energetics of azurin: a comparison of the native, zinc and apoprotein, *Biochim Biophys Acta*, **1342**, 19-27.
- Lee, C.F., Allen, M.D., Bycroft, M. and Wong, K.B. (2005) Electrostatic interactions contribute to reduced heat capacity change of unfolding in a thermophilic ribosomal protein l30e, *J Mol Biol*, **348**, 419-431.
- Lee, S.M., Grass, G., Rensing, C., Barrett, S.R., Yates, C.J., Stoyanov, J.V. and Brown, N.L. (2002) The Pco proteins are involved in periplasmic copper handling in *Escherichia coli*, *Biochem Biophys Res Commun*, **295**, 616-620.
- Leite, O.D., Lupetti, K.O., Fatibello-Filho, O., Vieira, I.C. and Barbosa Ade, M. (2003) Synergic effect studies of the bi-enzymatic system laccase-peroxidase in a voltammetric biosensor for catecholamines, *Talanta*, **59**, 889-896.
- LeMaster, D., Tang J, Paredes, D. and Hernández, G. (2005) Enhanced thermal stability achieved without increased conformational rigidity at physiological temperatures: spatial propagation of differential flexibility in rubredoxin hybrids, *Proteins*, **61**, 608-616.
- Leopold, P.E., Montal, M. and Onuchic, J.N. (1992) Protein folding funnels: a kinetic approach to the sequence-structure relationship, *Proc Natl Acad Sci U S A*, **89**, 8721-8725.
- Leslie, A. (1992) Joint CCP4, ESF-EAMCB, *Newsletter on Protein Crystallography*, **26**.
- Leslie, A.G. (2006) The integration of macromolecular diffraction data, *Acta Crystallogr D*, **62**, 48-57.

- Levinthal, C. (1968) Are there pathways for protein folding?, *J. Chim. Physique* **65**, 44–45.
- Lindley, P.F. (2001) Multi-Copper Oxidases. In Bertini, I., Sigel, A. and Sigel, H. (eds), *Handbook on Metalloproteins* Marcel Dekker, Inc., New York, 763–811.
- Liu, X., Gao, C., Zhang, A., Jin, P., Wang, L. and Feng, L. (2008) The nos gene cluster from gram-positive bacterium *Geobacillus thermodenitrificans* NG80-2 and functional characterization of the recombinant NosZ, *FEMS Microbiol Lett*, **289**, 46–52.
- Lumry, R. and Eyring, H. (1954) Conformation changes of proteins, *J Phys Chem*, **58**, 110–120.
- Lundell, T.K., Makela, M.R. and Hilden, K. (2010) Lignin-modifying enzymes in filamentous basidiomycetes--ecological, functional and phylogenetic review, *J Basic Microbiol*, **50**, 5–20.
- Luque, I., Leavitt, S.A. and Freire, E. (2002) The linkage between protein folding and functional cooperativity: two sides of the same coin?, *Annu Rev Biophys Biomol Struct*, **31**, 235–256.
- Ma, J.K., Bishop, G.R. and Davidson, V.L. (2005) The ligand geometry of copper determines the stability of amicyanin, *Arch Biochem Biophys*, **444**, 27–33.
- Machonkin, T.E., Quintanar, L., Palmer, A.E., Hassett, R., Severance, S., Kosman, D.J. and Solomon, E.I. (2001) Spectroscopy and reactivity of the type 1 copper site in Fet3p from *Saccharomyces cerevisiae*: correlation of structure with reactivity in the multicopper oxidases, *J Am Chem Soc*, **123**, 5507–5517.
- Macomber, L., Rensing, C. and Imlay, J.A. (2007) Intracellular copper does not catalyze the formation of oxidative DNA damage in *Escherichia coli*, *J Bacteriol*, **189**, 1616–1626.
- Madhavi, V. and Lele, S.S. (2009) Laccase: Properties and Applications, *Bioresources*, **4**, 1694–1717.
- Madsen, E. and Gitlin, J.D. (2007) Copper and iron disorders of the brain, *Annu Rev Neurosci*, **30**, 317–337.
- Maglio, O., Nistri, F., Pavone, V., Lombardi, A. and DeGrado, W.F. (2003) Preorganization of molecular binding sites in designed diiron proteins, *Proc Natl Acad Sci U S A*, **100**, 3772–3777.
- Marcus, R.A. and Sutin, N. (1985) Electron transfers in chemistry and biology, *BBA*, **811**, 265–322.

- Martele, Y., Callewaerta, K., Naessens, K., van Daeleb, P., Baetsb, R. and Schacht, E. (2003) Controlled patterning of biomolecules on solid surfaces, *Mater Sci Eng C BiomimMater Sens Syst*, **23**, 341-345.
- Martins, L.O., Soares, C.M., Pereira, M.M., Teixeira, M., Costa, T., Jones, G.H. and Henriques, A.O. (2002) Molecular and biochemical characterization of a highly stable bacterial laccase that occurs as a structural component of the *Bacillus subtilis* endospore coat, *J Biol Chem*, **277**, 18849-18859.
- Masino, L., Martin, S.R. and Bayley, P.M. (2000) Ligand binding and thermodynamic stability of a multidomain protein, calmodulin, *Protein Sci*, **9**, 1519-1529.
- Matsumura, M., Signor, G. and Matthews, B.W. (1989) Substantial increase of protein stability by multiple disulphide bonds, *Nature*, **342**, 291-293.
- Mayer, A.M. and Staples, R.C. (2002) Laccase: new functions for an old enzyme, *Phytochemistry*, **60**, 551-565.
- Mei, G., Di Venere, A., Campeggi, F.M., Gilardi, G., Rosato, N., De Matteis, F. and Finazzi-Agro, A. (1999) The effect of pressure and guanidine hydrochloride on azurins mutated in the hydrophobic core, *Eur J Biochem*, **265**, 619-626.
- Mellano, M.A. and Cooksey, D.A. (1988) Nucleotide sequence and organization of copper resistance genes from *Pseudomonas syringae* pv. tomato, *J Bacteriol*, **170**, 2879-2883.
- Melo, E.P., Fernandes, A.T., Durao, P. and Martins, L.O. (2007) Insight into stability of CotA laccase from the spore coat of *Bacillus subtilis*, *Biochem Soc Trans*, **35**, 1579-1582.
- Messerschmidt, A. (ed) (1997) *Multi-Copper Oxidases*. World Science Press, Singapore.
- Messerschmidt, A. (1997) *Multi-copper Oxidases*. World Science Press, Singapore.
- Messerschmidt, A., Luecke, H., Huber, R. (1992) X-ray Structures and Mechanistic Implications of Three Functional Dervatives of Ascorbate Oxidase from Zucchini, *J. Mol. Biol.*, **230**, 997-1014.
- Milardi, D., Grasso, D.M., Verbeet, M.P., Canters, G.W. and La Rosa, C. (2003) Thermodynamic analysis of the contributions of the copper ion and the disulfide bridge to azurin stability: synergism among multiple depletions, *Arch Biochem Biophys*, **414**, 121-127.

- Minussi, R.C., Pastore, G.M. and Duran, N. (2002) Potential applications of laccase in the food industry, *Trends in Food Science and Technology*, **3**, 205-216.
- Miura, T., Satoh, T. and Takeuchi, H. (1998) Role of metal-ligand coordination in the folding pathway of zinc finger peptides, *Biochim Biophys Acta*, **1384**, 171-179.
- Miyajima, H. (2002) Genetic disorders affecting proteins of iron and copper metabolism: clinical implications, *Intern Med*, **41**, 762-769.
- Miyazaki, K. (2005) A hyperthermophilic laccase from *Thermus thermophilus* HB27, *Extremophiles*, **9**, 415-425.
- Moczygemba, C., Guidry, J., Jones, K.L., Gomes, C.M., Teixeira, M. and Wittung-Stafshede, P. (2001) High stability of a ferredoxin from the hyperthermophilic archaeon *A. ambivalens*: involvement of electrostatic interactions and cofactors, *Protein Sci*, **10**, 1539-1548.
- Mohanraja, K., Dhanasekaran, M., Kundu, B. and Durani, S. (2003) Mechanism-based protein design: attempted "nucleation-condensation" approach to a possible minimal helix-bundle protein, *Biopolymers*, **70**, 355-363.
- Monsellier, E. and Bedouelle, H. (2005) Quantitative measurement of protein stability from unfolding equilibria monitored with the fluorescence maximum wavelength, *Protein Eng Des Sel*, **18**, 445-456.
- Moser, C.C. and Dutton, P.L. (1996). In Bendall, D.S. (ed), *Protein electron transfer*. Bios Scientific Publishers Ltd, 1-21.
- Murphy, M.E., Lindley, P.F. and Adman, E.T. (1997) Structural comparison of cupredoxin domains: domain recycling to construct proteins with novel functions, *Protein Sci*, **6**, 761-770.
- Murshudov, G.N., Vagin, A.A., Lebedev, A., Wilson, K.S. and Dodson, E.J. (1999) Efficient anisotropic refinement of macromolecular structures using FFT, *Acta Crystallogr D*, **55** ( Pt 1), 247-255.
- Myers, J.K., Pace, C.N. and Scholtz, J.M. (1995) Denaturant m values and heat capacity changes: relation to changes in accessible surface areas of protein unfolding, *Protein Sci*, **4**, 2138-2148.
- Nakamura, K. and Go, N. (2005) Function and molecular evolution of multicopper blue proteins, *Cell Mol Life Sci*, **62**, 2050-2066.
- Nersissian, A.M., Immoos, C., Hill, M.G., Hart, P.J., Williams, G., Herrmann, R.G. and Valentine, J.S. (1998) Uclacyanins, stellacyanins, and plantacyanins

are distinct subfamilies of phytocyanins: plant-specific mononuclear blue copper proteins, *Protein Sci*, **7**, 1915-1929.

Nersissian, A.M. and Shipp, E.L. (2002) Blue copper-binding domains, *Adv Protein Chem*, **60**, 271-340.

Nosanchuk, J.D. and Casadevall, A. (2003) The contribution of melanin to microbial pathogenesis, *Cell Microbiol*, **5**, 203-223.

Novotny, C., Erbanova, P., Cajthaml, T., Rothschild, N., Dosoretz, C. and Sasek, V. (2000) *Irpex lacteus*, a white rot fungus applicable to water and soil bioremediation, *Appl Microbiol Biotechnol*, **54**, 850-853.

Otzen, D.E. and Oliveberg, M. (2004) Correspondence between anomalous m- and DeltaCp-values in protein folding, *Protein Sci*, **13**, 3253-3263.

Outten, F.W., Huffman, D.L., Hale, J.A. and O'Halloran, T.V. (2001) The independent cue and cus systems confer copper tolerance during aerobic and anaerobic growth in *Escherichia coli*, *J Biol Chem*, **276**, 30670-30677.

Pace, C.N. (1986) Determination and analysis of urea and guanidine hydrochloride denaturation curves, *Methods Enzymol*, **131**, 266-280.

Pace, C.N., Hebert, E.J., Shaw, K.L., Schell, D., Both, V., Krajcikova, D., Sevcik, J., Wilson, K.S., Dauter, Z., Hartley, R.W. and Grimsley, G.R. (1998) Conformational stability and thermodynamics of folding of ribonucleases Sa, Sa2 and Sa3, *J Mol Biol*, **279**, 271-286.

Pace, C.N. and Laurents, D.V. (1989) A new method for determining the heat capacity change for protein folding, *Biochemistry*, **28**, 2520-2525.

Pace, N. and Scholtz, J. (1997) Measuring the conformational stability of a protein. In Creighton, T. (ed), *Protein Structure: A Practical Approach*. IRL Press, Oxford, 299-321.

Palmer, A.E., Lee, S.K. and Solomon, E.I. (2001) Decay of the peroxide intermediate in laccase: reductive cleavage of the O-O bond, *J Am Chem Soc*, **123**, 6591-6599.

Palmer, A.E., Szilagyi, R.K., Cherry, J.R., Jones, A., Xu, F. and Solomon, E.I. (2003) Spectroscopic characterization of the Leu513His variant of fungal laccase: effect of increased axial ligand interaction on the geometric and electronic structure of the type 1 Cu site, *Inorg Chem*, **42**, 4006-4017.

Palmieri, G., Giardina, P. and Sannia, G. (2005) Laccase-mediated Remazol Brilliant Blue R decolorization in a fixed-bed bioreactor, *Biotechnol Prog*, **21**, 1436-1441.

- Paraskevopoulos, K., Antonyuk, S.V., Sawers, R.G., Eady, R.R. and Hasnain, S.S. (2006) Insight into catalysis of nitrous oxide reductase from high-resolution structures of resting and inhibitor-bound enzyme from *Achromobacter cycloclastes*, *J Mol Biol*, **362**, 55-65.
- Pedersen, J.S., Christensen, G. and Otzen, D.E. (2004) Modulation of S6 fibrillation by unfolding rates and gatekeeper residues, *J Mol Biol*, **341**, 575-588.
- Pereira, L., Coelho, A.V., Viegas, C.A., Santos, M.M., Robalo, M.P. and Martins, L.O. (2009) Enzymatic biotransformation of the azo dye Sudan Orange G with bacterial CotA-laccase, *J Biotechnol*, **139**, 68-77.
- Pereira, L., Coelho, A.V., Viegas, C.A., Ganachaud, C., Iacazio, G., Tron, T., Robalo, M.P., Martins, L.O. (2009) On the mechanism of biotransformation of the anthraquinonic dye blue 62 by laccases., *Adv. Synth. Catal.*, **351**, 1857-1865.
- Pesci, E.C. and Pickett, C.L. (1994) Genetic organization and enzymatic activity of a superoxide dismutase from the microaerophilic human pathogen, *Helicobacter pylori*, *Gene*, **143**, 111-116.
- Petersen, L.C. and Degn, H. (1978) Steady-State Kinetics of Laccase from *Rhus vernicifera*, *Biochimica et Biophysica Acta*, **526**, 85-92.
- Petrak, J. and Vyoral, D. (2005) Hephaestin--a ferroxidase of cellular iron export, *Int J Biochem Cell Biol*, **37**, 1173-1178.
- Piontek, K., Antorini, M. and Choinowski, T. (2002) Crystal structure of a laccase from the fungus *Trametes versicolor* at 1.90-Å resolution containing a full complement of coppers, *J Biol Chem*, **277**, 37663-37669.
- Pitcher, R.S. and Watmough, N.J. (2004) The bacterial cytochrome cbb3 oxidases, *Biochim Biophys Acta*, **1655**, 388-399.
- Plakoutsi, G., Taddei, N., Stefani, M. and Chiti, F. (2004) Aggregation of the Acylphosphatase from *Sulfolobus solfataricus*: the folded and partially unfolded states can both be precursors for amyloid formation, *J Biol Chem*, **279**, 14111-14119.
- Pogni, R., Brogioni, B., Baratto, M. C., Sinicropi, A., Giardina, P., Pezzella, C., Sannia, G., Basosi, R. (2007) Evidence for a radical mechanism in biocatalytic degradation of synthetic dyes by fungal laccases mediated by violuric acid *Biocatalysis and Biotransformation* **25**, 269-275.
- Pozdnyakova, I., Guidry, J. and Wittung-Stafshede, P. (2001) Copper stabilizes azurin by decreasing the unfolding rate, *Arch Biochem Biophys*, **390**, 146-148.



- Pozdnyakova, I. and Wittung-Stafshede, P. (2001) Copper binding before polypeptide folding speeds up formation of active (holo) *Pseudomonas aeruginosa* azurin, *Biochemistry*, **40**, 13728-13733.
- Prajapati, R.S., Das, M., Sreeramulu, S., Sirajuddin, M., Srinivasan, S., Krishnamurthy, V., Ranjani, R., Ramakrishnan, C. and Varadarajan, R. (2007) Thermodynamic effects of proline introduction on protein stability, *Proteins*, **66**, 480-491.
- Ptitsyn, O.B. (1995) Molten globule and protein folding, *Adv Protein Chem*, **47**, 83-229.
- Quintanar, L., Stoj, C., Taylor, A.B., Hart, P.J., Kosman, D.J. and Solomon, E.I. (2007) Shall we dance? How a multicopper oxidase chooses its electron transfer partner, *Acc Chem Res*, **40**, 445-452.
- Radestock, S.G., H. (2008) Exploiting the Link between Protein Rigidity and Thermostability for Data-Driven Protein Engineering, *Eng. Life Sci.*, **5**, 507-522.
- Ragusa, S., Cambria, M.T., Pierfederici, F., Scire, A., Bertoli, E., Tanfani, F. and Cambria, A. (2002) Structure-activity relationship on fungal laccase from *Rigidoporus lignosus*: a Fourier-transform infrared spectroscopic study, *Biochim Biophys Acta*, **1601**, 155-162.
- Rakhit, G., Antholine, W.E., Froncisz, W., Hyde, J.S., Pilbrow, J.R., Sinclair, G.R. and Sarkar, B. (1985) Direct evidence of nitrogen coupling in the copper(II) complex of bovine serum albumin by S-band electron spin resonance technique, *J Inorg Biochem*, **25**, 217-224.
- Ranocha, P., McDougall, G., Hawkins, S., Sterjiades, R., Borderies, G., Stewart, D., Cabanes-Macheteau, M., Boudet, A.M. and Goffner, D. (1999) Biochemical characterization, molecular cloning and expression of laccases - a divergent gene family - in poplar, *Eur J Biochem*, **259**, 485-495.
- Rensing, C. and Grass, G. (2003) *Escherichia coli* mechanisms of copper homeostasis in a changing environment, *FEMS Microbiol Rev*, **27**, 197-213.
- Ricchelli, F., Buggio, R., Drago, D., Salmona, M., Forloni, G., Negro, A., Tognon, G. and Zatta, P. (2006) Aggregation/fibrillogenesis of recombinant human prion protein and Gerstmann-Straussler-Scheinker disease peptides in the presence of metal ions, *Biochemistry*, **45**, 6724-6732.
- Roberts, S.A., Weichsel, A., Grass, G., Thakali, K., Hazzard, J.T., Tollin, G., Rensing, C. and Montfort, W.R. (2002) Crystal structure and electron transfer kinetics of CueO, a multicopper oxidase required for copper homeostasis in *Escherichia coli*, *Proc Natl Acad Sci U S A*, **99**, 2766-2771.

- Roberts, S.A., Wildner, G.F., Grass, G., Weichsel, A., Ambrus, A., Rensing, C. and Montfort, W.R. (2003) A labile regulatory copper ion lies near the T1 copper site in the multicopper oxidase CueO, *J Biol Chem*, **278**, 31958-31963.
- Robertson, A.D. and Murphy, K.P. (1997) Protein Structure and the Energetics of Protein Stability, *Chem Rev*, **97**, 1251-1268.
- Robic, S., Guzman-Casado, M., Sanchez-Ruiz, J.M. and Marqusee, S. (2003) Role of residual structure in the unfolded state of a thermophilic protein, *Proc Natl Acad Sci U S A*, **100**, 11345-11349.
- Rooman, M., Yves, D., Kwasigroch, J., Biot, C. and Gilis, D. (2002) What is paradoxical about Levinthal Paradox?, *Journal of Biomolecular Structure and Dynamics* **20**, 327-329.
- Rose, G.D. and Wolfenden, R. (1993) Hydrogen bonding, hydrophobicity, packing, and protein folding, *Annu Rev Biophys Biomol Struct*, **22**, 381-415.
- Roy, J.J., Abraham, T.E., Abhijith, K.S., Sujith Kumar, P.V. and Thakur, M.S. (2005) Biosensor for the determination of phenols based on Cross-Linked Enzyme Crystals (CLEC) of laccase., *Biosens Bioelectron*, **21**, 206-211.
- Ryden, L.G. and Hunt, L.T. (1993) Evolution of protein complexity: the blue copper-containing oxidases and related proteins, *J Mol Evol*, **36**, 41-66.
- Salgueiro, C.A., Turner, D.L. and Xavier, A.V. (1997) Use of paramagnetic NMR probes for structural analysis in cytochrome c3 from *Desulfovibrio vulgaris*, *Eur J Biochem*, **244**, 721-734.
- Sali, A. (1995) Comparative protein modeling by satisfaction of spatial restraints, *Mol Med Today*, **1**, 270-277.
- Sali, A. and Blundell, T.L. (1993) Comparative protein modelling by satisfaction of spatial restraints, *J Mol Biol*, **234**, 779-815.
- Sali, A., Shakhnovich, E. and Karplus, M. (1994) How does a protein fold ? , *Nature*, **369**, 248-251.
- Sanchez-Amat, A., Lucas-Elio, P., Fernandez, E., Garcia-Borron, J.C. and Solano, F. (2001) Molecular cloning and functional characterization of a unique multipotent polyphenol oxidase from *Marinomonas mediterranea*, *Biochim Biophys Acta*, **1547**, 104-116.
- Sanchez-Ruiz, J.M. (1992) Theoretical analysis of Lumry-Eyring models in differential scanning calorimetry, *Biophys J*, **61**, 921-935.

- Sato, Y., Wuli, B., Sederoff, R. and Whetten, R. (2001) Molecular Cloning and Expression of Eight Laccase cDNAs in Loblolly Pine (*Pinus taeda*)\*, *Journal of Plant Research*, **114**, 147-255.
- Savini, I., D'Alessio, S., Giartosio, A., Morpurgo, L. and Avigliano, L. (1990) The role of copper in the stability of ascorbate oxidase towards denaturing agents, *Eur J Biochem*, **190**, 491-495.
- Schmid, A., Dordick, J.S., Hauer, B., Kiener, A., Wubbolts, M. and Witholt, B. (2001) Industrial biocatalysis today and tomorrow, *Nature*, **409**, 258-268.
- Scholtz, J.M. (1995) Conformational stability of HPr: the histidine-containing phosphocarrier protein from *Bacillus subtilis*, *Protein Sci*, **4**, 35-43.
- Sedlak, E. and Wittung-Stafshede, P. (2007) Discrete roles of copper ions in chemical unfolding of human ceruloplasmin, *Biochemistry*, **46**, 9638-9644.
- Sedlak, E., Ziegler, L., Kosman, D.J. and Wittung-Stafshede, P. (2008) In vitro unfolding of yeast multicopper oxidase Fet3p variants reveals unique role of each metal site, *Proc Natl Acad Sci U S A*, **105**, 19258-19263.
- Shi, X., Stoj, C., Romeo, A., Kosman, D.J. and Zhu, Z. (2003) Fre1p Cu<sup>2+</sup> reduction and Fet3p Cu<sup>1+</sup> oxidation modulate copper toxicity in *Saccharomyces cerevisiae*, *J Biol Chem*, **278**, 50309-50315.
- Silow, M., Tan, Y.J., Fersht, A.R. and Oliveberg, M. (1999) Formation of short-lived protein aggregates directly from the coil in two-state folding, *Biochemistry*, **38**, 13006-13012.
- Singh, A., Severance, S., Kaur, N., Wiltsie, W. and Kosman, D.J. (2006) Assembly, activation, and trafficking of the Fet3p.Ftr1p high affinity iron permease complex in *Saccharomyces cerevisiae*, *J Biol Chem*, **281**, 13355-13364.
- Singh, S.K., Grass, G., Rensing, C. and Montfort, W.R. (2004) Cuprous oxidase activity of CueO from *Escherichia coli*, *J Bacteriol*, **186**, 7815-7817.
- Sitthisak, S., Howieson, K., Amezola, C. and Jayaswal, R.K. (2005) Characterization of a multicopper oxidase gene from *Staphylococcus aureus*, *Appl Environ Microbiol*, **71**, 5650-5653.
- Solano, F., Garcia, E., Perez, D. and Sanchez-Amat, A. (1997) Isolation and Characterization of Strain MMB-1 (CECT 4803), a Novel Melanogenic Marine Bacterium, *Appl Environ Microbiol*, **63**, 3499-3506.
- Solomon, E.I., Augustine, A.J. and Yoon, J. (2008) O<sub>2</sub> reduction to H<sub>2</sub>O by the multicopper oxidases, *Dalton Trans*, **14**, 3921-3932.

Solomon, E.I., Baldwin M. J., Lowery, M. D. (1992) Electronic structures of active sites in copper proteins: contributions to reactivity, *Chem. Rev.*, **92**, 521-542.

Solomon, E.I., Chen, P., Metz, M., Lee, S.K. and Palmer, A.E. (2001) Oxygen Binding, Activation, and Reduction to Water by Copper Proteins, *Angew Chem Int Ed Engl*, **40**, 4570-4590.

Solomon, E.I., Sarangi, R., Woertink, J.S., Augustine, A.J., Yoon, J. and Ghosh, S. (2007) O<sub>2</sub> and N<sub>2</sub>O activation by Bi-, Tri-, and tetranuclear Cu clusters in biology, *Acc Chem Res*, **40**, 581-591.

Solomon, E.I., Sundaram, U.M. and Machonkin, T.E. (1996) Multicopper Oxidases and Oxygenases, *Chem Rev*, **96**, 2563-2606.

Somogyi, B., Punyiczki, M., Hedstrom, J., Norman, J.A., Prendergast, F.G. and Rosenberg, A. (1994) Coupling between external viscosity and the intramolecular dynamics of ribonuclease T1: a two-phase model for the quenching of protein fluorescence, *Biochim Biophys Acta*, **1209**, 61-68.

Spolar, R.S., Livingstone, J.R. and Record, M.T., Jr. (1992) Use of liquid hydrocarbon and amide transfer data to estimate contributions to thermodynamic functions of protein folding from the removal of nonpolar and polar surface from water, *Biochemistry*, **31**, 3947-3955.

Sreerama, N., Venyaminov, S.Y. and Woody, R.W. (1999) Estimation of the number of alpha-helical and beta-strand segments in proteins using circular dichroism spectroscopy, *Protein Sci*, **8**, 370-380.

Stanley, N.R., Palmer, T. and Berks, B.C. (2000) The twin arginine consensus motif of Tat signal peptides is involved in Sec-independent protein targeting in *Escherichia coli*, *J Biol Chem*, **275**, 11591-11596.

Stathopoulos, P.B., Rumfeldt, J.A., KARBASSI, F., Siddall, C.A., Lepock, J.R. and Meiering, E.M. (2006) Calorimetric analysis of thermodynamic stability and aggregation for apo and holo amyotrophic lateral sclerosis-associated Gly-93 mutants of superoxide dismutase, *J Biol Chem*, **281**, 6184-6193.

Sterner, R. and Liebl, W. (2001) Thermophilic adaptation of proteins, *Crit Rev Biochem Mol Biol*, **36**, 39-106.

Stirpe, A., Guzzi, R., Wijma, H., Verbeet, M.P., Canters, G.W. and Sportelli, L. (2005) Calorimetric and spectroscopic investigations of the thermal denaturation of wild type nitrite reductase, *Biochim Biophys Acta*, **1752**, 47-55.

Stirpe, A., Sportelli, L. and Guzzi, R. (2006) A comparative investigation of the thermal unfolding of pseudoazurin in the Cu(II)-holo and apo form, *Biopolymers*, **83**, 487-497.

- Stoj, C. and Kosman, D.J. (2003) Cuprous oxidase activity of yeast Fet3p and human ceruloplasmin: implication for function, *FEBS Lett*, **554**, 422-426.
- Stoj, C.S., Augustine, A.J., Solomon, E.I. and Kosman, D.J. (2007) Structure-function analysis of the cuprous oxidase activity in Fet3p from *Saccharomyces cerevisiae*, *J Biol Chem*, **282**, 7862-7868.
- Stoj, C.S., Augustine, A.J., Zeigler, L., Solomon, E.I. and Kosman, D.J. (2006) Structural basis of the ferrous iron specificity of the yeast ferroxidase, Fet3p, *Biochemistry*, **45**, 12741-12749.
- Stoj, C.S. and Kosman, D.J. (2005) Copper proteins: oxidases. In B., K.R. (ed), *Encyclopedia of Inorganic Chemistry*. John Wiley & Sons, New York, 1134-1159.
- Stutz, C. (1993) The use of enzymes in ultrafiltration, *Fruit Processing*, **3**, 248-252.
- Sugumaran, M., Giglio, L., Kundzicz, H., Saul, S. and Semensi, V. (1992) Studies on the enzymes involved in puparial cuticle sclerotization in *Drosophila melanogaster*, *Arch Insect Biochem Physiol*, **19**, 271-283.
- Suzuki, T., Endo, K., Ito, M., Tsujibo, H., Miyamoto, K. and Inamori, Y. (2003) A thermostable laccase from *Streptomyces lavendulae* REN-7: purification, characterization, nucleotide sequence, and expression, *Biosci Biotechnol Biochem*, **67**, 2167-2175.
- Tan, Y.J., Oliveberg, M. and Fersht, A.R. (1996) Titration properties and thermodynamics of the transition state for folding: comparison of two-state and multi-state folding pathways, *J Mol Biol*, **264**, 377-389.
- Taniguchi, T., Ichimura, K., Kawashima, S., Yamamura, T., Tachi'iri, Y., Satake, K. and Kihara, H. (1990) Binding of Cu(II), Tb(III) and Fe(III) to chicken ovotransferrin. A kinetic study, *Eur Biophys J*, **18**, 1-8.
- Tavares, P., Pereira, A.S., Moura, J.J. and Moura, I. (2006) Metalloenzymes of the denitrification pathway, *J Inorg Biochem*, **100**, 2087-2100.
- Tezuka, K., Hayashi, M., Ishihara, H., Onozaki, K., Nishimura, M. and Takahashi, N. (1993) Occurrence of heterogeneity of N-linked oligosaccharides attached to sycamore (*Acer pseudoplatanus* L.) laccase after excretion, *Biochem Mol Biol Int*, **29**, 395-402.
- Tsai, H.F., Wheeler, M.H., Chang, Y.C. and Kwon-Chung, K.J. (1999) A developmentally regulated gene cluster involved in conidial pigment biosynthesis in *Aspergillus fumigatus*, *J Bacteriol*, **181**, 6469-6477.

- Ubbink, M., Ejdeback, M., Karlsson, B.G. and Bendall, D.S. (1998) The structure of the complex of plastocyanin and cytochrome f, determined by paramagnetic NMR and restrained rigid-body molecular dynamics, *Structure*, **6**, 323-335.
- Uthandi, S., Saad, B., Humbard, M.A. and Maupin-Furlow, J.A. (2010) LccA, an archaeal laccase secreted as a highly stable glycoprotein into the extracellular medium by *Haloferax volcanii*, *Appl Environ Microbiol*, **76**, 733-743.
- Vagin, A. and Teplyakov, A. (1997) MOLREP: an Automated Program for Molecular Replacement, *J. Appl. Cryst.*, **30**, 1022-1025.
- van Waasbergen, L.G., Hildebrand, M. and Tebo, B.M. (1996) Identification and characterization of a gene cluster involved in manganese oxidation by spores of the marine *Bacillus* sp. strain SG-1, *J Bacteriol*, **178**, 3517-3530.
- Vassall, K.A., Stathopoulos, P.B., Rumfeldt, J.A., Lepock, J.R. and Meiering, E.M. (2006) Equilibrium thermodynamic analysis of amyotrophic lateral sclerosis-associated mutant apo Cu,Zn superoxide dismutases, *Biochemistry*, **45**, 7366-7379.
- Vieille, C. and Zeikus, G.J. (2001) Hyperthermophilic enzymes: sources, uses, and molecular mechanisms for thermostability, *Microbiol Mol Biol Rev*, **65**, 1-43.
- Vogt, G. and Argos, P. (1997) Protein thermal stability: hydrogen bonds or internal packing?, *Fold Des*, **2**, S40-46.
- Volkin, D.B. and Klivanov, A.M. (1989) Minimizing protein inactivation protein function. A practical approach. In TE, C. (ed), *Minimizing protein inactivation protein function. A practical approach*. IRL, Oxford, 1-24.
- Volkl, P., Huber, R., Drobner, E., Rachel, R., Burggraf, S., Trincone, A. and Stetter, K.O. (1993) *Pyrobaculum aerophilum* sp. nov., a novel nitrate-reducing hyperthermophilic archaeum, *Appl Environ Microbiol*, **59**, 2918-2926.
- Wang, C., Eufemi, M., Turano, C. and Giartosio, A. (1996) Influence of the carbohydrate moiety on the stability of glycoproteins, *Biochemistry*, **35**, 7299-7307.
- Wang, J., Kean, L., Yang, J., Allan, A.K., Davies, S.A., Herzyk, P. and Dow, J.A. (2004) Function-informed transcriptome analysis of *Drosophila* renal tubule, *Genome Biol*, **5**, R69.
- Whitehead, D.L., Brunet, P.C. and Kent, P.W. (1960) Specificity in vitro of a phenoloxidase system from *Periplaneta americana* (L.), *Nature*, **185**, 610.

- Widsten, P. and Kandelbauer, A. (2008) Laccase applications in the forest products industry: A review, *Enzyme and Microbial Technology*, **42**, 293-307.
- Wiethaus, J., Wildner, G.F. and Masepohl, B. (2006) The multicopper oxidase CutO confers copper tolerance to *Rhodobacter capsulatus*, *FEMS Microbiol Lett*, **256**, 67-74.
- Wilson, M.T. and Torres, J. (2004) Reactions of nitric oxide with copper containing oxidases; cytochrome c oxidase and laccase, *IUBMB Life*, **56**, 7-11.
- Wintrode, P.L., Zhang, D., Vaidehi, N., Arnold, F.H. and Goddard, W.A., 3rd (2003) Protein dynamics in a family of laboratory evolved thermophilic enzymes, *J Mol Biol*, **327**, 745-757.
- Wittung-Stafshede, P. (2004) Role of cofactors in folding of the blue-copper protein azurin, *Inorg Chem*, **43**, 7926-7933.
- Xu, F. (1996) Oxidation of phenols, anilines, and benzenethiols by fungal laccases: correlation between activity and redox potentials as well as halide inhibition, *Biochemistry*, **35**, 7608-7614.
- Xu, F. (1997) Effects of redox potential and hydroxide inhibition on the pH activity profile of fungal laccases, *J Biol Chem*, **272**, 924-928.
- Xu, F. (1999) Recent progress in laccase study: properties, enzymology, production and applications. In Flickinger M-C&Drew SW, e. (ed), *The Encyclopedia of Bioprocess Technology: Fermentation Biocatalysis, and Bioseparation*. John Wiley & Sons, Inc., New York, 1545-1554.
- Xu, F., Palmer, A.E., Yaver, D.S., Berka, R.M., Gambetta, G.A., Brown, S.H. and Solomon, E.I. (1999) Targeted mutations in a *Trametes villosa* laccase. Axial perturbations of the T1 copper, *J Biol Chem*, **274**, 12372-12375.
- Yoshida, H. (1883) Chemistry of lacquer (Urushi) – Part I, *J Chem Soc, Trans*, **43**, 472-486.
- Young, S.N. and Curzon, G. (1972) A method for obtaining linear reciprocal plots with caeruloplasmin and its application in a study of the kinetic parameters of caeruloplasmin substrates, *Biochem J*, **129**, 273-283.
- Zaitseva, I., Zaitsev, V., Card, G., Moshkov, K., Bax, B., Ralph, A. and Lindley, P. (1996) The X-ray structure of human serum ceruloplasmin at 3.1 angstrom: Nature of the copper centres, *J. Biol. Inorg. Chem.*, **1**, 15-23.
- Zettlmeissl, G., Rudolph, R. and Jaenicke, R. (1979) Reconstitution of lactic dehydrogenase. Noncovalent aggregation vs. reactivation. 1. Physical properties and kinetics of aggregation, *Biochemistry*, **18**, 5567-5571.

Zhang, J. and Matthews, C.R. (1998) The role of ligand binding in the kinetic folding mechanism of human p21(H-ras) protein, *Biochemistry*, **37**, 14891-14899.

Zhou, H.X. (2002) Toward the physical basis of thermophilic proteins: linking of enriched polar interactions and reduced heat capacity of unfolding, *Biophys J*, **83**, 3126-3133.

Zhou, X.X., Wang, Y.B., Pan, Y.J. and Li, W.F. (2008) Differences in amino acids composition and coupling patterns between mesophilic and thermophilic proteins, *Amino Acids*, **34**, 25-33.

Zhukhlistova, N., Zhukova, YN., Lyashenko, AV., Zaitsev, VN., Mikhaïlov AM. (2008) Three-dimensional organization of three-domain copper oxidases: A review *Crystallography Reports*, **53**, 92-109.

Zoppellaro, G., Sakurai, T. and Huang, H. (2001) A novel mixed valence form of *Rhus vernicifera* laccase and its reaction with dioxygen to give a peroxide intermediate bound to the trinuclear center, *Journal of biochemistry*, **129**, 949-953.

Zumft, W.G. (1997) Cell biology and molecular basis of denitrification, *Microbiol Mol Biol Rev*, **61**, 533-616.

Zumft, W.G. and Kroneck, P.M. (2007) Respiratory transformation of nitrous oxide (N<sub>2</sub>O) to dinitrogen by Bacteria and Archaea, *Adv Microb Physiol*, **52**, 107-227.

Zwanzig, R., Szabo, A. and Bagchi, B. (1992) Levinthal's paradox, *Proc Natl Acad Sci U S A*, **89**, 20-22.



## 8 ANNEXES

---



## **8.1. MCOA SUBSTRATE SPECIFICITY: CHARACTERIZATION OF MUTANT ENZYMES**

The substrate specificity in McoA is dependent on the addition of exogenous copper into the reaction media has shown previously (Fernandes, et al., 2007). In order to further elucidate the reaction mechanism of McoA we have mutated three methionines (M224, M402 and M449), two of these residues (M402 and M449) are conserved in CueO (M355 and M441), known to be involved in the binding of a fifth copper (Roberts, et al., 2003). The third methionine (M224) is putatively involved in copper ligation and eventually enzyme activation. These Met residues in CueO are thought to be involved in the binding of a fifth copper, providing a suitable electron transfer matrix between low valence metal substrates and the T1 center, or by modulating the Met rich region in order to exhibit a more exposed binding site to the bulkier substrates. We had compared the properties of these mutants with the wt enzyme and mutant lacking the Met-rich region ( $\Delta$ P321-V363) in order to get insight over the specificity of McoA towards metal ions

We have also intended to isolate a soluble McoA copper full loaded, using a similar methodology used for CotA. The enzyme produced was analyzed by UV-Vis and CD. The stability was also evaluated by measuring the kinetic stability (at 80 °C) and also the melting temperatures were measured by DSC.

### **8.1.1. EXPERIMENTAL PROCEDURES**

**Construction of the mutants.** Single amino acid substitutions in the *mcoA* were created using the QuickChange site-directed mutagenesis kit (Stratagene). Plasmid pATF-1 (containing the wildtype McoA sequence) was used as a template and the primers forward *mcoAM224Ad* (5' – CCCGATGGGACACGCGGGCTTCTGGGG – 3') and reverse *mcoAM224Ar* (5' – CCCCAGAAGCCCGCGTGTCCCATCGGG – 3') were used to generate

the M224A mutant in the pATF-11. The forward primer *mcoAM402Ad* (5' – GGATAACTCTAGGCGCGAGGAGAATGG – 3') and the reverse *mcoAM402Ar* (5' – CCATTCTCCTCGCGCCTAGAGTTATCC – 3') were used to generate the M402A mutant in the plasmid pATF-17. The forward primer *mcoAM449Ad* (5' – CAACACGGGTGCGTACCACCCCATGC – 3') and the reverse *mcoAM449Ar* (5' – GCATGGGGTGGTACGCACCCGTGTTG – 3') were used to generate the M449A mutant present in the plasmid pATF-12. The presence of the desired mutations in the resulting plasmids, pATF-11 (M224A), pATF-17 (M402A) and pATF-12 (M449A) and the absence of unwanted mutations in other regions of the insert were confirmed by DNA sequence analysis. For the mutation  $\Delta$ P321-V363, phosphorylated primers, *mcoAdel322r* (5'-GAAGTTGTAAAGCTTTATTACGTCATTTAC-3') and *mcoAdel362d* (5'-GTTATGGAGTTCAGGGTTACAAAGG-3') were used to amplify around plasmid pATF-1, excluding an internal fragment of *mcoA*. The PCR product was incubated with *DpnI*, to digest template DNA, self-ligated and introduced into *E. coli* DH5 $\alpha$  by transformation. The resulting plasmid pATF-9 containing *mcoA*, with an in-frame deletion corresponding to codons 964 to 1087, was then sequenced to confirm the desired mutation and the absence of unwanted mutations.

**Overproduction and purification.** The expression strain was freshly transformed with pGro7 (*Cm<sup>r</sup>*) (from Takara Bio Inc.), in which the L-arabinose inducible promoter (*araB*) was used to express the *groES/groEL* chaperones, before being transformed with the recombinant vectors. The co-expression of *mcoA* with *groES/groEL* find out that it enables the production of higher amounts of soluble McoA. The expression strain was grown in Luria-Bertani (LB) culture medium supplemented with ampicillin (100  $\mu$ g/mL), chloramphenicol (34  $\mu$ g/mL), arabinose (1 mg/mL) at 30°C. Growth was followed until OD<sub>600</sub>=0.6, at which time 100 $\mu$ M IPTG and 250 $\mu$ M CuCl<sub>2</sub> were added to the culture medium and the temperature lowered to 25°C. Incubation

was continued for further 4h when a change to microaerobic conditions was achieved by switching off the shaking function (Durao, et al., 2008). Cells were harvested by centrifugation (8000 x g, 15 min, 4°C) after a further 20h in microaerobic conditions. The cell sediment was suspended in 20mM Tris-HCl buffer (pH 7.6), containing DNase I (10µg/mL extract), MgCl<sub>2</sub> (5mM) and a mixture of protease inhibitors, antipain and leupeptin (2µg/mL extract). Cells were disrupted in a French pressure cell (at 19000 psi), followed by a centrifugation (18 000 x g, 60 min, 4°C) to remove cell debris. The crude extract was loaded onto an ion exchange SP-Sepharose column (bed volume 80 ml) equilibrated with Tris-HCl (20 mM, pH 7.6). Elution was carried out with a two-step linear NaCl gradient (0–0.5 and 0.5–1 M) in the same buffer. Fractions were collected and assayed for activity. Active fractions were pooled, concentrated by ultrafiltration (cut-off of 30 kDa), and equilibrated to 20 mM Tris-HCl (pH 7.6). The resulting sample was applied on a Superdex 75 HR 10/30 column (Amersham Biosciences) equilibrated with 20 mM Tris-HCl buffer, pH 7.6 containing 0.2 M NaCl. All purification steps were carried out at room temperature in a fast protein liquid chromatography system (Åkta-FPLC, Amersham Biosciences)

### **8.1.2. RESULTS**

**Characterization of the full loaded McoA.** McoA was previously produced following a method based in the denaturation/renaturation of inclusion bodies that resulted in a protein solution with a copper to protein ration lower than four (Fernandes, et al., 2007). The use of a recombinant plasmid coding for chaperones (*groES* and *groEL*) together with growing conditions that enabled the expression of the protein with full-copper loaded (3.4:1, Cu/protein as compared with 2.5:1, Cu/prot), (Figure 8.1) (Durao, et al., 2008).

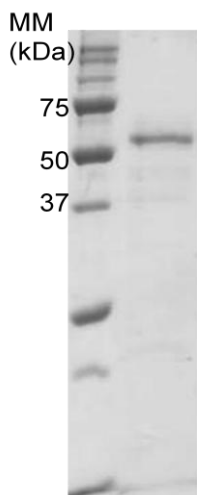


Figure 8.1: SDS-PAGE analysis of the purified McoA

The circular dichroism spectra Figure 8.2 shows that proteins prepared following different procedures present a similar secondary structure.

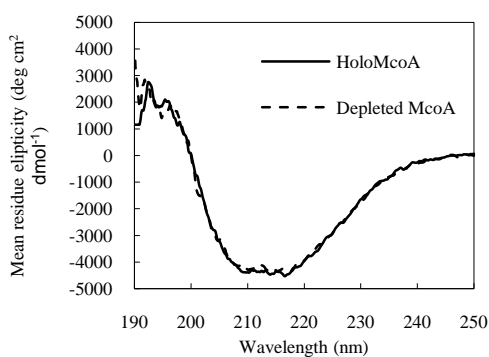


Figure 8.2: CD spectra in the far-UV region, of HoloMcoA (full line) and partially-copper depleted McoA (dashed line). Both spectra reflect high  $\beta$ -sheet content and the similarity between both forms of McoA.

Chemical unfolding of the tertiary structure was also measured by trp fluorescence and energy barriers (separating the native and the unfolded states) were similar in both preparations (Table 8.1).

Table 8.1: Chemical stability parameters

Protein	$\Delta G$ (kcal/mol)	$m$ (kcal/mol)	$M$ (M)
McoA recovered from IB	$2.8 \pm 0.6$	$-1.0 \pm 0.1$	$2.7 \pm 0.3$
McoA purified soluble fraction of crude extract	$3.3 \pm 0.3$	$-1.4 \pm 0.2$	$2.5 \pm 0.2$

These results show that the secondary structure and the chemical unfolding are similar in both proteins and thus independent of the production and purification method. Recently we have shown that copper content as well as copper incorporation have a direct impact on the thermal stability of CotA laccase from *B.subtilis* (Durao, et al., 2008). Accordingly, a higher long term stability with a  $t_{1/2}$  of 10 instead of 8 h (at 80°C) was calculated for this soluble form of McoA containing a higher copper content (Figure 8.3A). Similar to what was previously observed the activity decay along time could only be fitted by using the sum of two exponentials of this new form of McoA (Figure 8.3A), being one of the phases attributed to protein aggregation with an intermediary state with around 60% of activity, similar to the 50% determined for the other variant of McoA (Fernandes, et al., 2007). This result is in agreement with the results obtained by DSC where no unfolding was observed (no endothermic peak detected) up to 130°C, the maximum temperature reached by our DSC equipment.

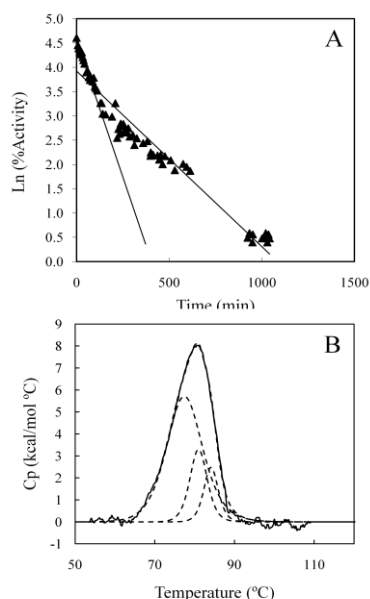


Figure 8.3: Thermal stability studies in HoloMcoA. (A) The logarithm of activity decay along time of McoA at 80°C shows clearly that the activity decay of McoA cannot be fitted by a single first-order process since it does not display an inverse linear relationship with time. (B) Excess heat capacity obtained from a DSC scan of McoA at (thick line) fitted with three independent transitions shown separately in dashed lines as one or two transitions could not fit accurately the experimental trace. The dashed line under the DSC trace is the resulting sum of the three independent transitions. The melting temperatures of the three transitions are 77.5, 80.5 and 84.1°C.

Therefore, we added subdenaturing concentrations of GdnHCl (500 mM) to the protein sample to provoke a slight destabilization of the structure which allowed the measuring melting temperatures of 77.5, 80.5 and 84.1 °C (Figure 8.3B). Furthermore, the DSC thermogram could only be fitted using three calorimetric domains and is an irreversible denaturation (no second peak in the second scan). These results of stability suggest the new copper-full loaded form of McoA is more stable, reinforcing our idea that copper ions have a fundamental role in the structural thermal stability of McoA. Furthermore, the aggregation phenomenon observed previously, when McoA is denatured using GdnHCl was also observed in this new form of McoA by using gel filtration chromatography (data not shown).

**Expression and purification.** McoA and mutants, M224A, M402A, M449A,  $\Delta$ P321-V363 were expressed in *E. coli* showing the same chromatographic pattern during purification when compared with that of McoA wild-type. Preparations were judged to be homogeneous by the



observation of a single band in Coomassie Blue stained SDS-PAGE. Copper content was measured for all the proteins and similar ratios of copper/protein ) (

Table 8.2).

Table 8.2: Redox potential, copper content, molar absorptivity of McoA wild-type and mutants

Species	T1 Copper redox potential (mV)	Copper equivalents	Absorptivity ( $\text{mM}^{-1} \text{cm}^{-1}$ )
<b>Wild-type</b>	535	$3.4 \pm 0.2$	2.0
<b>M224A</b>	410	$3.7 \pm 0.3$	1.3
<b>M402A</b>	510	$3.9 \pm 0.1$	1.9
<b>M449A</b>	475	$3.5 \pm 0.2$	1.6
<b><math>\Delta</math>P321-V363</b>	494	$3.6 \pm 0.3$	0.7

**Spectroscopic characterization.** The UV-Vis absorption spectra show that all proteins have an absorbance peak at 600 nm which corresponds to the charge transfer copper-cysteine at the T1 copper center. However, the mutations affected the maximal 600 nm absorption values (Figure 8.4 and Table 8.2). The deletion mutation  $\Delta$ P321-V363 had a profound impact on the 600 nm absorption with a decrease of almost 50% in absorptivity (Table 8.2), as previously observed (Fernandes, et al., 2007). Due to the overlapping peak of absorption at 280 nm it is not possible to draw conclusions about the alterations at the T3 copper center as its absorption at 330 nm may be masked.

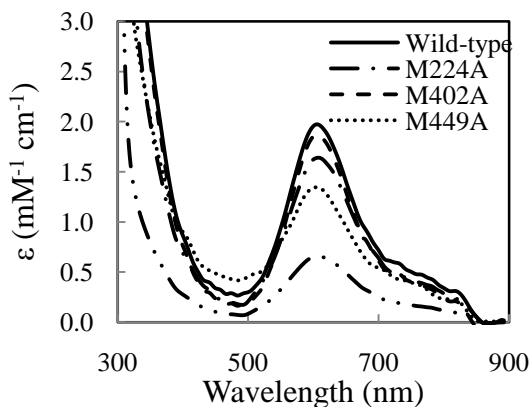


Figure 8.4: Absorption spectra of wild-type and mutant proteins. Absorbance is given as the millimolar extinction coefficient calculated from spectra normalized for protein concentration.

The lower absorption of T1 copper center is not the result of an incomplete copper loading as all the proteins were purified with around four coppers per protein molecule, thus it should reflect slight alterations in the properties of the T1 Cu site. The T1 redox potential was measured for all proteins following the decrease in absorption at 600 nm after reducing with sodium dithionite. All mutants show lower values than wt but M224A mutant was more severely affected, with a decrease of 120 mV comparing to the wild-type (Table 8.2).

**Kinetic analysis.** The higher copper:protein ratio in the new form of McoA resulted in an enzyme that globally has 10-fold more activity for all substrates tested. The maximal velocity versus substrate concentration was directly fitted according to the Michaelis-Menten equation (Fernandes, et al., 2007). The deletion of the Met-rich region had a profound impact in the protein resulting in a severe decrease in catalytic effectiveness for all the substrates with  $k_{cat}/K_m$  values ranging from 35-fold up to 1233-fold lower for DMP and  $\text{Cu}^+$ , respectively as compared with wt. this decrease relies essentially in the  $k_{cat}$  term, suggesting that the presence of the Met-rich motif and of its conformational arrangement are a key factor in the substrate modulation. In fact, this mutation caused an enzyme inert to the presence of exogenous copper, since no increase in the  $k_{cat}$  term towards metals (Table 8.3) or a decrease in the  $K_m$  towards the aromatic substrates was determined (Table 8.4).

Table 8.3: Steady-state kinetic constants of McoA wild-type and mutants proteins towards cuprous ( $\text{Cu}^+$ ) and ferrous ( $\text{Fe}^{2+}$ ) ions.

	Substrates	$K_m$ ( $\mu\text{M}$ )	$K_m$ ( $\mu\text{M}$ ) + $\text{Cu(II)}$	$k_{\text{cat}}$ ( $\text{min}^{-1}$ )	$k_{\text{cat}}$ ( $\text{min}^{-1}$ ) + $\text{Cu(II)}$	$k_{\text{cat}}/K_m$ ( $\text{s}^{-1}\text{M}^{-1}$ )	$k_{\text{cat}}/K_m$ ( $\text{s}^{-1}\text{M}^{-1}$ ) + $\text{Cu(II)}$
<b>Wild-type</b>	Cu(II)	$36 \pm 1$	$35 \pm 1$	$460 \pm 2$	$1280 \pm 68$	$2.1 \times 10^5$	$6.1 \times 10^5$
	Fe(II)	$9 \pm 0.4$	$12 \pm 2$	$205 \pm 46$	$657 \pm 23$	$3.8 \times 10^5$	$9.1 \times 10^5$
<b><math>\Delta\text{P321-V363}</math></b>	Cu(II)	$37 \pm 4$	$40 \pm 8$	$2 \pm 0.7$	$1 \pm 0.1$	$0.009 \times 10^5$	$0.004 \times 10^5$
	Fe(II)	$5 \pm 0.5$	$5 \pm 1$	$1 \pm 0.1$	$1 \pm 0.2$	$0.03 \times 10^5$	$0.03 \times 10^5$
<b>M224A</b>	Cu(II)	$42 \pm 7$	$51 \pm 7$	$304 \pm 19$	$310 \pm 17$	$1.2 \times 10^5$	$1.0 \times 10^5$
	Fe(II)	$13 \pm 0.7$	$13 \pm 3$	$157 \pm 38$	$128 \pm 6$	$2.0 \times 10^5$	$1.6 \times 10^5$
<b>M402A</b>	Cu(II)	$59 \pm 5$	$40 \pm 2$	$177 \pm 8$	$185 \pm 2$	$0.5 \times 10^5$	$0.8 \times 10^5$
	Fe(II)	$18 \pm 1$	$16 \pm 2$	$201 \pm 3$	$170 \pm 14$	$1.9 \times 10^5$	$1.8 \times 10^5$
<b>M449A</b>	Cu(II)	$46 \pm 8$	$50 \pm 8$	$312 \pm 20$	$323 \pm 20$	$1.1 \times 10^5$	$1.1 \times 10^5$
	Fe(II)	$13 \pm 2$	$10 \pm 2$	$147 \pm 12$	$156 \pm 43$	$1.8 \times 10^5$	$2.6 \times 10^5$

The catalytic properties of the M224A mutant showed that is the most similar to the wild-type, and the major difference is related to the absence of the increase of  $k_{\text{cat}}$  for metallic substrates oxidation ( $\text{Cu}^+$  and  $\text{Fe}^{2+}$ ) (Table 8.3).

Table 8.4: Steady-state kinetic constants of McoA wild-type and mutants towards aromatic substrates.

	Substrates	$K_m$ ( $\mu\text{M}$ )	$K_m$ ( $\mu\text{M}$ ) + Cu(II)	$k_{cat}$ ( $\text{min}^{-1}$ )	$k_{cat}$ ( $\text{min}^{-1}$ ) + Cu(II)	$k_{cat} / K_m$ ( $\text{s}^{-1}\text{M}^{-1}$ )	$k_{cat} / K_m$ ( $\text{s}^{-1}\text{M}^{-1}$ ) + Cu(II)
<b>Wild-type</b>	ABTS	$117 \pm 8$	$64 \pm 5$	$1136 \pm 99$	$1181 \pm 63$	$1.6 \times 10^5$	$3.1 \times 10^5$
	SGZ	$28 \pm 5$	$13 \pm 2$	$153 \pm 16$	$304 \pm 23$	$0.9 \times 10^5$	$3.9 \times 10^5$
	DMP	$167 \pm 9$	$84 \pm 3$	$56 \pm 4$	$55 \pm 1$	$0.05 \times 10^5$	$0.1 \times 10^5$
<b><math>\Delta\text{P321-V363}</math></b>	ABTS	$77 \pm 11$	$59 \pm 7$	$2 \pm 0.1$	$2 \pm 0.2$	$0.004 \times 10^5$	$0.005 \times 10^5$
	SGZ	$11 \pm 1$	$11 \pm 4$	$2 \pm 0.1$	$0.7 \pm 0.1$	$0.03 \times 10^5$	$0.01 \times 10^5$
	DMP	$73 \pm 9$	$55 \pm 5$	$0.5 \pm 0.1$	$1 \pm 0.1$	$0.001 \times 10^5$	$0.003 \times 10^5$
<b>M224A</b>	ABTS	$119 \pm 9$	$64 \pm 7$	$911 \pm 9$	$776 \pm 29$	$1.3 \times 10^5$	$2.2 \times 10^5$
	SGZ	$39 \pm 2$	$12 \pm 1$	$392 \pm 31$	$377 \pm 9$	$1.7 \times 10^5$	$5.2 \times 10^5$
	DMP	$170 \pm 25$	$73 \pm 1$	$37 \pm 3$	$36 \pm 2$	$0.04 \times 10^5$	$0.08 \times 10^5$
<b>M402A</b>	ABTS	$64 \pm 2$	$75 \pm 16$	$642 \pm 11$	$577 \pm 77$	$1.7 \times 10^5$	$1.3 \times 10^5$
	SGZ	$16 \pm 1$	$19 \pm 2$	$302 \pm 5$	$274 \pm 4$	$3.1 \times 10^5$	$2.4 \times 10^5$
	DMP	$80 \pm 6$	$66 \pm 5$	$20 \pm 1$	$27 \pm 3$	$0.04 \times 10^5$	$0.06 \times 10^5$
<b>M449A</b>	ABTS	$81 \pm 7$	$67 \pm 7$	$842 \pm 55$	$794 \pm 23$	$1.7 \times 10^5$	$1.9 \times 10^5$
	SGZ	$14 \pm 4$	$16 \pm 1$	$406 \pm 13$	$387 \pm 43$	$4.8 \times 10^5$	$4.0 \times 10^5$
	DMP	$64 \pm 5$	$81 \pm 8$	$35 \pm 1$	$39 \pm 2$	$0.09 \times 10^5$	$0.08 \times 10^5$

In fact, a decrease of 6-fold in M224A specificity was determined. Regarding the aromatic substrates (ABTS, SGZ and DMP) the M224A mutation did not affect the enzyme specificity, since those kinetic constants are quite similar to the wild-type enzyme except for minor variations in the  $k_{cat}$ . The activation observed for the aromatic substrates (a reduction in the  $K_m$  parameter) is maintained in this mutant (Table 8.4).

The M402 residue may probably have an important role in the electron transfer pathway from the substrate towards the  $\text{Cu}^+$  from the T1 copper center. This mutation is the most affected in the  $k_{\text{cat}}$ , where a reduction in activity of the enzyme towards metals by 4 and 7-fold towards  $\text{Cu}^+$  and  $\text{Fe}^{2+}$  was determined, respectively. On the other hand, in this mutant protein the  $K_m$  for aromatic substrates was highly affected.

The M449A mutation had the same effect of the M402A, with minor differences in the  $k_{\text{cat}}$  towards metals, where a decrease of 4-fold is observed compared with the wild-type. Like the 402 residue, also this Met449 should have a preponderant role in the specificity of the protein, because similarly to M402A this M449A also lost the effect of exogenous copper on the affinity towards aromatics (Table 8.4).

### **8.1.3. DISCUSSION**

HoloMcoA was obtained due to the co-expression of a plasmid containing molecular chaperones, and an improved expression method, which involves the creation of microaerobic conditions during the fermentation (Durao, et al., 2008). This methodology enabled the purification of a full loaded enzyme with around 10 times more activity towards the tested substrates, when compared with the depleted form (Fernandes, et al., 2007). The thermal stability studies show that the higher copper content in the protein contributed to a higher thermal stability. However, similar increase in stability was not observed in the chemical stability, most probably due to its depletion in a previous event to the unfolding of the structure (Fernandes, et al., 2009). Redox potential of the T1 center did not suffer alterations between the depleted and HoloMcoA, lying in 535mV. The relatively low epsilon at 600 nm ( $2 \text{ mM}^{-1} \text{ cm}^{-1}$ ) in McoA when compared to this family of enzymes could be related to small structural differences in the T1 copper center (Durao, et al., 2008). Near the T1 copper center, McoA has three methionines 224, 402 and 449 (Figure 8.5) that could be

involved in the binding of a fifth copper, just like happens in CueO from *E. coli* (Kataoka, et al., 2007; Roberts, et al., 2003). The study of their role in McoA could give further insights into the catalytic mechanism, as well as the enzyme substrate specificity. Contrarily, to the absorbance and to the catalytic properties the redox potential of the deletion mutant was not highly affected probably because this deletion could result in a higher exposition of the T1 copper center to the solvent, and therefore stabilizing the oxidized state. Alteration in the ligand field has been shown to significantly modulate the reduction potential of T1 copper sites, where second-sphere amino-acid residues affect the reduction potential (Stoj and Kosman, 2003; Stoj, et al., 2006). The M224A mutant presents a 120 mV decrease in the redox potential. This diminish in the redox potential could have compromised the thermodynamic driving force and thus result in a decreased electron transfer rate and hence of  $k_{\text{cat}}$  (Xu, 1997). However, this residue should not be involved in the modulation of the binding pocket, probably because it is the most distant one from T1 center and also the most faraway from other methionine that could eventually share the binding of the fifth copper. In CueO the fifth copper lays 7.5Å from the T1 copper and is buried under the methionine rich region (Roberts, et al., 2003). In McoA the M224 lies at near 9Å making it difficult to be a ligand of the fifth copper (Figure 8.5).



Figure 8.5: McoA T1 copper center. T1 copper is coordinated by H514, H451, C509 and M519. M402 and M224 are conserved residues present in CueO from *E. coli* and presumably involved in the coordination of a labile regulatory copper.

On the other hand, both M449 and M402, that are closer to the T1 center, seem to have an important role in the binding of a probable fifth copper due to the loss of activation for metal ions as well as the effect towards aromatic substrates.

In summary, these three methionines are between the Met-rich loop and the T1 copper center. M224A mutation had little effect in the catalytic, but a pronounced effect in the absorbance at 600 nm and in the redox potential. Both these effects could be related to some structural rearrangement in the vicinity of the T1 center, which could indicate the putative formation of an electron matrix. The M402 and M449 residues should have a determinant role in the putative binding of a fifth copper, once its mutations had a pronounced effect in the substrate modulation. Also, the M402 residue should be related to the electron transfer between the substrate and T1 copper since the  $k_{\text{cat}}$  for all substrates was affected. The deletion of the Met-rich loop had a profound impact on the catalytic capability of the enzyme, due to the decrease in the  $k_{\text{cat}}$  for all substrates. Furthermore, this mutant revealed the importance of the loop towards the formation of the putative electronic matrix coupling pathway (for metallic substrates) as well as in the modulation of the binding pocket towards aromatic substrates. These results show the importance that the putative ligands of the fifth copper as well as the Met-rich loop have in the catalytic mechanism of McoA.